Fine-Tuning the Quality of Fast Pyrolysis Bio-Oils During Condensation with the Aid of Thermodynamic Phase Equilibria Modeling

Zur Erlangung des akademischen Grades eines
DOKTORS DER INGENIEURWISSENSCHAFTEN (Dr.-Ing.)

von der KIT-Fakultät für Chemieingenieurwesen und Verfahrenstechnik des
Karlsruher Instituts für Technologie (KIT)
genehmigte

DISSERTATION

von

MEng George Kofi Parku
aus Aveme, Ghana

Tag der mündlichen Prüfung: 12. Dezember 2024
Erstgutachter: Prof. Dr. Nicolaus Dahmen
Zweitgutachter: Prof. Dr. Robert C. Brown

Abstract

The development of biomass fast pyrolysis oil refineries plays a pivotal role in advancing the sustainable production of biofuels and biochemicals. Fast pyrolysis bio-oil (FPBO) is a complex mixture of organic compounds, and the selective recovery of valuable chemicals from FPBO requires the application of multiple separation techniques, including fractional condensation, distillation, and liquid–liquid extraction. The overarching aim of this study was to optimize the recovery of selected chemicals from FPBOs by fine-tuning oil composition during condensation of hot pyrolysis volatiles, while investigating the underlying physicochemical phenomena through phase equilibria modeling. Key process parameters, including condensation temperature, condenser design, and quench media (QM) type, were systematically explored to elucidate their impact on product yield and composition. Phase equilibria modeling was implemented not only to reduce experimental effort but also to provide insights into otherwise unexplained trends in FPBO composition.

The first part of the study focused on the use of fractional condensation to optimize the aqueous condensate (AC) fraction for downstream microbial conversion. Optimum conditions were identified by integrating the Central Composite Design statistical method with vapor–liquid equilibrium flash calculations using the modified UNIFAC Dortmund (UNIFAC-DMD) model, and validated experimentally on a 10 kg/h fast pyrolysis unit. Model predictions indicated that maximum AC yield and enhanced substrate recovery, at the expense of inhibitors, were achieved at condenser temperatures of 120 °C and 50 °C in the first and second stages, respectively. Experimental data showed good agreement with predictions, although deviations were observed for inhibitory compounds present at trace concentrations. These deviations were attributed to the limitations of the UNIFAC-DMD model in capturing phase behavior of dilute organics in water and uncertainties in vapor pressure data. Overall, fractional condensation was demonstrated as an effective pre-treatment strategy for AC valorization, providing a foundation for subsequent downstream bioconversion processes.

The second part of the study evaluated the influence of four different QM (water, Isopar-V, ethanol, and glycol) on the yield and composition of FPBOs. Ratios of 0.5 and 2.0 of QM to hot pyrolysis volatiles (m_q/m_v), defining the extent of cooling, and quenching temperatures

ranging between 40 and 120 °C were investigated. A phase equilibria model was developed to predict the effects of these parameters on FPBO yield and composition, and selected conditions were validated experimentally on a 10 kg/h fast pyrolysis unit. Model predictions indicated that organic-rich condensate (ORC) yield decreased with increasing quenching temperature for all the investigated QM, except water. Glycol and ethanol formed a mixed product with the ORC, with the m_q/m_v ratio of 2.0 producing higher ORC yields than 0.5, whereas Isopar-V and water formed immiscible products, with higher ratios reducing ORC yields due to mass transfer limitations. Predicted concentrations of carboxylic acids (acids) in the ORC declined with increasing temperature for all QM and across all m_q/m_v ratios, with glycol retaining the highest acid content, followed by ethanol, Isopar-V, and water. Other functional groups, including ketones, phenols, guaiacols, furans, and sugars, exhibited similar trends, with their concentrations in the AC also rising at higher quenching temperatures. Experimental validations were performed at temperatures optimized for each QM: 40 °C (ethanol), 80 °C (glycol and Isopar-V), and 95 °C (water). Ethanol recovered the highest ORC yield, producing 50 wt.% more than glycol and 75 wt.% more than water or Isopar-V. Glycol retained the highest fractions of acids, ketones, and phenolic compounds in the ORC, consistent with model predictions. Isopar-V remained largely immiscible with the ORC, with minor interactions, whereas the water quench retained nearly all water-soluble compounds, particularly sugars, highlighting its potential for direct sugar recovery during condensation.

The final part of the study evaluated a novel method for recovering levoglucosan (LG), an anhydrosugar derived from fast pyrolysis volatiles, during direct-contact condensation, compared with the widely known liquid–liquid (solvent) extraction technique. The method employed quenching hot pyrolysis volatiles with water in a single step condensation so that the condensed ORC fraction was recovered together with the spent water quench in a single stage. Investigations revealed a 100% effective recovery of LG and other anhydrosugars in the recovered spent water quench following condensation. Compared to solvent extraction of LG from an already condensed ORC, this technique proved more efficient for LG extraction from FPBOs, as it required significantly lower solvent-to-feed ratios and eliminated downstream liquid–liquid extraction setups. Moreover, the application of AC as the solvent to recover LG from the ORC proved more efficient than freshwater, as demonstrated by bench-scale solvent extraction tests. These findings enhance the valorization potential of AC, reduce operational

costs, and provide a sustainable pathway for integrating sugar recovery into pyrolysis biorefineries.

Throughout the study, thermodynamic modeling using the UNIFAC-DMD model provided valuable guidance for predicting the non-ideal vapor–liquid and, to some extent, liquid–liquid equilibria of pyrolysis vapors and bio-oils. However, deviations were observed, particularly for functional group compounds, due to limitations in: (i) handling highly dilute organics in water, (ii) representing association and hydrogen-bonding interactions, and (iii) uncertainties of pure-component vapor pressure data. These findings suggest that more advanced models, such as the Group Contribution with Association Equation of State (GCA-EoS), should be considered for improved predictions. Additionally, experimental pyrolysis condensation systems rarely achieve equilibrium conditions, emphasizing the need for validation methods such as the Advanced Distillation Curve (ADC).

In conclusion, although limitations were observed in modeling predictions, the combination of experimental and modeling approaches provided comprehensive insights into quenching condensation phenomena and supported the optimized recovery of high-value chemicals from FPBO. The findings emphasize the importance of detailed parametric studies and establish a robust foundation for the design and operation of sustainable biomass fast pyrolysis biorefineries, with direct implications for biofuel and biochemical production.

Zusammenfassung

Die Entwicklung von Biomasse-Schnellpyrolyse-Bioraffinerien spielt eine zentrale Rolle bei der Förderung der nachhaltigen Produktion von Biokraftstoffen und Biochemikalien. Schnellpyrolyse-Bioöl (Fast Pyrolysis Bio-Oil, FPBO) ist ein komplexes Gemisch organischer Verbindungen; dahererfordert die selektive Gewinnung wertvoller Chemikalien aus FPBO den Einsatz mehrerer Trennverfahren einschließlich fraktionierter Kondensation, Destillation und Flüssig-Flüssig-Extraktion. Ziel dieser Arbeit war es, die Rückgewinnung ausgewählter Chemikalien aus FPBO durch Feinabstimmung der Ölzusammensetzung während der Kondensation heißer Pyrolysegase zu optimieren und gleichzeitig die zugrunde liegenden physikochemischen Phänomene mithilfe von Phasengleichgewichtsmodellierung zu untersuchen. Wichtige Prozessparameter, darunter Kondensationstemperatur, Kondensatoraufbau und Art des Quenchmediums (QM), wurden systematisch untersucht, um deren Einfluss auf Produktausbeute und -zusammensetzung zu bestimmen. Die Phasengleichgewichtsmodellierung diente nicht nur der Reduzierung des experimentellen Aufwands, sondern lieferte auch Erklärungen für bislang nicht aufgeklärte Trends in der FPBO-Zusammensetzung.

Der erste Teil der Arbeit konzentrierte sich auf die fraktionierte Kondensation zur Optimierung der wässrigen Kondensatfraktion (AC) für eine nachgelagerte mikrobielle Anreicherung und Umsetzung der darin enthaltenen Substrate. Die optimalen Bedingungen wurden durch die Kombination der Central-Composite-Design-Statistik mit Dampf-Flüssig-Gleichgewichts-Flash-Berechnungen unter Verwendung des modifizierten UNIFAC-Dortmund-Modells (UNIFAC-DMD) ermittelt und experimentell an einer 10-kg/h-Schnellpyrolyseanlage validiert. Modellvorhersagen zeigten, dass maximale AC-Ausbeute und verbesserte Substratrückgewinnung auf Kosten von Inhibitoren bei Kondensationstemperaturen von 120 °C und 50 °C in der ersten bzw. zweiten Stufe erreicht wurden. Experimentelle Daten stimmten weitgehend mit den Vorhersagen überein, Abweichungen bei Inhibitoren in Spurenkonzentrationen wurden auf die begrenzte Fähigkeit des UNIFAC-DMD-Modells zurückgeführt, das Phasenverhalten verdünnter organischer Verbindungen in Wasser und Dampfdruckunsicherheiten abzubilden. Insgesamt erwies sich die fraktionierte Kondensation

als effektive Vorbehandlungsstrategie für die AC-Valorisierung und legte die Grundlage für nachgelagerte biotechnologische Prozesse.

Der zweite Teil der Arbeit bewertete den Einfluss von vier verschiedenen Quenchmedien (Wasser, Isopar-V, Ethanol und Glykol) auf Ausbeute und Zusammensetzung von FPBO. Untersucht wurden Quenchmedien-Verhältnisse (m_q/m_v) von 0,5 und 2,0 sowie Quenchtemperaturen zwischen 40 und 120 °C. Ein Phasengleichgewichtsmodell wurde entwickelt, um die Auswirkungen dieser Parameter auf FPBO-Ausbeute und -Zusammensetzung vorherzusagen, und ausgewählte Bedingungen wurden wiederum experimentell validiert. Modellvorhersagen zeigten, dass die Ausbeute des organikreichen Kondensats (ORC) mit steigender Quenchtemperatur für alle untersuchten QM außer Wasser abnahm. Glykol und Ethanol bildeten ein gemischtes Produkt mit dem ORC; ein m_q/m_v-Verhältnis von 2,0 führte zu höheren ORC-Ausbeuten als 0,5. Isopar-V und Wasser bildeten immiscible Produkte; höhere Quenchmedienverhältnisse reduzierten die ORC-Ausbeute aufgrund von Stofftransportlimitierungen. Die Vorhersagen der Carbonsäurekonzentrationen im ORC zeigten einen Rückgang mit steigender Temperatur für alle QM und m_q/m_v-Verhältnisse, wobei Glykol die höchste Säurekonzentration hielt, gefolgt von Ethanol, Isopar-V und Wasser. Andere funktionelle Gruppen, darunter Ketone, Phenole, Guajakole, Furane und Zucker, zeigten ähnliche Trends, wobei ihre Konzentrationen im AC bei höheren Quenchtemperaturen ebenfalls anstiegen. Experimentelle Validierungen wurden bei optimierten, QM-spezifischen Temperaturen durchgeführt: 40 °C (Ethanol), 80 °C (Glykol und Isopar-V) und 95 °C (Wasser). Ethanol erzielte die höchste ORC-Ausbeute, Glykol die höchsten Anteile an Säuren, Ketonen und phenolischen Verbindungen, Isopar-V blieb weitgehend immiscible, während das Wasserquench nahezu alle wasserlöslichen Verbindungen, insbesondere Zucker, zurückhielt.

Der letzte Teil der Arbeit untersuchte eine neuartige Methode zur Rückgewinnung von Levoglucosan (LG) aus Pyrolyseöl, einem Anhydro-Zucker, im Vergleich zur bekannten Flüssig-Flüssig-(Lösungsmittel-)Extraktion. Das Verfahren nutzte das Quenchen heißer Pyrolysegase mit Wasser in einer einstufigen Kondensation, wodurch ORC und Wasserquench gemeinsam zurückgewonnen wurden. Die Untersuchungen zeigten eine vollständige Rückgewinnung von LG und anderen Anhydrozuckern. Im Vergleich zur Lösungsmittel-Extraktion aus bereits kondensiertem ORC erwies sich die Methode als effizienter, da geringere Lösungsmittel-zu-

Feed-Verhältnisse benötigt und zusätzliche Extraktionsschritte vermieden wurden. Der Einsatz von AC als Lösungsmittel für LG war zudem effizienter als Frischwasser, steigerte das Valorisierungspotenzial und senkt die Betriebskosten.

Die thermodynamische Modellierung unter Verwendung des UNIFAC-DMD-Modells lieferte wertvolle Hinweise zur Vorhersage des nichtidealen Dampf-Flüssig- und teilweise auch Flüssig-Flüssig-Gleichgewichts von Pyrolysedämpfen und Bioölen. Abweichungen traten wie erwartet vor allem bei funktionellen Gruppen auf, bedingt durch (i) die unzureichende Abbildung stark verdünnter Organika in Wasser, (ii) die eingeschränkte Darstellung von Assoziations- und Wasserstoffbrückenbindungen sowie (iii) Unsicherheiten in den Dampfdruckdaten reiner Komponenten. Diese Ergebnisse deuten darauf hin, dass fortschrittlichere Modelle wie die Group Contribution with Association Equation of State (GCA-EoS) für verbesserte Vorhersagen berücksichtigt werden sollten. Zudem erreichen experimentelle Pyrolyse-Kondensationssysteme selten Gleichgewichtszustände, wodurch die Anwendung von Validierungsmethoden wie der Advanced Distillation Curve (ADC) empfohlen wird.

Abschließend zeigt sich, dass trotz bestimmter Einschränkungen der Modellvorhersagen die Kombination aus experimentellen und modellbasierten Ansätzen umfassende Einblicke in die Quench-Kondensation von Pyrolysedämpfen ermöglicht und die Rückgewinnung hochwertiger Chemikalien aus FPBO unterstützte. Die Ergebnisse unterstreichen die Bedeutung detaillierter Parameterstudien und schaffen eine solide Grundlage für die Auslegung und den Betrieb nachhaltiger Biomasse-Schnellpyrolyse-Bioraffinerien mit direkten Auswirkungen auf die Produktion von Biokraftstoffen und Biochemikalien.

Acknowledgements

I would like to express my sincere gratitude to my academic supervisor, **Prof. Dr. Nicolaus Dahmen**, for his invaluable guidance throughout my study. I am also deeply indebted to **Dr.-Ing. Axel Funke**, my supervisor and team leader, for his academic and moral support, critical reviews of the study, and immense contributions. Most importantly, I am grateful to both advisors for believing in me and providing me with the opportunity.

Subsequently, I would like to express my heartfelt gratitude to **my family, especially my parents and siblings**, for their love and moral support throughout my studies.

Special thanks go to all the analytical team at the Institute of Catalysis Research and Technology (IKFT), especially **Ms. Birgit Rolli, Ms. Frank Melany, Ms. Jessica Heinrich, Ms. Petra Janke, Ms. Pia Griesheimer, Mr. Armin Lautenbach,** and **Ms. Veronika Holderied for** their enormous support.

A very special thanks to **Mr. Daniel Richter, the bioliq® team (Nicole Weih, Cornelius Pfitzer, and Andreas Niebel), and the bioliq® technicians** for their dedicated support with running experiments on the fast pyrolysis pilot unit (PYTHON), as well as their technical guidance on the operation of the bioliq®. Many thanks also go to **Mr. Norbert Sickinger** for his support with setup designs and installations. I am also very grateful to the staff at the mechanical workshop of the institute.

I would also like to thank **Mr. Roland Fritz** for his assistance with software and IT-related issues. I am additionally grateful to the IKFT institute head, secretaries, and administrators for their administrative support.

To all my past and present colleagues at IKFT (**Dr. Yannik Stark, Dr. Frederico Fonseca, Dr. Anke Krutof, Eugen Aschenbrenner, Ewelina Brunet, Dr. Joscha Zimmerman, Ana Araujo, Amir Jalalinejad, Kelechi John, Ankur Chowdhury, Dr. Bruno & Mariana Campos, Mahsa Ebrahim-Moghaddam, Naiara Telis, Dr. Myriam Rojas Salas, Max Wörner, and Henri Steinweg**), as well as other friends, colleagues at KIT, and loved ones, I would like to sincerely thank you for your consistent support and encouragement. It has been a pleasure to meet and work with you all!

I would also like to express my gratitude to all students who worked on the project and completed their end-of-study theses under my supervision.

A special thanks to the **German Federal Ministry of Education and Research (BMBF)** for their financial support.

Finally, I would also like to thank the **Karlsruhe House of Young Scientists (KHYS)** for their numerous funding opportunities and training programs, which have played a vital role in this journey.

Table of Contents

List of Figures

List of Tables

Nomenclature

Abbreviations

AAEMs – Alkali and alkaline earth metals

AARD – Average absolute relative deviation

AC – Aqueous condensate

ARD – Absolute relative deviation

FPBO – Fast pyrolysis bio-oil

GCA-EoS – Group Contribution with Association Equation of State

LG – Levoglucosan

LLE – Liquid–liquid equilibrium

NCG – Non-condensable gases

NRTL – Non-Random Two Liquid

ORC – Organic-rich condensate

PDU – Process Development Unit

QM – Quench media

RMSE – Root Mean Square Error

STOR – Solvent-to-oil-ratio

UNIFAC-DMD – Modified UNIFAC Dortmund

VLE – Vapor liquid equilibrium

Symbols

(m_q/m_v) – Mass flow rate ratio of the quench to the hot pyrolysis volatiles

Chapter 1

Introduction

1.1 Contextual Background

The projected depletion and rising carbon footprint associated with the use of fossil resources, coupled with growing energy demands have necessitated the production of fuels and chemicals from renewable sources such as biomass [1,2]. Various thermal and biochemical processes have been developed to valorize biomass residues as carbon-neutral feedstock [1,3,4]. Fast pyrolysis to convert lignocellulosic biomass into bio-based energy and chemicals has gained significant attention, due to its advantages of processing many types of biomass feedstock into energy-dense liquid and solid intermediates for further energetic or chemical use [3,5–8]. Fast pyrolysis decomposes lignocellulosic biomass at temperatures of around 500 °C in an inert environment to produce char (containing inorganics), fast pyrolysis bio-oil (FPBO) and non-condensable gases (NCGs), each of which can be used for fuel and chemical applications [1,4,9–15]. Following fast pyrolysis, up to 75 wt.% of initial dry biomass can be converted into FPBO [4,14]. Temperature, residence time of pyrolysis volatiles and the design of the condensation process are key factors that determine the final composition of FPBOs. Effects of these factors have been largely investigated experimentally [10,12,16–20]. However, in the quest to save time and effort required in thoroughly investigating the effects of these parameters in real setups, phase equilibria modeling of fast pyrolysis condensation processes has gained attention. Phase equilibria modeling has also demonstrated to be prospective towards further understanding unexplained experimental phenomena during the condensation of pyrolysis volatiles. In broadening this concept, phase equilibria modeling was extensively applied in this work to three different case studies on fine-tuning the composition of FPBOs during condensation. These include, (i) The optimization of the aqueous pyrolysis condensate fraction of the FPBO for its application for downstream microbial conversion, (ii) Evaluating the influence of selected quench media on the yield and quality of FPBOs and (iii) Assessing the efficiency of applying a novel recovery method of levoglucosan (LG) from fast pyrolysis volatiles during quenching (direct-contact condensation) as compared to the widely

known liquid–liquid (solvent) extraction technique. The rationale for these three studies has been elucidated in the subsequent section.

1.2 Motivation

FPBO is a complex mixture of numerous compounds, including organic acids, ketones, aldehydes, alcohols, furans, phenols, anhydrosugars, other oxygenates, and water [4,10,21–24]. Due to its complex nature, FPBO is often separated into various fractions to tailor its quality for specific applications [18]. For instance, FPBO intended for fuel applications should contain more organics and less water. Additionally, FPBO may spontaneously phase-separate when the water content is high, forming an organic-rich phase and an aqueous phase [25]. Fractional condensation of pyrolysis volatiles has been strongly considered over other separation techniques for separating FPBOs into useful fractions [2,10,26], owing to its cost-effectiveness. It allows for the separation of FPBOs into different fractions, particularly into the organic-rich (ORC) and aqueous condensate (AC) fractions [22,23,27]. The ORC, largely due to its heavy molecular weight constituents, has a high energy content, making it more suitable for fuel applications [24,28]. The AC, on the other hand, is composed primarily of up to 85 wt.% water and contains low molecular weight compounds such as carboxylic acids and acetol [12,24,28]. As a result, it is corrosive and low in energy content, which limits its direct application as fuel. Although the production of AC is avoided in industrial-scale setups by simply combusting this product fraction together with the NCGs, alternative value-added utilizations of this product have still been strongly considered. A more recent application is its use as a carbon source for microbial cultivation and as a substrate for anaerobic digestion. [24,28–32]. This is feasible due to the conspicuous presence of compounds such as carboxylic acids in this product, which have been reported to enhance microbial growth [28,29,33]. Nonetheless, the simultaneous presence of growth inhibitors makes this application quite challenging [34]. Several techniques have been developed to mitigate this, but most are more intricate and costly compared to fractional condensation. Since the use of fractional condensation to fine-tune the composition of the AC for application as a substrate in downstream microbial conversion is still a subject of ongoing investigations, it warrants further detailed study.

Subsequently, for the efficient cooling of pyrolysis volatiles to recover FPBO, the mode of condensation is crucial. Both direct-contact (spray/quench columns) and indirect-contact

(shell-and-tube) condensation systems have been widely exploited [4]. As a result of their competitive advantages, including improved economic and thermal performance, direct-contact heat exchangers have been predominantly used in industrial scale-systems. Nevertheless, the choice of quench media (QM) is critical as it significantly impacts the yield, stability, and composition of recovered FPBO. Different types of QM have been employed for various pyrolysis processes, ranging from the use of paraffinic and naphthenic hydrocarbon oils (usually immiscible with the recovered ORC fraction of FPBO) such as Isopar-V, to highly volatile QM like ethanol and liquid nitrogen, which vaporize almost entirely upon contact with hot pyrolysis volatiles. There is also a common practice in most state-of-the-art large and industrial-scale and industrial-scale systems where the produced ORC is reused as the quench. Since such processes require an initial start-up quench material, most industrial-scale processes use previously produced and stored ORC, whereas others (primarily R&D units) employ different starting materials such as ethylene glycol (glycol), due to the nature of their operations. Nonetheless, in most of these cases, the choice of QM is primarily based on practical and process optimization considerations. However, the complexities surrounding the impacts of these commonly used QM on the characteristics of FPBOs are not fully understood and remain a subject of ongoing investigation.

Consequently, anhydrosugars, particularly, levoglucosan (LG) obtained from FPBOs have been reported to be important precursors for the production of monomeric sugars such as glucose, which can, in turn be further processed into bioethanol [35,36]. Additionally, when isolated from other heavy, water-insoluble lignin-derived components, these sugars can serve as a substrate for microbial conversion [22,32]. Given that LG is highly soluble in water, solvent extraction using water has been widely employed for its recovery from FPBOs [37–40]. Although the method is well-established, it typically requires additional downstream liquid–liquid extraction steps (following the recovery of the ORC) for implementation. In the quest to optimize the integrated pyrolysis biorefinery concept, opportunities for further process development to enhance LG extraction have emerged. Commonly explored routes include feedstock pretreatment, and more recently, modification of the condensation process to limit secondary cracking of LG during the condensation of hot pyrolysis volatiles. This involves directly spraying hot pyrolysis volatiles with water so that condensed ORC and water are recovered together in a single stage, thereby enabling one-step condensation. While the former (feedstock pretreatment) has been extensively investigated in the literature, the latter

has received little attention. A study on the efficiency of LG capture using this technique, and how it compares with the conventional solvent extraction method, is both compelling and highlights a gap that warrants further investigation.

1.3 Study Aims and Objectives

1.3.1 Aim

This study aims to employ thermodynamic phase equilibria modeling to predict the behavior of fast pyrolysis volatiles and to help explain certain phenomena observed during the condensation of hot pyrolysis volatiles into fast pyrolysis bio-oils (FPBOs). The modeling will be applied to the three previously discussed case studies focused on fine-tuning the yield, stability, and composition of FPBOs during condensation. These cases are aligned with the study objectives outlined below.

1.3.2 Objectives

1. Using fractional condensation to optimize the aqueous pyrolysis condensate for downstream microbial conversion.
2. Investigating the influence of selected quench media (including ethylene glycol, ethanol, water and Isopar-V) used in direct-contact condensation on the yield and composition of fast pyrolysis bio-oils.
3. Evaluating the efficiency of water extraction of levoglucosan from fast-pyrolysis bio-oils in a single-step direct-contact condensation process and comparing it with conventional solvent extraction.

1.4 Thesis outline

The thesis is organized into 5 chapters. **Chapter 2** provides a literature overview covering the general concept of fast pyrolysis, fractionation processes of fast pyrolysis bio-oils, including fractional condensation, background of all the study objectives, and an overview of the phase equilibria modeling of fast pyrolysis condensation processes. **Chapter 3** details all materials, as well as the experimental and theoretical approaches employed. **Chapter 4** presents and discusses all results. Finally, **Chapter 5** outlines the conclusions drawn from the study and provides recommendations for future research.

Chapter 2

Literature Review

2.1 Fast Pyrolysis Bio-Oils: Production and Fractionation

2.1.1 Fast Pyrolysis

For the efficient industrial utilization of energy derived from biomass feedstock, the biomass must be transformed into high heating value products that are easy to handle, store, and transport. Through fast pyrolysis, solid biomass is primarily converted into fast pyrolysis bio-oil (FPBO), along with solid char and non-condensable gases. Currently, commercial fast pyrolysis processes rely exclusively on woody biomass as feedstock. To achieve a sustainable pyrolysis biorefinery concept in the future, a wider variety of lignocellulosic biomass (such as herbaceous and agricultural biomass residues) needs to be utilized to significantly increase the available biomass potential. Therefore, there is a need to adapt pyrolysis processes to these biomass feedstocks and to tailor them toward specific product specifications based on the intended application. This will require a better understanding of the key pyrolysis process steps, including the condensation and fractionation of hot pyrolysis volatiles into FPBOs.

Pyrolysis is a thermochemical conversion process in which dry organic materials (such as coal, refinery residues, wastes, or biomass) are thermally decomposed in an inert environment into a solid residue and volatiles, which are subsequently recovered as liquid and non-condensable gas under ambient conditions [9,41]. Fast pyrolysis has gained significant attention due to its ability to process various types of biomass feedstocks into energy-dense liquid and solid intermediates for further energetic or chemical use [3,5–8]. It is characterized by the rapid heating (at temperatures around 500 °C) of finely shredded feedstock, quick removal of char, short residence time of volatiles (up to 2 seconds), and immediate termination of further chemical reactions by quench-cooling the generated volatiles [41–43]. This consequently facilitates the optimum recovery of the liquid product, most commonly referred to as FPBO. Yields of up to 75 wt.% of FPBO can be achieved from the fast pyrolysis of biomass [43–45].

FPBO holds promise as a versatile precursor for the production of second-generation biofuels as well as platform chemicals [42].Depending on the type and nature of biomass feedstock, FPBO may contain significant amounts of water [12,41]. This can spontaneously cause phase separation, leading to the formation of an organic-rich phase and an aqueous phase [12,17,44]. Aging (defined as changes in the chemical composition of FPBO after recovery, mostly occurring during storage) also contributes to phase separation [44]. Additionally, FPBO is a complex product comprising numerous compounds, including organic acids, ketones, aldehydes, alcohols, furans, phenols, anhydrosugars, and other oxygenates [4,8,10,12,21,26,39,40,46], with a wide range of boiling points. This complexity has, in turn, prompted the fractionation of FPBOs to tailor their quality for specific applications [28].

2.1.2 Fractionation Techniques for Fast Pyrolysis Bio-Oils

Several fractionation methods for FPBOs exist. These include, but are not limited to, distillation (atmospheric, vacuum, and molecular), liquid–liquid/solvent extraction (e.g., water and organic solvent extraction), column chromatography, membrane separation, and fractional condensation [47]. Distillation, solvent extraction, and fractional condensation are discussed in this study, as they are the most commonly applied methods for upgrading FPBOs.

2.1.2.1 Distillation

Distillation involves the separation of components of a mixture based on differences in their boiling points and volatilities. The most common types include atmospheric, vacuum, and molecular distillation [47].

Atmospheric distillation typically occurs within a temperature range of 80 to 250 °C and is particularly suitable for extracting acids, alcohols, and aldehydes from FPBOs [47,48]. At temperatures above 250 °C, secondary reactions can lead to polymerization, resulting in coke formation [47,49,50]. Consequently, the recovery of higher molecular weight compounds with boiling points above 250 °C (such as lignin-derived phenolics) is not favored using this technique. Atmospheric distillation is generally limited in its capacity to fractionate FPBOs, as typically only about 50 wt.% of the FPBO can be distilled before the remaining material polymerizes into coke [50].

Vacuum distillation occurs under reduced pressure, which facilitates distillation at much lower temperatures compared to atmospheric distillation. As a result, polymerization reactions are

slowed, allowing for the fractionation of a broader spectrum of chemicals present in FPBOs [47,49].

Molecular distillation is a short-path distillation technique (involving the distillate travelling a very short distance), where thermally unstable compounds with closely spaced boiling points are separated under high vacuum conditions [47]. The process is characterized by extremely low pressures (around 0.0133 Pa) and short exposure times of the liquid distillate to high temperatures [51]. It is particularly suitable for separating thermally unstable materials, such as vitamins, as losses due to thermal decomposition are minimized [47,51]. Molecular distillation has also been widely employed for upgrading FPBOs [52,53].

2.1.2.2 Liquid–Liquid (Solvent) Extraction

Solvent extraction is one of the promising techniques also applied to separate FPBOs into various fractions [40,47]. It involves the transfer of a compound from one liquid to another due to differences in solubility or distribution coefficients between two immiscible liquids [54]. Compared to other separation techniques such as distillation and column chromatography, it is cost-effective as it requires low energy consumption, offers higher production capacity, and is much easier to implement in a continuous and large-scale operations [18,40,54]. Nonetheless, it is important to note that some solvents used in solvent extraction may be costly, and in such instances, processing costs may increase. Solvent extraction of FPBOs has mostly been conducted using water [36,55,56], as well as other organic solvents such as chloroform, hexane, ethyl acetate, and petroleum ether [39,40,54]. The addition of excess water to FPBO triggers phase separation into an aqueous phase and an organic-rich condensate fraction. Owing to its high organic content and calorific value, the organic-rich condensate has been extensively studied for applications as fuel, flavorings, resins, fertilizers, and emission control agents [47]. The aqueous fraction mostly contains highly polar compounds including acids, ketones, esters and sugars. Due to the presence of sugars in this fraction, it serves as a good precursor for bioethanol production [56,57]. An extensive overview of the water extraction of the anhydrosugar, levoglucosan (LG) from FPBOs is provided in Section 2.2.2.

Other known solvent extraction techniques include reactive liquid–liquid extraction (LLE), switchable hydrophilicity solvent extraction, supercritical fluid extraction, and ionic liquid extraction. These processes have been described in detail elsewhere [47].

2.1.2.3 Fractional Condensation

The fractionation of FPBOs is crucial for achieving a viable pyrolysis biorefinery. Fractional condensation is a key and efficient technology used to separate FPBOs into distinct fractions, as it enables the recovery of pyrolytic condensates based on differences in boiling point. During fractional condensation, pyrolysis volatiles pass through a series of condensation stages at progressively lower temperatures, allowing FPBO fractions of different physical and chemical properties to be collected separately [1,2,18,58,59]. Electrostatic precipitators are often integrated into the condensation system to capture aerosols [15,18,60]. The applications of the recovered FPBOs depend on their individual characteristics and may help reduce additional costs associated with further downstream upgrading or fractionation, thereby improving the overall economics of the fast pyrolysis process [2,18]. Several studies involving the fractional condensation of fast pyrolysis volatiles

to enhance product quality have been reported in the literature. Tumbalam Gooty et al. [1] used fractional condensation to separate water from the organic-rich phases in FPBOs during the pyrolysis of birch bark. Similarly, Ma et al. [2] employed fractional condensation to separate heavy phenolic-rich organics from water and acids following the pyrolysis of rice husk. Rover et al. [18] conducted similar investigations during the pyrolysis of red oak and reported maximum recovery of anhydrosugars in the organic-rich fraction. Other comparable studies were conducted by Pollard et al. [12], Johansson et al. [26], Sui et al. [6], Schulzke et al. [7], Siriwardhana [17], Chai et al. [13], Chen et al. [60], Papari et al. [10], and Yi et al. [16]. Most of these studies also demonstrated that the aging of the recovered FPBOs was minimized, as the oil components typically responsible for aging reactions were effectively separated [16,17]. Compared to other fractionation techniques (such as molecular distillation, centrifugation, and liquid chromatography), fractional condensation is more economical, less energy-intensive, and easier to implement on a larger scale [1,10,18].

Specific applications of condensation and fractional condensation for fine-tuning the quality of FPBOs during condensation of pyrolysis volatiles are discussed in the following sections.

2.2 Optimization Potential of Condensation and Fractional Condensation Processes for FPBOs

The following sections provide an overview of all three study objectives, highlighting the progress made, the gaps identified, and the justification for each respective study.

2.2.1 Overview of Fractional Condensation of FPBOs with Emphasis on Tailoring the Aqueous Condensate for Downstream Microbial Conversion

The complex chemical composition of FPBOs has led to several challenges, including poor stability during storage and instability during heating prior to upgrading. Fractional condensation, identified as an efficient and cost-effective fractionation technique, typically separates FPBOs into ORC and AC [30]. The ORC is viscous and contains lignin-rich, high-molecular-weight compounds such as phenolic oligomers and sugars. Owing to its concentrated organic content, it exhibits a promising higher heating value (HHV), averaging around 17 MJ/kg (approximately 40% of the calorific value of diesel) [1,58,61]. This makes the ORC a strong candidate for fuel applications [1,30,58].

In contrast, the AC primarily comprises water, along with other organics such as carboxylic acids, methanol, acetol, and aldehydes [19,24,62]. Depending on the pyrolysis and condensation conditions, traces of furanics and phenolic compounds may also be detected in the AC [19,24]. The AC is corrosive and has a comparatively low HHV due to its high acidity and water content. Consequently, its application as a fuel is limited [28,30]. As a result, condensation of the AC is avoided in industrial fast pyrolysis units. Instead, the generated water vapors are combusted alongside the non-condensable gases and char to supplement the pyrolysis process heat. In most cases, the AC is regarded as a by-product of the FPBO; hence, its valorization requires attention, as it is crucial to achieving a successful pyrolysis-based biorefinery [28].

Presently, a number of alternatives are being developed to utilize the AC. For instance, as gasifier feed following mixing with char [63,64]. The utilization of AC as a carbon source for microbial cultivation and as a substrate for anaerobic digestion (to produce biomethane) has also been demonstrated [22,24,28,30,31,33,65]. This potential is attributed to the high

concentrations of acids (e.g., acetic acid, propionic acid, and formic acid) in the AC, which have been reported to facilitate microbial growth [22,24,28,66].

Nonetheless, a major challenge commonly encountered when employing AC as a substrate is the presence of potential growth-inhibitory compounds such as furans, ketones, and some phenol derivatives [30,66–68]. Several techniques have been investigated to mitigate this issue, including liquid–liquid extraction [14], adsorption using pyrolysis char as activated carbon [30,65], rotary evaporation [24,33], and overliming [28,33,69–71]. While these methods show promise, most are implemented as separate downstream processes in addition to the fast pyrolysis step, which is not ideal for realizing an integrated and efficient pyrolysis-based biorefinery [31].

The use of an optimized fractional condensation system for the removal of inhibitory compounds from AC could potentially enable the development of a novel growth medium for microbial cultivation. In their study, Liaw et al. [31] adjusted the temperature conditions of only the first-stage condenser in a fractional condensation setup to investigate the composition of the recovered phases, with a focus on producing AC suitable for use as a substrate in biomethane production via anaerobic digestion. Although they observed a reduction in some inhibitory compounds, such as phenolics, with temperature adjustments in the first condensation stage, they were unable to fully verify the distribution of other known substrates and inhibitors in the AC and thus recommended further technical studies to clarify their observations.

Simultaneous temperature adjustments of all condensation stages, together with proper identification and classification of substrates and inhibitory compounds, will be crucial in assessing the practicability of this technique.

2.2.2 An Overview of Levoglucosan Extraction Techniques from FPBOs

Sugars are among the vital platform chemicals generated during the conversion of biomass to biofuels and can readily be converted into several compounds [72]. The conversion pathways of biomass into sugars that serve as substrates for fermentation remain key determinants of their applicability. One of the most commonly exploited pathways for extracting sugars from biomass is enzymatic or acid hydrolysis [72,73]. Through the catalytic action of enzymes or

acids, cellulose and hemicellulose are broken down into glucose and xylose. Although the enzymatic conversion pathway has proven promising, it is limited in terms of economic feasibility and commercial scale-up due to the high cost of enzymes, comparatively low product concentrations, and slow hydrolysis rates [72,73]. Additionally, challenges associated with acid use, particularly the regeneration of spent acids, discourage the application of acid hydrolysis at the industrial scale [72].

Thermochemical conversion methods such as fast pyrolysis have been identified as alternative pathways to overcome these challenges [72,74]. FPBOs have been reported to contain considerable amounts of anhydrosugars [72,75]. Levoglucosan (1,6-anhydro-β-D-glucopyranose) is the major anhydrosugar component present in FPBOs [36]. It is predominantly formed from the depolymerization of cellulose during fast pyrolysis, and levoglucosan (LG) yields of up to 70 wt.% can be obtained when microcrystalline cellulose is pyrolyzed [72].

Interest in the production of LG is based on the fact that it serves as a major precursor for the production of monomeric sugars such as glucose, which can further be utilized for the production of biofuels such as ethanol and butanol [35,36]. It also has significant potential in commercial applications for the synthesis of polymers, solvents, non-ionic surfactants, and pharmaceuticals [57,76]. Ultimately, these applications of LG promise to enhance the overall valorization of carbon present in biomass, thereby making biomass conversion more economically viable [14].

Given the tendency of FPBOs to phase-separate into an organic-rich and an aqueous fraction, Vitasari et al. [55] suggested that water extraction is the first important step toward the recovery of valuable chemicals from FPBOs, particularly for isolating polar water-soluble compounds into the aqueous phase [77]. As LG is highly soluble in water, its isolation from FPBOs via water extraction has proven successful. The optimal recovery of LG from FPBOs has received significant attention and has been widely investigated, leading to extensive process developments [38]. Numerous factors have been found to influence the optimal extraction of LG from biomass feedstocks. The most common include the type and nature of the biomass feedstock, its pretreatment, the pyrolysis process conditions and system modifications, and other downstream separation technologies such as solvent or liquid–liquid extraction.

2.2.2.1 Type and Nature of Biomass

2.2.2.1.1 Influence of Biomass Composition

Lignocellulosic biomass primarily comprises cellulose (40-60%), hemicellulose (15-30%) and lignin (15-30%), with traces of extractives and inorganic ash [3]. Cellulose is the most stable of the three major constituents [72]. Hemicellulose is the most reactive and degrades at the lowest temperatures, while lignin is known to devolatilize over a broad temperature range, overlapping those of cellulose and hemicellulose [78]. Lignocellulosic materials with high cellulose content are capable of yielding higher amounts of LG [72,73].

Although some studies [79,80] concluded that hardly any interactions occur among these components during their thermal degradation, others have provided evidence of such interactions [81]. This has led to divergent conclusions, particularly regarding how these interactions affect LG production. For instance, Zhang et al. [82] established from their study that no significant interactions were observed between cellulose and hemicellulose, whereas an obvious interaction was found in a herbaceous native cellulose-lignin mixture, which was responsible for the diminished LG yields. Interestingly, they also reported that no such interactions occurred in woody biomass. Stronger interactions between cellulose and lignin, compared to cellulose and hemicellulose, have also been reported [83,84].

Interactions of lignin or hemicellulose with cellulose broaden the thermal degradation temperature range of LG [85]. The presence of lignin restrains the thermal polymerization of LG and fosters the production of undesirable low molecular weight compounds from cellulose [84]. Ye et al. [86] found that the presence of a lignin model dimer suppressed LG formation from glucose. Shoji et al. [87] also postulated that the existence of aromatics could stabilize LG through solvation, protecting it from thermal degradation and thereby improving its selectivity. Interactions between cellulose and hemicellulose can effectively boost the production of hemicellulose-derived compounds (including acetic acid, furfural, and hydroxyacetaldehyde), while suppressing certain cellulose-derived compounds such as LG [83,85,88].

2.2.2.1.2 Influence of Mineral Compounds

Presence of minerals in lignocellulosic biomass strongly impacts the pyrolysis of cellulose [89]. The yield of LG is sensitive to the content and purity of cellulose present in the lignocellulosic

biomass feedstock, and the presence of even trace levels of impurities, particularly inorganic compounds, can significantly reduce the recovery of LG during thermal degradation [72,81]. Most studies have focused on the effects of alkali and alkaline earth metals (AAEMs) due to their strong catalytic influence on altering the decomposition rate and chemical pathways during cellulose degradation [72]. The presence of AAEMs has been reported to inhibit the primary polymerization pathway responsible for LG formation and instead promote secondary cracking reactions [38,81,90–92]. The mineral content in woody biomass is generally around 1 wt.%, while in herbaceous biomass (such as leaves, grasses and straw-based materials), it may exceed 10 wt.% [93]. This difference has been linked to higher LG recovery from FPBOs derived from woody biomass compared to those from herbaceous feedstocks [38].

2.2.2.2 Pretreatment of the Biomass Feedstock

Pretreatment of biomass feedstock helps condition the material by removing inhibitory compounds (such as minerals) or neutralizing (passivating) their effects, thereby promoting the recovery of LG during thermal degradation. Two main pretreatment strategies have been widely employed: demineralization via washing with water or mild acid [35,94], and the passivation of the catalytic influence of AAEMs through acid impregnation to form inert salts [95].

The water/hot-water pretreatment method is a green hydrothermal process in which lignocellulosic biomass is cooked in water without any chemical additives. At such elevated temperatures and pressures, the ionic concentration of water becomes significant, and the H^+ and OH^- ions act as acid and base, respectively [72]. This enables water to penetrate the plant cell structure, releasing hemicellulose and lignin and hydrating cellulose [72]. Water washing also significantly reduces the ash content of biomass, which further enhances selective conversion [96]. Compared to unwashed biomass feedstock, water-washed biomass has demonstrated notable improvements in thermal behavior and a reduction in undesirable inorganic compounds [96,97].

Regarding acid washing, numerous studies have been reported in the literature. Interestingly, most observed that significantly high yields of LG can be recovered even with minimal acid use [37]. Commonly used acids include H_2SO_4, HCl, HNO_3, H_3PO_4, and acetic acid, with H_2SO_4 being the most widely used [72].

Acid impregnation involves the application of a small amount of acid to the lignocellulosic biomass without subsequent washing. This converts the cations of AAEMs into thermally stable salts, thereby improving LG selectivity [72]. These salts not only reduce the catalytic activity of AAEMs but also provide a buffering effect [95]. The combined effects of passivation and buffering promote reaction pathways that favor LG production. Pecha et al. [93] concluded that a single pretreatment method does not yield optimal LG extraction and suggested that a combination of acid washing and acid impregnation may provide better results. Additional benefits from combined pretreatment methods were also observed by David et al. [98] and Zhou et al. [99]. Li et al. [35], however, coupled acid pretreatment with modifications to the pyrolysis condensation process to optimize LG recovery. Nonetheless, it is worth noting that while combined pretreatment methods can enhance LG recovery, they may also increase pretreatment costs.

Other reported pretreatment methods include alkaline infusion, bio-pretreatment (using microorganisms to alter the structure or chemical composition of biomass to facilitate sugar liberation), and microwave pretreatment in glycerol. More extensive discussions of these processes were carried out in the reviews by Jiang et al. [72] and Hakeem et al. [38]. Jiang et al. concluded that a successful pretreatment method should: (1) enhance LG formation during pyrolysis; (2) minimize inhibitory compounds in the pyrolysate; (3) avoid expensive pretreatment setups and high energy demands; (4) limit the need for waste disposal; and most importantly, (5) be environmentally friendly and economical.

2.2.2.3 Pyrolysis Process Conditions and Setup Modifications

2.2.2.3.1 Temperature and Vapor Residence Time

Pyrolysis temperatures at which the optimum yield of LG is obtained largely depend on the type of biomass [100]. According to the literature, optimum yield of LG is most commonly reported within a pyrolysis temperature range of 400 to 500 °C [38]. Further increases in temperature beyond this range lead to a significant decrease in LG recovery due to cracking into lower oligomers and levoglucosenone (a heterocyclic ketone) [38]. The residence time of pyrolysis volatiles in the hot zone of the reactor has also been reported to have significant effects on LG yield. Wang et al. [37] reported approximately a 20% decrease in yield of LG when vapor residence time increased from 1.4 to 6.8 seconds. These observations suggest

that moderate pyrolysis temperatures, coupled with very short vapor residence times are, most suitable for optimum LG production.

2.2.2.3.2 Pyrolysis Setups and Process Modifications

The mode and design of the pyrolysis reactor also significantly affect the yield of LG production. Higher yields of LG have been reported in micro-scale pyrolysis setups compared to bench- and pilot-scale setups. This was attributed to the increased occurrence of secondary cracking reactions in higher-throughput reactor setups [38]. Increased LG production has also been observed in vacuum pyrolysis systems [38], as well as in continuous-feeding pyrolysis systems with rapid quenching of pyrolysis volatiles [38].

As previously highlighted, Li et al. [35] introduced a water spray injection system just before the condensation train to rapidly cool hot pyrolysis volatiles. Consequently, the spray lowered the temperature of the volatiles from 400 °C to below 300 °C. However, a critical evaluation of their results revealed that this spray system had no significant effect on LG yield. The increased yield of LG reported in their study was primarily influenced by the acid pretreatment of the biomass feedstock.

Nonetheless, it is also important to note that the spray system only cooled the pyrolysis volatiles to just below 300 °C, a temperature still high enough for cracking reactions to occur. While the spray quenching system appears promising, it is essential that the volatiles are cooled more intensively to minimize or eliminate secondary cracking. Furthermore, the fact that Li et al. also employed fractional condensation of the volatiles after the spray quenching could have resulted in the dispersion of LG across multiple oil fractions. Their analysis of the combined oil fractions may not accurately reflect the actual amount of LG captured.

Additionally, since LG is highly soluble in water, a single-stage condensation setup, where the recovered FPBO and spray water are collected together, may enhance LG recovery, as the LG would be instantaneously transferred into the aqueous phase. If efficiently implemented, this technique could eliminate the need for downstream solvent extraction processes, thereby reducing costs and supporting the development of a sustainable pyrolysis-based biorefinery.

2.2.2.4 Liquid–Liquid (Solvent) Extraction of Levoglucosan from FPBOs

Solvent extraction is one of the most widely explored methods for the recovery of LG from FPBOs, as the differences in polarities, solubilities, and densities of the diverse compounds

present in FPBO are advantageous for the process [37–40]. A number of solvents have been employed to extract various compounds from FPBOs, including water, ethyl acetate, *n*-butanol, hexane, linoleic acid, chloroform, dichloromethane, methanol, toluene, and petroleum ether [38–40,72]. Among these solvents, water is readily available, environmentally friendly, and cost-effective [55,72]. Phase separation may occur when a certain threshold amount of water is added to FPBO [101], typically in the range of about 30 to 45 wt.% [55]. Following phase separation, the aqueous phase, which generally remains on top, is predominantly composed of polar carbohydrate-derived compounds, whereas the denser organic bottom phase is mostly enriched with less polar lignin-derived components [102]. LG is one of the major components that can be primarily extracted into the aqueous phase. A study by Vitasari et al. [55] demonstrated that, compared to other compounds that are also easily extracted into the aqueous phase (such as acetic acid, acetol, glycolaldehyde, etc.), LG has the highest distribution coefficient. This was attributed to hydrogen bonding interactions between LG and water.

The amount of water added to FPBO (water-to-oil ratio) is a key factor that determines the optimum recovery of LG. This has been investigated in numerous studies. Vitasari et al. [55] examined the effects of water-to-oil ratio and the stirring rate during LG extraction from forest residue- and pine-derived bio-oils. For water-to-oil ratios ranging from 0.3:1 to 0.8:1 (for forest-derived oil) and 0.4:1 to 0.9:1 (for pine-derived oil), the optimal ratios for maximum LG extraction were found to be 0.6–0.7:1 and 0.5:1, respectively. They also concluded that the stirring rate determines the time required to reach equilibrium but does not influence the equilibrium composition. Chan and Duff [71] investigated the water extraction of LG from bio-oil using a water-to-oil ratio ranging from 0.1:1 to 20:1. They reported that phase separation first occurred when 9.86 wt.% of water (approximately a 0.1:1 water-to-oil ratio) was added. The optimal LG recovery (4.98 wt.%) was achieved at 100 wt.% water addition (a 1:1 ratio). Bennett et al. [36] studied the effects of temperature, contact time, and water-to-oil ratio (within the range of 0.5:1 to 2:1) on LG extraction from Scots pine-derived bio-oil. They concluded that a water-to-oil ratio of 0.62:1, with a contact time of 22 minutes and a temperature of 34 °C, was sufficient for optimum extraction. Li et al. [77] also explored the impact of water-to-oil ratio (0.25:1 to 4.5:1) on LG extraction from FPBO derived from loblolly pinewood. They found that a water-to-oil ratio of 1.3:1 was optimal. They also confirmed that contact time and temperature had no significant effect on LG yield, and that the minimum

conditions tested (20 minutes and 25 °C) were sufficient for maximum recovery. Sukhbattar et al. [14], Wang et al. [103], Chi et al. [69], Lian et al. [104], and Rover et al. [73,76] all employed a 1:1 water-to-oil ratio to successfully isolate LG from the ORC fraction of FPBOs, which was further used as a substrate for ethanol fermentation.

The literature generally supports the conclusion that a 1:1 (w/w) water-to-oil ratio is sufficient for the optimal isolation of LG from FPBOs. Nevertheless, the optimum ratio also depends on the initial water content of the specific FPBO. It has also been established that temperature and contact time have minimal influence on the yield of LG, provided that a contact time of at least 20 minutes and ambient temperature are maintained.

Although water extraction is not a selective method for recovering LG, it has proven to be highly efficient. Up to 90 wt.% of LG has been successfully isolated using this technique. As part of this study, LG extraction from FPBOs via this process was compared to recovery in a single step during the condensation of hot pyrolysis volatiles.

2.2.3 Overview of the Effects of Selected Quench Media on the Yield and Composition of FPBOs in Direct-Contact Condensation

The yield and composition of FPBOs can be significantly enhanced by optimizing the downstream condensation systems of the volatiles generated from the hot zone of the reactor [4]. Condensation cools pyrolysis volatiles from temperatures around 500 °C to nearly room temperature, consequently yielding FPBOs. Various types of condensation setups have been employed for the capture of fast pyrolysis volatiles. Typically, the nature and quality of FPBOs to be recovered determine the type of condensation setup used. For instance, some studies have used a single-stage condensation setup, where all FPBOs are recovered in one stage. Several other studies [6,7,12,13,17,58,61] have employed fractional condensation setups, where FPBOs are recovered as different fractions at different stages. Based on the cooling mechanism, condensation of FPBOs can be implemented as either direct or indirect cooling.

Indirect-contact heat exchangers (shell-and-tube) have been widely used, mostly in laboratory bench-scale systems [105,106]. They are associated with comparatively low cooling rates and difficulties in removing highly viscous FPBOs, especially at lower temperatures [105]. They are also typically prone to pipeline and heat exchanger blockages, as well as fouling and corrosion, usually arising from the accumulation of lignin-derived components [20,43,107,108].

The use of direct-contact heat exchangers (quench/spray columns) for the condensation of FPBOs has been reported to overcome the above-mentioned limitations of indirect-contact heat exchangers and to facilitate greater contact area between the cooling fluid and pyrolysis volatiles [108,109]. This consequently enhances the rapid cooling of the pyrolysis volatiles, minimizing undesirable secondary cracking reactions that favor the production of non-condensable gases at the expense of FPBOs [20,43,102,107,110–112]. Due to their improved thermal performance, direct-contact heat exchangers typically require up to 60% less cooling fluid than their corresponding indirect counterparts [108]. These factors reduce overall process costs, making direct-contact heat exchangers more economically viable and the preferred choice for industrial applications [108–110].

Nevertheless, the use of direct-contact heat exchangers is associated with limitations, including interactions such as mixing, reactions, and mass transfer between the quench medium and the FPBO. These interactions can affect the yield, stability, and composition of the recovered FPBO. Consequently, potentially high costs of downstream separation and treatment methods are often required to obtain the desired FPBO [108,109]. To mitigate this, several studies have employed paraffinic and naphthenic hydrocarbon oils as QM, due to their immiscibility with the recovered organic-rich condensate (ORC) fraction of the FPBO. Westerhof et al. [113] used one such hydrocarbon, Shell Ondina 941 oil, as a QM to rapidly cool the hot pyrolysis volatiles generated from the fast pyrolysis of pine wood. In another study, the authors used a similar hydrocarbon liquid (Shell Ondina 917) with slightly different physicochemical properties [19]. Park et al. [20] also employed a hydrocarbon oil (primarily composed of paraffinic and naphthenic compounds) as a quench to condense the hot volatiles obtained from the fast pyrolysis of larch sawdust. Palla et al. [107] used octane at -5 °C as a direct-contact quench for the condensation of hot pyrolysis volatiles. The fast pyrolysis technology developed at CanmetENERGY-Ottawa, Canada, also utilized an isoparaffinic hydrocarbon mixture quench fluid (Isopar-V) to condense hot pyrolysis volatiles into FPBOs [114–116]. They cited low vapor pressure, thermal stability, and immiscibility with the ORC as the key reasons for its selection.

In contrast to the use of such high-boiling-point QM, other studies have employed highly volatile QM such as liquid nitrogen, ethanol, and acetone, which immediately flash into vapor upon contact with the hot pyrolysis volatiles and therefore do not mix with the recovered

ORC. For instance, Treedet et al. [106] used ethanol as a quench for recovering bio-oil generated from the fast pyrolysis of selected herbaceous and agricultural biomass feedstocks. Dalluge et al. [117] developed a novel quench system that employed liquid nitrogen to rapidly cool hot volatiles generated from the fast pyrolysis of cellulose. In the same study, water was used as a quench medium in a scaled-up version of the system, citing water as a more economic option, particularly for commercial applications. Elsewhere, the research group employed the same technique with liquid nitrogen as quench for sugar production from the pyrolysis of acid-infused lignocellulosic biomass [118]. The technology was also used in another study by Kim et al. [119], who investigated the recovery of resin acids from the fast pyrolysis of pine.

Furthermore, as a common practice for most state-of-the-art large and industrial-scale systems, the produced ORC fraction of the FPBO itself is utilized as a quench. In that case, an initial starting quench liquid is required; typically, in commercial units, this would be previously produced and stored ORC. There are also cases in R&D units where the produced ORC is recirculated as QM. However, due to the nature of their operation, a different startup QM is initially used. One example is the use of ethylene glycol (glycol) as the starting quench material, which is readily miscible with the produced FPBO [120–122]. The studies of Chang et al. [111] and Zheng Ji-lu et al. [123,124] also used acetone and ethanol as starting quench liquids, respectively, citing high volatility as the reason behind these choices.

In most of these cases, the choice of QM was based on pragmatic considerations (e.g., miscibility/immiscibility with FPBO) and/or process optimization considerations such as cost and boiling point. However, the complexities of how these commonly employed QM impact the characteristics of FPBOs have not yet been fully established and remain a subject of ongoing investigation.

Therefore, there is a need to test the hypothesis that the choice of QM affects phase equilibria and, consequently, the chemical composition of FPBOs. As part of this study, four commonly utilized QM, Isopar-V, water, glycol, and ethanol, were evaluated. Vapor–liquid equilibrium (VLE) modeling of all the direct-contact (quenching) condensation scenarios was applied to provide a theoretical basis for understanding the underlying effects, and specific condensation conditions were experimentally applied to validate the theoretical findings.

2.3 Phase Equilibria Modeling for the Prediction of Pyrolysis Condensation Processes

2.3.1 Overview

Factors such as condensation temperature, residence time of volatiles, and the design of the condensation setup play a critical role in determining the final composition of FPBOs. These factors have been extensively investigated experimentally and reported in numerous studies [10,12,16–20]. More recently, in an effort to save the time and resources required to investigate these parameters in real setups, theoretical phase equilibria modeling of FPBOs during fractional condensation has gained attention. To model such systems and predict their phase behavior, a detailed understanding of the phase equilibria of FPBOs is essential [5,15,125,126]. Westerhof et al. [19] demonstrated this by predicting the effects of condensation temperatures on the lightweight fractions of FPBOs. The authors also previously compared an equilibrium flash condensation model with experimental data when investigating water control in FPBOs [113]. Ille et al. [15] likewise applied thermodynamic phase equilibrium modeling to predict the behavior of unknown components detected in FPBOs.

Thermodynamic models include, but are not limited to, the following:

1. Cubic equations of state, such as the Redlich-Kwong and Peng-Robinson equations, which largely originate from the van der Waals equation of state [127].
2. Equilibrium models and associated liquid-phase activity coefficient models, including the Non-Random Two-Liquid (NRTL), the Universal Quasi-Chemical (UNIQUAC), the UNIQUAC Functional-Group Activity Coefficients (UNIFAC), and its more recent version, the UNIFAC Dortmund (UNIFAC-DMD) [128].
3. Models that consider hydrogen bonding, molecular association, and solvation, such as the Statistical Associating Fluid Theory (SAFT) [129–131] and the Group Contribution with Association Equation of State (GCA-EoS) [132].

Since pyrolysis volatiles and FPBOs are highly non-ideal and complex in nature, using advanced thermodynamic models that account for molecular association and other complex interactions is crucial for accurate modeling. Additionally, as most FPBO components lack model parameters in databases or literature, group-contribution models are favorable for

predicting their behavior. The modified UNIFAC Dortmund (UNIFAC-DMD) and the Group Contribution with Association Equation of State (GCA-EoS) are two prominent examples of such models.

2.3.2 UNIFAC-DMD

The UNIFAC (Universal Quasichemical Functional Group Activity Coefficients) group contribution method, first published by Fredenslund et al. [133,134], is used for estimating activity coefficients in liquid mixtures. It is the most popular group contribution method based on local compositions. In this method, molecules are built on the basis of functional groups, and the properties of binary or multicomponent solutions can be predicted directly from the binary parameters of each pair of groups. This makes it possible to predict a large number of mixtures from a relatively small number of binary parameters [135].

The calculation of activity coefficients by UNIFAC considers two main aspects: the combinatorial and the residual. The combinatorial aspect is temperature-independent and accounts for the size and shape of molecules (entropic contribution), whereas the residual aspect accounts for enthalpic interactions. The UNIFAC method has the advantage of describing the behavior of complex mixtures for which experimental data are rarely available and of representing the components of a solution as a sum of contribution groups. Nonetheless, it is characterized by two main limitations. These include the possible loss of information due to the simplification of a molecule into a sum of contribution groups, and the lack of a standardized method for dividing molecules into contribution groups, which may lead to different outcomes among users applying the same mixture [15].

The modified UNIFAC Dortmund (UNIFAC-DMD) is an extension of the original UNIFAC model [136]. It differs from the classical variant mainly in its temperature-dependent group interaction parameters [105]. Additionally, its empirically modified combinatorial part produces improved results for asymmetric systems. Furthermore, it allows for the modeling of compounds that include cyclic alkanes and formic acid. Unlike the classical variant, the following data can also be employed, in addition to VLE data, when fitting the temperature-dependent group interaction parameters: (1) activity coefficients at infinite dilution, (2) excess enthalpy data, (3) excess heat capacity, (4) LLE data, and (5) azeotropic data [128]. Since FPBOs

are multicomponent mixtures with most compounds present in minute concentrations, the reliable calculation of activity coefficients at infinite dilution is particularly relevant [105].

A large amount of experimental data has been collected in the Dortmund Data Bank (DDB) by the UNIFAC Consortium [137], much of which is publicly available. Due to its significance for process development, the applicability range of the UNIFAC-DMD is continuously being extended by addressing gaps in the UNIFAC-DMD parameter table [128]. Some existing parameters are also being revised.

The UNIFAC-DMD, as a predictive model, allows for easy comparison of various process alternatives, as well as the evaluation of suitable solvents for separation processes. It also enables the prediction of the influence of solvents on chemical equilibrium conversions [128]. Besides phase equilibrium prediction, the UNIFAC and UNIFAC-DMD models can also be used to calculate the flash points of liquid fuel mixtures [128]. This is particularly relevant for FPBOs when their quality is assessed for fuel applications.

Despite the many advantages associated with the UNIFAC-DMD model, it also has the following weaknesses: (1) its inability to predict the effects of isomers, (2) unreliable results from group contribution methods in cases involving a large number of functional groups, (3) unsatisfactory results at infinite dilution and for the solubility of hydrocarbons in water [128]. With the AC of FPBO being a typical example of such a mixture, extra attention should be paid when it is modeled with the UNIFAC-DMD. It is also worth noting that G^E models, including UNIFAC-DMD, are only valid up to a temperature and pressure limit of 120 °C and 4 bar, respectively [105]. As fast pyrolysis and condensation processes all occur at atmospheric pressure, pressure limitations are rarely an issue. Nonetheless, temperature levels can reach as high as 500 °C (for freshly generated fast pyrolysis volatiles). Hence, activity coefficients can be assumed to be constant at and beyond temperatures of 120 °C [128].

2.3.3 GCA-EoS

Compared to UNIFAC-DMD, the GCA-EoS (Group Contribution with Association Equation of State) is a significantly more advanced model. Additionally, it is characterized by a smaller number of group and interaction parameters. However, its implementation requires increased computational effort [105]. Unlike excess Gibbs energy (G^E) models, the GCA-EoS is not

constrained to limited ranges of pressure and temperature and can also be applied in the supercritical range.

The model, which was initially developed by Gros et al. [138] and more recently updated by Sánchez et al. [139], is an extension of the associating systems of the original GC-EoS [140], which is based on the generalized van der Waals theory. Three main terms contribute to the residual Helmholtz energy of the model, each representing the contribution of different intermolecular forces. These include: (1) the repulsive/free volume (A^{fv}), (2) attractive/dispersive forces (A^{att}), and (3) specific association forces (A^{assoc}). The residual Helmholtz energy (A^{r}) in the model is defined as:

$$A^r = A^{fv} + A^{att} + A^{assoc} \tag{2.1}$$

The free volume term (A^{fv}) follows the extended Carnahan-Starling equation for mixtures of hard spheres, developed by Mansoori et al. [141,142]. It is characterized by only one pure parameter (the critical diameter, d_c).

The attractive term (A^{att}) describes the dispersive forces between functional groups. It is a van der Waals expression combined with a density-dependent mixing rule based on a group contribution version of the NRTL model [105]. The term is also characterized by the number of surface segments of each group and the temperature-dependent surface energy. Each binary group interaction is defined by a symmetric temperature-dependent interaction parameter ($k_{ij} = k_{ji}$) and two asymmetric non-randomness parameters ($\alpha_{ij} \neq \alpha_{ji}$).

The association term (A^{assoc}) is a group contribution version of the SAFT equation, developed by Chapman et al. [143]. This term is characterized by the energy and volume of the association. A detailed description of the GCA-EoS model has been reported elsewhere [132,135,139].

Numerous GCA-EoS parameters for relevant groups of compounds have been reported in the literature. However, essential binary interaction parameters remain missing, particularly for aromatic ethers, phenols, and organic acids. Extensive work has recently been conducted on methoxy groups and multiple aromatic derivatives [5,144].

Group contribution models like the GCA-EoS permit the prediction of the phase behavior of compounds not included in the parameterization procedure. Furthermore, the current

interest in employing renewables as feedstock for the chemical industry has made the use of group contribution models particularly appealing, since natural products generally contain a large number of similar species that can be represented by a limited number of functional groups [132].

2.4 Validation of Theoretical Thermodynamic Models Using the Advanced Distillation Curve (ADC) Method

Experimental validation of thermodynamic models plays an integral role in confirming the accuracy of theoretical predictions. For VLE models, VLE cells have primarily been used for validation. Ille et al. [15] employed a VLE cell to generate experimental thermodynamic data in their investigation of the activity coefficient of water in pyrolysis oils. Although VLE cells generate high-quality data, the method can be very time-consuming [145,146].

The Advanced Distillation Curve (ADC) method has been developed and recognized as a more time- and cost-effective technique for generating experimental VLE data for multicomponent fluid mixtures, including FPBOs [50,145]. The ADC method also enables the modeling of VLE data using an equation of state (EoS) [50,145,147,148]. Compared to other distillation methods, the ADC offers several advantages, including: (1) quantified and identified composition data for each distillate fraction; (2) temperature, volume, and pressure data as true thermodynamic state points suitable for modeling with an EoS; (3) consistency with over a century of historical data, such as the ASTM D86; and (4) calculation of density and enthalpy, trace chemical analysis, and assessment of corrosivity for each distillate fraction [50,147–150].

Many ADC studies have been conducted under atmospheric pressure. However, distilling oils with low volatility under such conditions may lead to thermal degradation, cracking, or polymerization [50]. To address this, vacuum distillation (V-ADC) was successfully employed in studies by Windom and Bruno [146,149,151].

The ADC method has been extensively applied to characterize a variety of fuels, including alkanes, crude petroleum oil, bio- and petroleum-derived diesel, jet fuels, rocket fuels, marine fuels, and pyrolysis oils [147,148,150,152,153]. V-ADC has also been used to characterize temperature-sensitive fuels such as soy- and algae-based biodiesel, virgin and waste oils, and swine manure pyrolysis oil [147,154,155]. Krutof and Hawboldt [50] also used V-ADC to assess

the volatility of FPBOs obtained from pine and spruce softwood. They further applied the method to select surrogate/model compounds for modeling the distillation curve. Bulk fuel properties, including enthalpy (heating value, heat capacity, and flash point), flow properties (viscosity and density), and average molecular weight, were modeled and compared with experimental data from the V-ADC.

To improve the ADC approach, Harries et al. [145] recently developed the ADC with reflux (ADCR) method to address challenges in experimentally determining the VLE of fluids containing numerous compounds. The ADCR collects data on the chemical composition of both liquid and vapor phases across a range of temperatures, illustrating the two-phase region at constant pressure. The study concluded that ADCR is a useful method for determining the *T-P-x-y* behavior of multicomponent fluid mixtures.

Chapter 3

Materials & Methods

3.1 Introduction

This chapter details the stepwise experimental and theoretical approaches employed, along with a comprehensive description of all equipment used. Information on all materials used is also provided. The methodological descriptions are presented in separate sections, corresponding to the specific objectives addressed in this study, as outlined in Subsections 3.2, 3.3, and 3.4.

3.2 Methodology for the Study on Using Fractional Condensation to Optimize Aqueous Pyrolysis Condensates for Downstream Microbial Conversion

3.2.1 Materials

Three ash-rich biomass feedstocks were employed: wheat straw, *miscanthus* (a perennial grass), and coffee husk (an agricultural residue), all of which were available in large quantities. These materials were selected because they contain high levels of minerals, particularly potassium. Like most alkali metals, potassium is known to catalyze pyrolysis reactions, which consequently lead to increased formation of char and reaction water during fast pyrolysis [41,156]. As a result, fractionated condensation becomes more important in this context.

Wheat straw was supplied by Franz Kolb GmbH & Co. KG, Germany (firma-kolb.de), and was shredded in two batches: one of 200 kg (April 2019) and another of 300–400 kg (December 2020). The April 2019 batch was used to generate the initial AC for microbial tolerance tests (Section 3.2.2.1), while the December 2020 batch was used for validation experiments following model predictions (Section 3.2.3). Wheat straw was shredded using a shredder (HZR 1300) and subsequently milled using a cutting mill (TYP LM 450/1000-S5-2) to particle sizes below 5 mm. Both pieces of equipment were supplied and installed by Neue Herbold Maschinen- und Anlagenbau GmbH (Sinsheim, Germany).

Miscanthus was supplied by Miscanthus Falzberger, Pichl bei Wels, Austria, in large bales of approximately 500 kg each. The batch was harvested in April 2020. Particle size reduction followed the same procedure as that used for wheat straw, resulting in final particle sizes of 5 mm or smaller.

Colombian coffee husk was supplied by the Universidad Nacional de Colombia, Sede Medellín. The feedstock was originally obtained from "*ALMAVIVA,*" a logistics center for the National Federation of Coffee Growers in Medellín, Colombia. The batch was harvested in July 2019. For 90% of the particles, the maximum and minimum chord lengths were less than 7.5 mm and 4.2 mm, respectively, with particle thicknesses ranging between 0.1 and 0.2 mm. The coffee husk did not require further size reduction prior to pyrolysis.

3.2.2 Modeling the Optimization of the Fractional Condensation Process

3.2.2.1 Selection of Surrogate/Model Mixtures for Thermodynamic VLE Modeling

A surrogate mixture for the AC was designed following GC-MS analysis of a sample obtained from the fast pyrolysis of wheat straw on a 10 kg/h process development unit (PDU) (described in detail in Section 3.2.3), as well as tolerance and toxicity tests conducted on this sample. This followed a procedure similar to that employed elsewhere [23]. Toxicity and tolerance tests were conducted to assess the extent to which microbes can tolerate compounds present in a substrate such as AC. For example, toxicity testing confirmed that compounds such as acetic acid and acetol are good substrates (promoters) that aid microbial growth, whereas compounds such as furfural inhibit microbial growth.

The procedure used for selecting surrogate/model components followed a similar principle to that employed by Ille et al. [15], ensuring that compounds of interest to microbial conversion (as both substrates and inhibitors) were included. In general, the following factors were considered:

1. Representation of the surrogate mixtures to cover the full boiling point range of the individual components present in AC.
2. Representation of all relevant functional groups in the original AC mixture.

3. Relevance of the compounds to microbial conversion.
4. Mass fraction (wt.%) of the selected compounds.

The selection of surrogate compounds, based on the overall GC-MS characterization of the AC and toxicity testing of microbes, is presented in Section 1 of Appendix A. A similar procedure was followed to define surrogate mixtures for *miscanthus* and coffee husk. The resulting model compounds for all three biomass feedstocks were categorized into substrates and inhibitors, as summarized in Table 3.1.

The mass fractions (in wt.%) of the selected surrogate compounds of pyrolysis volatiles entering the first condensation unit were calculated using their corresponding mass fractions in the ORCs and ACs, the composition of the NCGs, and the respective flow rates for each of these streams. GC-undetectable lignin-derived components present in the ORC were represented as 3,4,4'-Biphenoltriol, following the approach of Ille et al. [15]. These calculated mass fractions subsequently served as input stream data for the thermodynamic VLE flash calculations (Section 3.2.2.3). The resulting surrogate mixtures with their respective mass fractions (of pyrolysis volatiles entering the first condensation unit) for all three biomass feedstocks, as well as the GC-MS data for all the respective AC and ORC samples, are presented in Table A4 (Section 1 of Appendix A) and Tables A9 to A14 (Section 3 of Appendix A).

Yields of ORC (Y_{ORC}) and AC (Y_{AC}) were estimated with respect to the total input vapor flow into the first condenser ($m_{tot\ vapours\ into\ C1}$), as defined by Equations (3.1) and (3.2).

$$Y_{ORC} = \frac{m_{ORC}}{m_{tot\ vapours\ into\ C1}} \tag{3.1}$$

$$Y_{AC} = \frac{m_{AC}}{m_{tot\ vapours\ into\ C1}} \tag{3.2}$$

Where:

$$m_{tot\ vapours\ into\ C1} = m_{ORC} + m_{AC} + m_{NCGs}.$$

Table 3.1. Grouping surrogate/model compounds in AC into substrates (promoters) and inhibitors for all three biomass feedstocks.

Substrates/Promoters	Inhibitors
Hydroxyacetaldehyde	3-Hydroxypropionaldehyde
Acetic Acid	2-Butanone
Propionic Acid	Methanol
Acetol	Furfural
Phenol	*o*-Cresol
Ethylene Glycol	*m*-Cresol
Guaiacol	Syringol
2-Methylpropanoic acid	5-Hydroxymethyl-2-furaldehyde
	Vanillin
	2,3-Butanedione (Diacetyl)
	1-Hydroxy-2-butanone

3.2.2.2 Central Composite Design (CCD)

A Central Composite Design (CCD) statistical method with five center points was used to ascertain the optimal temperature conditions at which the production of substrates exceeds that of inhibitors. *Design-Expert* software, version 12 (Stat-Ease Inc., Minneapolis, USA), was used to set up and evaluate the CCD. Condensation temperatures (recorded at the exit point of each condenser) of Condensers 1 (C1) and 2 (C2) were the factors investigated, whereas the mass fractions of substrates and inhibitory compounds (in wt.%) recovered in the AC, the yield of the AC, the ratio of substrates to inhibitors, and the mass fraction of water in the AC were the main response variables.

The temperature ranges investigated for C1 and C2 were 80 to 120 °C and 10 to 50 °C, respectively. These ranges were selected based on the operability limits of the condensers, while also avoiding condensation temperatures below 80 °C for C1, as such conditions

facilitate the recovery of two-phase liquid products. For C2, condensation temperatures above 50 °C led to significant losses of aqueous condensate products. The investigated factors and their respective ranges, as designed using the CCD, are presented in Table A5 in Section 2 of Appendix A.

3.2.2.3 Thermodynamic VLE Flash Calculations

Following the design of temperature ranges to be investigated using the CCD, thermodynamic VLE flash calculations were performed using the UNIFAC-DMD thermodynamic model. The UNIFAC-DMD model was programmed in MATLAB using the latest database obtained from the UNIFAC Consortium at the Dortmund Data Bank [137]. Thermodynamic VLE calculations were performed around the condensation unit of the fast pyrolysis PDU described in Section 3.2.3 and depicted in Fig. 3.1, in which Units 5 and 9 represent the first and second condensers that produce ORC and AC, respectively. It is important to note that aerosols formed during cooling in the first condensation stage were recovered in an electrostatic precipitator and added to the ORC. Consequently, it is feasible to represent each condenser by flash calculations. Flash calculations were performed for each biomass feedstock using temperature pairs for C1 and C2 that were defined by the CCD (Tables A6 to A8 in Section 2 of Appendix A), to obtain the corresponding response factor data.

The generalized laws of Raoult and Dalton (Equation (*3.3*) form the basis for modeling typical G^E models like the UNIFAC-DMD. VLE flash calculations were formulated using this relation, where x_i and y_i represent the mole (or mass) fractions of pure components in the liquid and vapor phases, respectively; p and p_i^0 denote the total pressure and saturated vapor pressure of pure components, respectively. The Poynting correction, Φ_i, defines the vapor-phase non-ideality, while the activity coefficient, γ_i, accounts for liquid-phase deviations from ideal solution behavior. It is important to note that the Poynting correction for high pressures was approximated as unity in this study since the condensation process was conducted at atmospheric pressure.

$$y_i \Phi_i p = x_i \gamma_i p_i^0 \tag{3.3}$$

The saturated vapor pressure of pure substances, p_i^0, was defined using the Wagner equation (Equation (*3.4*) [157–159].

$$\ln\frac{p_i^0}{p_c} = \frac{1}{T_r}[A(1-T_r) + B(1-T_r)^{1.5} + C(1-T_r)^{2.5} + D(1-T_r)^5 \quad (3.4)$$

$$T_r = T/T_c \quad (3.5)$$

Here, p_c and T_r represent the critical pressure and reduced temperature, respectively. T_r is a function of the thermodynamic temperature, T, and the critical temperature, T_c. The constants A, B, C, and D are the Wagner constants. The Wagner constants for the majority of the compounds were obtained from the literature [105,159], whereas the constants for all other substances were estimated using the Extended Antoine Equation from the Aspen Plus physical property system pure-component databank.

3.2.3 Experimental Validation on the Process Development Unit (PDU)

Subsequent to the modeling optimization study, optimum condensation temperatures were experimentally validated on a 10 kg/h pyrolysis PDU, a scaled-down version of the bioliq® process [120,156]. A detailed process description of this unit has been elaborated elsewhere [122,160]; therefore, only descriptions of the modifications made to the condensation system are provided in this study. A representation of the setup with the modified condensation system is shown in Fig. 3.1.

Validating the optimized temperature conditions from the CCD investigation required a modification of the PDU condensation system, since it was not initially designed to operate at these optimized condensation temperatures. These modifications include a third condensation unit, designed as a shell-and-tube condenser, that also operated at a temperature similar to C2, with its sole purpose of recovering any AC that could not condense

in C2 as a result of its higher condensation temperature (50 °C) compared to the default/conventional condensation temperature of 15 °C. All experiments were conducted in triplicate to ensure repeatability.

Because ORC and AC obtained from these main condensation loops are heavily diluted with the quenching liquids, ethylene glycol and water, respectively, a bypass condensation system (Units 14, 15 and 16 of Fig. 3.1) was installed and attached to the PDU to recover undiluted pyrolysis oil products. The bypass condensation loops consist of shell-and-tube condensers operating at condensation temperature conditions similar to those of the main quenching condensation loops. These undiluted pyrolysis products provide a more accurate representation of the pyrolysis condensates; hence, their GC-MS characterization results were used (for experimental validation) instead of the GC-MS characterization of the heavily diluted samples.

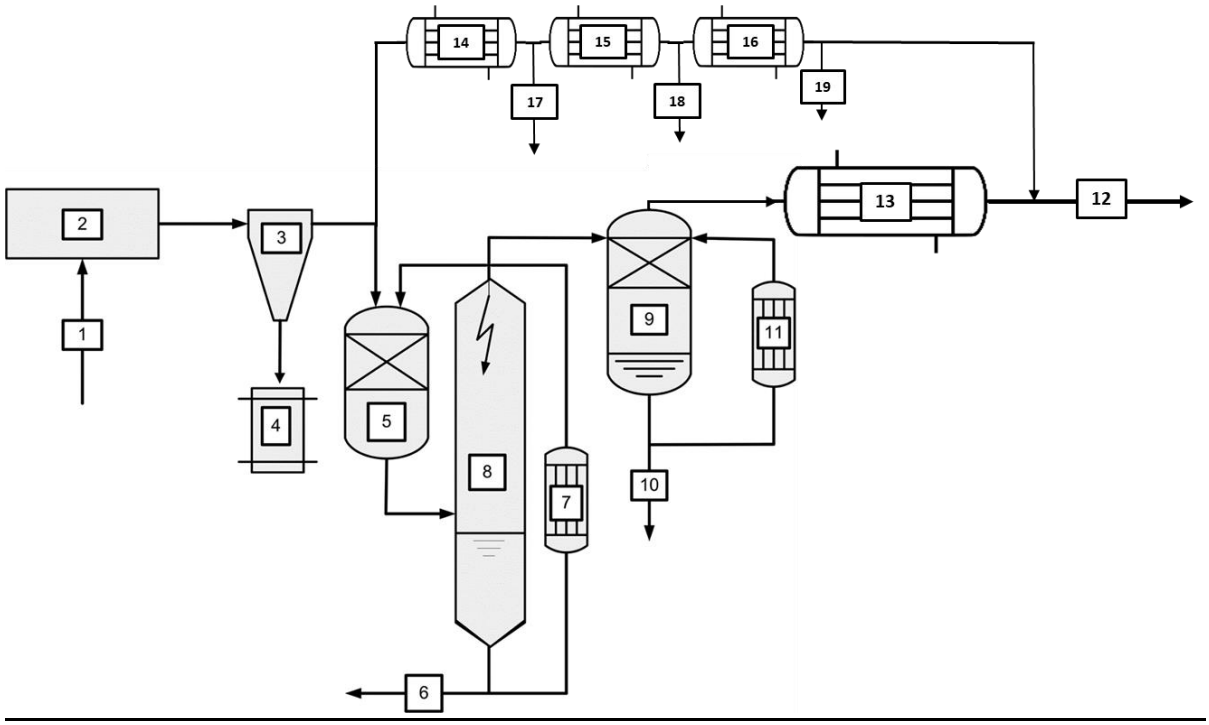

Fig. 3.1. Schematic representation of the fast pyrolysis Process Development Unit (PDU) showing the modified condensation system: 1: Biomass feed, 2: Pyrolysis screw reactor, 3: Cyclone, 4: Solid char products, 5: Quenching condenser 1, 6: Organic-rich condensate (ORC), 7: Heat exchanger 1, 8: Electrostatic precipitator, 9: Quenching condenser 2, 10: Aqueous condensate (AC), 11: Heat exchanger 2, 12: Incondensable gases, 13: Third condensation unit, 14: Bypass condenser 1, 15: Bypass condenser 2, 16: Bypass condenser 3, 17: ORC from bypass, 18: AC1 from bypass, 19: AC2 from bypass. (Adapted from Ille et al. [15], with permission from Elsevier).

3.2.4 Product Characterization

For every test conducted in the PDU, biomass samples, solid char, and all condensates were subjected to various analyses. The methods followed procedures similar to those employed elsewhere [160], with only summaries being highlighted here.

The moisture content of biomass feedstocks and char was measured in accordance with DIN EN 18134-3. Volumetric Karl-Fischer titration was performed using methanol with Hydranal Composite-V to determine water content in all condensates. The ash content of biomass feedstocks and solid char was determined per DIN EN ISO 18122, where samples were heated to 250 °C for 60 min, and subsequently to 550 °C for 120 min. The volatile matter content of biomass feedstocks was measured following DIN EN ISO 18123. Elemental analysis of solid char was carried out according to DIN EN 15104, and that of biomass feedstocks and ORCs was conducted according to DIN EN 51732.

The composition of non-condensable gases was characterized online using gas chromatography with neon gas as a tracer. The gas volumetric flow rate was additionally measured using an online flowmeter.

GC–MS analyses of all pyrolysis condensates were conducted by the Thünen Institute, Hamburg, Germany. The method is described in detail elsewhere [161].

3.3 Methodology for the Study on the Influence of Selected Quench Media for Direct-Contact Condensation on Yield and Composition of Fast Pyrolysis Bio-Oils

3.3.1 Materials

Wheat straw feedstock, as supplied and used in Section 3.2.1, was also used for all experiments conducted for this study objective.

Isopar-V, manufactured by Exxon Company, USA, and supplied by LCG Limited, UK, primarily contains C_{14}–C_{18} isoparaffinic hydrocarbons, with a boiling point range of 273–311 °C. It has an average molecular weight of 197 g/mol and a specific gravity of 0.82 at 15.6 °C.

Demineralized water, used for the water quenching experiments, was supplied by the facilities management of the Karlsruhe Institute of Technology (KIT) at ambient temperature and a pressure of 4 bar.

Ethanol (99.5 vol.%), denatured with approximately 1 vol.% methyl ethyl ketone, was manufactured by VWR Chemicals BDH, France, and supplied by Häffner GmbH & Co. KG, Asperg, Baden-Württemberg, Germany.

Ethylene glycol (glycol), supplied by Brenntag GmbH, Essen, Germany, has a molecular weight of 62.07 g/mol, a boiling point of 197.4 °C, and a density of 1.122 g/cm^3 at 20 °C.

3.3.2 Fast Pyrolysis Conversion and Direct-Contact Condensation Process

Fast pyrolysis of wheat straw was conducted on the 10 kg/h fast pyrolysis PDU, also equipped with a modified condensation system. Unlike the system employed for the first study objective in Section 3.2.3, the quenching of hot volatiles was performed directly in the bypass system, as this was a much simpler and easier approach to control the condensation process, particularly since several QM with different properties were being tested on the setup for the first time. Consequently, all pyrolysis volatiles exiting the hot part of the reactor were channeled solely through the bypass segment (Fig. 3.2). Before entering the bypass system, hot volatiles first passed through a filter to retain any solid particles. Unlike the main condensation loop, QM was externally supplied throughout the course of the experiment, without recirculation of the QM/ORC product (Fig. 3.2).

Following quenching, the quenched mixture at temperature T_1 (Fig. 3.2) proceeded to a heat exchanger, where it was further cooled to recover the ORC in the first condensation stage. Set temperatures T_2 (Table 3.2) for this heat exchanger were selected based on the volatility and boiling point of the specific QM. QM that did not mix with the ORC (i.e., Isopar-V and water) were further decanted at the end of the test to separate the recovered ORC from the spent quench. Volatiles that could not condense at this stage proceeded to an electrostatic precipitator, where aerosols were captured before passing on to a second heat exchanger, with a condensation temperature of 6 °C, to recover a water-rich AC (Fig. 3.2.). NCGs were then analyzed using an online gas chromatograph before being discarded. During the

experiment, entry to the main quench loop was completely closed to ensure that all volatiles were channeled into the bypass. To accommodate the comparatively low volume capacity of the bypass, the biomass feed rate was adjusted to between 1.5 and 2 kg/h.

The mass flow rate ratio of the quench to hot pyrolysis volatiles (m_q/m_v) defines the quenching temperature and, consequently, the extent of cooling of the hot pyrolysis volatiles. Two different m_q/m_v ratios, 0.5 and 2.0, were investigated. The temperature of the pyrolysis volatiles exiting the reactor prior to quenching ranged between 380 and 385 °C, and the temperature of the resultant QM/ORC product was primarily dependent on the properties of the QM and its heat of evaporation. These temperatures (T_1) are presented in Table 3.3. All experiments in the PDU were conducted in duplicate to ensure repeatability.

Table 3.2. Set condensation temperatures (T_2) of the ORC condensation stage for all investigated QM (selected based on their volatility and boiling point).

Quench	Set condensation temperature on ORC recovery stage (°C)
Isopar-V	80
Water	95
Ethanol	40
Glycol	80

Table 3.3. Temperatures of QM/ORC product (T_1) following direct-contact with respective QM.

Quench	Temperatures of QM/ORC mixture (°C)	
	m_q/m_v – 0.50	m_q/m_v– 2.0
Isopar-V	179	133
Water	169	86
Ethanol	148	50
Glycol	153	115

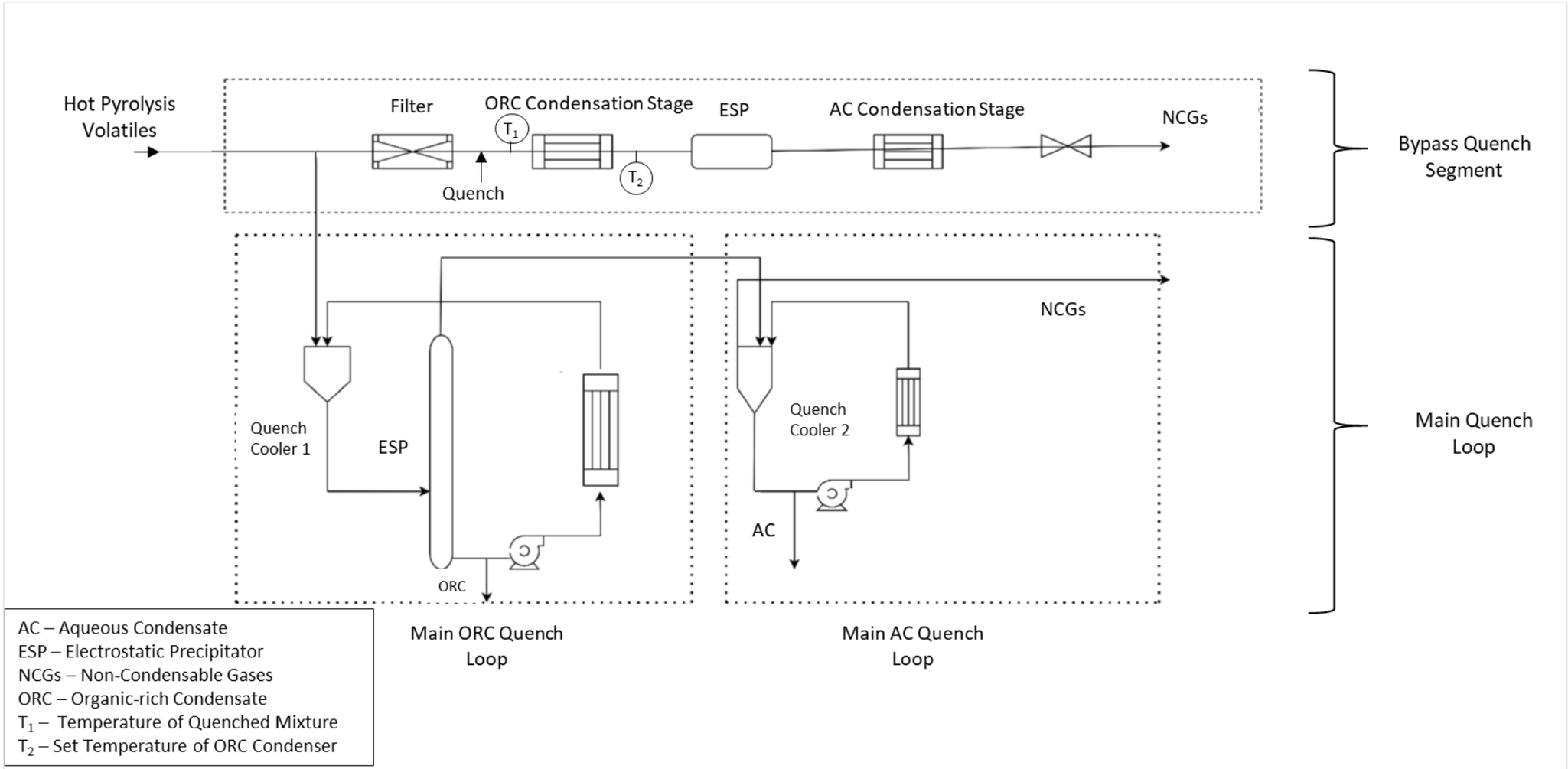

Fig. 3.2. Schematic representation of the fast pyrolysis process development unit (PDU) demonstrating the main and bypass condensation systems (all QM tests were conducted using the bypass system, as it was a much simpler and easier approach to control the condensation process).

3.3.3 Product Characterization

Moisture content and GC–MS/FID characterization of all recovered condensates were carried out in accordance with the methods described in Section 3.2.4. GC–MS analyses of all condensates are presented in Tables B6 to B15 of Appendix B.

3.3.4 Aspen Plus Model Simulation of the Quenching Condensation Process

The phase equilibrium under the given conditions during condensation was simulated in Aspen Plus® V12 to predict how the variable parameters (QM, flash temperature, and m_q/m_v) affect the yield and composition of FPBOs.

The wheat straw surrogate mixture, previously defined in Section 3.2.2.1, was also employed here to represent the composition of hot pyrolysis volatiles that entered the first condensation unit. For the modeling scenario that investigated the ORC as a quench (subsequently discussed in Section 4.3.3), surrogate mixtures defined for the ORC are presented in Table C11 of Appendix C.

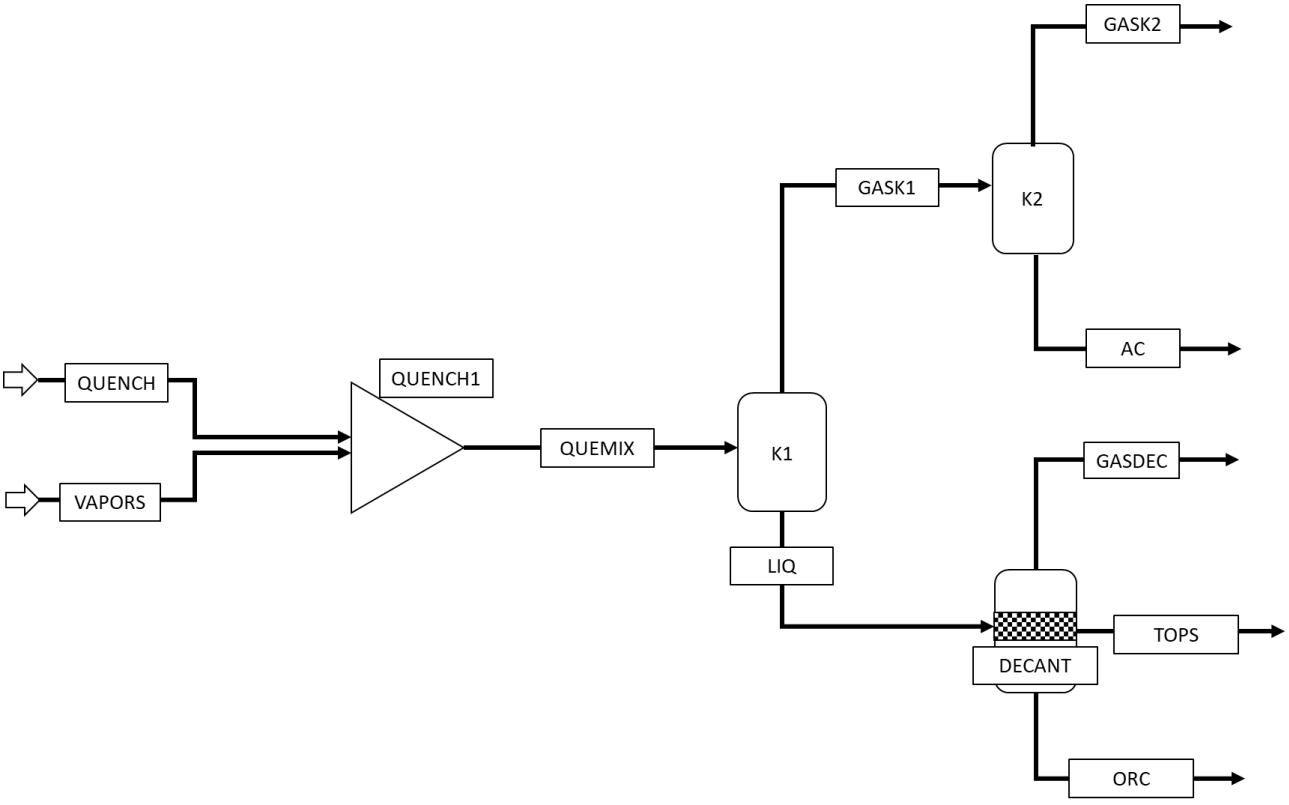

Fig. 3.3. Aspen flowchart of the quenching condensation process as implemented in the bypass system.

Following the definition of the surrogate mixture, the Aspen flowchart simulation was set up as shown in Fig. 3.3. The quenching of hot volatiles (VAPORS) by the respective QM (QUENCH) was modeled as a mixer (QUENCH1) operating at 1 bar. Thereafter, the QM/ORC product (QUEMIX) proceeds to the first condensation stage (K1), which was modeled using the Aspen flash module. In this stage, the phase equilibrium of the mixture is modeled at the respective set temperatures to recover the condensate, which comprises a mixture of the ORC and the spent QM (LIQ). For the investigations examining the predicted effects of quenching temperature, a temperature range of 40–120 °C was used, whereas set temperatures (Table 3.2) were used for experimental validations. For the cases of Isopar-V and water, which are immiscible with the ORC, the ORC/QM (LIQ) mixture is subsequently subjected to downstream separation, modeled as an adiabatic decanter at 1 bar (DECANT). At this stage, the spent QM (TOPS) is separated from the ORC. Virtually no gases (GASDEC) are generated in this unit.

Volatiles that could not condense in K1 proceed to the second condensation stage (K2), where they are cooled to 6 °C to recover the AC (modeled using the Aspen flash module). NCGs (GASK2) are then expelled. Again, the UNIFAC-DMD was employed to estimate the physical properties of all defined components.

Deviations of theoretically predicted model data ($Z_{calc,i}$) from the corresponding experimental data ($Z_{exp,i}$) were quantified using the absolute relative deviation (ARD%) and the average absolute relative deviation (AARD%) for N data points. These are defined by Equations (3.6) and (3.7), respectively:

$$(ARD\%)_i = \left| \frac{Z_{exp,i} - Z_{calc,i}}{Z_{exp,i}} \right| * 100 \tag{3.6}$$

$$AARD\% = \frac{1}{N} \sum_{i}^{N} ARD_i \tag{3.7}$$

3.4 Methodology for the Comparative Study on Levoglucosan Extraction from FPBOs Using Solvent Extraction and Extraction During Direct-Contact Condensation of Hot Pyrolysis Volatiles

3.4.1 Materials

ORC and AC used for solvent extraction were obtained from the fast pyrolysis of wheat straw and *miscanthus* at the bioliq® fast pyrolysis plant. The GC-MS compositions of these condensates are presented in Tables C7 to C10 in Appendix C. Demineralized water used as a solvent was supplied under the same conditions as previously reported in Section 3.3.1.

3.4.2 Bench-Scale Solvent Extraction of Levoglucosan

Two solvents (water and the AC) were investigated for LG extraction from the respective ORCs. Six different solvent-to-oil ratios (STORs), namely, 0.2:1, 0.5:1, 1:1, 2:1, 5:1, and 10:1, were tested. 50 g of ORC was mixed with the corresponding amount of solvent according to the STOR in Schott bottles. Following mixing, the solvent–ORC mixture was vigorously shaken by hand and then placed on a CERTOMAT® shaker table set at a rotation speed of 250 min^{-1} for approximately 4 hours to ensure thorough mixing and equilibrium. Reaching phase equilibrium typically takes at least 20 minutes; therefore, 4 hours ensures it is fully established.

After mixing, the mixture was left undisturbed overnight at room temperature to allow for separation of the raffinate (mostly containing heavy phenolic fractions) from the extract phase. The extract phase was then gently decanted and analyzed for LG content. Knowing the mass of LG originally contained in the ORC ($mass\ of\ LG\ in\ ORC$) and that determined from the characterization of the extract ($mass\ of\ LG\ in\ extract$), the percentage of LG transferred into the extract phase ($\%\ LG\ extracted$) was calculated using Equation (3.8). Average standard deviations for the percentage of LG extracted (for both water and AC solvent systems) were less than 1.30% for wheat straw and 0.19% for *miscanthus*.

$$\%\ LG\ extracted = \frac{mass\ of\ LG\ in\ extract}{mass\ of\ LG\ in\ ORC} * 100\% \quad (3.8)$$

3.4.3 Levoglucosan Extraction During Direct-Contact Condensation with Water as the Quenching Medium

LG extraction during quenching followed the same procedure used for direct-contact experiments (Section 3.3.2) that employed water as the quench, except that in this instance, the first condensation stage was set to a lower temperature of 40 °C to allow for the optimal recovery of almost all condensates together with the spent water quench. This facilitates a single-step condensation of both ORC and the solvent (water) on the same condensation stage, which enhances the transfer of water-soluble compounds, particularly LG, into the spent water quench phase. The single-stage condensed product of the ORC fraction and the spent water quench was collected and separated using a separating funnel, after which both phases were characterized for LG.

3.4.4 Product Characterization

For bench-scale experiments, since the concentrations of LG present in the ORC feedstocks are known, only the water extract phase was analyzed for LG. This was conducted using a compact IC Flex Amperometric system equipped with a 945 Professional Amperometric Detector and a Metrosep Carb 2 250/4.0 column. The column has dimensions of 250 × 4 mm and contains a styrene-divinylbenzene copolymer as the stationary phase, which is well suited for the characterization of carbohydrates and anhydrosugars. The mobile phases, comprising NaOH (100 mmol/L) and CH_3COONa (10 mmol/L), were diluted with pure water with a resistivity greater than 18 MΩ·cm at 25 °C. The 838 Advanced Sample Processor injected 20 µL of the sample into the mobile phase, which was pumped by an ion chromatographic (IC) pump at a flow rate of 0.5 mL/min. The temperature of the column was maintained at 35 °C using an oven, and the system pressure was maintained at 11.5 MPa. The measurement span was 100 ms. Prior to injection into the Amperometric detector, the samples were first filtered using 0.2 µm CHROMAFIL Xtra PA-20/13 disposable syringe filters. The filtered samples were then diluted to concentrations within the calibration range (2–20 mg/L) of the Amperometric detector.

Since the concentration of LG in hot pyrolysis volatiles is virtually impossible to quantify, it is important to characterize LG concentrations in both the extract and raffinate phases of the products recovered from the single-step direct-contact condensation process to enable

calculation of LG distribution between the two phases. As the raffinate fraction could not be characterized using amperometry, both products were subjected to GC-MS/FID characterization and subsequent moisture analysis using methodologies consistent with those described in Section 3.2.4. The results of the GC-MS/FID characterizations of all raffinates, extracts, and corresponding ACs are presented in Tables C1 to C6 in Section 1 of Appendix C.

3.4.5 Aspen Plus Model Simulations of LG Extraction

3.4.5.1 Bench-Scale Solvent Extraction

The phase equilibrium under the given conditions during solvent extraction at bench scale was simulated in Aspen Plus® V12 to predict how STOR influences LG extraction from the ORC. The simulation was conducted separately for water and AC solvents at the ratios investigated experimentally.

Surrogate mixtures for the ORC (feedstock) and AC (one of the solvents employed), derived from wheat straw and *miscanthus* (Table C11 in Appendix C), were first defined. Thereafter, the simulation of solvent extraction was set up according to the Aspen flowchart depicted in Fig. 3.4. The mixing of solvents (water and AC) with the ORC, both at ambient temperature, was modeled as a mixer operating at 1 bar.

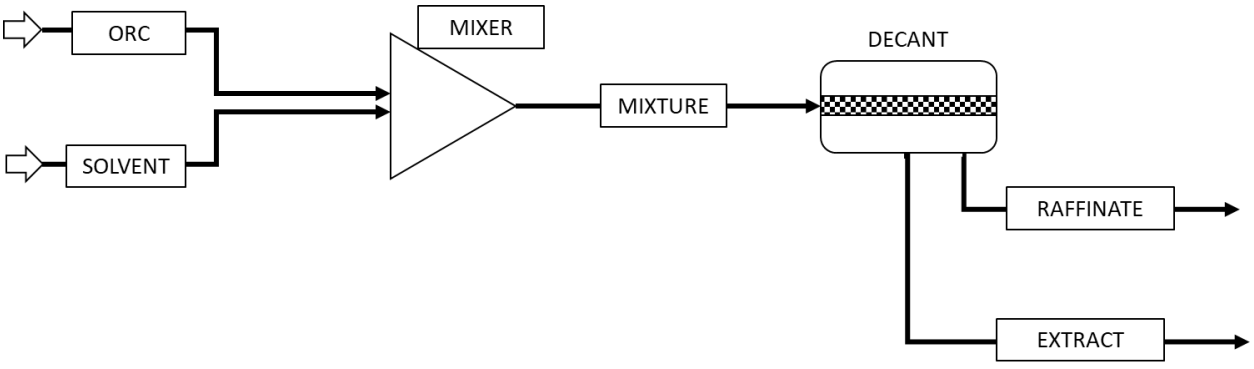

Fig. 3.4. Aspen flowchart of the bench-scale solvent extraction of LG from ORC using water and AC as solvents.

Following mixing, the mixture was decanted to separate the extract from the raffinate. Root Mean Square Error (RMSE) (Equation (*3.9*)) was used to quantify the deviation of model predictions from experimental data.

$$RMSE = \sqrt{\frac{1}{n}\sum_{i=1}^{n}(y_i - \hat{y}_i)^2} \quad (3.9)$$

Where:

n represents the number of observations in the dataset.

y_i represents the experimental value for observation i.

$\hat{y}_i$ represents the model predicted value for observation i.

3.4.5.2 Extraction During Direct-Contact Condensation

Simulation of phase equilibrium conditions during direct-contact condensation followed the exact procedures described in Section 3.3.4, except that the condensation temperature in the first condensation stage was set to 40 °C to allow for single-step condensation, as implemented in the experimental investigation previously described in Section 3.4.3. A mass flow rate ratio of water quench to hot pyrolysis volatiles (m_q/m_v) of 2.0 was utilized. As a result, virtually no product ended up in the second condensation stage.

Chapter 4

Results & Discussions

4.1 Introduction

This chapter presents and discusses the results of all objectives investigated in this study. The discussion begins with studies on the optimization of the fractional condensation setup to fine-tune the composition of the aqueous pyrolysis condensate for downstream microbial conversion. This is followed by a discussion on the influence of selected quenching media on the yield and composition of fast pyrolysis bio-oils (FPBOs). Next is a comparative study of levoglucosan (LG) extraction from FPBOs using both conventional solvent extraction and a novel approach (developed as part of this study) involving extraction during direct-contact condensation of hot pyrolysis volatiles. The chapter concludes with key reflections on the shortcomings of the theoretical model predictions for the condensation system.

4.2 Using Fractional Condensation to Optimize Aqueous Pyrolysis Condensates for Downstream Microbial Conversion

4.2.1 Modeling Optimization of the Fractional Condensation Process

The two-unit condensation setup (described in Section 3.2.3) was modeled to determine the effects of condensation temperatures on the variation in mass fractions of substrate (promoter) and inhibitor compounds in the recovered AC. Temperature ranges of 80–120 °C were investigated for the first condenser, while 10–50 °C were considered for the second condenser. The influence of condenser temperatures on the mass fractions of substrate and inhibitor compounds (grouped according to the selected surrogate mixtures shown in Table 3.1) present in the AC was evaluated. Additionally, substrate-to-inhibitor ratio parameters were used to support the identification of conditions under which substrate recovery was optimized. Furthermore, the effects of temperature variation on the yields and water content of the AC were also investigated. The study was conducted using three different biomass feedstocks: wheat straw, *miscanthus*, and coffee husk.

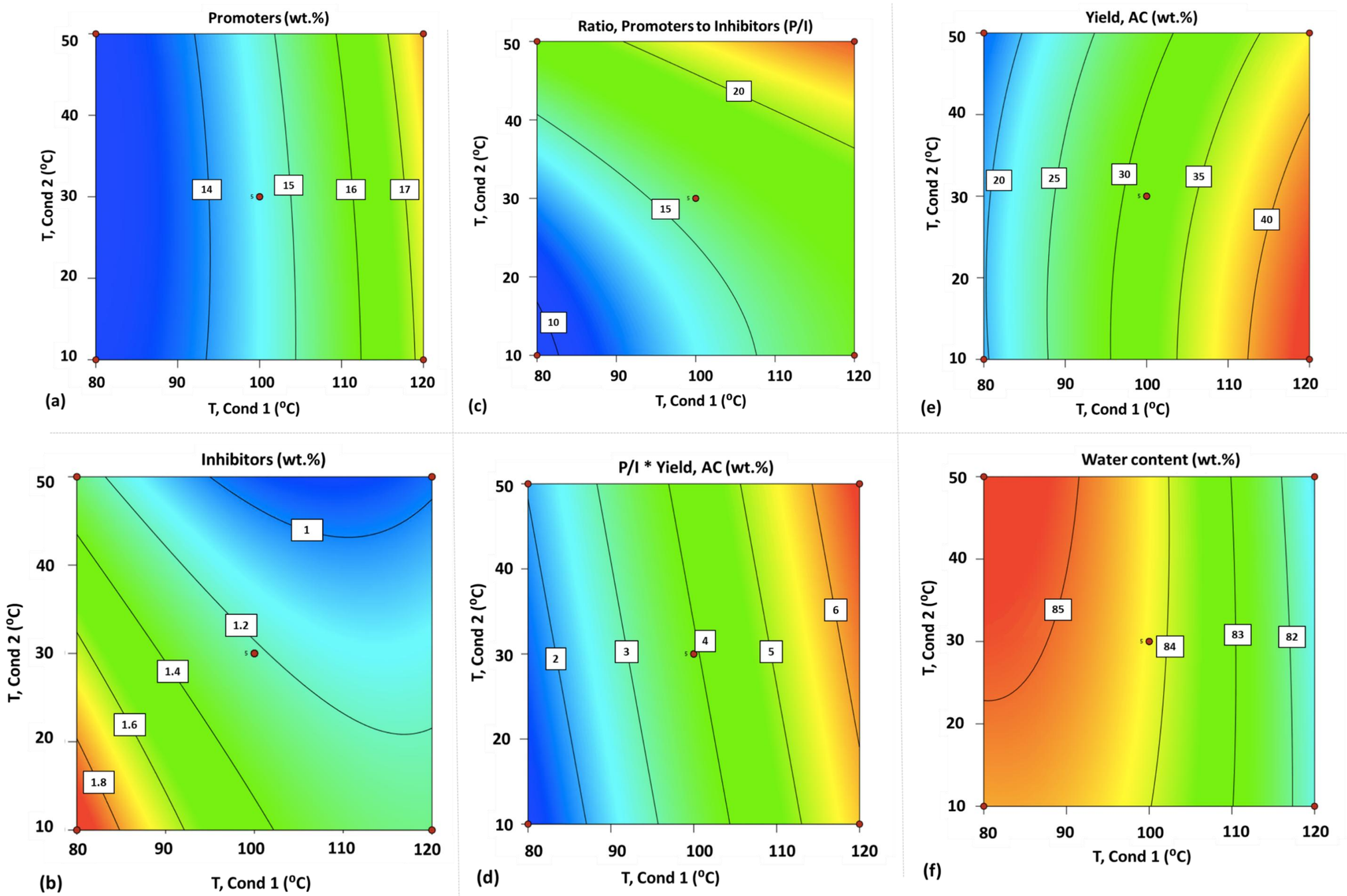

Fig. 4.1. ***Wheat Straw****: Effects of condensation temperatures on: (a) mass fraction of the sum of promoter/substrate compounds in AC; (b) mass fraction of the sum of inhibitory compounds in AC; (c) ratio of promoters (P) to inhibitors (I); (d) proportion of promoters to inhibitors relative to AC yield; (e) AC yield (relative to the total amount of pyrolysis volatiles entering the first condenser); and (f) water content in AC. (Note: Cond = Condenser)*

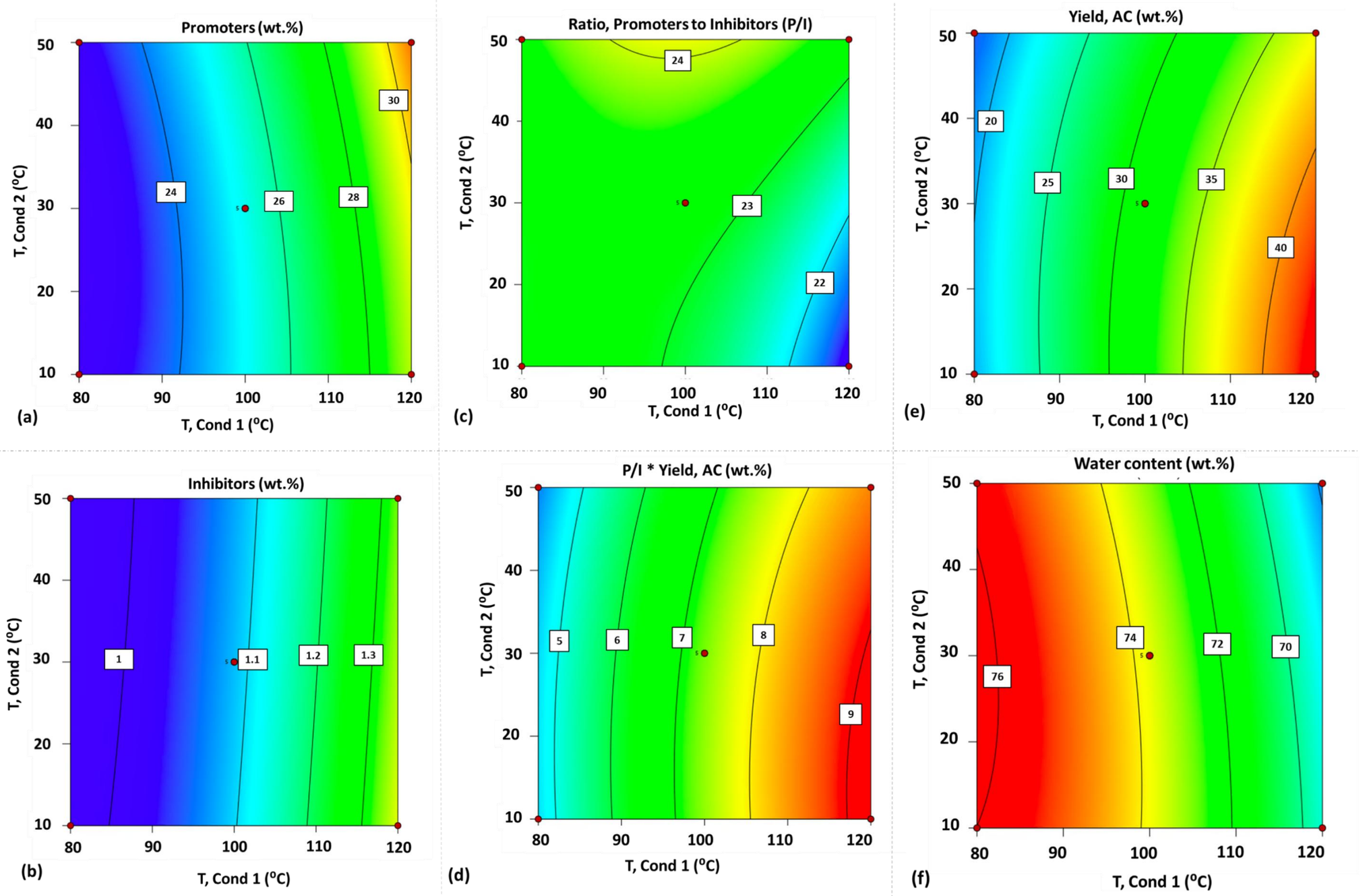

Fig. 4.2. ***Miscanthus****: Effects of condensation temperatures on: (a) mass fraction of the sum of promoter/substrate compounds in AC; (b) mass fraction of the sum of inhibitory compounds in AC; (c) ratio of promoters (P) to inhibitors (I); (d) proportion of promoters to inhibitors relative to AC yield; (e) AC yield (relative to the total amount of pyrolysis volatiles entering the first condenser); and (f) water content in AC. (Note: Cond = Condenser)*

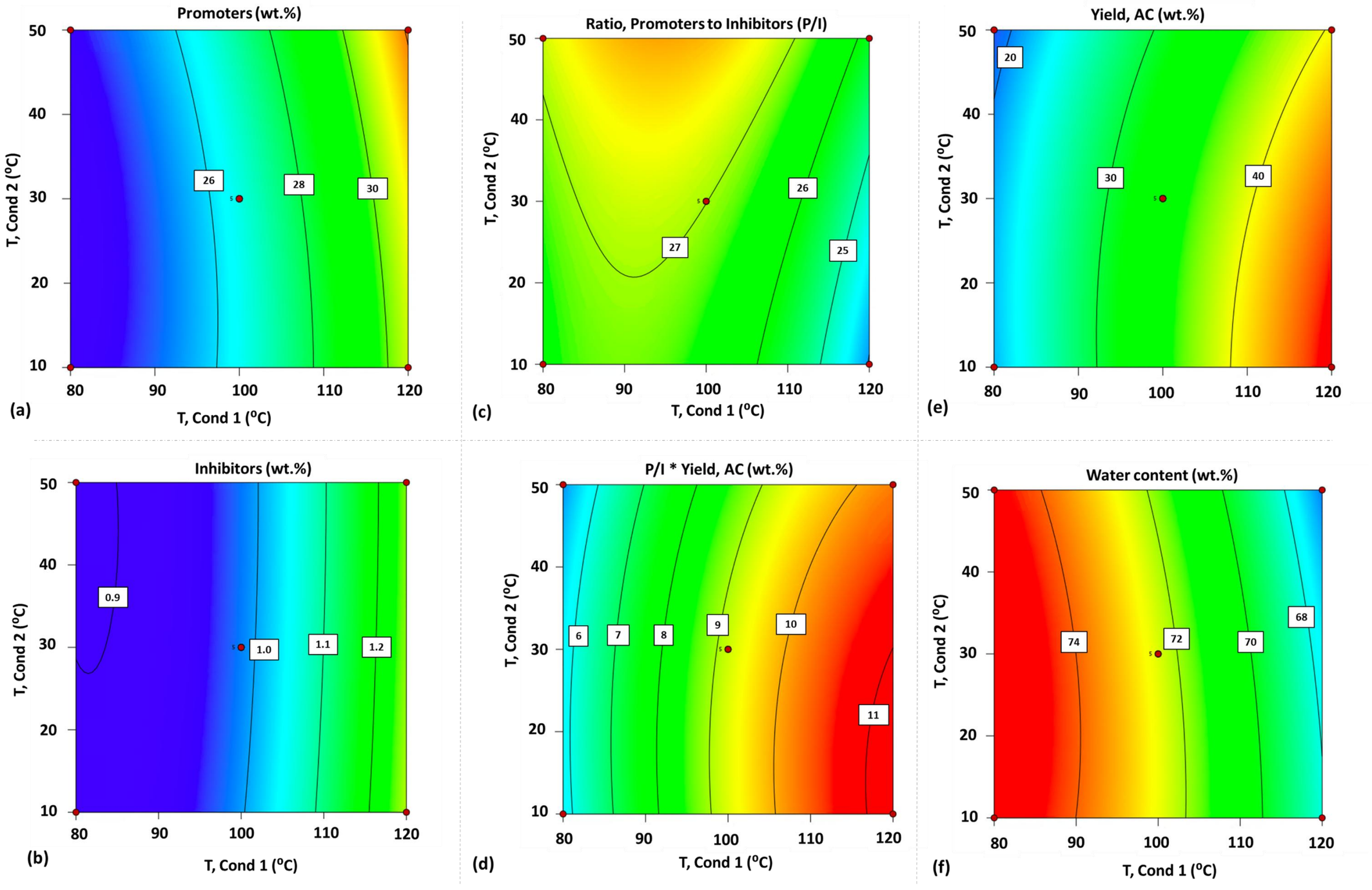

Fig. 4.3. ***Coffee Husk****: Effects of condensation temperatures on: (a) mass fraction of the sum of promoter/substrate compounds in AC; (b) mass fraction of the sum of inhibitory compounds in AC; (c) ratio of promoters (P) to inhibitors (I); (d) proportion of promoters to inhibitors relative to AC yield; (e) AC yield (relative to the total amount of pyrolysis volatiles entering the first condenser); and (f) water content in AC. (Note: Cond = Condenser)*

4.2.1.1 Wheat Straw

In Fig. 4.1a, it was observed that increasing the condensation temperature of the first condenser from 80 to 120 °C had the greatest effect on the recovery of substrates in the AC, with the substrate mass fraction increasing from about 13 to 18 wt.%. This increase occurred because, at higher temperatures, more substrate compounds (especially acetic acid, propionic acid, and acetol) remained in the vapor phase in the first condenser and condensed into the AC only during the next condensation stage. Similar observations were made by Liaw et al. [31], who also reported an increase in the mass fractions of compounds such as acetic acid and acetol in their AC when the temperature of the first-stage condenser was increased.

Generally, the influence of temperature in the second-stage condenser on the mass fraction of substrates in the AC was insignificant. At a lower C1 temperature (80 °C), virtually no change in the mass fraction of substrates was observed when the temperature of C2 increased from 10 to 50 °C. Also, for the same temperature range of C2, only a slight increase (about 0.5 wt.%) in the mass fraction of substrates was observed at a higher condensation temperature of C1 (120 °C). The highest yield of substrate (about 18 wt.%) was recorded at a temperature combination of 120 °C and 50 °C for C1 and C2, respectively.

From Fig. 4.1b, throughout the temperature range of C1 (80–120 °C), a decrease in the mass fraction of inhibitors in the AC was observed when the temperature of C2 increased from 10 to 50 °C. Reductions from 1.98 to 1.28 wt.% (at C1 temperature of 80 °C) and from 1.26 to 0.98 wt.% (at a C1 temperature of 120 °C) were observed. The lowest mass fraction of inhibitors in the AC (about 0.98 wt.%) was recorded at the highest condensation temperature combinations of both condensers, since these conditions promoted the fractional condensation of most of the higher molecular weight compounds (including furfural, syringol, *m*-cresol, and *o*-cresol), which form the majority fraction of inhibitors, in the first-stage condenser. Due to their comparatively higher boiling points, they tend to be retained in C1, which operates at higher temperatures, resulting in a significantly smaller fraction of these components progressing to the next condensation stage. Also, it is evident that the concentrations of most low molecular weight compounds that make up the substrate fraction increased and consequently predominated in the AC at higher temperature combinations of C1 and C2, thereby diluting the concentrations of the minor high molecular weight compounds (most of which constitute the inhibitors) that ended up in this fraction. It is also important to

mention that at higher condensation temperatures of both condensers, the inhibitor methanol remained in the vapor phase, indicating that its concentration in the recovered AC remained below toxic thresholds.

To provide a clearer understanding of the recovery of substrates/promoters (P) and inhibitory (I) compounds in the AC, the ratio of their respective mass fractions was multiplied by the yield of AC to generate the parameter "(P/I) × AC Yield". This parameter confirmed that an increase in temperature in both condensation units facilitated the production of substrates at the expense of inhibitors at an optimal recovery of AC, as depicted in Fig. 4.1d. Proportions of inhibitors were suppressed by approximately sixfold when condensation temperatures of both condensers increased from the lowest to the highest. Even more striking with this trend was the direct ratio of promoters to inhibitors (P/I) (Fig. 4.1c), which showed an exponential rise from about 10 to 25 as the temperatures of both condensation stages were increased from their lowest to their highest ranges investigated.

From Fig. 4.1e, the yield of AC (relative to the total amount of pyrolysis volatiles entering the first condenser) was strongly influenced by temperature changes in the first condenser. By increasing the temperature of the first condenser from 80 to 120 °C, an increase in the yield of AC from about 18 wt.% to 35–45 wt.% was observed. This is expected, as higher temperatures in this unit would not be conducive to the condensation of water (boiling point: 100 °C), and hence more water was passed on and recovered in the second condensation stage. Westerhof et al. [19] made similar observations when they varied C1 temperatures between 20 and 81 °C and recorded a gradual increase in the yield of their AC at different biomass pyrolysis temperatures. Increasing the temperature in the second condensation stage had a comparatively weaker influence on AC yield. At a fixed upper-limit temperature of 120 °C in the first condenser, the yield decreased from approximately 45 to 35 wt.% as the second condenser temperature increased from 10 to 50 °C. At a fixed lower-limit temperature of 80 °C in the first condenser, hardly any change in AC yield was observed with an increase in temperature in the second condensation stage (Fig. 4.1e).

In Fig. 4.1f, the influence of condensation temperature in the second-stage condenser did not significantly affect the mass fraction of water (water content) in the AC. Although temperature decrease from 50 to 10 °C in C2 would be expected to enhance water condensation, given the significant difference in vapor pressure, this was not clearly reflected in the results. This was attributed to the simultaneous condensation of other low-boiling-point components (evident

in the peaked condensation of inhibitory compounds in Fig. 4.1b) at 10 °C, which diluted the increased water concentration. Nevertheless, with increasing temperature in the first condenser, the water content slightly decreased from approximately 85 to 80 wt.%.
The observed trends for all the parameters discussed suggest that, within the investigated temperature ranges, a combination of 120 °C (first-stage condenser) and 50 °C (second-stage condenser) provided optimum conditions for maximum substrate recovery, minimum inhibitor content, and optimal AC yield.

4.2.1.2 *Miscanthus* and Coffee Husk

As with wheat straw, similar trends were observed in the evolution of substrate content with increasing condenser temperatures for the cases where *miscanthus* and coffee husk were used as biomass feedstock. The highest substrate mass fraction (about 31 and 32 wt.%, respectively, for *miscanthus* and coffee husk) was recorded at temperature combinations of 120 and 50 °C in the first- and second-stage condensers, respectively.

It is interesting to note that the corresponding mass fractions of substrates were about twice as high in ACs recovered from *miscanthus* and coffee husk compared to those from wheat straw. This was attributed to the relatively higher amounts of carboxylic acids, such as acetic and propionic acids, which constitute the major fraction of substrate compounds originally present in the volatiles generated following the pyrolysis of these feedstocks (Table A4, Appendix A). As shown in Table A4, the mass fractions of acetic and propionic acid in the volatiles from *miscanthus* and coffee husk were about twice as high as those recorded from wheat straw. This also suggests possible similarities in the chemical compositions and degradation mechanisms of *miscanthus* and coffee husk.

Unlike wheat straw, where a decrease in the mass fraction of inhibitors was observed with increasing condensation temperatures, the mass fraction of inhibitors in ACs from *miscanthus* and coffee husk increased notably, especially with a temperature rise in C1. Increases in inhibitor yield of about 0.38 and 0.37 wt.% were observed for *miscanthus* (Fig. 4.2b) and coffee husk (Fig. 4.3b), respectively, when the temperature of C1 rose from 80 to 120 °C. Nonetheless, an increase in C2 temperature had no significant effect on the inhibitor mass fractions. Again, in contrast to wheat straw, the lowest inhibitor mass fractions were recorded at temperature combinations of 80 and 10 °C in C1 and C2, respectively, for both feedstocks.

These contrasting trends for *miscanthus* and coffee husk compared to wheat straw result from the varying compositions of the inhibitor, 3-hydroxypropionaldehyde, in the pyrolysis volatiles of these biomass feedstocks (Table A4, Appendix A). This strong inhibitor was present only in negligible amounts in the wheat straw pyrolysis volatiles and was hardly detected in its subsequently recovered AC. Its concentration in the volatiles of *miscanthus* and coffee husk was, however, fairly significant and increased in the AC with rising C1 temperature, though only at lower corresponding C2 temperatures. It was also noted that the mass fractions of other inhibitors, such as vanillin and furfural, were at least three times higher in the pyrolysis volatiles of *miscanthus* and coffee husk than in those from wheat straw (Table A4, Appendix A).

In effect, the evolution of the substrate-to-inhibitor ratio (P/I) with increasing temperature in both condensers followed a different pattern for *miscanthus* and coffee husk compared to wheat straw. Unlike wheat straw, where this ratio increased steadily and peaked at 120 °C/50 °C (C1/C2), it first increased for *miscanthus* and coffee husk with rising temperatures in both C1 and C2, peaked at 100 °C/50 °C (for miscanthus) (Fig. 4.2c) and about 95 °C/50 °C (for coffee husk) (Fig. 4.3c), and then decreased with further temperature increases. This corroborates the observation that inhibitory compounds became more pronounced at higher condensation temperatures for *miscanthus* and coffee husk, unlike wheat straw, where inhibitor mass fractions were suppressed at elevated temperatures in both condensers.

Yields of AC and water content for *miscanthus* (Fig. 4.2e and Fig. 4.2f) and coffee husk (Fig. 4.3e and Fig. 4.3f) followed similar trends to wheat straw, except that water content was about 10 wt.% lower under all comparable temperature conditions. This is expected, as wheat straw volatiles contain more water than those from *miscanthus* and coffee husk (Table A4, Appendix A), another observation supporting similarities in composition and degradation mechanisms between *miscanthus* and coffee husk.

Unlike wheat straw, which showed optimal AC and substrate yields with minimal inhibitor content at C1/C2 = 120 °C/50 °C (Fig. 4.1d), the optimal conditions for *miscanthus* and coffee husk were less distinct (Fig. 4.2d and Fig. 4.3d). Although maximum substrate yields with minimal inhibitors occurred at 100 °C/50 °C (*miscanthus*) and about 95 °C/50 °C (coffee husk), the AC yield at these conditions was not maximal. Maximum AC yields were only observed at C1/C2 = 120 °C /10 °C (Fig. 4.2e and Fig. 4.3e), although inhibitor content was highest at these

settings. Nonetheless, the 120 °C/50 °C combination appears to be the best compromise, producing significantly higher substrate levels relative to inhibitors (only 1–2.5 units below optimum values in Fig. 4.2c and Fig. 4.3c) and AC yields only 5–6 wt.% below their peak values.

It is, however, important to highlight that the ORC is the main product of the fast pyrolysis process, while AC is a side stream. Under the recommended optimal condensation conditions for valorizing substrates from AC, the yield of the main product (ORC) decreased compared to normal conditions. Table 4.1 shows ORC yields for wheat straw, *miscanthus*, and coffee husk decreased by 23, 15, and 17%, respectively, when C1 temperature increased from the conventional 90 °C to 120 °C. This trade-off may affect the economic feasibility of the new concept (valorizing AC while recovering viable amounts of ORC). Nonetheless, minimal changes were observed in the total energy recovered from the ORC at higher condensation temperatures, indicating that the yield loss is largely due to reduced water content in the ORC.

Table 4.1. ORC yields at conventional (90 °C) and optimal (120 °C) C1 condensation temperatures, with corresponding percentage decreases for wheat straw, miscanthus, and coffee husk

	ORC yield (wt.%) at different C1 temperatures		
C1 Temperature (°C)	Wheat straw	*Miscanthus*	Coffee Husk
90 (conventional)	60	65	65
120 (optimized)	46	55	54
Percentage decrease	23.3	15.4	16.9

Note: The percentage decrease represents the reduction in ORC yield as the temperature increased from conventional to optimized conditions.

4.2.2 Experimental Validation of Theoretical Models Using a 10 kg/h PDU

4.2.2.1 Comparison of Experimental Data with Model Predictions for Yields of Substrates, Inhibitors, AC, and Water Content

The recommended optimum conditions (120 and 50 °C in the first- and second-stage condensers, respectively) for substrate recovery in the AC, as obtained from the modeling study, were implemented on a 10 kg/h pyrolysis PDU (described earlier in Section 3.2.3) to validate the model predictions for all three biomass feedstocks (wheat straw, *miscanthus*, and

coffee husk). Subsequently, comparisons between the model predictions and experimental data were also performed under conventional condensation temperature conditions in the PDU (90 and 15 °C in the first- and second-stage condensers, respectively), and these model predictions and experimental data were then compared with those obtained under the recommended optimum conditions for wheat straw (Fig. 4.4) and *miscanthus* (Fig. 4.5a,b). Comparisons of model predictions with experimental data for coffee husk were made only under the recommended optimum temperature combination, due to limited data availability (Fig. 4.5c).

For wheat straw, aside from significant deviations between the model and experimental data for inhibitory compounds, the theoretical model generally agreed with experimental results from the PDU (Fig. 4.4). Model predictions were even more accurate at conventional condensation temperatures (C1/C2 = 90 °C/15 °C), with percentage deviations of only 1% (under-prediction), 8% (under-prediction), and 14% (over-prediction) observed for AC water content, AC yield, and mass fraction of substrates, respectively (Fig. 4.4a). Similar trends were observed under optimum condensation temperatures (C1/C2 = 120 °C/50 °C), except that deviations at these temperature conditions (for all parameters except inhibitors) were comparatively higher (Fig. 4.4b), which is consistent with the model's known limitations, as G^E models like UNIFAC-DMD are valid only up to a maximum temperature of 120 °C (as noted earlier in Section 2.3.2 of the literature review).

Interestingly, the deviations observed for AC yield and its corresponding water content were not as pronounced compared to those for inhibitory and substrate components. This is because the calculation of AC yield was primarily based on the overall mass balance of the process without considering interaction parameters between components. For water content, the minimal deviations observed were attributed to the fact that water comprises the major fraction of the AC and hence its interaction with the highly dilute components is negligible and not complex enough to fall outside the predictive range of UNIFAC-DMD.

The trends were no different for *miscanthus* and coffee husk biomass feedstocks, where model predictions were also largely in agreement with experimental data (Fig. 4.5).

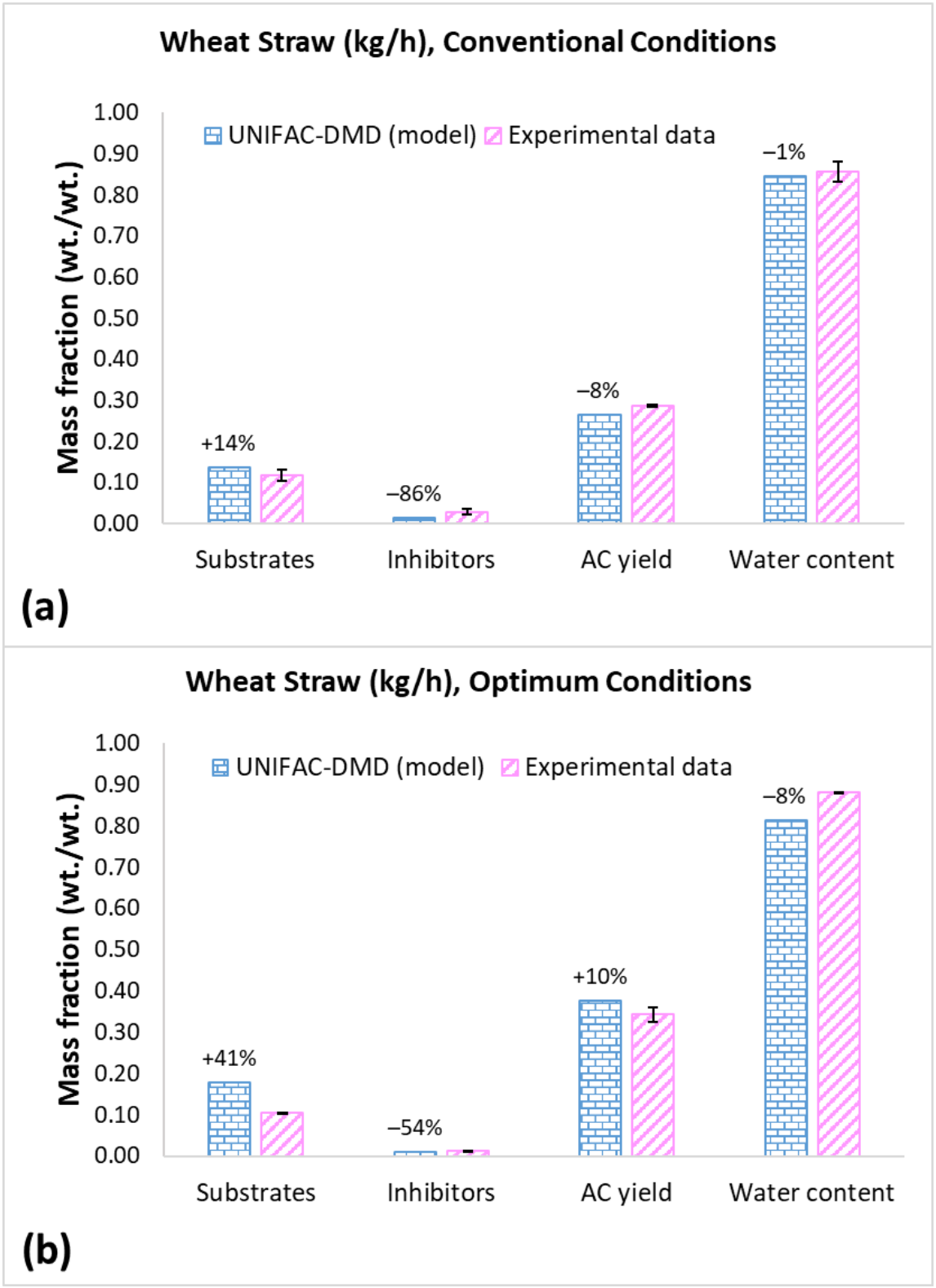

Fig. 4.4. Comparison of theoretical UNIFAC-DMD model predictions with experimental data from the PDU for wheat straw pyrolysis, showing percentage deviations: (a) conventional condensation temperatures (C1/C2 = 90 °C/15 °C); (b) optimum condensation temperatures (C1/C2 = 120 °C/50 °C). Experimental data represent the mean values from three replicates, with error bars indicating the corresponding standard deviations.

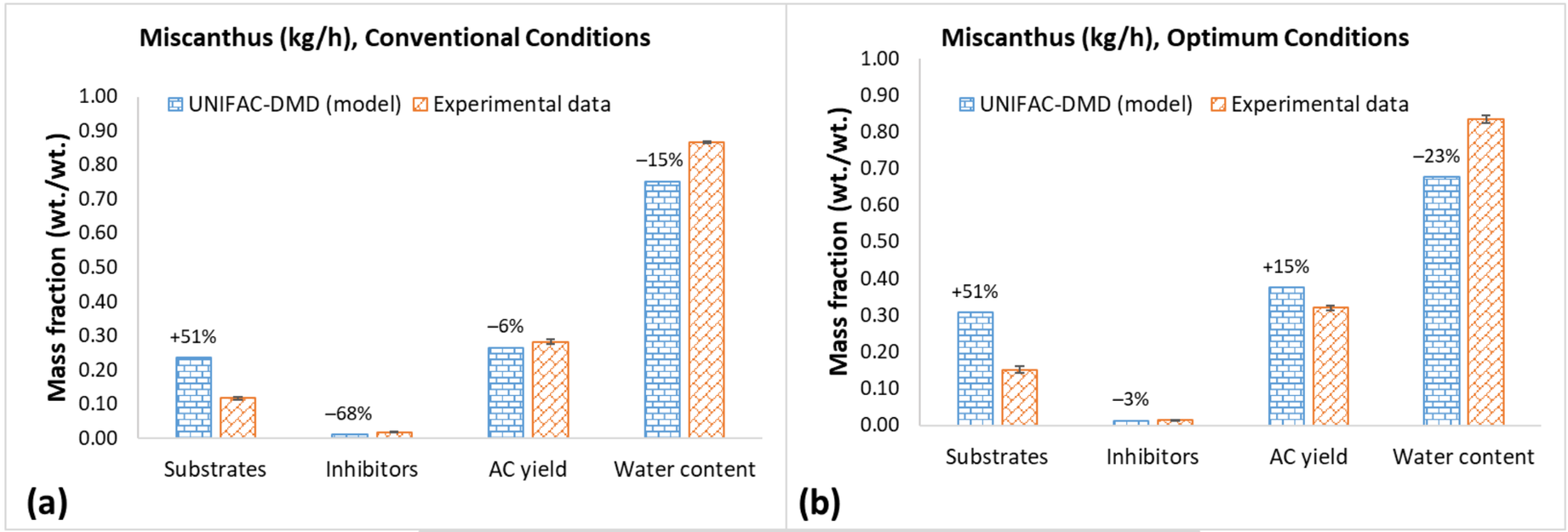

Fig. 4.5. Comparison of theoretical UNIFAC-DMD model predictions with experimental data from the PDU for miscanthus and coffee husk, showing percentage deviations: (a) conventional condensation temperatures (C1/C2 = 90 °C/15 °C) for miscanthus; (b) optimum condensation temperatures (C1/C2 = 120 °C/50 °C) for miscanthus; and (c) optimum condensation temperatures (C1/C2 = 120 °C/50 °C) for coffee husk. Experimental values represent the means of three replicate runs, with error bars indicating the corresponding standard deviations.

For all three biomass feedstocks, at all temperature combinations investigated, the mass fractions of substrates and inhibitors tend to be the parameters with the strongest deviations, particularly for inhibitors. This is attributed to their comparatively low concentrations relative to the overall amount of AC. As discussed in Section 2.3.2 of the literature review, one known limitation of the UNIFAC-DMD model is its inability to accurately handle the infinite dilution of hydrocarbons in water. Given the significantly low concentrations of these organic compounds in AC, the stronger deviations observed are understandable. The deviations may also be due to the uncertainties in the pure-component vapor pressure data for some of the compounds. This is particularly the case for compounds estimated using the Extended Antoine equation (due to lack of experimental data), for which some associated uncertainties are definite. It is also worth noting that the thermodynamic modeling is based on the assumption that the condensation system was in equilibrium. As this is rarely the case for the experimental setup, the deviations observed between model predictions and experimental data were to be expected. Regardless, the UNIFAC-DMD thermodynamic model, to a large extent, predicted the VLE behavior of the fast pyrolysis volatiles, although its limitations in handling highly dilute concentrations of organic compounds in water became evident. In that regard, more complex group contribution models, such as the Group Contribution Associating Equation of State (GCA-EoS), can potentially lead to a better prediction of these phase equilibria and should be considered in future studies.

4.2.2.2 Assessment of Experimental Data for the Secondary Parameters "P/I" and "P/I × AC Yield" Compared with Model Predictions

The experimental data for the parameters, "P/I" and "(P/I) × AC Yield," at optimum condensation temperature conditions (C1/C2 = 120 °C/50 °C) were compared with those at conventional condensation temperature conditions (C1/C2 = 90 °C/15 °C). Based on the available experimental data, the assessment was primarily conducted for wheat straw and *miscanthus* biomass feedstocks. Experimental data were also compared with model predictions.

In the assessment of "(P/I) × AC Yield" for wheat straw and *miscanthus* biomass feedstocks, experimental data confirmed that the optimum condensation temperature conditions were highly effective in promoting substrate formation over inhibitors at an optimal recovery of AC. Experimental data recorded for this parameter increased by about threefold (wheat straw)

and twofold (*miscanthus*) as condensation temperatures increased from conventional to optimum conditions (Table 4.2). It is important to note that this parameter is a secondary computation of different terms, and cumulative errors associated with each of the terms led to significant percentage deviations (within the ranges of +54 and +69%) of corresponding model-predicted values recorded. Regardless of model prediction deviations from experimental values, the trends observed as temperature conditions increased from conventional to optimized conditions were quite consistent.

Similar observations were made for the assessment of experimental data for "P/I," where data (for wheat straw and *miscanthus*) recorded at optimum conditions were nearly twice those recorded at conventional conditions (Table 4.3). As observed in the case of "(P/I) × AC Yield," substantial deviations of model-predicted data from experimental data were also observed, again attributed to the accumulation of errors associated with the individual terms that make up the parameter (i.e., weight percent of promoters, P, and inhibitors, I).

Interestingly, *miscanthus* and coffee husk recorded higher experimental values of "P/I" and "(P/I) × AC Yield" at optimum conditions than wheat straw. This suggests that *miscanthus* and coffee husk tend to be more promising sources of substrate recovery in AC as compared to wheat straw.

These deductions underpin the fact that a carefully controlled fractional condensation of pyrolysis volatiles has a significant impact on the distribution of substrates and inhibitors in pyrolysis condensates. Similar pronouncements were made by Liaw et al. [31] when they investigated the effects of temperature variations in the first condensation unit (at a fixed temperature of the second) on the yield of AC and product distribution of compounds in AC from the fast pyrolysis of Douglas Fir Wood. They also reported increased production of substrates and AC yield at the expense of inhibitory compounds at high temperatures of C1. Their study, however, did not take into consideration the simultaneous variations of temperatures of both condensation units.

Table 4.2. Comparison of experimental and model-predicted values of the parameter '(P/I) × AC Yield' under optimum (C1/C2 = 120 °C/50 °C) and conventional (C1/C2 = 90 °C/15 °C) condensation temperatures for all three biomass feedstocks.

C1/C2 temperature combinations (°C)	Wheat straw			*Miscanthus*			Coffee husk		
	(P/I) × AC Yield (exp.)	Model prediction	PD (%)	(P/I) × AC Yield (exp.)	Model prediction	PD (%)	(P/I) × AC Yield (exp.)	Model prediction	PD (%)
120/50	2.61 (±0.00)	7.01	+63	3.53 (±0.20)	8.51	+59	4.03 (±0.33)	10.42	+61
90/15	1.15 (±0.03)	2.49	+54	1.92 (±0.21)	6.19	+69	N/A	7.74	N/A

Note: exp.= experimental data; PD = percent deviation of model prediction from experimental data; N/A = no experimental data available.

Table 4.3. Comparison of experimental and model-predicted values of the parameter 'P/I' under optimum (C1/C2 = 120 °C/50 °C) and conventional (C1/C2 = 90 °C/15 °C) condensation temperatures for all three biomass feedstocks.

C1/C2 temperature combinations (°C)	Wheat straw			*Miscanthus*			Coffee husk		
	P/I (exp.)	Model prediction	PD (%)	P/I (exp.)	Model prediction	PD (%)	P/I (exp.)	Model prediction	PD (%)
120/50	7.58 (±0.10)	19.70	+62	11.04 (±0.47)	23.11	+52	10.35 (±0.42)	25.37	+59
90/15	4.02 (±0.45)	8.74	+54	6.80 (±0.59)	23.26	+71	N/A	26.91	N/A

Note: exp.= experimental data; PD = percent deviation of model prediction from experimental data; N/A = no experimental data available.

4.3 Influence of Selected Quench Media for Direct-Contact Condensation on the Yield and Composition of Fast Pyrolysis Bio-Oils

This sub-chapter discusses the influence of four selected quench media (QM) used for direct-contact condensation on the yield and composition of fast pyrolysis bio-oils (FPBOs): Isopar-V, water, ethylene glycol (glycol), and ethanol. Thermodynamic flash model simulations were first used to predict the effects of quenching temperature and the mass flow rate ratios of QM to pyrolysis volatiles (m_q/m_v) for all investigated QM. Subsequently, experimental validations of the model predictions were conducted at selected temperatures (for each QM) that enabled the practical condensation of the FPBOs. The integration of theoretical model predictions with experimental validations helped clarify previously unexplained experimental phenomena, broadening the applicability of phase equilibria modeling for fast pyrolysis systems.

4.3.1 Predicted Effects of Quench Temperature and m_q/m_v Ratio on FPBO Yield and Composition

Thermodynamic phase equilibria modeling was used to investigate the influence of quenching temperature (in the first stage condenser) and m_q/m_v ratio on product yield and the distribution of major chemical compounds in the FPBOs (i.e., the organic-rich (ORC) and the aqueous condensate (AC) fractions) for all the above-mentioned QM. Temperature ranges of 40 to 120 °C, together with the two extreme m_q/m_v ratio points of 0.5 and 2.0, were investigated.

4.3.1.1 Effects on FPBO Product Yield

The effects of the investigated ranges of quenching temperature and m_q/m_v on the yield of ORC and AC for all QM are shown in Fig. 4.6. The yield distribution for both fractions was reported on a dry, QM-free basis, relative to the total amount of pyrolysis volatiles entering the first condensation stage. Except for the water quench, the distribution of the ORC showed a downward trend as quenching temperature increased from 40 to 120 °C for both m_q/m_v ratios (Fig. 4.6a). For instance, at an m_q/m_v of 2.0, the ORC yield recovered using the glycol quench decreased steadily from about 43 to 37 wt.% as condensation temperature increased from 40 to 120 °C. Likewise, the m_q/m_v = 0.5 scenario recovered slightly lower yields of ORC,

also decreasing steadily from about 38 to 28 wt.% over the same temperature range. The decrease in ORC yield with increasing quenching temperature was attributed to the loss of compounds that could not be condensed at elevated temperatures and are only recovered in the subsequent low-temperature condensation stages. Similar observations were made for the ethanol QM.

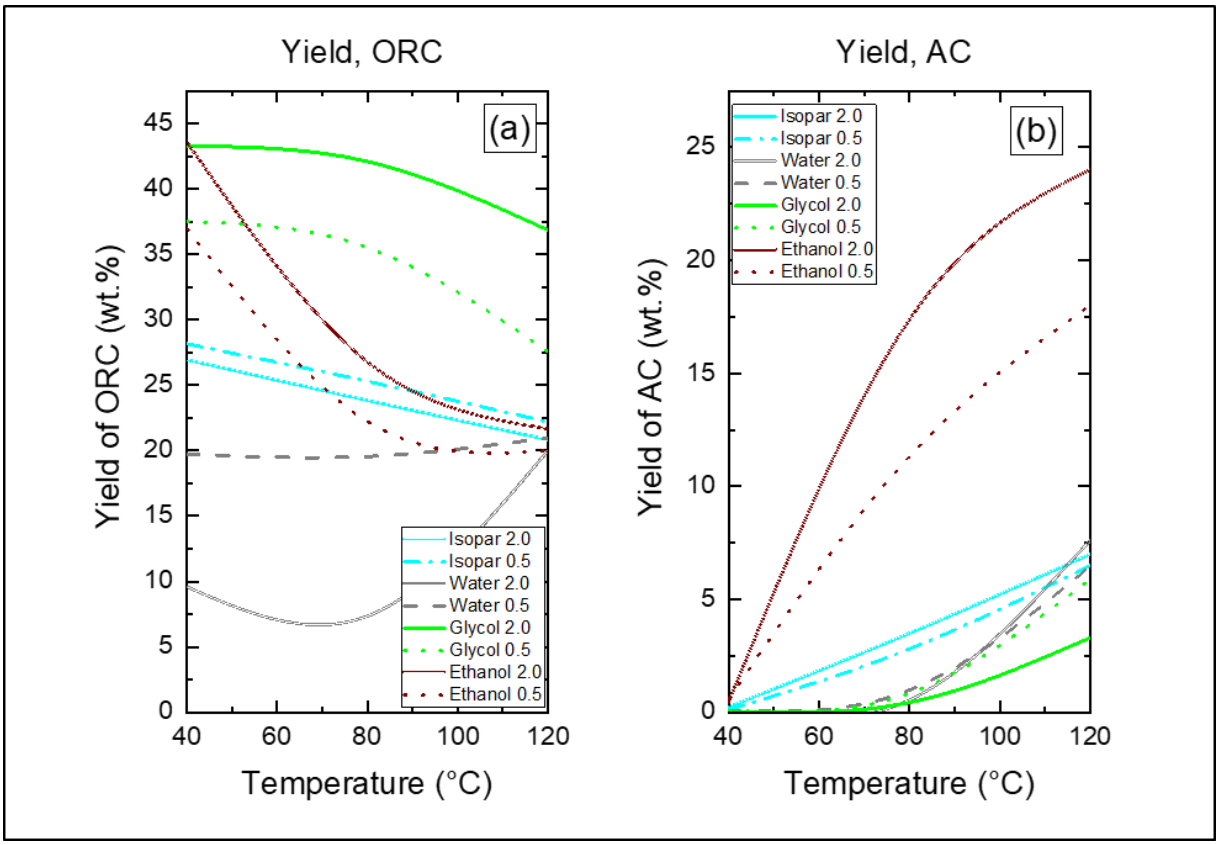

Fig. 4.6. Model-predicted effects of quenching temperature and the mass flow rate ratios of QM to pyrolysis volatiles (m_q/m_v) for all investigated QM on the yield of FPBOs: (a) ORC and (b) AC. Yields are reported on a dry, QM-free basis and relative to the total amount of volatiles that entered the first condensation stage.

At 40 °C, the lowest temperature investigated, both glycol and ethanol yielded the highest ORC fraction (about 43 wt.%) at an m_q/m_v = 2.0, closely followed by the m_q/m_v = 0.5, yielding about 38 wt.% at the same temperature. Both glycol and ethanol formed a miscible product with the recovered ORC. Isopar-V, which formed an immiscible product with the ORC, showed a steady decline in ORC yield from about 27 to 21 wt.% as temperature increased from 40 to 120 °C at an m_q/m_v = 2.0 (Fig. 4.6a). Similar observations were made for m_q/m_v = 0.5, except that for this QM, the lower m_q/m_v ratio recorded slightly higher ORC yields at all temperatures, attributed to increased mass transfer of components from the ORC to the quench at the higher QM ratio. A similar but more pronounced trend was observed for the

water QM, which also formed an immiscible product with the ORC (Fig. 4.6a). For this QM, an m_q/m_v = 2.0 at 40 °C resulted in a significantly low ORC yield (about 10 wt.%), attributed to substantial mass transfer of water-soluble components into the water quench. Interestingly, as the temperature rose, ORC yield sharply increased, reaching twice the yield obtained at 40 °C when the temperature reached 120 °C. At quenching temperatures above the boiling point of water, this is expected because much of the water quench remains in the vapor phase and is only recovered in subsequent stages, thereby minimizing mass transfer between the recovered quench and the ORC in this condensation stage and therefore increasing ORC yield. For m_q/m_v = 0.5, hardly any change in ORC yield was observed with the increase of quenching temperature.

Across all temperatures, the glycol quench recovered the highest ORC fraction, regardless of the m_q/m_v ratio. This was followed closely by ethanol, although its recovered ORC yield decreased substantially above 70 °C. The water quench essentially produced the lowest ORC yield at nearly all the temperatures investigated, while Isopar-V's recovery efficiency was intermediate between glycol and water.

The corresponding yields of all AC fractions increased for all QM as quenching temperature progressed from 40 to 120 °C (Fig. 4.6b). For all QM, very little AC was produced at 40 °C, suggesting that at such low temperatures, nearly all products were recovered in the first condensation stage. This makes such conditions favorable for single-stage condensation processes, as was later used for the recovery of anhydrosugars during pyrolysis vapor condensation, discussed further in Section 4.4.

The increase in AC yield with temperature rise was the sharpest for ethanol, rising from about 0.4 to 24 wt.% when temperature increased from 40 to 120 °C at m_q/m_v = 2.0. The m_q/m_v = 0.5 case exhibited similar trends but with generally lower AC yields. Although all the other investigated QM exhibited similar trends with temperature rise, their AC yields at all temperatures were significantly lower than ethanol (Fig. 4.6b). Ethanol's high volatility (boiling point ≈ 78 °C) meant that at quenching temperatures near or above this value, it vaporizes and barely induces condensation in the first stage. Vaporized ethanol then proceeds to the much colder second-stage, where it condenses and is recovered with the AC (i.e., the quenching effect of ethanol was only realized in the second condensation stage at increased condensation temperature in the first stage).

After ethanol, the Isopar-V quench recovered the highest AC fractions across most of the investigated temperature ranges and both m_q/m_v ratios, compared with the glycol and water quenches, which yielded the least fractions of the AC.

4.3.1.2 Effects on FPBO Composition: Moisture Content

The effects of quenching temperature and the m_q/m_v ratio on the moisture content of recovered FPBOs (ORC and AC) for all investigated QM are shown in Fig. 4.7. The moisture content has been reported on an 'as received' basis. For the water quench, the moisture content of its ORC at m_q/m_v = 0.5 slightly increased by about 0.5 wt.% as temperature increased from 40 °C to 80 °C, after which a further increase in temperature led to a drastic decrease of about 25 wt.% (Fig. 4.7a). Very similar trends were observed for the m_q/m_v = 2.0, but with slightly lower moisture content recorded for most of the temperature conditions investigated. Moisture content of the ORC recovered using the Isopar-V quench was also seen to decrease sharply from around 35–38 wt.% to just about 2 wt.% with temperature rise for both m_q/m_v ratios. Again, m_q/m_v = 0.5 showed relatively higher moisture at all temperatures. Moisture content of the ORC recorded using glycol and ethanol QM only slightly decreased with temperature rise for both m_q/m_v ratios (Fig. 4.7a). For these QM, m_q/m_v = 0.5 consistently showed higher moisture contents than the corresponding m_q/m_v = 2.0 across all temperatures, in a more pronounced manner. The lower moisture recorded at the higher m_q/m_v ratios is attributed to increased interaction between the ORC and its respective QM at higher dosing of the QM, resulting in greater transfer or loss of moisture from the ORC into the quench. This is further supported by the prominence of this phenomenon for the QM that formed a mixed product with the ORC (i.e., ethanol and glycol), where QM–ORC interactions are expected to be maximal.

The effects of quenching temperature and m_q/m_v ratio on the moisture content of the AC for all QM are shown in Fig. 4.7b. For the water quench, changes in either parameter hardly affected the moisture of the AC. Unsurprisingly, moisture content virtually remained at about 95 wt.% (for m_q/m_v = 2.0) and 90 wt.% (for m_q/m_v = 0.5) as temperature increased from 40 to 120 °C. For Isopar-V, a decrease from about 92–96 wt.% to around 72–73 wt.% for both m_q/m_v ratios was observed for the same temperature range. Glycol also showed decreases in AC moisture from about 76 to 60 wt.% (at m_q/m_v = 2.0) and 83 to 67 wt.% (at m_q/m_v =

0.5) as quenching temperature increased from 40 to 120 °C. Compared with all the other investigated QM, the ethanol quench recovered significantly less moisture in the AC (Fig. 4.7b). Only about 24 wt.% (at m_q/m_v = 0.5) and 8 wt.% (at m_q/m_v = 2.0) were recovered on average across all temperatures, showing minimal influence from temperature changes. The evidently decreased moisture content observed for the ethanol quench reflects interactions between ethanol and water, whereby vaporized ethanol forms an inseparable mixture with uncondensed water vapor, which proceeds downstream. This is supported by evidence of azeotrope formation between ethanol and water at around 78 °C, the boiling point of ethanol (Fig. B1, Appendix B), indicating that inseparable water vapor from uncondensed ethanol contributes to the marked decrease in moisture content of the resultant AC.

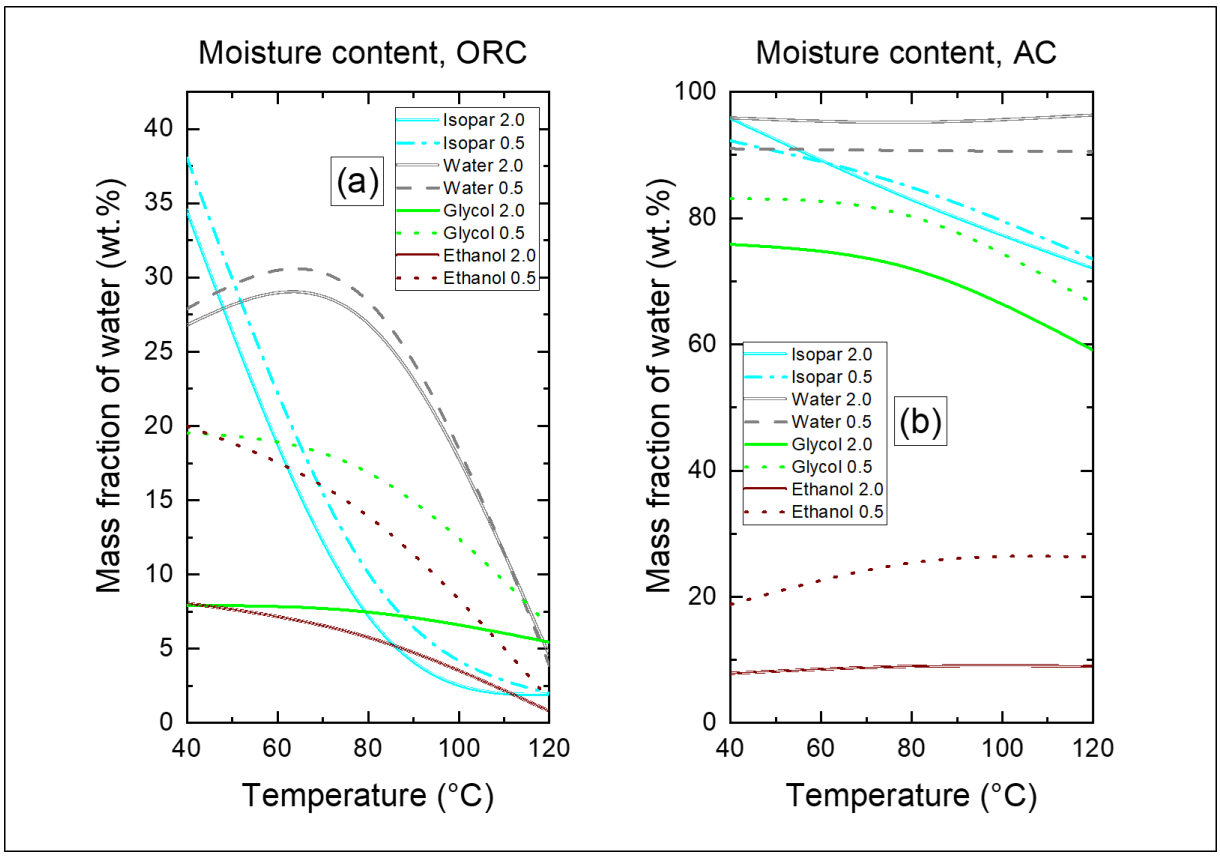

Fig. 4.7. Model-predicted effects of quenching temperature and the mass flow rate ratios of QM to pyrolysis volatiles (m_q/m_v) of all investigated QM on the moisture content of FPBOs: (a) ORC and (b) AC. Moisture content is reported on an "as-received" basis.

4.3.1.3 Effects on FPBO Composition: Distribution of Major Functional Group Compounds

The effects of quenching temperature and m_q/m_v ratios for all investigated QM on the distribution of several key functional group compounds that constitute the ORC and AC have been represented in Fig. 4.8 through Fig. 4.10. The functional group compounds investigated include carboxylic acids (acids), ketones, phenols, guaiacols, furans, and sugars. Mass fractions (concentrations) of all compounds have been reported on a dry and QM-free basis and relative to the total amount of volatiles that entered the first condensation stage.

In the ORC, acid concentrations generally decreased with increasing quenching temperature for all QM, regardless of m_q/m_v ratio (Fig. 4.8a). The most pronounced decrease occurred for the ethanol quench, followed by Isopar-V and glycol, with water showing the smallest decline. This trend is not surprising, as increased quenching temperature would increase the tendency of the acids to remain in the vapor phase and be recovered in the low-temperature second condensation stage.

For glycol, the m_q/m_v = 2.0 ratio consistently produced higher acid concentrations than m_q/m_v = 0.5 across all temperatures, whereas the opposite was observed for water. As acetic acid is highly water-soluble, higher water-quench ratios favor its transfer to the spent quench phase, explaining the lower acid content in the ORC for m_q/m_v = 2.0. In contrast, higher glycol ratios lower condensation temperatures (Table 3.3), enhancing acid retention in the ORC.

Aside from the glycol and water quench, where distinctive trends were noted for the m_q/m_v ratios, the trends observed for the other QM (ethanol and Isopar-V) did not follow any clear patterns. For instance, between the temperature range of 40 and 65 °C, the acids recovered by the ethanol quench at m_q/m_v = 2.0 were higher than those at m_q/m_v = 0.5, with the converse true at temperatures above 65 °C (Fig. 4.8a). Additionally, the differences in concentrations observed between the two m_q/m_v ratios across all temperatures were negligible. Comparable observations were also made for the Isopar-V quench.

Overall, the highest acid concentrations in the ORC were consistently achieved with glycol, regardless of temperature or ratio, followed by ethanol. Isopar-V generally retained more acids than water, except above 75 °C, where the water quench at m_q/m_v = 0.5 surpassed it. This pattern mirrors the ORC product yield trends (Fig. 4.6a) discussed in Section 4.3.1.1.

Compared to the deductions made for the distribution of acids in the ORC, very similar trends were observed for all the other functional group compounds investigated, particularly for the ketones (Fig. 4.8c), phenols (Fig. 4.9a), guaiacols (Fig. 4.9c) and furans (Fig. 4.10a), predominantly with increasing quenching temperature, which resulted in the steady decrease in concentrations of these functional group compounds in the ORC. However, the rate of decrease in the concentration of sugars in the ORC with increasing temperature was less severe than for the other investigated compounds (Fig. 4.10c). For the water quench, the concentrations of sugars even increased slightly with increasing temperature (Fig. 4.10c). Sugars are highly soluble in water, and at higher quenching temperatures, a significant fraction of the water quench is lost as vapor to subsequent condensation stages. This implies that, under higher water quench conditions (which would typically occur at low quenching temperatures and at a higher m_q/m_v ratio), lower concentrations of sugars in the ORC would occur. This, therefore, explains the increased concentration of sugars in the ORC observed with increasing temperature and the comparatively lower sugar concentrations recorded for the m_q/m_v = 2.0 ratio.

The concentrations of acids recovered in the AC for all investigated QM increased with the increase in quenching temperature for all m_q/m_v ratios (Fig. 4.8b). However, the rate of increase was more noticeable for the ethanol quench, which recorded a sharp increase from around 0.46 to 11.12 wt.% (at m_q/m_v = 0.5) and 0.27 to 12.92 wt.% (at m_q/m_v = 2.0) as quenching temperature increased from 40 to 120 °C. With the highly volatile nature of ethanol, a major fraction of this quench was only condensed in the low-temperature second-stage condenser when the first condensation stage operated at higher quenching temperatures. Acids are highly water-soluble, and as ethanol forms an azeotropic mixture with water (i.e., the aqueous fraction), acids retained in the azeotropic mixture, which could not condense in the first condensation stage at high temperatures, were only recovered in the low-temperature second-stage condenser as AC. Aside from ethanol, a steady increase in the concentration of acids was noted for the Isopar-V quench. Additionally, the Isopar-V quench generated comparatively higher concentrations of acids in the AC for most of the investigated temperature range compared to glycol and water. Nevertheless, the concentrations recorded were much lower (up to a maximum of about 4 wt.% recorded at m_q/m_v = 0.5) than those recorded for the ethanol quench. Concentrations of acids in the AC recovered using the glycol

and water QM also showed sudden increases when quenching temperatures reached about 70 °C, which then progressed steadily until 120 °C. This was most particularly evident for their m_q/m_v = 0.5 scenarios, where acid concentrations reached 4.0 wt.% at 120 °C for both QM (Fig. 4.8b).

Very similar evolution of concentrations in the AC with increasing quenching temperature and m_q/m_v ratio was observed for ketones (Fig. 4.8d) and furans (Fig. 4.10b), where an increase in temperature saw a steady increase in the concentrations of these compounds in the AC for all investigated QM. Just as observed for the acids, the rate of increase was the most severe for the ethanol quench and the least severe for the glycol quench. The concentrations of phenols (Fig. 4.9b), guaiacols (Fig. 4.9d), and sugars (Fig. 4.10d) only began to increase after the quenching temperature reached 70 °C for all investigated QM. Notably, for all QM, very low concentrations (less than 0.10 wt.%) of sugars were detected in the AC compared to all the other functional group compounds investigated. Among all these functional group compounds, sugars have the highest average molecular weight and hence the highest boiling point. This implies that most of this compound would be retained in the high-temperature first condensation stage, with only traces proceeding to the second-stage condenser and hence the very low concentrations detected in this stage.

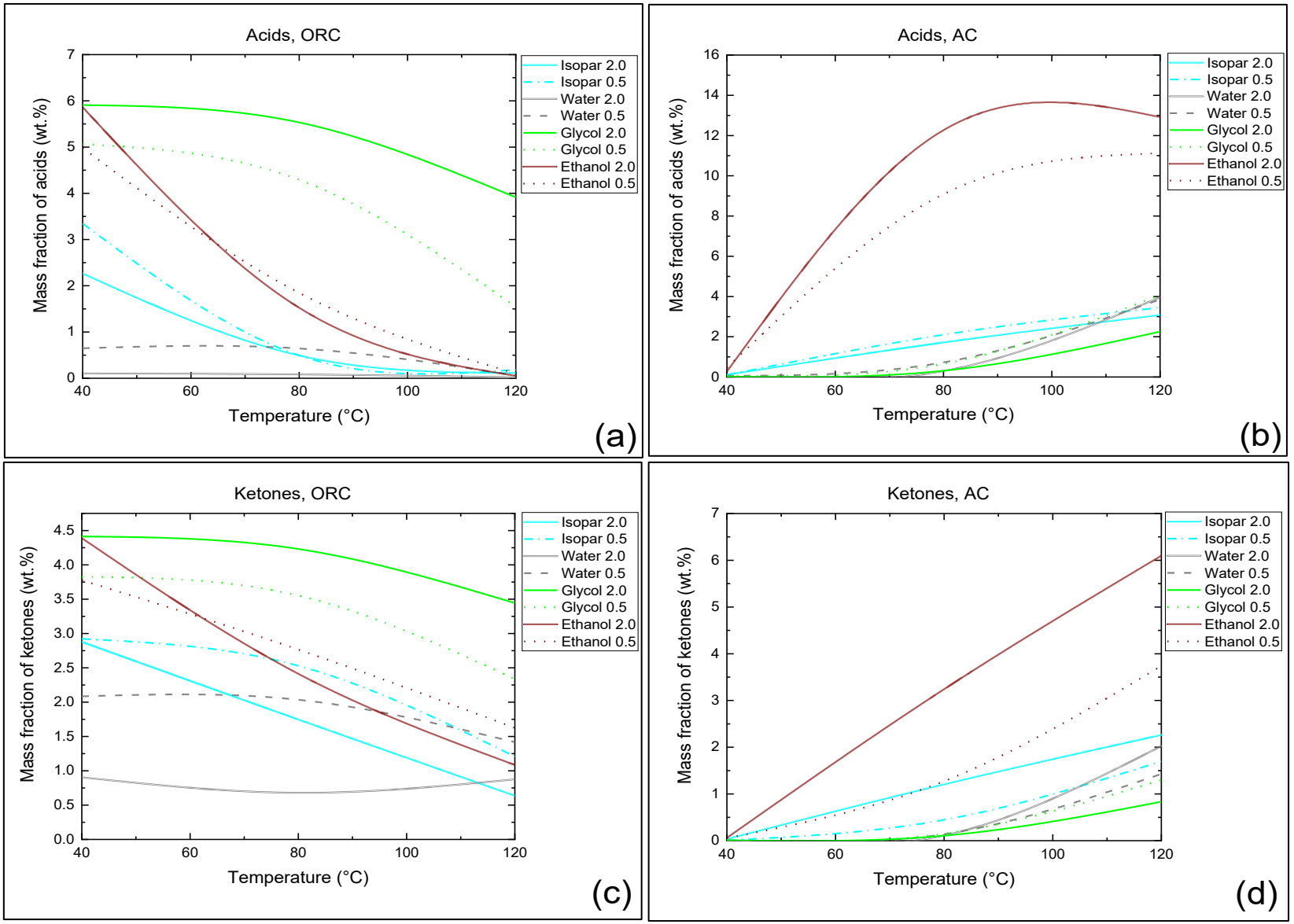

Fig. 4.8. Model-predicted effects of quenching temperature and the mass flow rate ratio of QM to pyrolysis volatiles (m_q/m_v) on the concentrations of acids and ketones in FPBOs: (a) acids in ORC, (b) acids in AC, (c) ketones in ORC, and (d) ketones in AC. Concentrations are reported on a dry, QM-free basis, relative to the total volatile input to the first condensation stage.

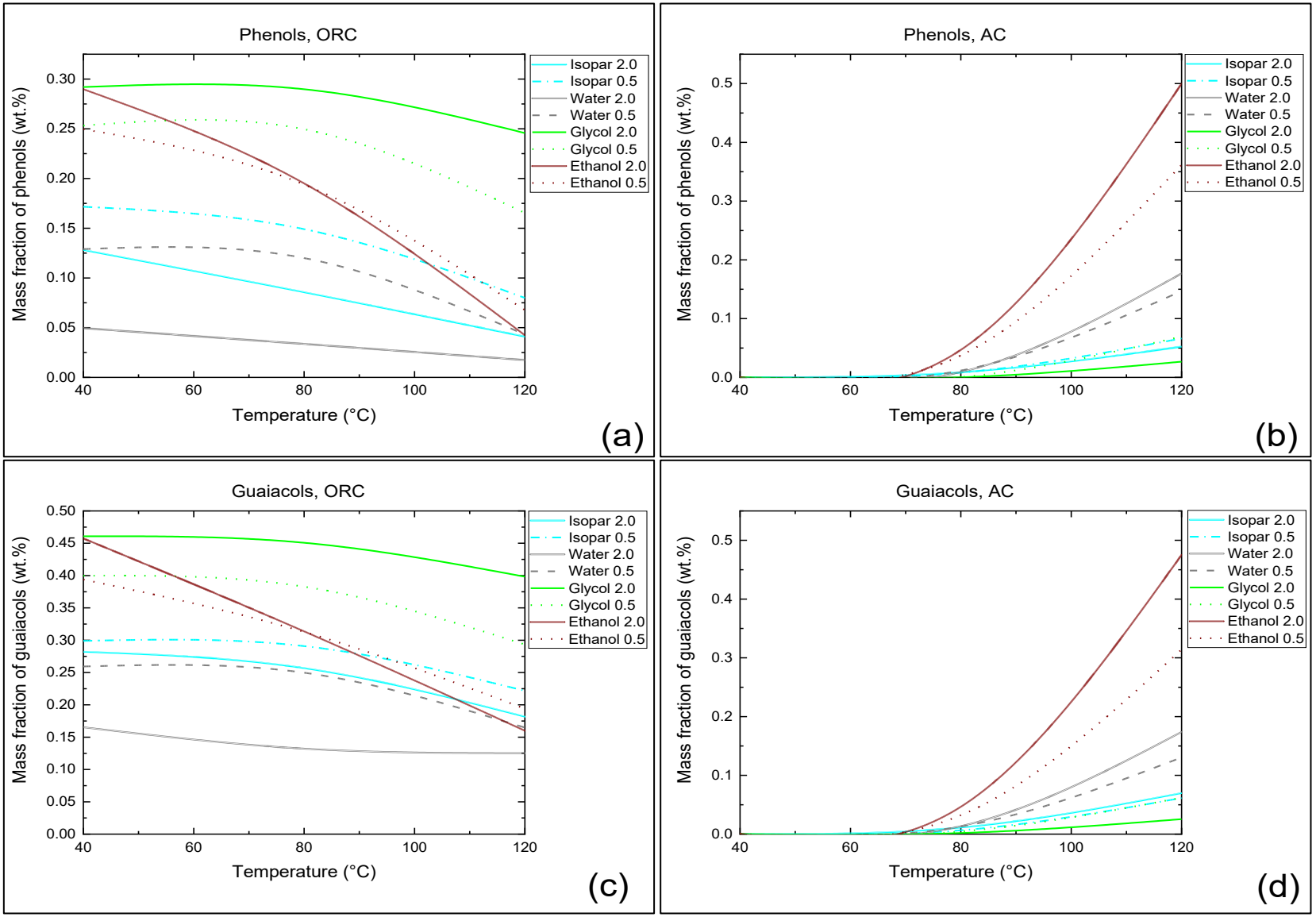

Fig. 4.9. Model-predicted effects of quenching temperature and the mass flow rate ratios of QM to pyrolysis volatiles (m_q/m_v) on the concentrations of phenols and guaiacols in the FPBOs: (a) phenols in ORC, (b) phenols in AC, (c) guaiacols in ORC and (d) guaiacols in AC. Concentrations are reported on a dry, QM-free basis, relative to the total volatile input to the first condensation stage.

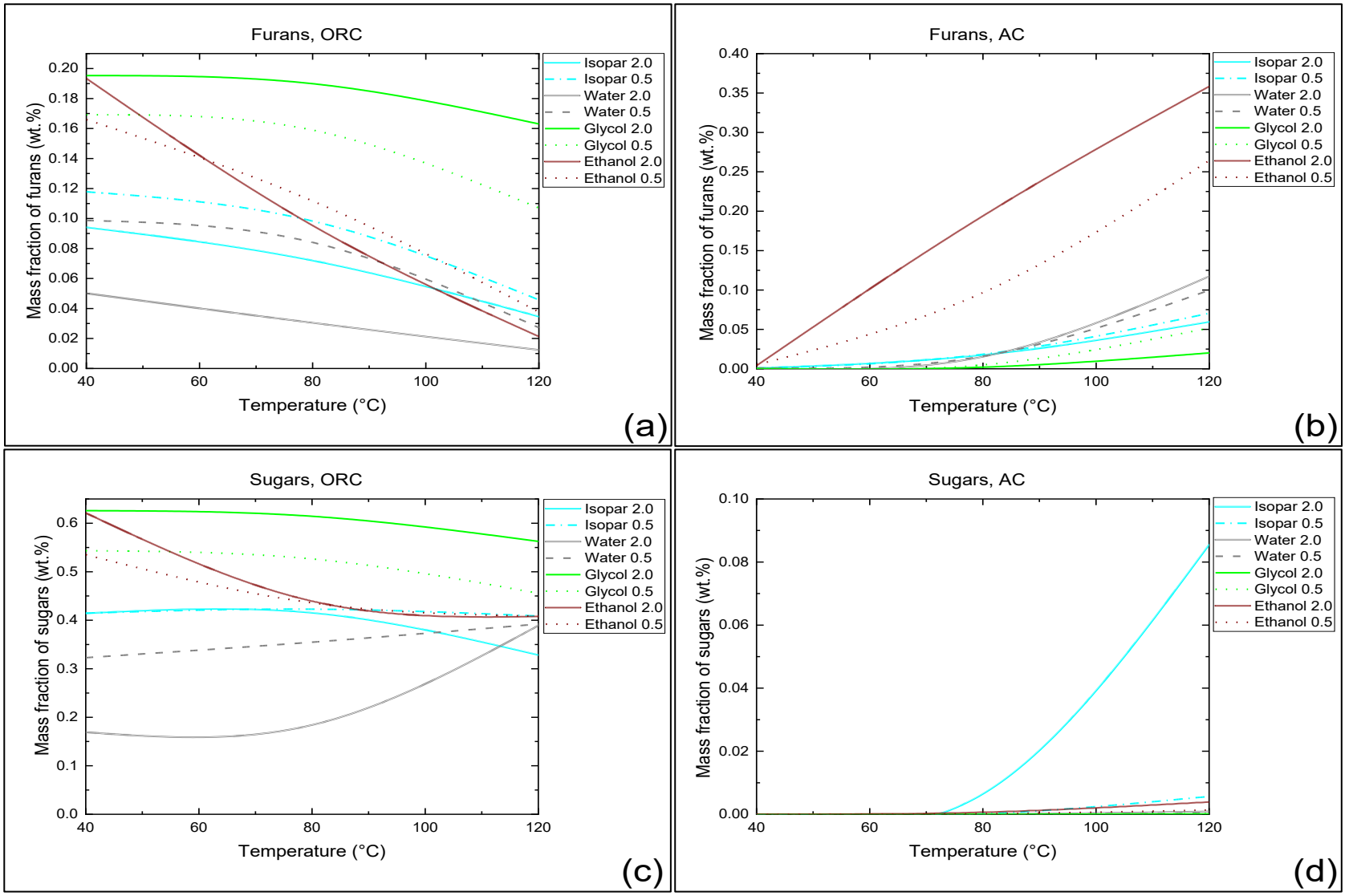

Fig. 4.10. Model-predicted effects of quenching temperature and the mass flow rate ratios of QM to pyrolysis volatiles (m_q/m_v) on the concentrations of furans and sugars in the FPBOs: (a) furans in ORC, (b) furans in AC, (c) sugars in ORC and (d) sugars in AC. Concentrations are reported on a dry, QM-free basis, relative to the total volatile input to the first condensation stage.

4.3.1.4 Key Findings from Model Predictions

Except for the water quench, an increase in quenching temperature resulted in a decrease in the yield of the resulting ORCs for all the other investigated QM. Ethanol and glycol formed miscible products with the recovered ORC, and in particular, glycol recorded the highest ORC yields across most of the temperature conditions investigated. For both ethanol and glycol, an m_q/m_v ratio of 2.0 resulted in higher ORC yields compared to the corresponding ratio of 0.5. In contrast, Isopar-V and water formed immiscible products with the recovered ORC, and for these two QM, higher m_q/m_v ratios led to lower ORC yields at all temperatures, consistent with enhanced mass transfer between these QM and the ORC. Increasing the quenching temperature also increased AC yields for all investigated QM, with the effect being most pronounced for the ethanol quench.

Substantial decreases in moisture content of the ORC were observed for the QM that formed immiscible products with the ORC (i.e., water and Isopar-V) as quenching temperature increased. In contrast, for QM that formed miscible products with the ORC (i.e., ethanol and glycol), the corresponding ORCs exhibited only a modest reduction in moisture content with increasing temperature. As expected, when water was used as the quench, the AC moisture content remained above 90 wt.% and was largely unaffected by either quenching temperature or the m_q/m_v ratio. For Isopar-V and glycol, AC yields steadily decreased with increasing quenching temperature. Although the AC moisture content obtained with ethanol quenching was relatively insensitive to temperature, yields were markedly lower (only about 24 wt.% at most) compared with those from the other quenches. This effect was attributed to interactions between vaporized ethanol and water vapor.

For functional group compounds, the concentration of acids in the ORC decreased with an increase in quenching temperature for all QM, irrespective of the m_q/m_v ratio. The ethanol quench showed the steepest decline, while water showed the least. In the case of glycol, an m_q/m_v = 2.0 yielded higher acid concentrations than 0.5, whereas the opposite trend was observed for water. The effects of m_q/m_v ratio showed no consistent trends for the Isopar-V and ethanol quenches. Across all temperatures, glycol retained the highest concentrations of acids in the ORC, followed by ethanol, Isopar-V and water. Ketones, phenols, guaiacols, furans, and sugars exhibited trends comparable to those reported for acids. However, an additional observation was that sugar concentrations in the ORC increased with rising quenching

temperature when water was used as the quench. This was attributed to the high solubility of sugars in water, as higher temperatures are associated with less water, which also explains the relatively lower sugar concentrations observed for m_q/m_v = 2.0.

In the AC, acid concentrations increased with temperature regardless of the m_q/m_v ratio, with the effect being most pronounced for ethanol. Similar trends were observed for the other compound groups, while only negligible amounts of sugars were recovered in the AC across all QM, owing to their high molecular weight and boiling point.

Overall, the thermodynamic phase equilibria model predictions demonstrated that both quenching temperature and m_q/m_v ratio influence the yield and composition of FPBOs, independent of the QM type. Model performance compared with selected experimental data is discussed in the following section.

4.3.2 Experimental Validation of Model Predictions

In this section, selected data points from the theoretical model predictions were experimentally validated on a 10 kg/h PDU, and deviations from the experimental data were assessed. The comparison was carried out for both product yield distributions and product compositions. Due to the varying volatilities and boiling points of the different QM, experiments were conducted at distinct condensation temperatures (previously presented in Table 3.2) to enable efficient recovery of FPBOs via fractional condensation, particularly for ethanol and water. Consequently, it was not possible to apply identical temperature conditions across all QM, which represents a limitation when comparing different QM with distinct physical properties under experimental conditions.

4.3.2.1 Investigation of FPBO Yield Distribution

4.3.2.1.1 Experimental Investigations

On average, 92 and 99 wt.%, respectively, of the total Isopar-V and glycol originally utilized were recovered with their corresponding ORCs in the first condensation stage (Table 4.4). In contrast, ethanol, due to its high volatility and low boiling point, was more widely distributed, with about 45 and 30 wt.% recovered in the first and second stages, respectively. An additional 20–25 wt.% was lost as vapor with the non-condensable gases. As water formed a homogeneous mixture with the AC, recovery in the second stage could not be quantified.

Nevertheless, over 80 wt.% (m_q/m_v = 2.0) and 50 wt.% (m_q/m_v = 0.5) of the water quench were recovered in the first condenser (Table 4.4).

Table 4.4. Fractions of spent QM recovered (wt.%) at each condensation stage.

	$m_q/m_v - 2.0$		$m_q/m_v - 0.5$	
Quench	Condenser 1	Condenser 2	Condenser 1	Condenser 2
Isopar-V	95.8	0.1	89.0	0.52
Ethylene glycol	>99.0	<1	95.0	<1
Ethanol	60.1	18.5	30.3	42.4
Water	81.7	n/a	50.1	n/a

Note: n/a.= not applicable.

The effects of the investigated QM on the product yield distribution of both ORC and AC are shown in Fig. 4.11. Yields of all FPBOs are presented on a dry, QM-free basis, relative to the total volatiles entering the first condensation stage. Consistent with model predictions, the experiments were conducted at two extreme QM-to-volatile mass ratios (m_q/m_v = 0.5 and 2.0), which determine the quenching temperature and cooling extent of the hot volatiles. Theoretical predictions of the condensation effects associated with each QM (Fig. 4.11b) were compared with experimental results (Fig. 4.11a).

At m_q/m_v = 2.0, ethanol produced the highest fraction of ORC, recovering about 54 wt.% of pyrolysis volatiles as ORC. This was followed by ethylene glycol, which yielded about 26 wt.%. Water and Isopar-V gave the lowest ORC yield, recovering only about 13 wt.% each (Fig. 4.11a). Similar trends were observed at m_q/m_v = 0.5, except that the ORC yield with ethanol dropped to about 29 wt.%. This indicates that a higher ethanol-to-volatile ratio enhanced interactions (as subsequently observed and discussed in Section 4.3.2.3) with major compounds such as carboxylic acids and ketones, increasing their condensation into the ORC. At this ratio, ethanol also produced a lower QM/ORC mixture temperature (50 °C; Table 3.3), sufficient to suppress secondary cracking reactions and enable comparatively higher ORC recovery.

It was subsequently observed that the QM that formed mixed phases with the ORC (ethanol and ethylene glycol) yielded more ORC than the immiscible QM (Isopar-V and water). This was

corroborated by the loss of organic compounds from the ORC, arising from molecular mass transfer between the ORC and the immiscible QM. This is consistent with earlier observations made from model predictions, discussed in Section 4.3.1.1. Although Isopar-V has demonstrated physical immiscibility with the ORC, some mass transfer was evident from the coloration of the spent quench. A similar emulsification phenomenon was reported by Bronson et al. [116], particularly for ash-rich feedstocks such as wheat straw.

For all QM and at both m_q/m_v ratios, the fractions of pyrolysis volatiles recovered as AC in the second condensation stage were below 10 wt.% (Fig. 4.11a). Ethanol generated the highest AC fraction at both ratios, producing nearly double that of the other QM, whose AC yields averaged about 4 wt.%.

4.3.2.1.2 Model Predictions and Extent of Deviation from Experimental Data

Average absolute relative deviations (AARDs), defined as the average of the individual Absolute Relative Deviations (ARDs) of model-predicted data with respect to experimental data for the ORC yields of all QM, ranged between 45% (at m_q/m_v = 0.5) and 50% (at m_q/m_v = 2.0). The deviations were even more widespread for ACs, spanning from 56% (m_q/m_v = 0.5) to 63% (m_q/m_v = 2.0) (Fig. 4.11b). These deviations are attributable to the complex interactions that typically occur between pyrolysis volatiles and the QM, which are difficult to accurately represent in the theoretical model. The known limitation of the UNIFAC-DMD model in accurately predicting infinite dilution of organic compounds in water is also responsible for the greater deviations observed for AC [59,128]. In addition, the uncertainties in the pure-component vapor pressure data for some of the surrogate compounds contribute significantly to the observed deviations. Nonetheless, despite these deviations, the qualitative trends predicted by the models generally matched the experimental data.

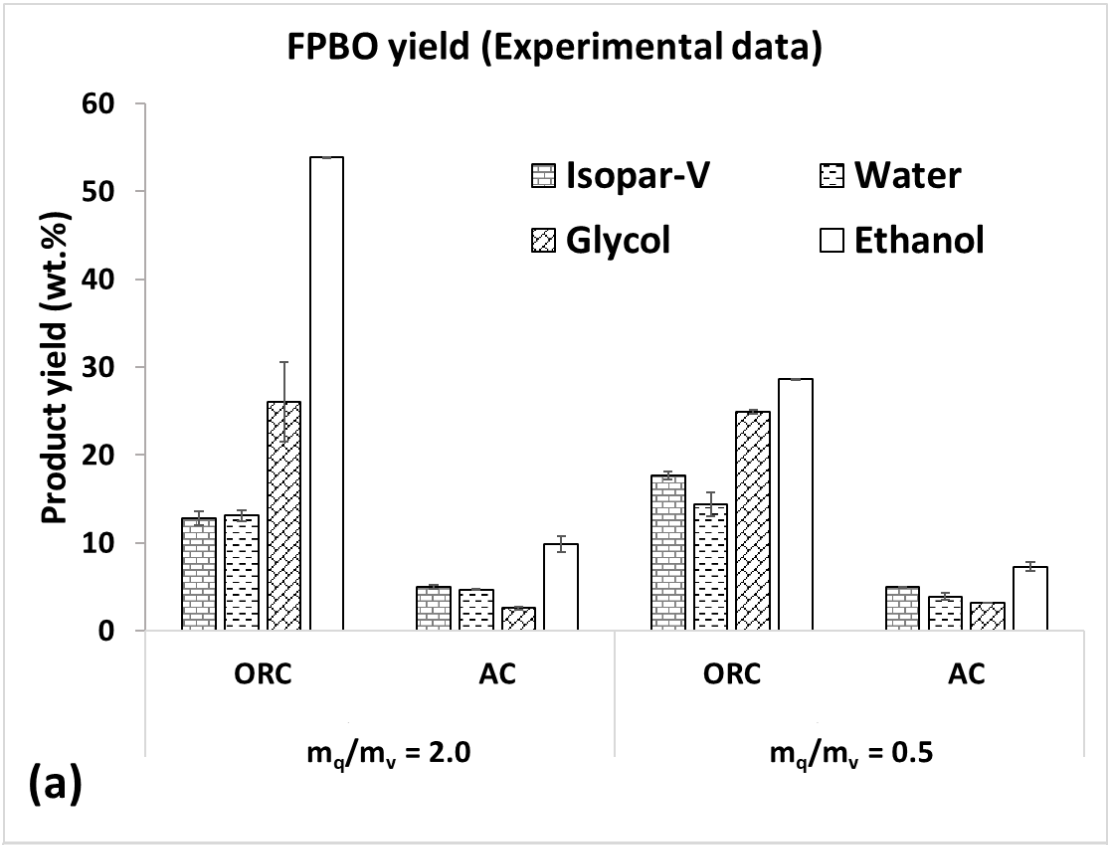

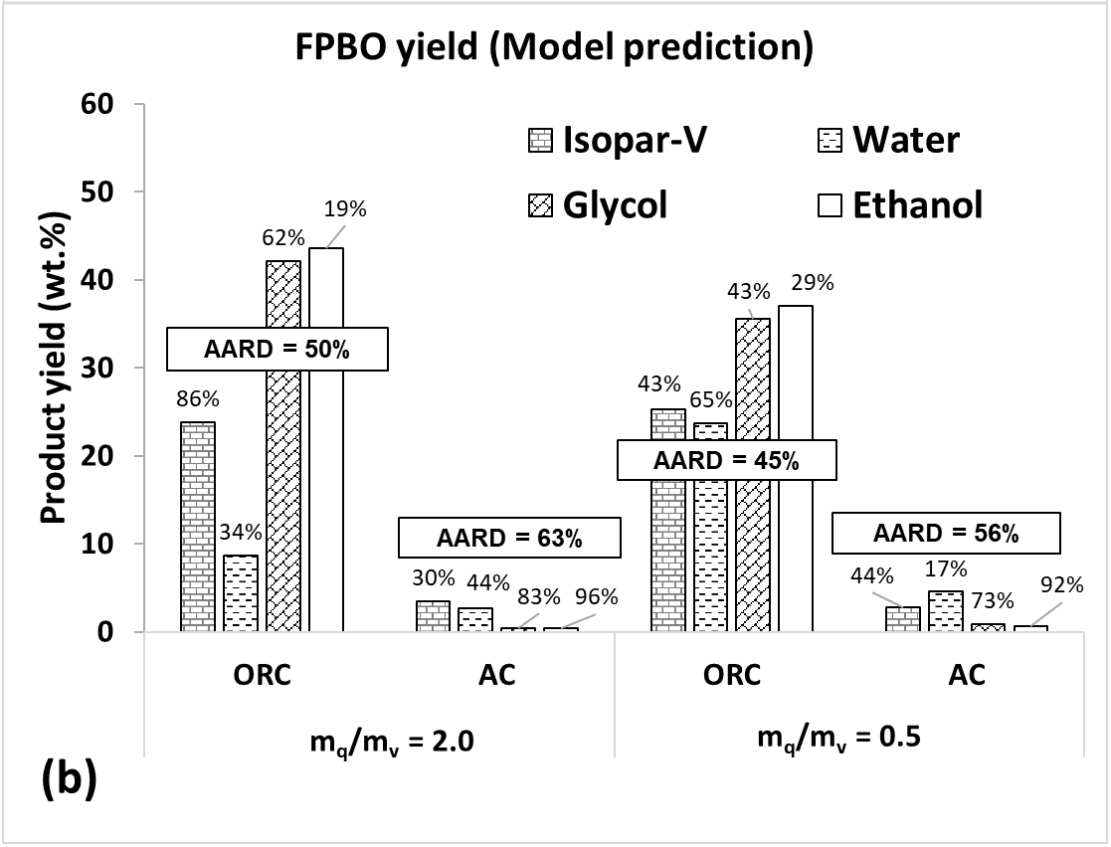

Fig. 4.11. Effects of the investigated QMs on FPBO yields (ORC and AC): (a) experimental results and (b) model predictions, including individual absolute relative deviations (ARDs) and average absolute relative deviations (AARDs) with respect to experimental data. Yields are reported on a dry, QM-free basis relative to the total volatiles entering the first condensation stage.

4.3.2.2 Investigation of FPBO Composition: Moisture content

4.3.2.2.1 Experimental Investigations

The moisture content of the ORC significantly influences FPBO quality, as it determines key physicochemical properties such as viscosity and calorific value and is critical for its stability. The effects of QM type on the moisture content of the FPBOs are shown in Fig. 4.12a. Moisture content was reported on an 'as received' basis, rather than relative to the total volatiles entering the first condensation stage. For m_q/m_v = 2.0, water content in the ORCs was approximately 10, 14, 7, and 15 wt.% for Isopar-V, water, glycol, and ethanol, respectively (Fig. 4.12a). These values fall within the typical range reported for ORCs derived from ash-rich biomass feedstocks, such as wheat straw [15,162]. A similar trend was observed for m_q/m_v = 0.5, except that under this condition, the ethanol quench scenario exhibited substantially higher moisture content (about 42 wt.%). This indicates strong interactions between water and ethanol during quenching, where an increased supply of ethanol leads to greater interaction with, and consequent absorption of, water by ethanol, resulting in lower moisture content in the resulting ORC, as evidenced for the m_q/m_v = 2.0 case. Comparable trends were observed for the model predictions at distinct temperatures discussed earlier in Section 4.3.1.2.

As expected, the moisture content of all corresponding ACs, for all QM except ethanol, exceeded 80 wt.% regardless of the m_q/m_v ratio. The markedly lower moisture content for the ethanol quench scenario further confirms the azeotropic interactions between ethanol and water, consistent with earlier model predictions (Section 4.3.1.2).

4.3.2.2.2 Comparison of Model Predictions with Experimental Data

Generally, model predictions (Fig. 4.12b) were comparable to experimental data. ORC AARDs of 66 and 47% were recorded for m_q/m_v of 0.5 and 2.0, respectively. It is, however, noteworthy that the high ARDs recorded for the water-quench scenario significantly contributed to the increased AARDs recorded for the ORCs (Fig. 4.12b). Water, being an exceedingly polar compound, has a strong tendency to undergo association and hydrogen bonding interactions with condensing volatiles. Given that the UNIFAC-DMD model is limited in accurately predicting such complex interactions, the conspicuous deviations observed for this quench scenario are not surprising.

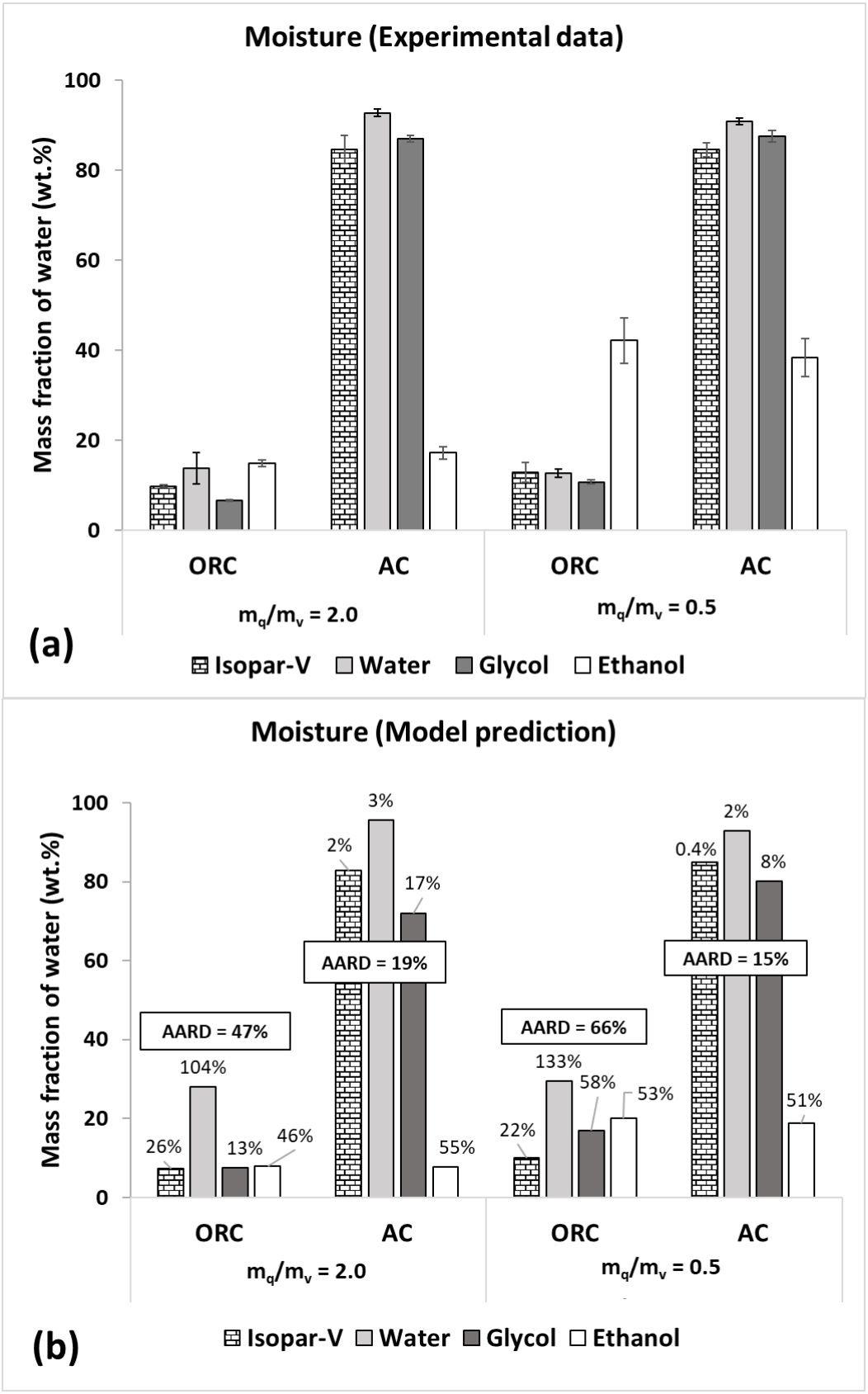

Fig. 4.12. Moisture content of FPBOs (ORC and AC) based on the effects of all QM: (a) experimental data and (b) corresponding model predicted data, showing individual absolute relative deviations (ARDs) and average absolute relative deviations (AARDs) with respect to experimental data. Moisture content was reported on 'as received' basis.

Similar to the ORCs, the model predictions for ACs also showed good agreement with experimental data (Fig. 4.12b), yielding even lower AARDs that ranged between 15% (m_q/m_v = 0.5) and 19% (m_q/m_v = 2.0). Nonetheless, ARDs for ethanol were quite extensive, once again highlighting the limitations of the UNIFAC-DMD model in accurately predicting the highly associated systems present in water–ethanol mixtures.

4.3.2.3 Investigation of FPBO Composition: Distribution of Major Functional Group Compounds

As demonstrated by model predictions, all investigated QM influence the composition of the recovered condensates (ORC and AC). The selectivity of QM towards this is presented and discussed in terms of the distribution of major functional group compounds in the condensates. Fig. 4.13 to Fig. 4.16 show both the experimental data and the corresponding theoretical predictions of the selectivity fingerprints of these functional group compounds, reported on a dry and QM-free basis relative to the total amount of volatiles entering the first condensation stage. The average standard deviations of mass fractions (experimental data) for all functional group compounds were less than 0.20 wt.% for the ORC and 0.05 wt.% for the AC.

4.3.2.3.1 Experimental investigations

As previously noted, Isopar-V formed an immiscible product with the recovered ORC. For this QM, carboxylic acids (primarily acetic and propionic acids) were the dominant detectable fractions in the ORC recovered using Isopar-V (Fig. 4.13a), with mass fractions (concentrations) just below 2 wt.% detected for both m_q/m_v ratios. Nonaromatic ketones (chiefly acetol, 2-butanone, and cyclopentanone) were the next most abundant fraction, with concentrations of about 1.25 wt.% (m_q/m_v = 0.50) and 0.80 wt.% (m_q/m_v = 2.0). Lignin-derived phenols (mainly phenol and *o-, m-, and p*-cresols) and guaiacols were also present in substantial amounts in the ORC, ranging between 0.46 and 0.83 wt.% across both ratios. These were followed by anhydrosugars (particularly levoglucosan) and syringols, with concentrations of about 0.45 wt.% (m_q/m_v = 0.5) and 0.32 wt.% (m_q/m_v = 2.0). Furans (primarily furfural, 2(5H)-furanone, and 2-furfural alcohol) and nonaromatic alcohols were among the compounds with the lowest concentrations detected in the ORC. Their fractions ranged between 0.14 and 0.32 wt.%. No aldehydes were detected in the ORCs.

In the AC, nonaromatic ketones and carboxylic acids also formed the dominant fractions at both ratios (Fig. 4.13b). In comparison, alcohols, furans, lignin-derived phenols, guaiacols and syringols were only detected in trace amounts, and no sugars were present. Unlike the ORC, trace levels (0.01–0.02 wt.%) of nonaromatic aldehydes (particularly hydroxyacetaldehyde and crotonaldehyde) were present in the AC.

Notably, fractions of aliphatic hydrocarbons (mainly C_{14}–C_{17} alkanes) were detected in both FPBOs (i.e., ORC and AC). These alkanes were similar in composition to those typically present in Isopar-V, indicating that some quench fractions were retained in the FPBOs. This observation aligns with the losses recorded for the total Isopar-V quench originally supplied (Table 4.4). Conversely, trace amounts of all functional group compounds typically found in FPBOs were also identified in the recovered spent Isopar-V quench, confirming mass transfer of components between both phases. Similar inferences were reported by Mazerolle et al. [114] and Zacher et al. [115], who also employed Isopar-V in condensing hot pyrolysis volatiles.

For the water quench scenario (also immiscible with the ORC), the mass fractions of acids and ketones in the ORC were less pronounced than in the Isopar-V case (Fig. 4.14a). Acid concentrations of 0.57 wt.% (m_q/m_v = 0.5) and 0.47 wt.% (m_q/m_v = 2.0) were recorded, alongside ketone concentrations of 0.59 wt.% and 0.32 wt.%, respectively. Unlike Isopar-V, no aliphatic hydrocarbons were detected in the ORC, confirming that those observed previously (for the case of Isopar-V) originated directly from the QM.

Phenolic compounds (lignin-derived phenols, guaiacols, and syringols) were also present in substantial amounts compared with acids and ketones, with concentrations ranging between 0.45 and 0.67 wt.% for both m_q/m_v ratios (Fig. 4.14a). Because water is a highly soluble solvent for many FPBO components (e.g., sugars, ketones and acids), its use as a quench causes these compounds to transfer into the spent water QM (extract), thereby enriching the ORC in heavier molecular weight fractions such as lignin-derived phenols, guaiacols, and syringols. This transfer is evident from the elevated concentrations of acids and ketones in the spent water QM, particularly at m_q/m_v = 2.0 (Fig. 4.14c), where increases of approximately 200 and 155% relative to their ORC levels were observed, respectively. Nearly all sugars were also recovered in this phase. At m_q/m_v = 2.0, 100% of generated sugars were transferred, highlighting the potential for single-step sugar extraction via quench condensation. This technique was later employed for the recovery of anhydrosugars from hot pyrolysis vapors

(Section 4.4). Alcohols were present in the spent quench at concentrations of 0.08 (m_q/m_v = 2.0) to 0.20 wt.% (m_q/m_v = 0.5), while lignin-derived phenols, guaiacols, and syringols appeared only in trace amounts (with concentrations below 0.1 wt.% at all ratios).

The product distribution in the ACs of the water-quench scenario was very similar to that of Isopar-V. Ketones (1.30 wt.% on average) and acids (0.82 wt.% on average) formed the most prevalent fractions (Fig. 4.14b). Like the ORC, no aliphatic compounds were present, further substantiating that those detected in the AC of the Isopar-V quench originated from the QM. Again, sugars were absent and compared with acids and ketones, all other compounds appeared only in minute concentrations. With the increased condensation of water in the second condensation stage, the presence of these compounds only in trace amounts was expected.

All the QM that formed homogeneous mixtures with the ORCs (i.e., glycol and ethanol) showed the highest fractions of acids and ketones in the ORC (Fig. 4.15a and Fig. 4.16a). This aligns with model predictions (Section 4.3.1.3), where glycol and ethanol also retained the highest concentrations of these compounds, particularly acids in the ORC across all quenching temperatures and m_q/m_v ratios. Acid concentrations ranged from around 4.0 wt.% (m_q/m_v of 0.5) to 7.5 wt.% (m_q/m_v of 2.0) for ethanol, while glycol reached 10 wt.% at m_q/m_v = 0.5. Notably, no acids were detected in the ORC for the glycol m_q/m_v = 2.0 scenario, due to severe dilution from the quench, which lowered concentrations below the quantification limits of the GC-FID/MS. The substantial concentration of acids (ca. 0.50 wt.%) in the corresponding AC (Fig. 4.15b) confirms this. Treedet et al. [106] reported similar results when they employed ethanol as a quench for the condensation of pyrolysis volatiles generated from Napier grass, sugarcane, and rubber leaves, noting dominant carboxylic acid concentrations relative to other ORC compounds. Ketone concentrations ranged from approximately 7.0 wt.% (m_q/m_v = 0.5) to 17.0 wt.% (m_q/m_v = 2.0) for glycol, and from 4.50 wt.% (m_q/m_v = 0.5) to 6.60 wt.% (m_q/m_v = 2.0) for ethanol.

The ORC recovered with glycol also contained the highest fractions of lignin-derived phenolic compounds (phenols, guaiacols, and syringols) compared to all the other investigated QM. Their concentrations were, on average, about four times higher than those in the corresponding ORCs recovered using ethanol and five times more than in ORCs recovered using Isopar-V and water. This is consistent with model predictions (Section 4.3.1.3), where

phenols and guaiacols predominated in the ORC recovered with glycol across all quenching temperatures and m_q/m_v ratios. In contrast, the concentrations of these compounds in the corresponding ACs recovered using the glycol-quench were negligible (below 0.01 and 0.03 wt.% for ethanol and glycol, respectively).

For both QM, particularly glycol, the concentrations of most compounds (especially acids and ketones) detected in the ORC were higher at an m_q/m_v of 2.0 than at 0.5, with similar results observed for the Isopar-V quench. This indicates that higher mass ratios of these organic QM (ethanol, Isopar-V, and glycol) to the pyrolysis volatiles (an effect associated with lower condensation temperatures) enhanced the recovery of most compounds in the ORC. This trend did not apply to the water-quench, as most of these compounds were water-soluble and instead ended up in the spent water-quench phase.

Ketones were the dominant organic compounds in the ACs recovered with ethanol and glycol. Concentrations of 1.62 wt.% (m_q/m_v = 0.5) and 1.22 wt.% (m_q/m_v = 2.0) were recorded for glycol (Fig. 4.15b), whereas ethanol showed concentrations of about 1.30 wt.% at both m_q/m_v ratios (Fig. 4.16b). Acids were also significant, at 0.68 wt.% (m_q/m_v = 0.5) and 0.49 wt.% (m_q/m_v = 2.0) for glycol, and 0.33 wt.% (m_q/m_v = 0.5) and 0.20 wt.% (m_q/m_v = 2.0) for ethanol. Aldehydes, furans, phenols, and guaiacols were present only in trace amounts for both QM, while sugars and syringols were absent.

4.3.2.3.2 Comparison of Experimental Data with Model Predictions

Model predictions of the concentrations of all major functional group compounds in the FPBOs generally followed a similar qualitative trend as their corresponding experimental data (also represented in Figures Fig. 4.13 to Fig. 4.16). Notwithstanding, some substantial deviations were observed, particularly in the predictions for the ACs and in cases where water was used as the quench. These discrepancies can be attributed to the limitation of the UNIFAC-DMD model in accurately predicting highly dilute concentrations of organic compounds in water.

AARDs for all major functional group compounds under all process conditions are presented in Table 4.5. Except for the glycol quench, model predictions for the ORCs deviated less than for their AC counterparts. Among the ORC products, the ethanol-quench showed the lowest AARD (about 44% on average), followed by Isopar-V (64% on average) and glycol (about 79% on average). The water-quench gave the highest AARD, averaging slightly over 150%. As noted

earlier, water, being a polar compound, undergoes complex association interactions such as solvation and hydrogen bonding, interactions that the UNIFAC-DMD does not account for [5]. In particular, for the AC, the UNIFAC-DMD model is limited in handling infinitely dilute hydrocarbons in water. Since the AC was substantially diluted with the water QM, the high deviations observed are not surprising.

Table 4.5. Average absolute relative deviations (AARD, %) of major functional group compounds in FPBOs for all QM investigated.

	ORC (AARD, %)		AC (AARD, %)	
Quench	$m_q/m_v - 0.5$	$m_q/m_v - 2.0$	$m_q/m_v - 0.5$	$m_q/m_v - 2.0$
Isopar-V	64	65	146	407
Water	182	124	439	352
Glycol	74	83	65	73
Ethanol	49	38	85	86

To establish the selective recovery of the yields and chemical compositions of the ORCs and the ACs, the corresponding ratios (for product yield and composition) of ORC to AC were calculated for both experimental and corresponding model-predicted data (Tables B1 to B5, Appendix B). Comparing the deviations of model-predicted ratios to experimental data permitted further evaluation of model performance. It was deduced from the data that, although significant differences were observed between experimental and model-predicted ratios, their qualitative trends were still generally well replicated. Interestingly, all product yield and nearly all composition ratios were well above unity, suggesting that a significant fraction of the condensed volatiles was recovered as ORC, with a majority of the compounds also retained in this phase. Notably, the recovery of sugars solely in the ORC, as per experimental findings, was accurately reproduced by the model predictions.

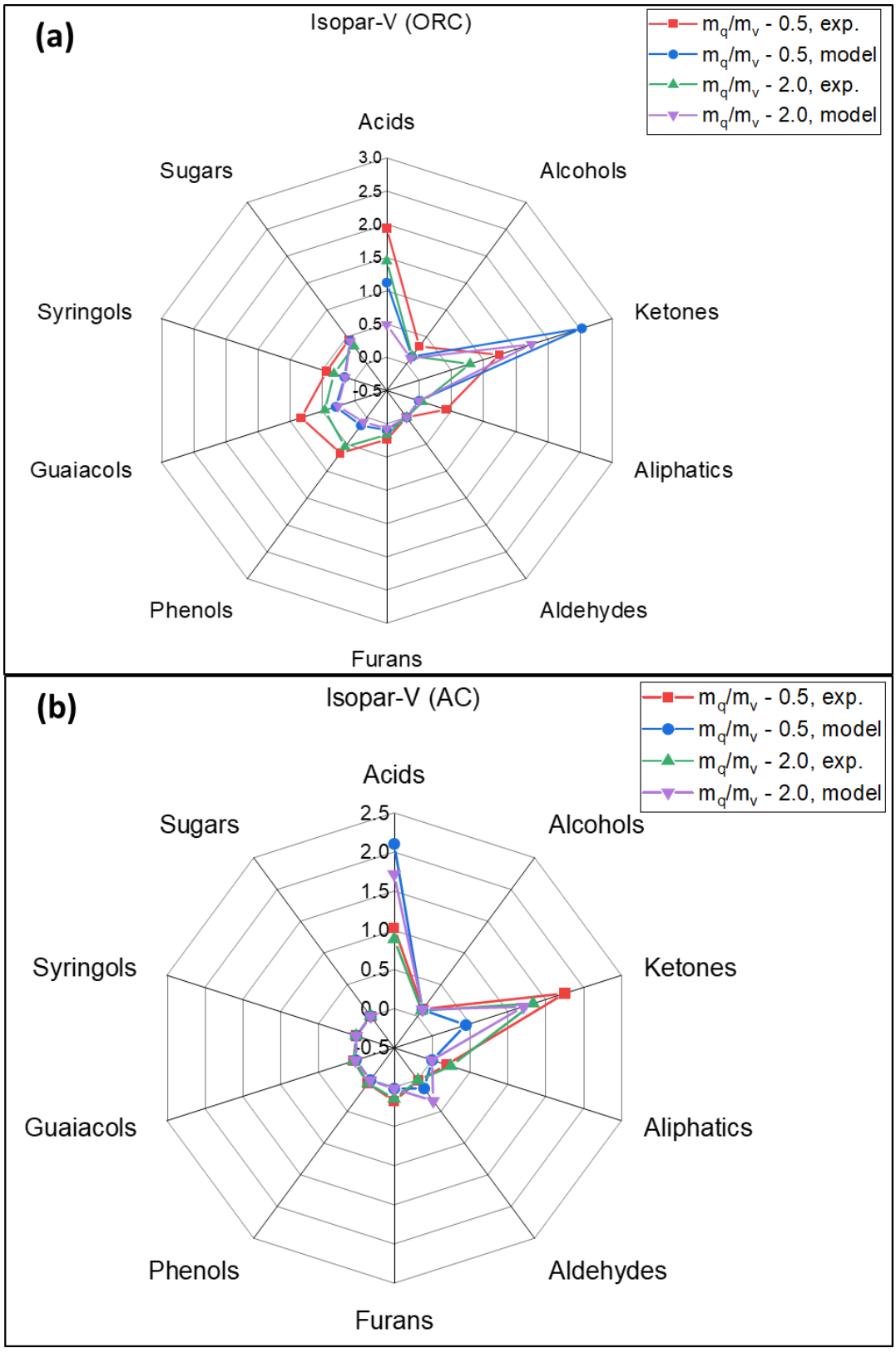

Fig. 4.13. Effects of Isopar-V QM on the mass fractions of major functional group compounds in FPBOs, with model predictions for (a) ORC and (b) AC. Mass fractions are reported on a dry, QM-free basis relative to the total volatiles that entered the first condensation stage.

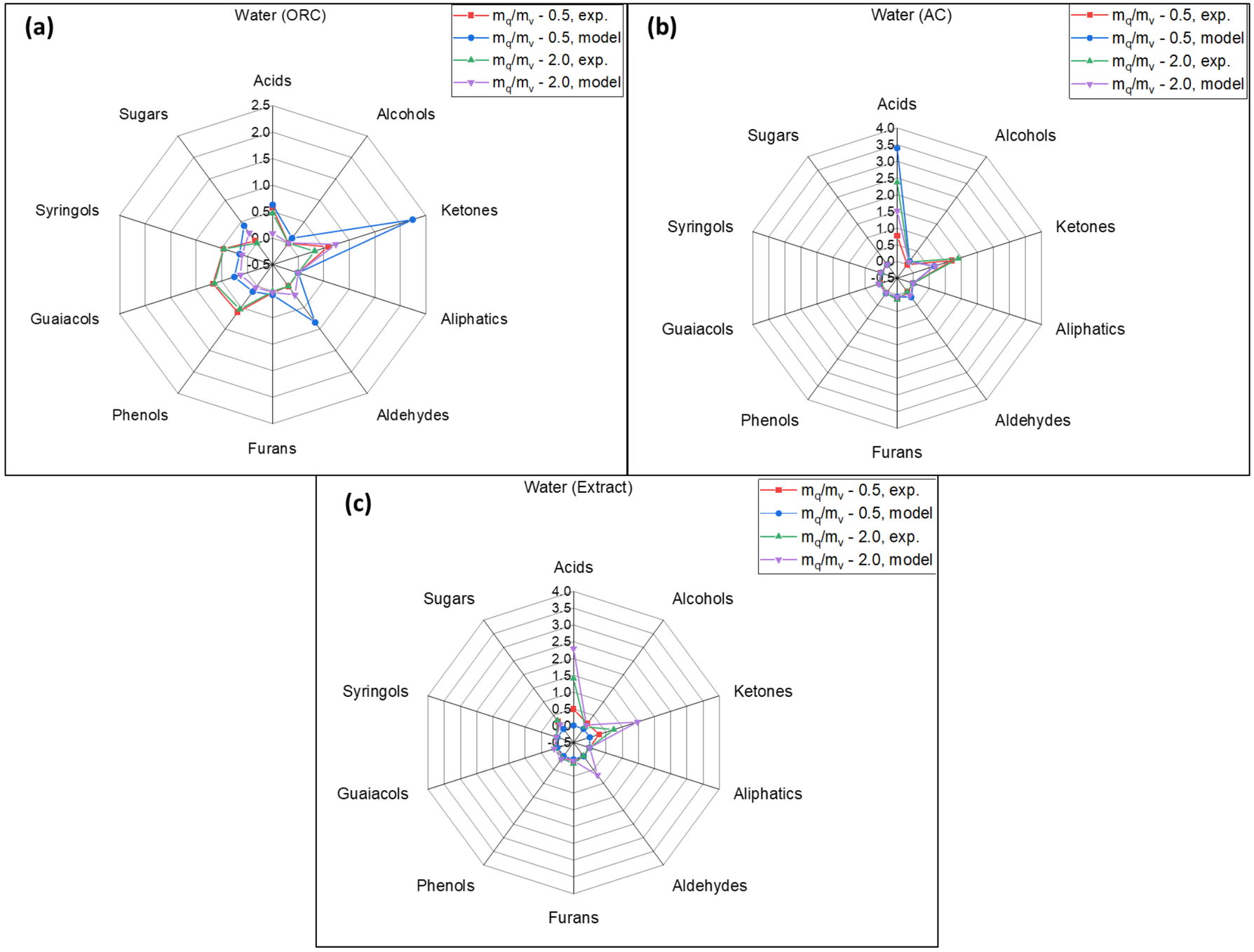

Fig. 4.14. Effects of water QM on the mass fractions of major functional group compounds in FPBOs, with model predictions for (a) ORC, (b) AC, and (c) the phase-separated spent water QM (extract) from the ORC fraction. Mass fractions are reported on a dry, QM-free basis relative to the total volatiles that entered the first condensation stage.

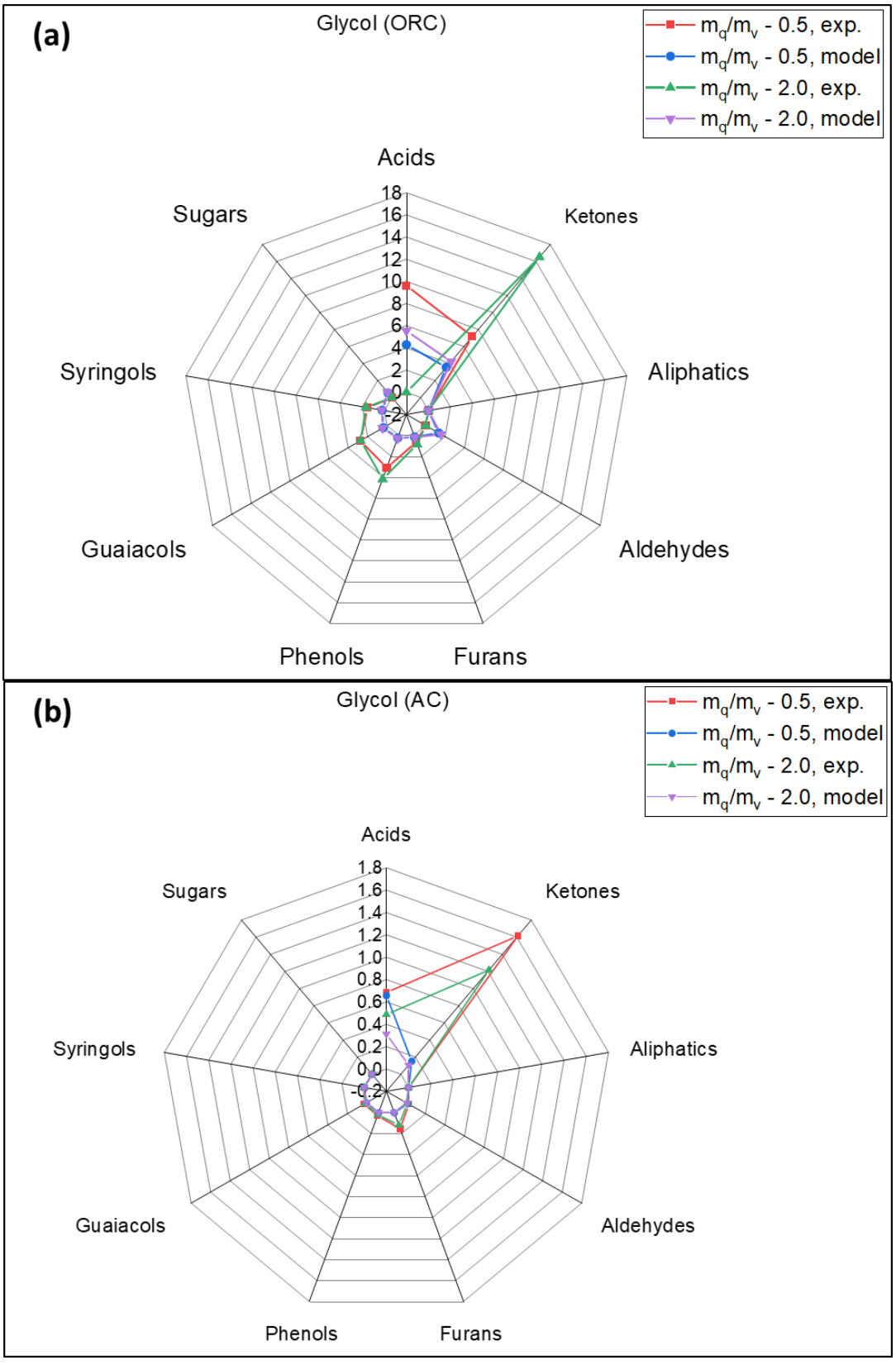

Fig. 4.15. Effects of glycol QM on the mass fractions of major functional group compounds in FPBOs, with model predictions for (a) ORC and (b) AC. Mass fractions are reported on a dry, QM-free basis relative to the total volatiles that entered the first condensation stage.

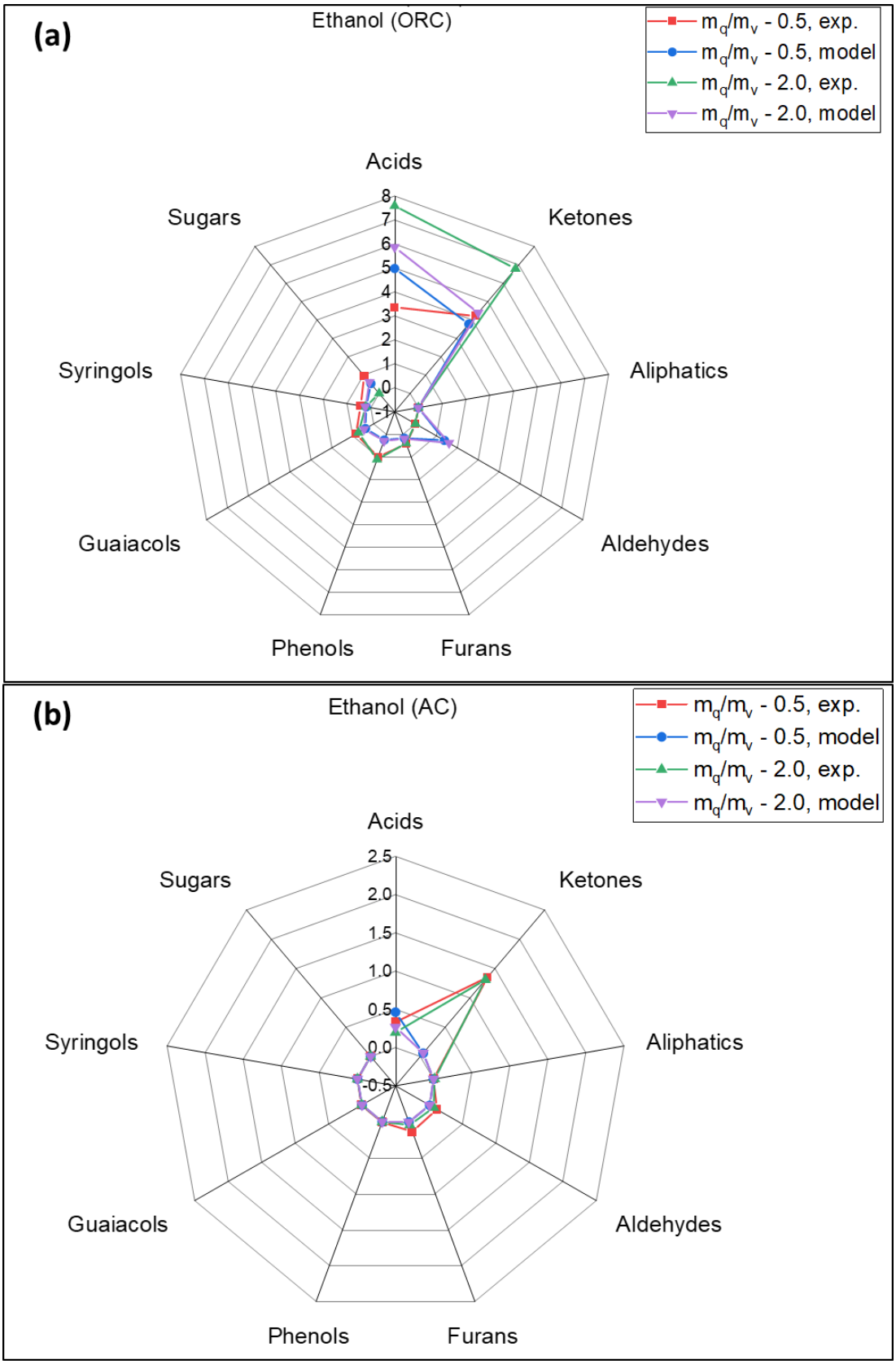

Fig. 4.16. Effects of ethanol QM on the mass fractions of major functional group compounds in FPBOs, with model predictions for (a) ORC and (b) AC. Mass fractions are reported on a dry, QM-free basis relative to the total volatiles that entered the first condensation stage.

4.3.3 Model Predictions for ORC-as-Quench Compared to All Investigated QM

To evaluate how the investigated QM in this study compare with using the ORC as quench (a common practice for industrial-scale pyrolysis systems), the UNIFAC-DMD model was applied to predict the yield distribution and composition of FPBOs. Only theoretical predictions were considered, as the PDU has not yet been fully designed or optimized to implement this process. Predictions followed similar methods outlined in Section 3.3.4, with a quenching temperature of 80 °C.

4.3.3.1 FPBO Yield Distribution

Relative to the other QM, the m_q/m_v ratios for the ORC-as-quench case had little effect on FPBO yield distribution (Table 4.6). For both m_q/m_v ratios, the average ORC yield (ca. 25 wt.%) exceeded that obtained with water (ca. 16 wt.%), was comparable to Isopar-V (ca. 25 wt.%), and fell below ethanol and glycol (ca. 40 wt.%). The AC yield using ORC quench (ca. 2.3 wt.%) was lower than for Isopar-V and water (3.12 and 3.58 wt.%, respectively) but higher than for ethanol and glycol (0.48 and 0.64 wt.%, respectively).

Table 4.6. Model-predicted yields (wt.%) of ORC and AC from condensation using ORC quench, reported on a dry, QM-free basis relative to the total volatiles that entered the first condensation stage.

m_q/m_v – 0.5		m_q/m_v – 2.0	
ORC (wt.%)	AC (wt.%)	ORC (wt.%)	AC (wt.%)
25.8	2.2	25.0	2.4

4.3.3.2 FPBO Composition: Moisture and Major Functional Group Compounds Distribution

Average moisture content of the ORC recovered was about 27 wt.% (Table 4.7), which is closer to that of the water quench scenario. Similar to the cases of Isopar-V, water, and glycol, the moisture content of the recovered AC (using ORC quench) was at least 80 wt.%.

The distribution of mass fractions in the respective FPBOs (ORC and AC) is shown in Fig. 4.17. Acids and ketones were the most dominant fractions in the ORC, with concentrations of about 2.0 and 3.5 wt.% for acids and similar values for ketones at m_q/m_v ratios of 0.5 and 2.0,

respectively. Aldehydes followed, with concentrations of about 1.0 wt.% (m_q/m_v = 0.5) and 1.5 wt.% (m_q/m_v = 2.0). In contrast, furans, phenols, guaiacols, syringols, and sugars were detected only in traces. The qualitative distribution trends of the functional group compounds largely mirrored those observed for the Isopar-V quench. The AC primarily contained acids at concentrations of about 2 wt.% for both m_q/m_v ratios, while ketones were present in comparatively small amounts, unlike the case for all other investigated QM (Fig. 4.17).

Table 4.7. Model-predicted moisture content (wt.%) of ORC and AC from condensation using ORC quench, reported on an 'as-received' basis.

m_q/m_v – 0.5		m_q/m_v – 2.0	
ORC (wt.%)	AC (wt.%)	ORC (wt.%)	AC (wt.%)
26.5	80.9	28.3	79.7

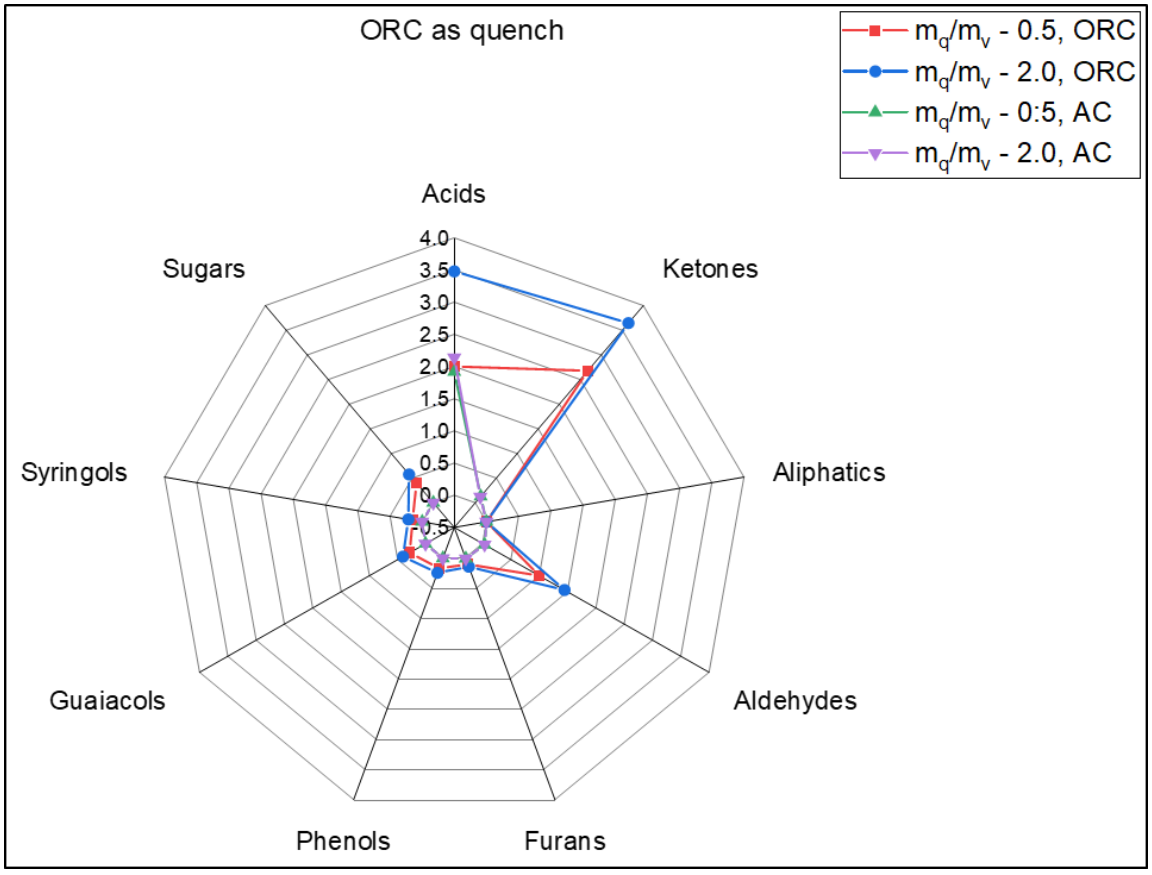

Fig. 4.17. Model-predicted effects of ORC quench on the mass fractions of major functional group compounds in FPBOs (ORC and AC). Mass fractions are reported on a dry basis relative to the total volatiles that entered the first condensation stage.

4.4 Water Extraction of Levoglucosan (LG) from Fast Pyrolysis Bio-Oils: A Comparative Study of Solvent Extraction and Extraction during Quenching of Hot Pyrolysis Volatiles

This sub-chapter presents and discusses results on the comparative study of levoglucosan (LG) extraction from FPBOs using liquid–liquid (solvent) extraction and extraction during the direct-contact condensation of hot pyrolysis volatiles. For the first time in this study, the UNIFAC-DMD model was also applied to predict liquid–liquid equilibrium. The efficiency of a single-stage condensation process, employing water as a quench to capture sugars from FPBOs, was also discussed in this section.

4.4.1 Bench-Scale Solvent Extraction

4.4.1.1 Experimental Investigations

The evolution of levoglucosan (LG) concentration in the extract phase with increasing solvent-to-oil ratio (STOR) for the ORC derived from *miscanthus* using both water and the AC solvents is shown in Fig. 4.18. When water was employed as the solvent, the LG concentration steadily increased from just below 20 wt.% to 100 wt.% as STOR rose from 0.2 to 10 (Fig. 4.18b). Unlike the studies of Bennett et al. [36], Chan and Duff [71], Sukhbattar et al. [14], and Vitasari et al. [55], which reported optimum LG recovery at ratios between 0.5:1 and 1:1, the optimum water-to-oil ratio in this study was achieved only at 10:1. This difference is attributable to the substantially lower water content (ca. 14 wt.%) originally present in the ORC used in this study, compared with the 21–34 wt.% reported in those studies. For ORC feedstocks with higher inherent water content, only smaller amounts of additional water are needed to induce phase separation and thereby facilitate optimum LG extraction. Hence, the higher optimum water-to-oil ratio of 10:1 observed in this study is consistent with the lower initial water content of the ORC.

Similar behavior was observed when AC was used as the solvent, where a steady increase in LG concentration was recorded as STOR increased from 0.5 to 10 (Fig. 4.18a). For the AC, no phase separation occurred at a STOR of 0.2. Because AC is already saturated with trace amounts of organic compounds, ratios as low as 0.2 are likely insufficient to establish the concentration gradient required to trigger phase separation.

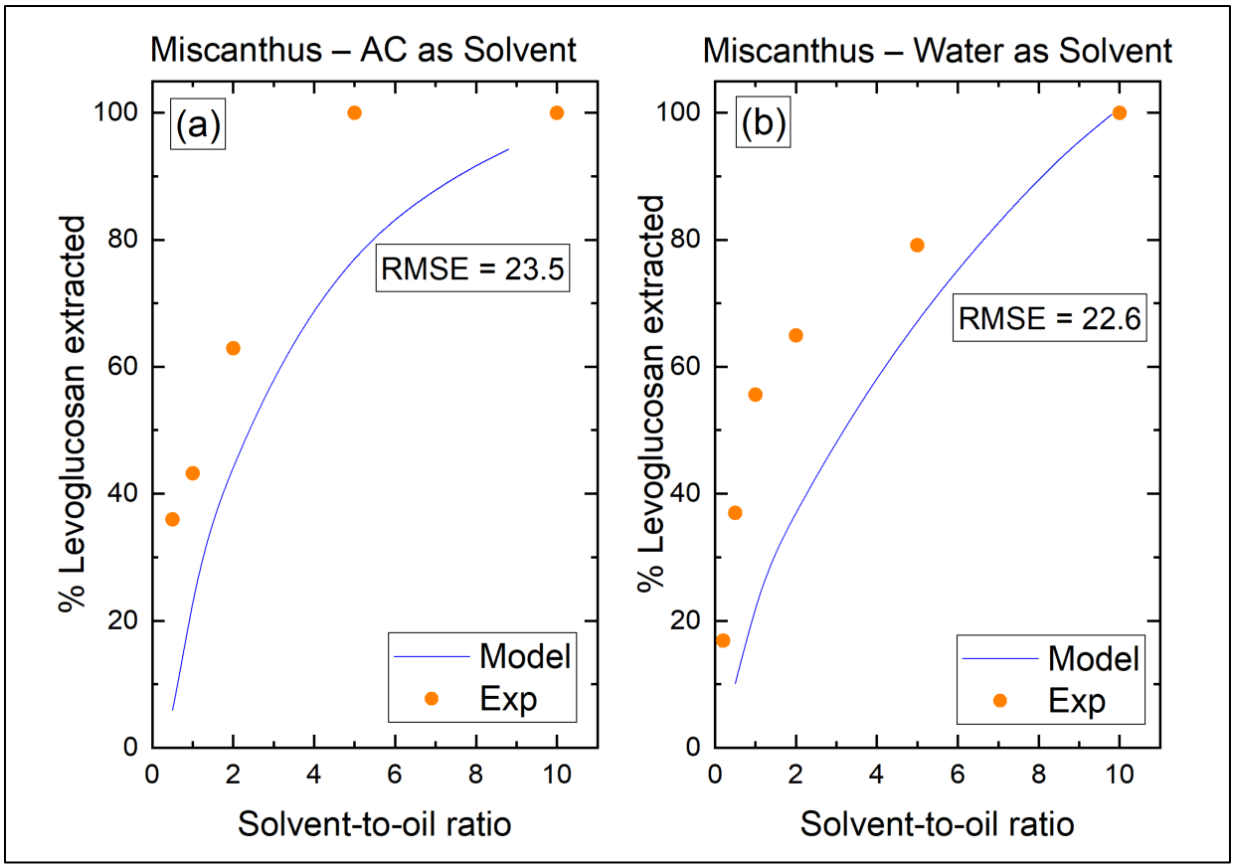

Fig. 4.18. Miscanthus: Experimental versus model-predicted effects of solvent-to-oil ratio (STOR) on LG extraction from ORC, with RMSE values: (a) AC as the solvent and (b) water as the solvent.

For wheat straw, employing water as the solvent resulted in a sharp rise in extracted LG from about 40 to 75 wt.% when STOR increased from 0.2:1 to 10:1 (Fig. 4.19b). Similar trends were observed when AC was used as the solvent (Fig. 4.19a). However, for this biomass, only about 80–85 wt.% of LG was extracted at the maximum STOR investigated, compared to the nearly 100% for *miscanthus*. This is attributable to the lower initial concentration of LG in the wheat-straw-derived ORC. Possible mass transfer limitations associated with mixing of solvent and oil may have hindered equilibrium, especially at low LG concentrations in the ORC. This suggests that higher STORs beyond the investigated range may be required to extract nearly all LG from the ORC, as indicated by model predictions (Fig. 4.19).

Remarkably, for both *miscanthus* and wheat straw, peak LG extraction was first attained at a lower STOR with AC than with water. For *miscanthus*, peak LG extraction was reached at a STOR of 5:1, while for wheat straw, the percentage of LG extracted was relatively higher when AC was employed as the solvent at STORs of 5:1 and beyond. This is noteworthy because, with the AC already containing trace amounts of organic compounds, one would expect a larger

solvent-to-ORC ratio (compared to water) to be required for optimal LG extraction. The divergent trends are explained by the substantial amounts of carboxylic acids, particularly acetic acid, in the AC, which increases the relative polarity. This, in turn, enhances the affinity of AC for polar compounds such as LG, thereby explaining its superior performance over water.

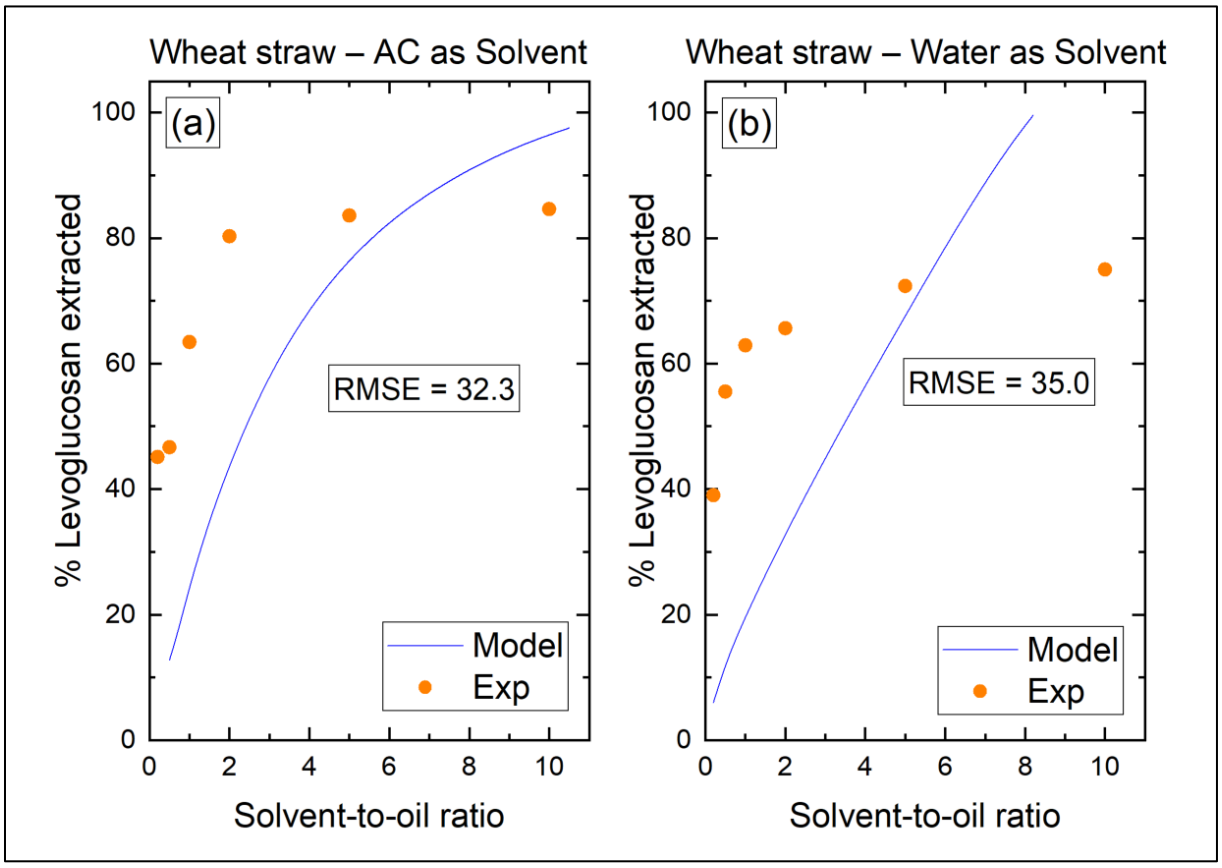

Fig. 4.19. Wheat Straw: Experimental versus model-predicted effects of solvent-to-oil ratio (STOR) on LG extraction from ORC, with RMSE values: (a) AC as the solvent and (b) water as the solvent.

4.4.1.2 Comparison of Experimental Results with Model Predictions

Both qualitative and quantitative trends of model predictions for LG extraction closely matched experimental data, particularly for *miscanthus*, which showed lower Root Mean Square Error (RMSE) compared with wheat straw. RMSE values for *miscanthus* (22.6 for water and 23.5 for AC) were about ten times lower than those for wheat straw (35.0 for water and 32.3 for AC). In most cases, the model under-predicted extracted LG fractions across all STOR conditions, again likely due to the limitations of the UNIFAC-DMD model in capturing low concentrations of organic compounds in aqueous media, as well as the unavailability and high

uncertainty of pure-component vapor pressure data for LG. Moreover, the UNIFAC-DMD model was primarily developed from vapor-liquid equilibrium (VLE) data and might be less accurate for modeling liquid–liquid equilibrium (LLE) systems, typical of LG extraction. Notably, the superior performance of AC over water in LG extraction was also well reproduced by the model, further confirming the enhanced effectiveness of the AC.

4.4.2 Extraction During Quenching Condensation

4.4.2.1 Experimental Investigations

The distributions of LG and other anhydrosugars in recovered products following the extraction of LG during quenching condensation are presented in Table 4.8 (*miscanthus*) and Table 4.9 (wheat straw). It is important to highlight that, due to time and resource constraints, only the water quench was experimentally interrogated for this scenario. However, model predictions for both the water and the AC quench were investigated and compared. These were subsequently discussed in Section 4.4.2.2.

For *miscanthus*, a 100% extraction of LG into the spent water quench phase was achieved. Additionally, all other anhydrosugars ended up in this fraction. No LG was detected in the other recovered condensate fractions (ORC and AC). Similar observations were made in the case of wheat straw, except that no LG was detected in the recovered spent water quench phase or in any of the other recovered product fractions.

Ash contents for the wheat straw and *miscanthus* biomass feedstocks employed in this study have been previously reported as 5.7 wt.% [156] and 2.3 wt.% [163], respectively. With the comparatively high ash content of wheat straw, it has a greater tendency to yield lower concentrations of LG due to catalyzed secondary cracking reactions aided by the alkali and alkaline earth metals (AAEMs) present in ash. This is in agreement with deductions made from the literature previously discussed in Section 2.2.2.1.2.

Degradation of LG in a filter cake that follows the hot pyrolysis segment used for coke separation could also be largely responsible for the absence of LG in the recovered liquid products. This is evident in the presence of other, more stable anhydrosugars such as Dianhydro-α-D-glucopyranose, 1,4:3,6-, that were still recovered in the spent water quench (extract) phase.

Table 4.8. Distribution of levoglucosan (LG) and other anhydrosugars in the recovered condensate fractions following quenching of hot pyrolysis volatiles with water (miscanthus case).

Condensate fraction	Percentage of sugar extracted	
	LG	Other anhydrosugars
ORC (Raffinate)	n.d.	n.d.
Spent water quench (Extract)	100	100
AC	n.d.	n.d.

Note: n.d. – LG not detected

Table 4.9. Distribution of levoglucosan (LG) and other anhydrosugars in the recovered condensate fractions following quenching of hot pyrolysis volatiles with water (wheat straw case).

Condensate fraction	Percentage of sugar extracted	
	LG	Other anhydrosugars
ORC (Raffinate)	n.d.	n.d.
Spent water quench (Extract)	n.d.	100
AC	n.d.	n.d.

Note: n.d. – LG not detected

4.4.2.2 Model Predictions Compared to Experimental Investigations

The effects of the ratio of solvent quench (water and AC) to pyrolysis vapors (m_q/m_v) on the fraction of LG extracted into the resulting spent solvent-quench (extract) phase were also investigated for both biomass feedstocks. For the water quench, LG extracted sharply increased with m_q/m_v for both feedstocks, reaching peak values at ratios of about 5.0 for wheat straw and slightly over 6.0 for *miscanthus* (Fig. 4.20). According to available experimental data, an m_q/m_v ratio of 2.0 was sufficient to optimally extract all LG (Fig. 4.20). For the AC quench, LG extraction increased steadily with m_q/m_v, peaking at 8.0 for both feedstocks. Divergences between model predictions and experimental data again highlight complex association and hydrogen-bonding interactions that occur between water and hot pyrolysis vapors, most of which the modified UNIFAC Dortmund (UNIFAC-DMD) model cannot fully capture, as previously discussed in Section 4.3.2.3.2.

Comparing solvent extraction to extraction during quenching condensation, the latter offers several advantages. These include requiring significantly lower solvent volumes to extract LG efficiently. Quenching of the hot pyrolysis volatiles rapidly cools them, minimizing further decomposition of LG into more stable products such as cellobiosan and xylose. For solvent extraction, LG is only recovered after the ORC has been obtained. Since the ORC is highly susceptible to aging reactions from the moment of its production, the LG it contains gradually diminishes, reducing the concentration gradient and necessitating higher STOR values to achieve maximal extraction. Furthermore, extraction during quenching eliminates the need for downstream liquid–liquid extraction, reducing both energy and cost requirements in LG recovery from FPBOs.

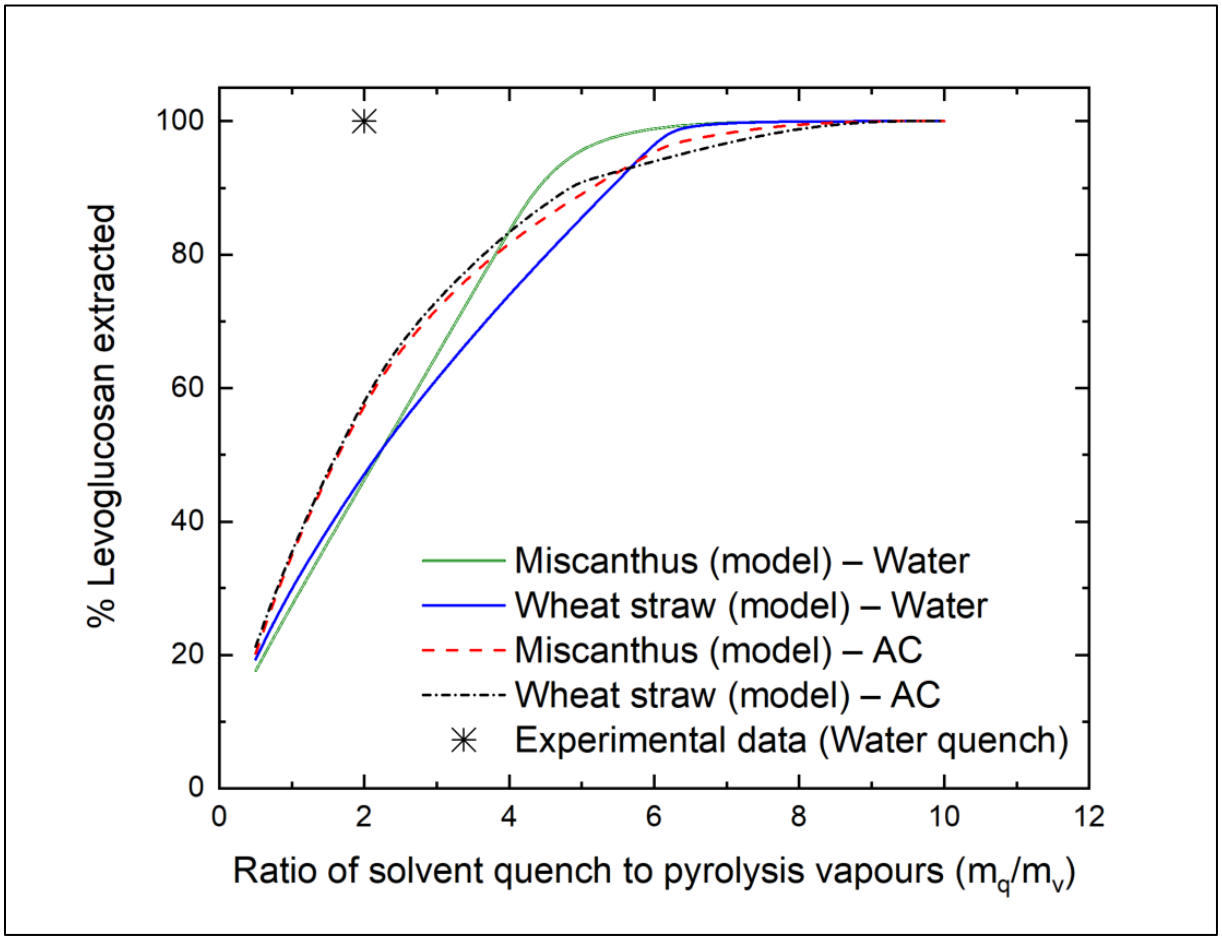

Fig. 4.20. Model-predicted effects of the ratio of solvent quench to pyrolysis vapors (m_q/m_v) on the fraction of levoglucosan extracted. Experimental data point (for water) is the same for both wheat straw and miscanthus.

Chapter 5

Conclusions & Outlook

Fine-tuning the composition of fast pyrolysis bio-oils (FPBOs) during condensation is essential for improving their quality in downstream applications. Phase equilibria modeling has proven a crucial tool for explaining complex phenomena, such as association and hydrogen-bonding interactions, while also reducing the need for extensive experimental investigations. In this work, modeling combined with experimental validation was used to study the effects of temperature, condenser design, and enthalpy of evaporation on FPBO yield and composition. Three scenarios were investigated: (i) optimizing aqueous condensate (AC) for microbial conversion, (ii) evaluating quench media effects in direct-contact condensation, and (iii) optimizing levoglucosan (LG) recovery during quenching compared with liquid–liquid extraction. The main findings, outlook, and recommendations are presented in this chapter.

The study on optimizing the AC of FPBO for downstream microbial conversion demonstrated that fractional condensation of biomass fast pyrolysis vapors can be tuned to optimize the composition of low-temperature ACs for use as microbial substrates. Within the examined condensation temperature ranges, the combination of 120 °C and 50 °C in the first and second staged condensers, respectively, was found to maximize both substrate recovery and AC yield. Since maximizing AC yield reduces that of the main pyrolysis product (i.e., the organic-rich condensate, ORC), future work should incorporate techno-economic analysis to ensure the concept remains economically viable.

Subsequently, the study demonstrated that the choice of quench media (QM) strongly influences the characteristics and composition of the resulting FPBOs. Phase equilibria model predictions revealed that increasing quenching temperature decreased the ORC yields for all the QM investigated (i.e., Isopar-V, ethanol, and glycol), except for water. Glycol and ethanol formed a mixed product with the recovered ORC, and for both QM, a mass flow rate ratio of QM to the hot pyrolysis volatiles (m_q/m_v) of 2.0 produced higher ORC yields than 0.5 at all temperatures. In contrast, Isopar-V and water formed an immiscible product with the ORC, and for these QM, higher m_q/m_v ratios reduced ORC yields at all temperatures, due to mass

transfer limitations. The choice of QM also affected the moisture content of the recovered ORC. Substantial decreases were observed at higher quenching temperatures, most notably for Isopar-V and water. Low moisture content was more pronounced at higher m_q/m_v ratios, especially for QM forming a mixed product with the ORC (glycol and ethanol), reflecting increased interactions at higher feed rates. Compared with other QM, ethanol consistently produced the lowest moisture yields in the AC (about 40 wt.%) under all quenching conditions. This trend was corroborated by azeotrope formation between vaporized ethanol and water vapor, which limited water recovery in the AC, as the resulting mixture condensed only downstream. Model predictions further indicated a decline in carboxylic acids concentrations in the ORC with increasing temperature for all QM, irrespective of m_q/m_v ratio. Glycol retained the highest acid concentration at all temperatures, followed by ethanol, Isopar-V, and water. Other functional groups, including ketones, phenols, guaiacols, furans, and sugars, showed similar behavior. Their concentrations in the AC increased with quenching temperature for all QM, regardless of m_q/m_v ratio. Due to their high boiling points and molecular weights, hardly any sugars were detected in this fraction. Experimental validations on a 10 kg/h fast pyrolysis setup were conducted to confirm the reliability of the theoretical phase equilibria model predictions. Tests were performed at suitable, QM-specific temperature conditions to account for volatility and boiling point differences. Ethanol quench consistently recovered the highest yield of ORC, particularly at an m_q/m_v ratio of 2.0, where it produced 50 wt.% more ORC than glycol and 75 wt.% more than water or Isopar-V. In contrast, Isopar-V remained largely immiscible with the ORC, although slight interactions were observed. The water quench transferred nearly all water-soluble compounds, especially sugars, into the quench phase, demonstrating its potential for direct sugar recovery during condensation. Glycol recovered the highest fractions of acids, ketones, and phenolic compounds in the ORC, results that were fully consistent with model predictions. Ethanol and glycol proved most effective overall, yielding not only higher ORC quantities but also higher concentrations of major functional groups. Despite their advantages, both ethanol and glycol formed homogeneous mixtures with the ORC, necessitating arduous and costly downstream separation to isolate these QMs from the recovered oils.

Furthermore, the study investigating direct-contact condensation of hot pyrolysis vapors with water as the quench proved highly effective for recovering anhydrosugars, particularly LG. All

LG and other anhydrosugars were retained in the spent water quench following condensation. Compared to solvent extraction of LG from pre-condensed ORC, the technique demonstrated superior efficiency, requiring a much lower solvent-to-feed ratio and eliminating the need for downstream liquid–liquid extraction. This represents a novel approach to LG recovery within a pyrolysis biorefinery concept. Using AC as a solvent for liquid–liquid LG recovery from ORC was also more effective than freshwater in bench-scale extractions, thereby enhancing the valorization potential of AC and avoiding additional costs associated with sourcing freshwater. Further work should investigate the direct use of AC as a quench for LG recovery during condensation.

The UNIFAC-DMD model has provided valuable insights into predicting the highly non-ideal vapor-liquid and, to some extent, liquid–liquid equilibria behavior of fast pyrolysis vapors and bio-oils, thereby supporting early-stage process development. However, notable deviations from qualitative trends were observed, particularly in predicting functional group compounds. These limitations stem from the model's (i) inability to adequately account for dilute organics in water, (ii) restricted accuracy in representing specific association and hydrogen-bonding interactions, and (iii) uncertainties in pure-component vapor pressure data, much of which is theoretically estimated due to the lack of experimental measurements. More advanced thermodynamic frameworks, such as the Group Contribution with Association Equation of State (GCA-EoS), which has been shown by Ille et al. [5] to overcome these drawbacks, should therefore be considered. Pyrolysis condensation systems rarely achieve equilibrium, suggesting that the predictive performance of the UNIFAC-DMD model could improve under true equilibrium conditions. Accordingly, the application of the Advanced Distillation Curve (ADC) method to validate model performance should be pursued in further studies.

In essence, although the model predictions for the processes investigated using the UNIFAC-DMD model were not without setbacks, its implementation in this study provides a valuable contribution to understanding the condensation process. Consequently, the challenges identified are crucial for detailed parametric studies of quenching condensation systems. Inasmuch as quenching condensation is a complex process involving highly dynamic heat and mass transfer phenomena, this study focused solely on phase equilibria, which constitute an essential prerequisite for investigating actual dynamic systems, and for understanding fundamental aspects of process design and their influence on product quality.

References

[1] A. Tumbalam Gooty, D. Li, C. Briens, F. Berruti, Fractional condensation of bio-oil vapors produced from birch bark pyrolysis, Sep. Purif. Technol. 124 (2014) 81–88. https://doi.org/10.1016/j.seppur.2014.01.003.

[2] S. Ma, L. Zhang, L. Zhu, X. Zhu, Preparation of multipurpose bio-oil from rice husk by pyrolysis and fractional condensation, J. Anal. Appl. Pyrolysis. 131 (2018) 113–119. https://doi.org/10.1016/j.jaap.2018.02.017.

[3] S. Wang, G. Dai, H. Yang, Z. Luo, Lignocellulosic biomass pyrolysis mechanism: A state-of-the-art review, Prog. Energy Combust. Sci. 62 (2017) 33–86. https://doi.org/10.1016/j.pecs.2017.05.004.

[4] S. Papari, K. Hawboldt, A review on condensing system for biomass pyrolysis process, Fuel Process. Technol. 180 (2018) 1–13. https://doi.org/10.1016/j.fuproc.2018.08.001.

[5] Y. Ille, F.A. Sánchez, N. Dahmen, S. Pereda, Multiphase Equilibria Modeling of Fast Pyrolysis Bio-Oils. Group Contribution Associating Equation of State Extension to Lignin Monomers and Derivatives, Ind. Eng. Chem. Res. 58 (2019) 7318–7331. https://doi.org/10.1021/acs.iecr.9b00227.

[6] H. Sui, H. Yang, J. Shao, X. Wang, Y. Li, H. Chen, Fractional condensation of multicomponent vapors from pyrolysis of cotton stalk, Energy and Fuels. 28 (2014) 5095–5102. https://doi.org/10.1021/ef5006012.

[7] T. Schulzke, S. Conrad, J. Westermeyer, Fractionation of flash pyrolysis condensates by staged condensation, Biomass and Bioenergy. 95 (2016) 287–295. https://doi.org/10.1016/j.biombioe.2016.05.022.

[8] A.N. Huang, C.P. Hsu, B.R. Hou, H.P. Kuo, Production and separation of rice husk pyrolysis bio-oils from a fractional distillation column connected fluidized bed reactor, Powder Technol. 323 (2018) 588–593. https://doi.org/10.1016/j.powtec.2016.03.052.

[9] F.-X. Collard, M. Carrier, J.F. Gorgens, Fractionation of Lignocellulosic Material With Pyrolysis Processing, in: S.I. Mussatto (Ed.), Biomass Fractionation Technol. a Lignocellul. Feed. Based Biorefinery, Elsevier Inc, 2016: pp. 81–101. https://doi.org/10.1016/C2014-0-01890-4.

[10] S. Papari, K. Hawboldt, P. Fransham, Study of selective condensation for woody biomass pyrolysis oil vapours, Fuel. 245 (2019) 233–239. https://doi.org/10.1016/j.fuel.2019.02.055.

[11] R. Yin, R. Liu, Y. Mei, W. Fei, X. Sun, Characterization of bio-oil and bio-char obtained from sweet sorghum bagasse fast pyrolysis with fractional condensers, Fuel. 112 (2013) 96–104. https://doi.org/10.1016/j.fuel.2013.04.090.

[12] A.S. Pollard, M.R. Rover, R.C. Brown, Characterization of bio-oil recovered as stage fractions with unique chemical and physical properties, J. Anal. Appl. Pyrolysis. 93 (2012) 129–138. https://doi.org/10.1016/j.jaap.2011.10.007.

[13] M. Chai, Y. He, Nishu, C. Sun, R. Liu, Effect of fractional condensers on characteristics, compounds distribution and phenols selection of bio-oil from pine sawdust fast pyrolysis, J. Energy Inst. (2019) 1–11. https://doi.org/10.1016/j.joei.2019.05.001.

[14] B. Sukhbaatar, Q. Li, C. Wan, F. Yu, E.B. Hassan, P. Steele, Inhibitors removal from bio-oil aqueous fraction for increased ethanol production, Bioresour. Technol. 161 (2014) 379–384. https://doi.org/10.1016/j.biortech.2014.03.051.

[15] Y. Ille, F. Kröhl, A. Velez, A. Funke, S. Pereda, K. Schaber, N. Dahmen, Activity of water in pyrolysis oil—Experiments and modelling, J. Anal. Appl. Pyrolysis. 135 (2018) 260–270. https://doi.org/10.1016/j.jaap.2018.08.027.

[16] W. Yi, X. Wang, K. Zeng, H. Yang, J. Shao, S. Zhang, H. Chen, Improving bio-oil stability by fractional condensation and solvent addition, Fuel. 290 (2021) 119929. https://doi.org/10.1016/j.fuel.2020.119929.

[17] M. Siriwardhana, Fractional condensation of pyrolysis vapours as a promising approach to control bio-oil aging: Dry birch bark bio-oil, Renew. Energy. 152 (2020) 1121–1128. https://doi.org/10.1016/j.renene.2020.01.095.

[18] M.R. Rover, P.A. Johnston, L.E. Whitmer, R.G. Smith, R.C. Brown, The effect of pyrolysis temperature on recovery of bio-oil as distinctive stage fractions, J. Anal. Appl. Pyrolysis. 105 (2014) 262–268. https://doi.org/10.1016/j.jaap.2013.11.012.

[19] R.J.M. Westerhof, D.W.F. Brilman, M. Garcia-Perez, Z. Wang, S.R.G. Oudenhoven, W.P.M. Van Swaaij, S.R.A. Kersten, Fractional condensation of biomass pyrolysis vapors, Energy and Fuels. 25 (2011) 1817–1829. https://doi.org/10.1021/ef2000322.

[20] H.C. Park, H.S. Choi, J.E. Lee, Heat transfer of bio-oil in a direct contact heat exchanger during condensation, Korean J. Chem. Eng. 33 (2016) 1159–1169. https://doi.org/10.1007/s11814-015-0256-y.

[21] T.P. Vispute, G.W. Huber, Production of hydrogen, alkanes and polyols by aqueous phase processing of wood-derived pyrolysis oils, Green Chem. 11 (2009) 1433–1445. https://doi.org/10.1039/b912522c.

[22] S. Arnold, K. Moss, N. Dahmen, M. Henkel, R. Hausmann, Pretreatment strategies for microbial valorization of bio-oil fractions produced by fast pyrolysis of ash-rich lignocellulosic biomass, GCB Bioenergy. 11 (2019) 181–190. https://doi.org/10.1111/gcbb.12544.

[23] S. Dörsam, J. Kirchhoff, M. Bigalke, N. Dahmen, C. Syldatk, K. Ochsenreither, Evaluation of pyrolysis oil as carbon source for fungal fermentation, Front. Microbiol. 7 (2016) 1–11. https://doi.org/10.3389/fmicb.2016.02059.

[24] J. Lian, M. Garcia-Perez, R. Coates, H. Wu, S. Chen, Yeast fermentation of carboxylic acids obtained from pyrolytic aqueous phases for lipid production, Bioresour. Technol. 118 (2012) 177–186. https://doi.org/10.1016/j.biortech.2012.05.010.

[25] A. Oasmaa, T. Sundqvist, E. Kuoppala, M. Garcia-Perez, Y. Solantausta, C. Lindfors, V. Paasikallio, Controlling the phase stability of biomass fast pyrolysis bio-oils, Energy and Fuels. 29 (2015) 4373–4381. https://doi.org/10.1021/acs.energyfuels.5b00607.

[26] A.C. Johansson, K. Iisa, L. Sandström, H. Ben, H. Pilath, S. Deutch, H. Wiinikka, O.G.W. Öhrman, Fractional condensation of pyrolysis vapors produced from Nordic feedstocks in cyclone pyrolysis, J. Anal. Appl. Pyrolysis. 123 (2017) 244–254. https://doi.org/10.1016/j.jaap.2016.11.020.

[27] S. Arnold, T. Tews, M. Kiefer, M. Henkel, R. Hausmann, Evaluation of small organic acids present in fast pyrolysis bio-oil from lignocellulose as feedstocks for bacterial bioconversion, GCB Bioenergy. 11 (2019) 1159–1172. https://doi.org/10.1111/gcbb.12623.

[28] H. Zhou, R.C. Brown, Z. Wen, Anaerobic digestion of aqueous phase from pyrolysis of biomass: Reducing toxicity and improving microbial tolerance, Bioresour. Technol. 292 (2019) 121976. https://doi.org/10.1016/j.biortech.2019.121976.

[29] S. Arnold, K. Moss, N. Dahmen, M. Henkel, R. Hausmann, Pretreatment strategies for microbial valorization of bio-oil fractions produced by fast pyrolysis of ash-rich lignocellulosic biomass, GCB Bioenergy. 11 (2019) 181–190. https://doi.org/10.1111/gcbb.12544.

[30] C. Wen, C.M. Moreira, L. Rehmann, F. Berruti, Feasibility of anaerobic digestion as a treatment for the aqueous pyrolysis condensate (APC) of birch bark, Bioresour. Technol. 307 (2020) 123199. https://doi.org/10.1016/j.biortech.2020.123199.

[31] S.S. Liaw, V.H. Perez, R.J.M. Westerhof, G.F. David, C. Frear, M. Garcia-Perez, Biomethane Production from Pyrolytic Aqueous Phase: Biomass Acid Washing and Condensation Temperature Effect on the Bio-oil and Aqueous Phase Composition, Bioenergy Res. 13 (2020) 878–886. https://doi.org/10.1007/s12155-020-10100-3.

[32] D. Fabbri, C. Torri, Linking pyrolysis and anaerobic digestion (Py-AD) for the conversion of lignocellulosic biomass, Curr. Opin. Biotechnol. 38 (2016) 167–173. https://doi.org/10.1016/j.copbio.2016.02.004.

[33] C. Kubisch, K. Ochsenreither, Detoxification of a pyrolytic aqueous condensate from wheat straw for utilization as substrate in Aspergillus oryzae DSM 1863 cultivations, Biotechnol. Biofuels Bioprod. 15 (2022) 1–21. https://doi.org/10.1186/s13068-022-02115-z.

[34] S. Ren, X.P. Ye, A.P. Borole, P. Kim, N. Labbé, Analysis of switchgrass-derived bio-oil and associated aqueous phase generated in a semi-pilot scale auger pyrolyzer, J. Anal. Appl. Pyrolysis. 119 (2016) 97–103. https://doi.org/10.1016/j.jaap.2016.03.013.

[35] Q. Li, P.H. Steele, F. Yu, B. Mitchell, E.B.M. Hassan, Pyrolytic spray increases levoglucosan production during fast pyrolysis, J. Anal. Appl. Pyrolysis. 100 (2013) 33–40. https://doi.org/10.1016/j.jaap.2012.11.013.

[36] N.M. Bennett, S.S. Helle, S.J.B. Duff, Extraction and hydrolysis of levoglucosan from pyrolysis oil, Bioresour. Technol. 100 (2009) 6059–6063. https://doi.org/10.1016/j.biortech.2009.06.067.

[37] J. Wang, Q. Wei, J. Zheng, M. Zhu, Effect of pyrolysis conditions on levoglucosan yield from cotton straw and optimization of levoglucosan extraction from bio-oil, J. Anal. Appl. Pyrolysis. 122 (2016) 294–303. https://doi.org/10.1016/j.jaap.2016.09.013.

[38] I.G. Hakeem, P. Halder, M.H. Marzbali, S. Patel, S. Kundu, J. Paz-Ferreiro, A. Surapaneni, K. Shah, Research progress on levoglucosan production via pyrolysis of lignocellulosic biomass and its effective recovery from bio-oil, J. Environ. Chem. Eng. 9 (2021). https://doi.org/10.1016/j.jece.2021.105614.

[39] Y. Wei, H. Lei, L. Wang, L. Zhu, X. Zhang, Y. Liu, S. Chen, B. Ahring, Liquid-liquid extraction of biomass pyrolysis bio-oil, Energy and Fuels. 28 (2014) 1207–1212. https://doi.org/10.1021/ef402490s.

[40] S. Ren, X.P. Ye, A.P. Borole, Separation of chemical groups from bio-oil water-extract via sequential organic solvent extraction, J. Anal. Appl. Pyrolysis. 123 (2017) 30–39. https://doi.org/10.1016/j.jaap.2017.01.004.

[41] A. Funke, M. Tomasi Morgano, N. Dahmen, H. Leibold, Experimental comparison of two bench scale units for fast and intermediate pyrolysis, J. Anal. Appl. Pyrolysis. 124 (2017) 504–514. https://doi.org/10.1016/j.jaap.2016.12.033.

[42] D. Meier, B. Van De Beld, A. V. Bridgwater, D.C. Elliott, A. Oasmaa, F. Preto, State-of-the-art of fast pyrolysis in IEA bioenergy member countries, Renew. Sustain. Energy Rev. 20 (2013) 619–641. https://doi.org/10.1016/j.rser.2012.11.061.

[43] A. V. Bridgwater, Review of fast pyrolysis of biomass and product upgrading, Biomass and Bioenergy. 38 (2012) 68–94. https://doi.org/10.1016/j.biombioe.2011.01.048.

[44] A. Oasmaa, I. Fonts, M.R. Pelaez-Samaniego, M.E. Garcia-Perez, M. Garcia-Perez, Pyrolysis Oil Multiphase Behavior and Phase Stability: A Review, Energy and Fuels. 30 (2016) 6179–6200. https://doi.org/10.1021/acs.energyfuels.6b01287.

[45] X. Chen, Q. Che, S. Li, Z. Liu, H. Yang, Y. Chen, X. Wang, J. Shao, H. Chen, Recent developments in lignocellulosic biomass catalytic fast pyrolysis: Strategies for the optimization of bio-oil quality and yield, Fuel Process. Technol. 196 (2019) 106180. https://doi.org/10.1016/j.fuproc.2019.106180.

[46] F. Stankovikj, A.G. McDonald, G.L. Helms, M. V. Olarte, M. Garcia-Perez, Characterization of the Water-Soluble Fraction of Woody Biomass Pyrolysis Oils, Energy and Fuels. 31 (2017) 1650–1664. https://doi.org/10.1021/acs.energyfuels.6b02950.

[47] K. Drugkar, W. Rathod, T. Sharma, A. Sharma, J. Joshi, V.K. Pareek, L. Ledwani, U. Diwekar, Advanced separation strategies for up-gradation of bio-oil into value-added chemicals: A comprehensive review, Sep. Purif. Technol. 283 (2022) 120149. https://doi.org/10.1016/j.seppur.2021.120149.

[48] X.-S. Zhang, G.-X. Yang, H. Jiang, W.-J. Liu, H.-S. Ding, Mass production of chemicals from biomass-derived oil by directly atmospheric distillation coupled with co-pyrolysis, Sci. Rep. 3 (2013) 1120. https://doi.org/10.1038/srep01120.

[49] Q. Lu, X. Yang, X. Zhu, Analysis on chemical and physical properties of bio-oil pyrolyzed from rice husk, J. Anal. Appl. Pyrolysis. 82 (2008) 191–198. https://doi.org/10.1016/j.jaap.2008.03.003.

[50] A. Krutof, K.A. Hawboldt, Thermodynamic model of fast pyrolysis bio-oil advanced distillation curves, Fuel. 261 (2020) 116446. https://doi.org/10.1016/j.fuel.2019.116446.

[51] L. V Fregolente, E.B. Moraes, P.F. Martins, C.B. Batistella, M.R. Wolf Maciel, A.P. Afonso, M.H.M. Reis, Enrichment of natural products using an integrated solvent-free process : molecular distillation, Inst. Chem. Eng. Symp. Ser. 152 (2006) 648–656. https://skoge.folk.ntnu.no/prost/proceedings/distillation06/CD-proceedings/paper062.pdf (accessed February, 23, 2024).

[52] Z.G. Guo, S.R. Wang, Y.Y. Zhu, Z.Y. Luo, K.F. Cen, Separation of acid compounds for refining biomass pyrolysis oil, Ranliao Huaxue Xuebao/Journal Fuel Chem. Technol. 37 (2009) 49–52. https://doi.org/10.1016/s1872-5813(09)60010-4.

[53] S. Rahman, R. Helleur, S. MacQuarrie, S. Papari, K. Hawboldt, Upgrading and isolation of low molecular weight compounds from bark and softwood bio-oils through vacuum distillation, Sep. Purif. Technol. (2017). https://doi.org/https://doi.org/10.1016/j.seppur.2017.11.033.

[54] H. Chen, L. Wang, Posttreatment strategies for biomass conversion, in: *Posttreatment Strategies for Biomass Conversion*, Metallurgical Industry Press (2017), 201. https://doi.org/10.1016/B978-0-12-802417-1.00008-9.

[55] C.R. Vitasari, G.W. Meindersma, A.B. de Haan, Water extraction of pyrolysis oil: The first step for the recovery of renewable chemicals, Bioresour. Technol. 102 (2011) 7204–7210. https://doi.org/10.1016/j.biortech.2011.04.079.

[56] K. Jacobson, K.C. Maheria, A. Kumar Dalai, Bio-oil valorization: A review, Renew. Sustain. Energy Rev. 23 (2013) 91–106. https://doi.org/10.1016/j.rser.2013.02.036.

[57] C. Tessini, M. Vega, N. Müller, L. Bustamante, D. von Baer, A. Berg, C. Mardones, High performance thin layer chromatography determination of cellobiosan and levoglucosan in bio-oil obtained by fast pyrolysis of sawdust, J. Chromatogr. A. 1218 (2011) 3811–3815. https://doi.org/10.1016/j.chroma.2011.04.037.

[58] A. Tumbalam Gooty, D. Li, F. Berruti, C. Briens, Kraft-lignin pyrolysis and fractional condensation of its bio-oil vapors, J. Anal. Appl. Pyrolysis. 106 (2014) 33–40. https://doi.org/10.1016/j.jaap.2013.12.006.

[59] G.K. Parku, A. Krutof, A. Funke, D. Richter, N. Dahmen, Using Fractional Condensation to Optimize Aqueous Pyrolysis Condensates for Downstream Microbial Conversion, Ind. Eng. Chem. Res. (2023). https://doi.org/10.1021/acs.iecr.2c03598.

[60] T. Chen, C. Deng, R. Liu, Effect of selective condensation on the characterization of bio-oil from pine sawdust fast pyrolysis using a fluidized-bed reactor, Energy and Fuels. 24 (2010) 6616–6623. https://doi.org/10.1021/ef1011963.

[61] P. Kim, S. Weaver, N. Labbé, Effect of sweeping gas flow rates on temperature-controlled multistage condensation of pyrolysis vapors in an auger intermediate pyrolysis system, J. Anal. Appl. Pyrolysis. 118 (2016) 325–334. https://doi.org/10.1016/j.jaap.2016.02.017.

[62] B.A. Black, W.E. Michener, K.J. Ramirez, M.J. Biddy, B.C. Knott, M.W. Jarvis, J. Olstad, O.D. Mante, D.C. Dayton, G.T. Beckham, Aqueous Stream Characterization from Biomass Fast Pyrolysis and Catalytic Fast Pyrolysis, ACS Sustain. Chem. Eng. 4 (2016) 6815–6827. https://doi.org/10.1021/acssuschemeng.6b01766.

[63] T. Nicoleit, N. Dahmen, J. Sauer, Production and Storage of Gasifiable Slurries Based on Flash-Pyrolyzed Straw, Energy Technol. 4 (2016) 221–229. https://doi.org/10.1002/ente.201500273.

[64] N. Dahmen, J. Abeln, M. Eberhard, T. Kolb, H. Leibold, J. Sauer, D. Stapf, B. Zimmerlin, The bioliq process for producing synthetic transportation fuels, Wiley Interdiscip. Rev. Energy Environ. 6 (2017). https://doi.org/10.1002/wene.236.

[65] C. Torri, D. Fabbri, Biochar enables anaerobic digestion of aqueous phase from intermediate pyrolysis of biomass, Bioresour. Technol. 172 (2014) 335–341. https://doi.org/10.1016/j.biortech.2014.09.021.

[66] Y. Liang, X. Zhao, Z. Chi, M. Rover, P. Johnston, R. Brown, L. Jarboe, Z. Wen, Utilization of acetic acid-rich pyrolytic bio-oil by microalga Chlamydomonas reinhardtii: Reducing bio-oil toxicity and enhancing algal toxicity tolerance, Bioresour. Technol. 133 (2013) 500–506. https://doi.org/10.1016/j.biortech.2013.01.134.

[67] L.N. Jayakody, C.W. Johnson, J.M. Whitham, R.J. Giannone, B.A. Black, N.S. Cleveland, D.M. Klingeman, W.E. Michener, J.L. Olstad, D.R. Vardon, R.C. Brown, S.D. Brown, R.L. Hettich, A.M. Guss, G.T. Beckham, Thermochemical wastewater valorization: Via enhanced microbial toxicity tolerance, Energy Environ. Sci. 11 (2018) 1625–1638. https://doi.org/10.1039/c8ee00460a.

[68] X. Zhao, Z. Chi, M. Rover, R. Brown, L. Jarboe, Z. Wen, Microalgae Fermentation of Acetic Acid-Rich Pyrolytic Bio-Oil: Reducing Bio-Oil Toxicity by Alkali Treatment, Environ. Prog. Sustain. Energy. 32 (2013) 676–680. https://doi.org/10.1002/ep.

[69] Z. Chi, M. Rover, E. Jun, M. Deaton, P. Johnston, R.C. Brown, Z. Wen, L.R. Jarboe, Overliming detoxification of pyrolytic sugar syrup for direct fermentation of levoglucosan to ethanol, Bioresour. Technol. 150 (2013) 220–227. https://doi.org/10.1016/j.biortech.2013.09.138.

[70] X. Zhao, K. Davis, R. Brown, L. Jarboe, Z. Wen, Alkaline treatment for detoxification of acetic acid-rich pyrolytic bio-oil for microalgae fermentation: Effects of alkaline species and the detoxification mechanisms, Biomass and Bioenergy. 80 (2015) 203–212. https://doi.org/10.1016/j.biombioe.2015.05.007.

[71] J.K.S. Chan, S.J.B. Duff, Methods for mitigation of bio-oil extract toxicity, Bioresour. Technol. 101 (2010) 3755–3759. https://doi.org/10.1016/j.biortech.2009.12.054.

[72] L.Q. Jiang, Z. Fang, Z.L. Zhao, A.Q. Zheng, X.B. Wang, H. Bin Li, Levoglucosan and its hydrolysates via fast pyrolysis of lignocellulose for microbial biofuels: A state-of-the-art review, Renew. Sustain. Energy Rev. 105 (2019) 215–229. https://doi.org/10.1016/j.rser.2019.01.055.

[73] M.R. Rover, P.A. Johnston, T. Jin, R.G. Smith, R.C. Brown, L. Jarboe, Production of clean pyrolytic sugars for fermentation, ChemSusChem. 7 (2014) 1662–1668. https://doi.org/10.1002/cssc.201301259.

[74] K.S. So, R.C. Brown, Economic analysis of selected lignocellulose-to-ethanol conversion technologies, Appl. Biochem. Biotechnol. - Part A Enzym. Eng. Biotechnol. 77–79 (1999) 633–640. https://doi.org/10.1385/abab:79:1-3:633.

[75] S. Czernik, A. V. Bridgwater, Overview of applications of biomass fast pyrolysis oil, Energy and Fuels. 18 (2004) 590–598. https://doi.org/10.1021/ef034067u.

[76] M.R. Rover, A. Aui, M.M. Wright, R.G. Smith, R.C. Brown, Production and purification of crystallized levoglucosan from pyrolysis of lignocellulosic biomass, Green Chem. 21 (2019) 5980–5989. https://doi.org/10.1039/c9gc02461a.

[77] Q. Li, P.H. Steele, B. Mitchell, L.L. Ingram, F. Yu, The addition of water to extract maximum levoglucosan from the bio-oil produced via fast pyrolysis of pretreated loblolly pinewood, BioResources. 8 (2013) 1868–1880. https://doi.org/10.15376/biores.8.2.1868-1880.

[78] C.H. Pang, S. Gaddipatti, G. Tucker, E. Lester, T. Wu, Relationship between thermal behaviour of lignocellulosic components and properties of biomass, Bioresour. Technol. 172 (2014) 312–320. https://doi.org/10.1016/j.biortech.2014.09.042.

[79] S.D. Stefanidis, K.G. Kalogiannis, E.F. Iliopoulou, C.M. Michailof, P.A. Pilavachi, A.A. Lappas, A study of lignocellulosic biomass pyrolysis via the pyrolysis of cellulose, hemicellulose and lignin, J. Anal. Appl. Pyrolysis. 105 (2014) 143–150. https://doi.org/10.1016/j.jaap.2013.10.013.

[80] H. Yang, R. Yan, H. Chen, C. Zheng, D.H. Lee, D.T. Liang, Investigation of plant biomass two-stage pyrolysis based on three major components: cellulose, hemicellulose, and lignin, Biomass Convers. Biorefinery. (2006) 388–393. https://doi.org/https://doi.org/10.1021/ef0580117.

[81] F.X. Collard, J. Blin, A review on pyrolysis of biomass constituents: Mechanisms and composition of the products obtained from the conversion of cellulose, hemicelluloses and lignin, Renew. Sustain. Energy Rev. 38 (2014) 594–608. https://doi.org/10.1016/j.rser.2014.06.013.

[82] J. Zhang, Y.S. Choi, C.G. Yoo, T.H. Kim, R.C. Brown, B.H. Shanks, Cellulose-hemicellulose and cellulose-lignin interactions during fast pyrolysis, ACS Sustain. Chem. Eng. 3 (2015) 293–301. https://doi.org/10.1021/sc500664h.

[83] S. Wu, D. Shen, J. Hu, H. Zhang, R. Xiao, Cellulose-hemicellulose interactions during fast pyrolysis with different temperatures and mixing methods, Biomass and Bioenergy. 95 (2016) 55–63. https://doi.org/10.1016/j.biombioe.2016.09.015.

[84] T. Hosoya, H. Kawamoto, S. Saka, Cellulose-hemicellulose and cellulose-lignin interactions in wood pyrolysis at gasification temperature, J. Anal. Appl. Pyrolysis. 80 (2007) 118–125. https://doi.org/10.1016/j.jaap.2007.01.006.

[85] S. Wang, X. Guo, K. Wang, Z. Luo, Influence of the interaction of components on the pyrolysis behavior of biomass, J. Anal. Appl. Pyrolysis. 91 (2011) 183–189. https://doi.org/10.1016/j.jaap.2011.02.006.

[86] X. Ye, L. Qiang, X. Jiang, X. Wang, B. Hu, W. Li, C. Dong, Interaction characteristics and mechanism in the fast co-pyrolysis of cellulose and lignin model compounds: A joint experimental and theoretical study, J. Therm. Anal. Calorim. 130 (2017) 975–984. https://doi.org/10.1007/s10973-017-6465-3.

[87] T. Shoji, H. Kawamoto, S. Saka, Complete inhibition of char formation from cellulose in fast pyrolysis with aromatic substance, J. Anal. Appl. Pyrolysis. 124 (2017) 638–642. https://doi.org/10.1016/j.jaap.2016.12.026.

[88] Q. Liu, Z. Zhong, S. Wang, Z. Luo, Interactions of biomass components during pyrolysis: A TG-FTIR study, J. Anal. Appl. Pyrolysis. 90 (2011) 213–218. https://doi.org/10.1016/j.jaap.2010.12.009.

[89] D. Carpenter, T.L. Westover, S. Czernik, W. Jablonski, Biomass feedstocks for renewable fuel production: A review of the impacts of feedstock and pretreatment on the yield and product distribution of fast pyrolysis bio-oils and vapors, Green Chem. 16 (2014) 384–406. https://doi.org/10.1039/c3gc41631c.

[90] J. Piskorz, D. Radlein, D.S. Scott, On the mechanism of the rapid pyrolysis of cellulose, J. Anal. Appl. Pyrolysis. 9 (1986) 121–137. https://doi.org/10.1016/0165-2370(86)85003-3.

[91] C. Di Blasi, A. Galgano, C. Branca, Influences of the chemical state of alkaline compounds and the nature of alkali metal on wood pyrolysis, Ind. Eng. Chem. Res. 48 (2009) 3359–3369. https://doi.org/10.1021/ie801468y.

[92] S.A. Rollag, J.K. Lindstrom, R.C. Brown, Pretreatments for the continuous production of pyrolytic sugar from lignocellulosic biomass, Chem. Eng. J. 385 (2020) 123889. https://doi.org/10.1016/j.cej.2019.123889.

[93] B. Pecha, P. Arauzo, M. Garcia-Perez, Impact of combined acid washing and acid impregnation on the pyrolysis of Douglas fir wood, J. Anal. Appl. Pyrolysis. 114 (2015) 127–137. https://doi.org/10.1016/j.jaap.2015.05.014.

[94] D.S. Scott, L. Paterson, J. Piskorz, D. Radlein, Pretreatment of poplar wood for fast pyrolysis: Rate of cation removal, J. Anal. Appl. Pyrolysis. 57 (2001) 169–176. https://doi.org/10.1016/S0165-2370(00)00108-X.

[95] N. Kuzhiyil, D. Dalluge, X. Bai, K.H. Kim, R.C. Brown, Pyrolytic sugars from cellulosic biomass, ChemSusChem. 5 (2012) 2228–2236. https://doi.org/10.1002/cssc.201200341.

[96] A. Zhurinsh, G. Dobele, V. Jurkjane, K. Meile, A. Volperts, A. Plavniece, Impact of hot water pretreatment temperature on the pyrolysis of birch wood, J. Anal. Appl. Pyrolysis. 124 (2017) 515–522. https://doi.org/10.1016/j.jaap.2017.01.030.

[97] N. Hao, T.L. Bezerra, Q. Wu, H. Ben, Q. Sun, S. Adhikari, A.J. Ragauskas, Effect of autohydrolysis pretreatment on biomass structure and the resulting bio-oil from a pyrolysis process, Fuel. 206 (2017) 494–503. https://doi.org/10.1016/j.fuel.2017.06.013.

[98] G.F. David, V.H. Perez, O. Rodriguez Justo, M. Garcia-Perez, Effect of acid additives on sugarcane bagasse pyrolysis: Production of high yields of sugars, Bioresour. Technol. 223 (2017) 74–83. https://doi.org/10.1016/j.biortech.2016.10.051.

[99] S. Zhou, Z. Wang, S.S. Liaw, C.Z. Li, M. Garcia-Perez, Effect of sulfuric acid on the pyrolysis of Douglas fir and hybrid poplar wood: Py-GC/MS and TG studies, J. Anal. Appl. Pyrolysis. 104 (2013) 117–130. https://doi.org/10.1016/j.jaap.2013.08.013.

[100] T. Shoji, H. Kawamoto, S. Saka, Boiling point of levoglucosan and devolatilization temperatures in cellulose pyrolysis measured at different heating area temperatures, J. Anal. Appl. Pyrolysis. 109 (2014) 185–195. https://doi.org/10.1016/j.jaap.2014.06.014.

[101] R. Venderbosch, W. Prins, Fast pyrolysis technology development, Biofuels, Bioprod. Biorefining. 4 (2010) 178–208. https://doi.org/https://doi.org/10.1002/bbb.205.

[102] D. Mohan, J. Charles U. Pittman, P.H. Steele, Pyrolysis of Wood/Biomass for Bio-oil: A Critical Review, Energy & Fuels. 20 (2006) 848–889. https://doi.org/https://doi.org/10.1021/ef0502397.

[103] H. Wang, D. Livingston, R. Srinivasan, Q. Li, P. Steele, F. Yu, Detoxification and fermentation of pyrolytic sugar for ethanol production, Appl. Biochem. Biotechnol. 168 (2012) 1568–1583. https://doi.org/10.1007/s12010-012-9879-1.

[104] J. Lian, M. Garcia-Perez, S. Chen, Fermentation of levoglucosan with oleaginous yeasts for lipid production, Bioresour. Technol. 133 (2013) 183–189. https://doi.org/10.1016/j.biortech.2013.01.031.

[105] Y.H. Stark, Modellierung der Kondensation von Pyrolysedämpfen unter Berücksichtigung der Aerosolbildung. München: Verlag Dr. Hut. (2020). [Doctoral dissertation, Karlsruher Institut für Technologie (KIT)]. https://www.dr.hut-verlag.de/978-3-8439-4483-0.html. (accessed January 15, 2022).

[106] W. Treedet, R. Suntivarakorn, I. Mufandi, P. Singbua, Improvement of Bio-oil Production System by Using Spray Condenser: Investigation of Yields, Properties, and Production Cost, Bioenergy Res. 15 (2022) 1579–1594. https://doi.org/10.1007/s12155-021-10372-3.

[107] K.K. Palla, V. S., K. Papadikis, S. Gu, Computational modelling of the condensation of fast pyrolysis vapours in a quenching column. Part B: Phase change dynamics and column size effects, Fuel Process. Technol. 144 (2016) 42–55. https://doi.org/10.1016/j.fuproc.2015.12.013.

[108] H.B. Mahood, A.N. Campbell, R.B. Thorpe, A.O. Sharif, Experimental measurements and theoretical prediction for the volumetric heat transfer coefficient of a three-phase direct contact condenser, Int. Commun. Heat Mass Transf. 66 (2015) 180–188. https://doi.org/10.1016/j.icheatmasstransfer.2015.05.020.

[109] H.B. Mahood, R.B. Thorpe, A.N. Campbell, A.O. Sharif, Experimental measurements and theoretical prediction for the transient characteristic of a two-phase two-component direct contact condenser, Appl. Therm. Eng. 87 (2015) 161–174. https://doi.org/10.1016/j.applthermaleng.2015.04.071.

[110] K.K. Palla, V. S., K. Papadikis, S. Gu, Computational modelling of the condensation of fast pyrolysis vapours in a quenching column. Part A: Hydrodynamics, heat transfer and design optimisation, Fuel Process. Technol. 131 (2015) 59–68. https://doi.org/10.1016/j.fuproc.2014.11.007.

[111] C.C. Chang, S.R. Wu, C.C. Lin, H.P. Wan, H.T. Lee, Fast pyrolysis of biomass in pyrolysis gas: Fractionation of pyrolysis vapors using a spray of bio-oil, Energy and Fuels. 26 (2012) 2962–2967. https://doi.org/10.1021/ef201858h.

[112] B. Li, X. Xie, L. Zhang, D. Lin, S. Wang, S. Wang, H. Xu, J. Wang, Y. Huang, S. Zhang, D. Liu, Coke formation during rapid quenching of volatile vapors from fast pyrolysis of cellulose, Fuel. 306 (2021) 121658. https://doi.org/10.1016/j.fuel.2021.121658.

[113] R.J.M. Westerhof, N.J.M. Kuipers, S.R.A. Kersten, W.P.M. Van Swaaij, Controlling the water content of biomass fast pyrolysis oil, Ind. Eng. Chem. Res. 46 (2007) 9238–9247. https://doi.org/10.1021/ie070684k.

[114] D. Mazerolle, B. Bronson, B. Kruczek, Experimental Evaluation and Empirical Modeling of Cross-Flow Microfiltration for Solids and Ash Removal from Fast Pyrolysis Bio-Oil, Energy and Fuels. 34 (2020) 11014–11025. https://doi.org/10.1021/acs.energyfuels.0c01641.

[115] A.H. Zacher, D.C. Elliott, M. V. Olarte, D.M. Santosa, F. Preto, K. Iisa, Pyrolysis of woody residue feedstocks: Upgrading of bio-oils from Mountain-pine-beetle-killed trees and hog fuel, Energy and Fuels. 28 (2014) 7510–7516. https://doi.org/10.1021/ef5017945.

[116] B. Bronson, D. Mazerolle, Robinson, T. Consequences of Using an Immiscible Quench Fluid for Engineering Scale R&D in Fast Pyrolysis. PYNE 45 Newsl. 2019, No. December, 1−33. https://task34.ieabioenergy.com/wp-content/uploads/sites/3/2019/12/PyNe-45_final.pdf. (accessed July 31, 2023).

[117] D.L. Dalluge, L.E. Whitmer, J.P. Polin, Y.S. Choi, B.H. Shanks, R.C. Brown, Comparison of direct and indirect contact heat exchange to improve recovery of bio-oil, Appl. Energy. 251 (2019) 113346. https://”doi.org/10.1016/j.apenergy.2019.113346.

[118] D.L. Dalluge, T. Daugaard, P. Johnston, N. Kuzhiyil, M.M. Wright, R.C. Brown, Continuous production of sugars from pyrolysis of acid-infused lignocellulosic biomass, Green Chem. 16 (2014) 4144–4155. https://doi.org/10.1039/c4gc00602j.

[119] K.H. Kim, T.J. Daugaard, R. Smith, M. Mba-Wright, R.C. Brown, Recovery of resin acids from fast pyrolysis of pine, J. Anal. Appl. Pyrolysis. 138 (2019) 132–136. https://doi.org/10.1016/j.jaap.2018.12.016.

[120] C. Pfitzer, N. Dahmen, N. Tröger, F. Weirich, J. Sauer, A. Günther, M. Müller-Hagedorn, Fast Pyrolysis of Wheat Straw in the Bioliq Pilot Plant, Energy and Fuels. 30 (2016) 8047–8054. https://doi.org/10.1021/acs.energyfuels.6b01412.

[121] F.G. Fonseca, A. Funke, A. Niebel, A.P. Soares Dias, N. Dahmen, Moisture content as a design and operational parameter for fast pyrolysis, J. Anal. Appl. Pyrolysis. 139 (2019) 73–86. https://doi.org/10.1016/j.jaap.2019.01.012.

[122] A. Funke, D. Richter, A. Niebel, N. Dahmen, J. Sauer, Fast pyrolysis of biomass residues in a twin-screw mixing reactor, J. Vis. Exp. 2016 (2016) 1–8. https://doi.org/10.3791/54395.

[123] Z. Ji-lu, Bio-oil from fast pyrolysis of rice husk: Yields and related properties and improvement of the pyrolysis system, J. Anal. Appl. Pyrolysis. 80 (2007) 30–35. https://doi.org/10.1016/j.jaap.2006.12.030.

[124] J. Zheng, W. Yi, N. Wang, Bio-oil production from cotton stalk, Energy Convers. Manag. 49 (2008) 1724–1730. https://doi.org/10.1016/j.enconman.2007.11.005.

[125] T.M. Soria, A.E. Andreatta, S. Pereda, S.B. Bottini, Thermodynamic modeling of phase equilibria in biorefineries, Fluid Phase Equilib. 302 (2011) 1–9. https://doi.org/10.1016/j.fluid.2010.10.029.

[126] J. Gmehling, R. Wittig, J. Lohmann, R. Joh, A modified UNIFAC (Dortmund) model. 4. Revision and extension, Ind. Eng. Chem. Res. 41 (2002) 1678–1688. https://doi.org/10.1021/ie0108043.

[127] I.G. Economou, Cubic and Generalized van der Waals Equations of State, in: A.R. Goodwin, J. Sengers, C.J. Peters (Eds.)*, Applied Thermodynamics of Fluids, RSC Publishing*, (2011) 123–135. https://doi.org/10.1039/9781849730983-00053.

[128] J. Gmehling, B. Kolbe, M. Kleiber, J. Rarey, Chemical Thermodynamics for Process Simulation, Wiley-VCH Verlag GmbH & Co. KGaA, Boschstr. 12, 69469 Weinheim, Germany All, 2019.

[129] I.G. Economou, Statistical Associating Fluid Theory: A Successful Model for the Calculation of Thermodynamic and Phase Equilibrium Properties of Complex Fluid Mixtures, Ind. Eng. Chem. Res. (2002). https://doi.org/10.1021/ie0102201.

[130] W. Feng, H.J. Van Der Kooi, J. De Swaan Arons, Application of the SAFT equation of state to biomass fast pyrolysis liquid, Chem. Eng. Sci. 60 (2005) 617–624. https://doi.org/10.1016/j.ces.2004.08.023.

[131] S.P. Tan, H. Adidharma, M. Radosz, Recent advances and applications of statistical associating fluid theory, Ind. Eng. Chem. Res. 47 (2008) 8063–8082. https://doi.org/10.1021/ie8008764.

[132] S. Pereda, E. Brignole, S. Bottini, Equations of State in Chemical Reacting Systems, in: A.R. Goodwin, J. Sengers, C.J. Peters (Eds.), *Applied Thermodynamics of Fluids*, *RSC Publishing* (2011) 433–459. https://doi.org/10.1039/9781849730983-00433.

[133] A. Fredenslund, R.L. Jones, John M. Prausnitz, Group-Contri bution Estimation of Activity Coefficients in Nonideal Liquid Mixtures, AIChE J. 21 (1975) 1086–1099. https://doi.org/https://doi.org/10.1002/aic.690210607.

[134] H.K. Hansen, P. Rasmussen, A. Fredenslund, M. Schiller, J. Gmehling, Vapor-Liquid Equilibria by UNIFAC Group Contribution. 5. Revision and Extension, Ind. Eng. Chem. Res. 30 (1991) 2352–2355. https://doi.org/10.1021/ie00058a017.

[135] E. Brignole, S. Pereda, Phase Equilibrium Engineering, 2013. https://www.elsevier.com/books/phase-equilibrium-engineering/brignole/978-0-444-56364-4.

[136] J. Lohmann, R. Joh, J. Gmehling, From UNIFAC to modified UNIFAC (Dortmund), Ind. Eng. Chem. Res. 40 (2001) 957–964. https://doi.org/10.1021/ie0005710.

[137] Dortmund Data Bank, (n.d.). http://www.ddbst.de/unifac-consortium.html (accessed April 29, 2020).

[138] H.P. Gros, S. Bottini, E.A. Brignole, A group contribution equation of state for associating mixtures, Fluid Phase Equilib. 116 (1996) 537–544. https://doi.org/https://doi.org/10.1016/0378-3812(95)02928-1.

[139] F.A. Sánchez, S. Pereda, E.A. Brignole, GCA-EoS: A SAFT group contribution model-Extension to mixtures containing aromatic hydrocarbons and associating compounds, Fluid Phase Equilib. 306 (2011) 112–123. https://doi.org/10.1016/j.fluid.2011.03.024.

[140] S. Skjold-Jørgensen, Group Contribution Equation of State (GC-EOS): A Predictive Method for Phase Equilibrium Computations Over Wide Ranges of Temperature and Pressures up to 30 MPa, Ind. Eng. Chem. Res. 27 (1988) 110–118. https://doi.org/10.1021/ie00073a021.

[141] G.A. Mansoori, N.F. Carnahan, K.E. Starling, T.W. Leland, Equilibrium thermodynamic properties of the mixture of hard spheres, J. Chem. Phys. 54 (1971) 1523–1526. https://doi.org/10.1063/1.1675048.

[142] N.F. Carnahan, K.E. Starling, Equation of state for nonattracting rigid spheres, J. Chem. Phys. 51 (1969) 635–636. https://doi.org/10.1063/1.1672048.

[143] W.G. Chapman, K.E. Gubbins, G. Jackson, M. Radosz, SAFT: Equation-of-state solution model for associating fluids, Fluid Phase Equilib. 52 (1989) 31–38. https://doi.org/10.1016/0378-3812(89)80308-5.

[144] F.A. Sánchez, Y. Ille, N. Dahmen, S. Pereda, GCA-EOS extension to mixtures of phenol ethers and derivatives with hydrocarbons and water, Fluid Phase Equilib. 490 (2019) 13–21. https://doi.org/10.1016/j.fluid.2019.02.017.

[145] M.E. Harries, M.L. Huber, T.J. Bruno, A Distillation Approach to Phase Equilibrium Measurements of Multicomponent Fluid Mixtures, Energy and Fuels. 33 (2019) 7908–7915. https://doi.org/10.1021/acs.energyfuels.9b01366.

[146] B.C. Windom, T.J. Bruno, Improvements in the measurement of distillation curves. 5. Reduced pressure advanced distillation curve method, Ind. Eng. Chem. Res. 50 (2011) 1115–1126. https://doi.org/10.1021/ie101784g.

[147] P.Y. Hsieh, T.J. Bruno, Pressure-controlled advanced distillation curve analysis and rotational viscometry of swine manure pyrolysis oil q, FUEL. 132 (2014) 1–6. https://doi.org/10.1016/j.fuel.2014.04.039.

[148] M.E. Harries, A.G. McDonald, T.J. Bruno, Measuring the distillation curves of non-homogeneous fluids: Method and case study of two pyrolysis oils, Fuel. 204 (2017) 23–27. https://doi.org/10.1016/j.fuel.2017.04.066.

[149] B.C. Windom, T.J. Bruno, Pressure-controlled advanced distillation curve analysis of biodiesel fuels: Assessment of thermal decomposition, Energy and Fuels. 26 (2012) 2407–2415. https://doi.org/10.1021/ef3000642.

[150] M.E. Harries, B. Kunwar, B.K. Sharma, T.J. Bruno, Application of the Advanced Distillation Curve Method to Characterize Two Alternative Transportation Fuels Prepared from the Pyrolysis of Waste Plastic, Energy and Fuels. 30 (2016) 9671–9678. https://doi.org/10.1021/acs.energyfuels.6b02068.

[151] B.C. Windom, T.J. Bruno, Novel reduced pressure-balance syringe for chromatographic analysis, J. Chromatogr. A. 1217 (2010) 7434–7439. https://doi.org/10.1016/j.chroma.2010.09.045.

[152] L.S. Ott, B.L. Smith, T.J. Bruno, Advanced distillation curve measurement: Application to a bio-derived crude oil prepared from swine manure, Fuel. 87 (2008) 3379–3387. https://doi.org/10.1016/j.fuel.2008.04.038.

[153] P.Y. Hsieh, K.R. Abel, T.J. Bruno, Analysis of marine diesel fuel with the advanced distillation curve method, Energy and Fuels. 27 (2013) 804–810. https://doi.org/10.1021/ef3020525.

[154] P.Y. Hsieh, J.A. Widegren, T.J. Fortin, T.J. Bruno, Chemical and thermophysical characterization of an algae-based hydrotreated renewable diesel fuel, Energy and Fuels. 28 (2014) 3192–3205. https://doi.org/10.1021/ef500237t.

[155] B.C. Windom, T.J. Bruno, Application of pressure-controlled advanced distillation curve analysis: Virgin and waste oils, Ind. Eng. Chem. Res. 52 (2013) 327–337. https://doi.org/10.1021/ie302399v.

[156] A. Niebel, A. Funke, C. Pfitzer, N. Dahmen, N. Weih, D. Richter, B. Zimmerlin, Fast Pyrolysis of Wheat Straw - Improvements of Operational Stability in 10 Years of Bioliq Pilot Plant Operation, Energy and Fuels. 35 (2021) 11333–11345. https://doi.org/10.1021/acs.energyfuels.1c00851.

[157] L.A. Forero G., J.A. Velásquez J., Wagner liquid-vapour pressure equation constants from a simple methodology, J. Chem. Thermodyn. 43 (2011) 1235–1251. https://doi.org/10.1016/j.jct.2011.03.011.

[158] T. Nichols, V. Utgikar, Wagner equation predicting entire curve for pure fluids from limited VLE data: Critical point & four Antoine analytic points, Fluid Phase Equilib. 460 (2018) 1–16. https://doi.org/10.1016/j.fluid.2017.12.022.

[159] VDI Heat Atlas. Second edition, Springer-Verlag Berlin Heidelberg, 2010. Ed. Verein Deutscher Ingenieure VDI-Gesellschaft Verfahrenstechnik und Chemieingenieurwesen (GVC). https://doi.org/10.1007/978-3-540-77877-6.

[160] F.G. Fonseca, A. Funke, A. Niebel, A.P. Soares Dias, N. Dahmen, Moisture content as a design and operational parameter for fast pyrolysis, J. Anal. Appl. Pyrolysis. 139 (2019) 73–86. https://doi.org/10.1016/j.jaap.2019.01.012.

[161] N. Charon, J. Ponthus, D. Espinat, F. Broust, G. Volle, J. Valette, D. Meier, Multi-technique characterization of fast pyrolysis oils, J. Anal. Appl. Pyrolysis. 116 (2015) 18–26. https://doi.org/10.1016/j.jaap.2015.10.012.

[162] J.O. Ajikashile, M.J. Alhnidi, G.K. Parku, A. Funke, A. Kruse, A study on the fast pyrolysis of millet and sorghum straws sourced from arid and semi-arid regions of Nigeria in a twin-screw mixing reactor, Mater. Sci. Energy Technol. 6 (2023) 388–398. https://doi.org/10.1016/j.mset.2023.03.007.

[163] N. Weih, A. Niebel, C. Pfitzer, A. Funke, G.K. Parku, N. Dahmen, Operational experience with miscanthus feedstock at the bioliq ® fast pyrolysis plant, J. Anal. Appl. Pyrolysis. 177 (2024). https://doi.org/https://doi.org/10.1016/j.jaap.2023.106338.

Appendix A: *Additional Information on Using Fractional Condensation to Optimize Aqueous Pyrolysis Condensates for Downstream Microbial Conversion*

Section 1: Surrogate Mixture Selection

Table A1. Analysis for selecting surrogate compounds for aqueous condensate (AC) (wheat straw–derived AC used as the basis).

	Factors					
Compounds	**Boiling point range (64.7 – 291.5 °C)**	**Functional group**	**Interest to microbial conversion**	**Concentration**	**Decision**	**Inference (basis for selection or rejection)**
ACIDS						
Acetic acid	Within range	Carboxylic acid	(+) Of interest; promotes microbial conversion	High	Selected	High concentration; interest to microbes
Propionic acid	Within range	Carboxylic acid	(+) Of interest; promotes microbial conversion	High	Selected	High concentration; interest to microbes
Butyric acid	Within range	Carboxylic acid	No Impact	Low	Not selected	Not of interest to microbes; low concentration
2-Methylpropanoic acid	Within range	Carboxylic acid	(+/-) Of interest; inhibits Bacillus and E. coli at concentrations at and above 21 and 13.7 g/L respectively	Low	Selected	Of interest to microbes
NONAROMATIC ALCOHOLS						
Ethylene glycol	Within range	Ethylene alcohol	(+/-) Of interest; inhibits microbial growth at concentrations above 40 g/L	High	Selected	High concentration; of interest to microbes
Methanol	lowest boiling point compound in mixture (bp 64.7 °C)	Alcohol	Inhibitor	High	Selected	High concentration; of interest to microbes; lowest boiling point compound in mixture
NONAROMATIC ALDEHYDES						
Hydroxy acetaldehyde (Glycol aldehyde)	Within range	Hydroxy aldehyde	(+/-) Of interest; concentration range of 0.05-0.1% is inhibiting to Bacillus and E. coli	Moderate	Selected	Moderate concentration; of interest to microbes
3-hydroxypropionaldehyde	Within range	Hydroxy aldehyde	(+/-) Of interest; strong inhibitor for some bacillus and fungi	Low	Selected	Of interest to microbes
Crotonaldehyde, trans	Within range	Aldehyde	No conclusive impact reported	Low	Not selected	Low concentration; interest to microbes is not completely defined

NONAROMATIC KETONES						
Hydroxyacetone (Acetol)	Within range	Hydroxy ketone	(+) Of interest; promotes microbial conversion	High	Selected	High concentration; of interest to microbes
2-Butanone	Within range	Ketone	Of interest to microbes (+/-); complete inhibition of bacillus and E. coli at concentrations above 30 and 18 g/L (i.e. 3.0 and 1.8 wt.%) respectively	Moderate	Selected	Moderate concentration; of interest to microbes
1-hydroxy-2-butanone	Within range	Ketone	Of interest, (+/-) high concentration enhances inhibition (numbers?? Consult partners)	High	Selected	High concentration; of interest to microbes
2,3-Butanedione (Diacetyl)	Within range	Diketone	Of interest; (+/-) inhibiting to some bacillus at concentrations above 0.14 g/L	Moderate	Selected	Moderate concentration; of interest to microbes
Acetoin (3-Hydroxy-2-butanone)	Within range	Hydroxy ketone	Not of interest	Moderate	Not selected	not of interest to microbes
Cyclopentanone	Within range	Cyclic ketone	Not of interest	Moderate	Not selected	Not of interest to microbes
2-Cyclopenten-1-one	Within range	Cyclic ketone	Not of interest	Moderate	Not selected	Not of interest to microbes
2-methyl-2-Cyclopenten-1-one	Within range	Cyclic ketone	Not of interest	Moderate	Not selected	Not of interest to microbes
2-Cyclohexen-1-one	Within range	Cyclic ketone	Not of interest	Very low	Not selected	Not of interest to microbes; concentration too low
3-methyl-1,2-Cyclopentanedione	Within range	Cyclic ketone	Not of interest	Moderate	Not selected	Not of interest to microbes
2-hydroxy-1-methyl-1-Cyclopenten-3-one	Within range	Cyclic ketone	Not of interest	Moderate	Not selected	Not of interest to microbes
poss: 3-Buten-2-one = 2-Butenone	Within range	-	Not of interest	Moderate	Not selected	Not of interest to microbes
2-hydroxy-2-Cyclopenten-1-one	Within range	Hydroxy cyclic ketone	Not of interest	Very low	Not selected	Not of interest to microbes; concentration too low
3-Penten-2-one	Within range	Ketone	Not of interest	Moderate	Not selected	Not of interest to microbes
FURANS						
2-Furfuryl alcohol	Within range	Hydroxymethyl furan	Not of interest	Low	Not selected	Not of interest to microbes; concentration low
2-Furaldehyde (Furfural)	Within range	Furan aldehyde	(-) Of interest; strong inhibitor	Moderate	Selected	Moderate concentration; of interest to microbes

3-Furaldehyde	Within range	Furan aldehyde	Not of interest	Very low	Not selected	Not of interest to microbes; concentration too low
5-methyl-2-Furaldehyde	Within range	Methylfuran aldehyde	Not of interest	Very low	Not selected	not of interest to microbes; concentration too low
5-hydroxymethyl-2-Furaldehyde	Highest boiling point compound in mixture (291.5 °C)	Hydroxymethyl furan aldehyde	(+/-) Of interest; known inhibitor to some microbes, complete inhibition to E. coli and Bacillus subtilis above 2 g/L	Very low	Selected	Of interest to microbes; highest boiling point compound in the mixture
γ -Butyrolactone	Within range	Dihydrofuran	Not of interest	Low	Not selected	Not of interest to microbes; low concentration
BENZENES						
Naphthalene	Within range	Benzene	(+/-) Of interest; inhibiting at concentrations above 0.5 g/L	Very low (negligible)	Not selected	Concentration is too low (approx. zero)
AROMATIC ALDEHYDES						
Benzaldehyde	Within range	Aromatic aldehyde	Not of interest; metabolite of some aromatics	Very low	Not selected	Not of interest to microbes; concentration too low
LIGNIN-DERIVED PHENOLS						
Phenol	Within range	Phenol	Of interest; inhibiting at concentrations above 0.8 g/L but suitable as single carbon source	Low	Selected	Of interest to microbes
o-Cresol	Within range	Methylphenol	(-) Of interest; inhibiting towards bacterial growth	Low	Selected	Of interest to microbes
m-Cresol	Within range	Methylphenol	(+/-) Of interest; potentially inhibiting but can serve as single carbon source	Very low	Selected	Of interest to microbes
p-Cresol	Within range	Methylphenol	Not of interest	Very low	Not selected	Not of interest to microbes, concentration is very low
GUAIACOLS (METHOXY PHENOLS)						
Guaiacol	Within range	Methoxyphenol	(+/-) Of interest; inhibiting but facilitates microbial growth for low concentrations of less than 0.1 g/L	Moderate	Selected	Moderate concentration; of interest to microbes
3-methyl-guaiacol	Within range	Methoxy methylphenol	Not of interest	Very low	Not selected	Not of interest to microbes; concentration too low
4-methyl-guaiacol	Within range	Methoxy methylphenol	Not of interest	Low	Not selected	Not of interest to microbes; concentration too low
4-ethyl-guaiacol	Within range	Ethyl methoxyphenol	Not of interest	Very low	Not selected	Not of interest to microbes; concentration too low

4-vinyl-guaiacol	Within range	Ethenyl methoxyphenol	Not of interest	Very low	Not selected	Not of interest to microbes; concentration too low
Vanillin	Within range	Hydroxymethoxybenzaldehyde	(-) Of interest; strong inhibitor	Very low	Selected	Concentration very low but of interest to microbes
SYRINGOLS (DIMETHOXY PHENOLS)						
Syringol	Within range	Dimethoxy phenol	(+/-) Of interest; inhibitor but can potentially be metabolized	Very low	Selected	concentration very low but of potential interest to microbes
4-methyl-syringol	Within range	Dimethoxy methylphenol	Not of interest	Very low (negligible)	Not selected	concentration too low (approx. zero) and not of interest to microbes
4-ethyl-syringol	Within range	Dimethoxy ethylphenol	Not of interest	Very low (negligible)	Not selected	concentration too low (approx. zero) and not of interest to microbes
4-vinyl-syringol	Within range	Dimethoxy ethenylphenol	Not of interest	Very low (negligible)	Not selected	concentration too low (approx. zero) and not of interest to microbes
Water	Within range		Main composition of Aqueous condensate (AC)	Very high	Selected	Forms the majority fraction of AC

Note: The categorization of sample concentrations is presented in Table A2.

Key / Symbols

(+) Substrate
(-) Inhibitor
(+/-) Possible substrate or inhibitor, depending on concentration

Surrogate compounds for aqueous condensate (AC) were selected following GC-MS analysis and microbial tolerance screening conducted by project partners. In selecting the compounds, the following factors were considered.

1. Representation of the surrogate mixtures such that they cover the entire boiling point range of the individual components present in AC.
2. Representation of all relevant functional groups in the original AC mixture.
3. Interest of the compounds to microbial conversion.
4. Concentration of the compounds.

The analysis for selecting surrogate compounds is presented in detail in Table A1. Based on the tolerance test results, concentration ranges have been categorized as shown in Table A2.

Table A2. Concentration categories used in selecting surrogate compounds.

Concentration	**Category**
Less than 0.03 wt.%	Very low
Between 0.03 and 0.1 wt.%	Low
Between 0.1 and 0.5 wt.%	Moderate
Above 0.5 wt.%	High

All surrogate compounds selected from Table A1 are listed in Table A3. The boiling point range of the components in the original AC is well represented in the surrogate mixture, with all selected compounds falling within the range of 64.7 °C (methanol) and 291.5 °C (5-hydroxymethyl-2-Furaldehyde), as shown in Table A3. Furthermore, all relevant functional groups are represented, except aromatic aldehyde, since the only compound detected under

this functional group, benzaldehyde, had negligible concentration and had no impact on microbial conversion.

Additionally, all compounds that were of interest for microbial conversion (i.e., promoting or inhibiting microbial conversion) were selected, regardless of their concentration, except for naphthalene, which had a near-zero concentration. This results in more than one compound representing almost all functional groups in the surrogate mixture. Lastly, water, which forms the majority composition of AC, was added to the selected organic compounds.

Concentrations (in wt.%) of surrogate mixtures (Table A3) were estimated by normalizing the original GC-MS concentrations of selected surrogate compounds relative to the total concentration of AC (dry basis) in the original mixture.

Table A3. Generated surrogate/model mixture (based on wheat straw-derived AC).

SN	Component	wt.% in AC	Boiling Point (°C) at 1 atm.
1	Water	83.25	100.0
2	Acetic acid	4.28	117.1
3	Propionic acid	1.15	141.7
4	2-Methylpropanoic acid	0.04	155.2
5	Ethylene glycol	1.54	197.5
6	Methanol	1.75	64.7
7	Hydroxy acetaldehyde (Glycol aldehyde)	0.19	131.3
8	3-hydroxypropionaldehyde	0.04	215.5
9	Hydroxyacetone (Acetol)	5.70	145.5
10	2-Butanone	0.24	75.6

SN	Component	wt.% in AC	Boiling Point (°C) at 1 atm.
11	1-hydroxy-2-butanone	0.77	160.0
12	2,3-Butanedione (Diacetyl)	0.28	88.0
13	2-Furaldehyde (Furfural)	0.35	161.8
14	5-hydroxymethyl-2-Furaldehyde	0.03	291.5
15	Phenol	0.07	181.8
16	*o*-Cresol	0.05	191.0
17	*m*-Cresol	0.03	202.3
18	Guaiacol	0.20	205.0
19	Vanillin	0.01	282.6
20	Syringol	0.03	264.4

Table A4. Surrogate/model mixtures of pyrolysis vapors entering the first condensation unit and their respective mass fractions for the three biomass feedstocks.

Surrogate compound	Mass fraction (wt.%) of surrogate mixtures for each biomass feedstock			
	Wheat Straw (tolerance tests)	**Wheat Straw (validation)**	***Miscanthus***	**Coffee husk**
Water	0.2783	0.2160	0.1867	0.2044
Acetic acid	0.0425	0.0552	0.0650	0.0809
Propionic acid	0.0155	0.0446	0.0441	0.0446
2-Methylpropanoic acid	4.44E-05	0.0000	0.0000	0.0000
Ethylene glycol	0.0017	0.0000	0.0000	0.0000
Methanol	0.0019	0.0000	0.0000	0.0000
Hydroxy acetaldehyde (Glycol aldehyde)	0.0157	0.0002	0.0153	0.0010
3-hydroxypropionaldehyde	0.00004	0.0000	0.0018	0.0011
Hydroxyacetone (Acetol)	0.0415	0.0416	0.0481	0.0465
2-Butanone	0.0004	0.0008	0.00008	0.0001
1-hydroxy-2-butanone	0.0009	0.0089	0.0059	0.0072
2,3-Butanedione (Diacetyl)	0.0004	0.0002	0.0001	0.0003
2-Furaldehyde (Furfural)	0.0019	0.0022	0.0040	0.0043
5-hydroxymethyl-2-Furaldehyde	0.00003	0.0000	0.0000	0.0000
Phenol	0.0015	0.0041	0.0028	0.0017
m-Cresol	0.0007	0.0019	0.0009	0.0010
o-Cresol	0.0006	0.0022	0.0011	0.0013

Surrogate compound	Mass fraction (wt.%) of surrogate mixtures for each biomass feedstock			
	Wheat Straw (tolerance tests)	**Wheat Straw (validation)**	***Miscanthus***	**Coffee husk**
Guaiacol	0.0030	0.0052	0.0023	0.0046
Vanillin	0.0015	0.0038	0.0044	0.0059
Syringol	0.0023	0.0040	0.0018	0.0034
Levoglucosan	0.0061	0.0053	0.0530	0.0464
Lignin (unknowns)	0.2857	0.3010	0.3094	0.3014
N_2	0.1099	0.0975	0.0925	0.0815
CO	0.0559	0.0644	0.0601	0.0606
CO_2	0.1318	0.1410	0.1003	0.1015
H_2	0.0003	0.0002	0.0003	0.0002

Section 2: Central Composite Design (CCD)

Table A5. Central Composite Design (CCD) factors and their respective ranges investigated for all biomass feedstocks.

Factors	Lower level (−)	Center point (0)	Upper level (+)	Lower axial (−δ)	Higher axial (+δ)
T, Cond 1 (°C)	10	30	50	1.71573	58.2843
T, Cond 2 (°C)	80	100	120	71.7157	128.284

Note: T, Cond 1 = Temperature of Condenser 1; T, Cond 2 = Temperature of Condenser 2.

Table A6. Data for the range of condenser temperatures investigated and their corresponding response factors for wheat straw.

T, Cond 1 (°C)	T, Cond 2 (°C)	Promoters (wt.%)	Inhibitors (wt.%)	P/I	Yield, AC (wt.%)	P/I × AC Yield	Water (wt.%)
80	10	13.3067	1.9252	7	19.0469	1	84.7681
120	10	17.3077	1.2782	14	43.8601	6	81.4141
100	30	14.5841	1.1861	12	31.6431	4	84.2298
100	30	14.5841	1.1861	12	31.6431	4	84.2298
128.284	30	18.8102	1.1540	16	45.2957	7	80.0358
100	1.71573	14.5449	1.4931	10	33.1026	3	83.9620
100	58.2843	14.9374	0.7547	20	25.6085	5	84.3077
100	30	14.5841	1.1861	12	31.6431	4	84.2298
80	50	13.1619	1.2033	11	17.5963	2	85.6350
71.7157	30	12.8862	1.2073	11	12.9203	1	85.9065
100	30	14.5841	1.1861	12	31.6431	4	84.2298

T, Cond 1 (°C)	T, Cond 2 (°C)	Promoters (wt.%)	Inhibitors (wt.%)	P/I	Yield, AC (wt.%)	P/I × AC Yield	Water (wt.%)
120	50	17.8888	0.9201	19	38.2816	7	81.1911
100	30	14.5841	1.1861	12	31.6431	4	84.2298

Note: T, Cond 1 = Temperature of Condenser 1; T, Cond 2 = Temperature of Condenser 2.

Table A7 Data for the condenser temperatures investigated and their corresponding response factors for *miscanthus*.

T, Cond 1 (°C)	T, Cond 2 (°C)	Promoters (wt.%)	Inhibitors (wt.%)	P/I	Yield, AC (wt.%)	P/I × AC Yield	Water (wt.%)
71.7157	30	22.7517	0.9852	23	14.5718	3	76.2633
100	1.71573	25.0297	1.1064	23	32.7913	7	73.8640
120	10	29.5242	1.3715	22	42.8419	9	69.1043
100	30	25.2409	1.0839	23	31.4338	7	73.6752
128.284	30	31.9876	1.5170	21	44.4212	9	66.4954
100	58.2843	26.5283	1.0541	25	25.6341	6	72.4174
100	30	25.2409	1.0839	23	31.4338	7	73.6752
80	10	22.9039	0.9948	23	19.5594	5	76.1012
80	50	22.9369	1.0049	23	18.1052	4	76.0583
100	30	25.2409	1.0839	23	31.4338	7	73.6752
120	50	30.9390	1.3421	23	37.5026	9	67.7189
100	30	25.2409	1.0839	23	31.4338	7	73.6752
100	30	25.2409	1.0839	23	31.4338	7	73.6752

Note: T, Cond 1 = Temperature of Condenser 1; T, Cond 2 = Temperature of Condenser 2.

Table A8. Data on the condenser temperatures investigated and their corresponding response factors for coffee husk.

T, Cond 1 (°C)	T, Cond 2 (°C)	Promoters (wt.%)	Inhibitors (wt.%)	P/I	Yield, AC (wt.%)	P/I × AC Yield	Water (wt.%)
100	1.71573	26.3563	1.0059	26	35.4630	9	72.6378
100	30	26.5715	0.9838	27	34.0034	9	72.4447
100	30	26.5715	0.9838	27	34.0034	9	72.4447
100	30	26.5715	0.9838	27	34.0034	9	72.4447
100	30	26.5715	0.9838	27	34.0034	9	72.4447
80	50	24.2192	0.9122	27	19.0975	5	74.8687
80	10	24.1633	0.9120	26	20.8445	6	74.9246
120	10	30.9109	1.2792	24	46.4504	11	67.8099
71.7157	30	23.9832	0.9137	26	15.4262	4	75.1027
128.284	30	33.2746	1.4411	23	48.1744	11	65.2843
100	30	26.5715	0.9838	27	34.0034	9	72.4447
100	58.2843	27.8765	0.9678	29	27.6978	8	71.1557
120	50	32.2183	1.2698	25	41.0773	10	66.5120

Note: T, Cond 1 = Temperature of Condenser 1; T, Cond 2 = Temperature of Condenser 2.

Section 3: GC-MS Analysis of All ORC and AC Products

Table A9. GC-MS data for aqueous condensate (AC) recovered under optimum condensation temperature conditions (C1/C2 = 120 °C/50 °C) for wheat straw.

		Run 1			Run 2			Run 3			Run 4		
CAS No.	**Compound**	**wt.% wet**		**wt.% dry**	**wt.% wet**		**wt.% dry**	**wt.% wet**		**wt.% dry**	**wt.% wet**		**wt.% dry**
	NONAROMATIC COMPOUNDS												
	Acids	**4.025**		**27.95**	**4.195**		**29.13**	**4.298**		**33.32**	**4.313**		**33.44**
64-19-7	Acetic acid	3.115	c	21.634	3.273	c	22.730	3.365	c	26.082	3.391	c	26.285
79-09-4	Propionic acid	0.766	c	5.321	0.774	c	5.372	0.800	c	6.201	0.795	c	6.160
107-92-6	Butyric acid	0.122	c	0.847	0.128	c	0.892	0.133	c	1.032	0.128	c	0.992
	Propanoic acid, 2-methyl- (NIST MQ 87)	0.021	#	0.147	0.020	#	0.140	-		-	-		-
	Nonaromatic Esters	**0.008**		**0.05**	**0.008**		**0.05**	**0.008**		**0.06**	**0.008**		**0.06**
554-12-1	Propanoic acid methyl ester	0.008	c	0.053	0.008	c	0.053	0.008	c	0.064	0.008	c	0.059
	Nonaromatic Alcohols	**0.025**		**0.17**	**0.024**		**0.17**	**0.004**		**0.03**	**0.029**		**0.22**
	Propanol, 1-	0.025	#	0.171	0.024	#	0.166	0.004	#	0.027	0.003	#	0.025
	2-Propen-1-ol (NIST MQ 91)	-		-	-		-	-			0.025	#	0.197
	Nonaromatic Aldehydes	**0.287**		**1.99**	**0.275**		**1.91**	**0.162**		**1.26**	**0.230**		**1.78**
141-46-8	Acetaldehyde, hydroxy-	0.162	c	1.125	0.150	c	1.043	0.045	c	0.351	0.111	c	0.858
123-72-8	Butanal	0.007	c	0.047	0.007	c	0.051	0.008	c	0.065	0.008	c	0.064
15798-64-8	Crotonaldehyde, cis	0.025	c	0.172	0.025	c	0.175	0.026	c	0.204	0.025	c	0.196
123-73-9	Crotonaldehyde, trans	0.014	c	0.098	0.014	c	0.100	0.016	c	0.127	0.017	c	0.129
	Butanedial or Propanal (NIST MQ 88)	0.079	#	0.548	0.078	#	0.543	0.066	#	0.511	0.069	#	0.534
	Nonaromatic Ketones	**6.438**		**44.71**	**6.281**		**43.62**	**6.362**		**49.32**	**6.271**		**48.61**
116-09-6	Acetol (Hydroxypropanone)	4.252	c	29.527	4.137	c	28.729	4.135	c	32.056	4.072	c	31.569
78-93-3	Butanone, 2-	0.064	c	0.445	0.065	c	0.455	0.077	c	0.599	0.078	c	0.604
5077-67-8	Butanone, 1-hydroxy-2-	0.670	c	4.652	0.653	c	4.536	0.667	c	5.167	0.661	c	5.128
431-03-8	Butandione, 2,3- (Diacetyl)	0.076	c	0.527	0.078	c	0.540	0.086	c	0.665	0.081	c	0.624
513-86-0	Acetoin (Hydroxy-2-butanone, 3-)	0.155	c	1.078	0.152	c	1.054	0.131	c	1.016	0.137	c	1.059
592-20-1	Propan-2-one, 1-acetyloxy-	0.056	c	0.387	0.050	c	0.349	0.077	c	0.599	0.070	c	0.544
120-92-3	Cyclopentanone	0.058	c	0.404	0.061	c	0.421	0.064	c	0.496	0.062	c	0.479
930-30-3	Cyclopenten-1-one, 2-	0.422	c	2.929	0.412	c	2.858	0.436	c	3.380	0.430	c	3.331
1121-05-7	Cyclopenten-1-one, 2,3-dimethyl-2-	0.027	c	0.186	0.028	c	0.193	0.029	c	0.221	0.027	c	0.212

		Run 1			Run 2			Run 3			Run 4		
CAS No.	**Compound**	**wt.% wet**		**wt.% dry**	**wt.% wet**		**wt.% dry**	**wt.% wet**		**wt.% dry**	**wt.% wet**		**wt.% dry**
1120-73-6	Cyclopenten-1-one, 2-methyl-2-	0.131	c	0.907	0.131	c	0.910	0.124	c	0.958	0.126	c	0.979
2758-18-1	Cyclopenten-1-one, 3-methyl-2-	0.075	c	0.521	0.073	c	0.510	0.078	c	0.604	0.075	c	0.579
5682-69-2	Cyclopenten-1-one, 3-ethyl-2-	-		-	-		-	0.012	#	0.090	0.012	#	0.090
80-71-7	Cyclopenten-1-one, 2-hydroxy-3-methyl-2-	0.120	c	0.837	0.117	c	0.816	0.120	c	0.933	0.122	c	0.945
21835-01-8	Cyclopenten-1-one, 3-ethyl-2-hydroxy-2-	0.017	c	0.120	0.016	c	0.112	0.016	c	0.126	0.017	c	0.132
930-68-7	Cyclohexen-1-one, 2-	0.008	c	0.059	0.009	c	0.059	0.009	c	0.072	0.009	c	0.069
	3-Buten-2-one (NIST MQ 88)	0.008	#	0.054	0.008	#	0.053	0.010	#	0.074	0.009	#	0.072
	Butanone, 3-methyl-2- (NIST MQ 88)	-		-	-		-	0.010	#	0.074	0.008	#	0.064
	3-Buten-2-one, 3-methyl- (NIST MQ 88)	-		-	-		-	0.005	#	0.039	0.005	#	0.038
	2-Pentanone (NIST MQ 94)	0.012	#	0.080	0.012	#	0.085	0.015	#	0.115	0.014	#	0.106
	2,3-Pentanedione	0.020	#	0.136	0.019	#	0.135	0.022	#	0.171	0.021	#	0.166
	3-Penten-2-one (NIST MQ 84)	0.017	#	0.120	0.017	#	0.120	0.020	#	0.158	0.019	#	0.150
	3-Pentanone, 2-hydroxy- (NIST MQ 82)	0.008	#	0.056	0.008	#	0.055	0.016	#	0.121	-		-
	Cyclopentanone, 2-methyl- (NIST MQ 87)	0.015	#	0.104	0.015	#	0.102	0.025	#	0.192	0.014	#	0.106
	Isomere of 2-Cyclopenten-1-one, 3-methyl-	0.023	#	0.160	0.022	#	0.155	0.034	#	0.261	0.024	#	0.188
	2-Butanone, 1-hydroxy-3-methyl- (NIST MQ 78)	0.034	#	0.235	0.033	#	0.228	0.018	#	0.141	0.034	#	0.260
	2-Cyclopenten-1-one, x,y-dimethyl-	0.017	#	0.117	0.017	#	0.115	0.017	#	0.130	0.017	#	0.135
	2-Cycolpenten-1-one, x,y-dimethyl-	0.016	#	0.109	0.015	#	0.106	0.013	#	0.098	0.016	#	0.124
	1,2-Cyclopentanedione (NIST MQ 86)	0.014	#	0.099	0.014	#	0.096	0.014	#	0.109	0.012	#	0.095
	2,5-Hexanedione (NIST MQ 89)	0.014	#	0.094	0.014	#	0.100	0.026	#	0.205	0.013	#	0.103
	Isomere of Cyclopenten-1-one, 2,3-dimethyl-2-	0.026	#	0.178	0.025	#	0.174	0.016	#	0.127	0.026	#	0.199
	2-Cyclopenten-1-one, x,y-dimethyl-	0.016	#	0.112	0.016	#	0.110	0.012	#	0.096	0.016	#	0.125
	2-Cyclopenten-1-one, 2,3,4-trimethyl- (NIST MQ 88)	0.012	#	0.086	0.012	#	0.086	0.010	#	0.074	0.012	#	0.097
	Isomer of Cyclopenten-1-one, 3-ethyl-2-hydroxy-	0.018	#	0.128	0.018	#	0.123	0.018	#	0.140	0.018	#	0.137
	2-Cyclopenten-1-one, trimethyl- (NIST MQ 87)	0.006	#	0.040	0.005	#	0.037	0.006	#	0.043	0.005	#	0.042

		Run 1			Run 2			Run 3			Run 4		
CAS No.	**Compound**	**wt.% wet**		**wt.% dry**	**wt.% wet**		**wt.% dry**	**wt.% wet**		**wt.% dry**	**wt.% wet**		**wt.% dry**
	poss: 2-Cyclopenten-1-one, trimethyl- (NIST MQ 82)	0.010	#	0.069	0.009	#	0.059	0.005	#	0.040	0.005	#	0.040
	similar to 2-Cyclopenten-1-one, 3-ethyl-	0.013	#	0.093	0.013	#	0.091	-		-	-		-
	poss: 2-Cyclopenten-1-one, trimethyl- (NIST MQ 82)	0.005	#	0.033	0.005	#	0.032	-		-	0.005	#	0.040
	2-Cyclopenten-1-one, 4-ethyl-2-hydroxy- (NIST MQ 80)	0.003	#	0.021	0.003	#	0.018	-		-	-		-
	Aliphatic Hydrocarbons	**0.000**		**0.00**	**0.000**		**0.00**	**0.000**		**0.00**	**0.000**		**0.00**
	HETEROCYCLIC COMPOUNDS												
	Furans	**0.569**		**3.95**	**0.552**		**3.84**	**0.583**		**4.52**	**0.572**		**4.43**
98-00-0	Furfuryl alcohol, 2-	0.048	c	0.330	0.045	c	0.316	0.042	c	0.323	0.039	c	0.304
497-23-4	Furanone, 2(5H)-	0.035	c	0.244	0.035	c	0.242	0.036	c	0.278	0.035	c	0.269
98-01-1	Furaldehyde, 2-	0.269	c	1.871	0.263	c	1.823	0.276	c	2.137	0.273	c	2.114
498-60-2	Furaldehyde, 3-	0.012	c	0.083	0.011	c	0.075	0.013	c	0.103	0.011	c	0.084
620-02-0	Furaldehyde, 5-methyl-2-	0.018	c	0.128	0.018	c	0.127	0.019	c	0.151	0.019	c	0.147
1192-62-7	Ethanone, 1-(2-furanyl)-	0.026	c	0.183	0.026	c	0.180	0.027	c	0.211	0.026	c	0.205
591-11-7	Furan-2-one, 5-methyl-, (5H)-	0.014	#	0.095	0.014	#	0.095	0.013	#	0.100	0.013	#	0.099
22122-36-7	Furan-2-one, 3-methyl-, (5H)-	0.015	c	0.105	0.015	c	0.103	0.015	c	0.119	0.015	c	0.119
	Furan-2-one, 2,5-dihydro-3,5-dimethyl-	0.017	#	0.121	0.016	#	0.112	0.017	#	0.130	0.016	#	0.126
108-29-2	Valerolactone, γ- (gamma-Butyrolactone, 1-methyl-)	-		-	-		-	0.008	c	0.061	-		-
96-48-0	Butyrolactone, γ-	0.100	c	0.694	0.098	c	0.683	0.104	c	0.808	0.008	c	0.060
	Furan, tetrahydro-2-methoxy- (NIST MQ (/)	0.008	#	0.056	0.008	#	0.055	0.009	#	0.067	0.104	c	0.808
	Furan-2-one, 4-methyl-(5H)- (NIST MQ 88)	0.006	#	0.039	0.004	#	0.026	0.004	#	0.033	0.008	#	0.063
	Pyrans	**0.000**		**0.00**	**0.000**		**0.00**	**0.000**		**0.00**	**0.000**		**0.00**
	AROMATIC COMPOUNDS												
	Benzenes	**0.000**		**0.00**	**0.000**		**0.00**	**0.002**		**0.02**			

		Run 1			Run 2			Run 3			Run 4		
CAS No.	**Compound**	**wt.% wet**		**wt.% dry**	**wt.% wet**		**wt.% dry**	**wt.% wet**		**wt.% dry**	**wt.% wet**		**wt.% dry**
83-33-0	Inden-1-one, 2,3-dihydro-1H-							0.002	c	0.016	0.002	c	0.015
	Catechols	**0.000**		**0.00**	**0.000**		**0.00**	**0.000**		**0.00**	**0.000**		**0.00**
	Aromatic Alcohols	**0.000**		**0.00**	**0.000**		**0.00**	**0.000**		**0.00**	**0.000**		**0.00**
	Aromatic Aldehydes	**0.003**		**0.02**	**0.003**		**0.02**	**0.003**		**0.02**	**0.003**		**0.02**
100-52-7	Benzaldehyde	0.003	c	0.020	0.003	c	0.019	0.003	c	0.024	0.003	c	0.022
	Aromatic Ketones	**0.002**		**0.02**	**0.002**		**0.01**	**0.002**		**0.02**	**0.002**		**0.02**
98-86-2	Acetophenone	0.002	c	0.016	0.002	c	0.014	0.002	c	0.019	0.002	c	0.017
	Aromatic Esters	**0.000**		**0.00**	**0.000**		**0.00**	**0.000**		**0.00**	**0.000**		**0.00**
	Lignin-derived Phenols	**0.131**		**0.91**	**0.130**		**0.90**	**0.152**		**1.18**	**0.149**		**1.15**
108-95-2	Phenol	0.061	c	0.425	0.060	c	0.417	0.065	c	0.502	0.063	c	0.492
95-48-7	Cresol, o-	0.023	c	0.163	0.024	c	0.166	0.025	c	0.193	0.024	c	0.187
106-44-5	Cresol, p-	0.010	c	0.067	0.010	c	0.067	0.010	c	0.079	0.010	c	0.077
108-39-4	Cresol, m-	0.013	c	0.088	0.013	c	0.089	0.014	c	0.107	0.014	c	0.107
95-87-4	Phenol, 2,5-dimethyl-	0.008	c	0.052	0.007	c	0.050	0.008	c	0.059	0.007	c	0.057
105-67-9	Phenol, 2,4-dimethyl-	0.004	c	0.025	0.004	c	0.025	0.003	c	0.027	0.003	c	0.027
576-26-1	Phenol, 2,6-dimethyl-	-		-	-		-	0.002	c	0.016	0.002	c	0.015
526-75-0	Phenol, 2,3-dimethyl-	-		-	-		-	0.001	c	0.011	0.001	c	0.010
108-68-9	Phenol, 3,5-dimethyl-	-		-	-		-	0.001	c	0.007	0.001	c	0.006
90-00-6	Phenol, 2-ethyl-	-		-	-		-	0.002	c	0.015	0.002	c	0.015
620-17-7	Phenol, 3-ethyl-	-		-	-		-	0.009	c	0.068	0.009	c	0.067
123-07-9	Phenol, 4-ethyl-	0.013	c	0.093	0.013	c	0.092	0.012	c	0.096	0.012	c	0.094
	Guaiacols (Methoxy phenols)	**0.152**		**1.05**	**0.148**		**1.02**	**0.141**		**1.09**	**0.139**		**1.08**
90-05-1	Guaiacol	0.110	c	0.767	0.107	c	0.743	0.102	c	0.793	0.101	c	0.786
18102-31-3	Guaiacol, 3-methyl-	0.003	#	0.024	0.003	#	0.024	0.003	#	0.025	0.003	#	0.025
93-51-6	Guaiacol, 4-methyl-	0.018	c	0.123	0.017	c	0.121	0.017	c	0.131	0.017	c	0.129
2785-89-9	Guaiacol, 4-ethyl-	0.020	c	0.140	0.020	c	0.137	0.019	c	0.144	0.018	c	0.141

		Run 1			Run 2			Run 3			Run 4		
CAS No.	Compound	wt.% wet		wt.% dry	wt.% wet		wt.% dry	wt.% wet		wt.% dry	wt.% wet		wt.% dry
	Syringols (Dimethoxy phenols)	**0.000**		**0.00**	**0.000**		**0.00**	**0.000**		**0.00**	**0.000**		**0.00**
	CARBOHYDRATES												
	Sugars	**0.000**		**0.00**	**0.000**		**0.00**	**0.000**		**0.00**	**0.000**		**0.00**
	OTHER ORGANIC COMPOUNDS												
	N-compounds	**0.014**		**0.10**	**0.014**		**0.10**	**0.013**		**0.10**	**0.013**		**0.10**
110-86-1	Pyridine	0.012	c	0.085	0.012	c	0.086	0.013	c	0.103	0.013	c	0.099
	Pyridine, 2-methyl- (NIST MQ 92)	0.002	#	0.013	0.002	#	0.012	-		-	-		-
	Acetates	**0.000**		**0.00**	**0.000**		**0.00**	**0.000**		**0.00**	**0.000**		**0.00**
	Terpenes	**0.000**		**0.00**	**0.000**		**0.00**	**0.000**		**0.00**	**0.000**		**0.00**
	unknown compounds	**0.000**		**0.00**	**0.000**		**0.00**	**0.000**		**0.00**	**0.000**		**0.00**
	Miscellaneous	**0.007**		**0.05**	**0.006**		**0.04**	**0.008**		**0.06**	**0.008**		**0.06**
	1,3-Dioxolane, 2,2,4-trimethyl- (NIST MQ 86)	-		-	-		-	0.002	#	0.014	0.002	#	0.014
	poss: 1,4-Dioxin, 2,3-dihydro-	0.007	#	0.045	0.006	#	0.044	0.006	#	0.050	0.006	#	0.049

Table A10. GC-MS data for aqueous condensate (AC) recovered under optimum condensation temperature conditions (C1/C2 = 120 °C/50 °C) for *miscanthus*

		Run 1			Run 2			Run 3			Run 4		
CAS No.	**Compound**	**wt.% wet**		**wt.% dry**	**wt.% wet**		**wt.% dry**	**wt.% wet**		**wt.% dry**	**wt.% wet**		**wt.% dry**
	NONAROMATIC COMPOUNDS												
	Acids	**6.242**		**32.51**	**6.190**		**32.24**	**7.067**		**31.41**	**7.058**		**31.37**
64-19-7	Acetic acid	5.357	c	27.902	5.315	c	27.684	6.207	c	27.589	6.193	c	27.522
79-09-4	Propionic acid	0.757	c	3.944	0.748	c	3.894	0.738	c	3.280	0.740	c	3.288
107-92-6	Butyric acid	0.127	c	0.662	0.127	c	0.664	0.122	c	0.540	0.125	c	0.557
	Nonaromatic Esters	**0.007**		**0.03**	**0.006**		**0.03**	**0.007**		**0.03**	**0.006**		**0.03**
554-12-1	Propanoic acid methyl ester	0.007	c	0.035	0.006	c	0.033	0.007	c	0.031	0.006	c	0.028
	Nonaromatic Alcohols	**0.047**		**0.24**	**0.047**		**0.24**	**0.050**		**0.22**	**0.050**		**0.22**
	2-Propen-1-ol (NIST MQ 91)	0.047	#	0.244	0.047	#	0.243	0.050	#	0.221	0.050	#	0.220
	Nonaromatic Aldehydes	**0.875**		**4.56**	**0.841**		**4.38**	**1.574**		**6.99**	**1.518**		**6.75**
141-46-8	Acetaldehyde, hydroxy-	0.633	c	3.295	0.589	c	3.068	1.160	c	5.157	1.118	c	4.971
2134-29-4	Propionaldehyde, 3-hydroxy	0.062	#	0.323	0.069	#	0.362	0.135	#	0.601	0.132	#	0.585
123-72-8	Butanal	0.010	c	0.051	0.010	c	0.051	0.011	c	0.047	0.010	c	0.045
15798-64-8	Crotonaldehyde, cis	0.050	c	0.261	0.050	c	0.260	0.058	c	0.259	0.058	c	0.258
123-73-9	Crotonaldehyde, trans	0.014	c	0.073	0.015	c	0.076	0.014	c	0.064	0.012	c	0.052
	Butanedial or Propanal (NIST MQ 88)	0.106	#	0.553	0.109	#	0.566	0.195	#	0.865	0.188	#	0.835
	Nonaromatic Ketones	**6.716**		**34.98**	**6.687**		**34.83**	**6.814**		**30.29**	**6.763**		**30.06**
116-09-6	Acetol (Hydroxypropanone)	5.121	c	26.670	5.113	c	26.628	5.381	c	23.915	5.343	c	23.748
78-93-3	Butanone, 2-	0.059	c	0.309	0.061	c	0.318	0.049	c	0.218	0.048	c	0.213
5077-67-8	Butanone, 1-hydroxy-2-	0.480	c	2.499	0.479	c	2.497	0.424	c	1.883	0.417	c	1.853
431-03-8	Butandione, 2,3- (Diacetyl)	0.099	c	0.515	0.097	c	0.505	0.105	c	0.465	0.104	c	0.463
513-86-0	Acetoin (Hydroxy-2-butanone, 3-)	0.093	c	0.483	0.094	c	0.489	0.087	c	0.385	0.086	c	0.382
592-20-1	Propan-2-one, 1-acetyloxy-	0.218	c	1.138	0.208	c	1.082	0.186	c	0.826	0.186	c	0.827
120-92-3	Cyclopentanone	0.033	c	0.174	0.033	c	0.170	0.029	c	0.130	0.029	c	0.128
930-30-3	Cyclopenten-1-one, 2-	0.259	c	1.348	0.258	c	1.344	0.215	c	0.957	0.214	c	0.953
1121-05-7	Cyclopenten-1-one, 2,3-dimethyl-2-	0.010	c	0.055	0.011	c	0.056	0.008	c	0.037	0.008	c	0.036
1120-73-6	Cyclopenten-1-one, 2-methyl-2-	0.042	c	0.220	0.044	c	0.227	0.039	c	0.175	0.039	c	0.171
2758-18-1	Cyclopenten-1-one, 3-methyl-2-	0.038	c	0.199	0.037	c	0.193	0.031	c	0.138	0.031	c	0.137

		Run 1			Run 2			Run 3			Run 4		
CAS No.	**Compound**	**wt.% wet**		**wt.% dry**	**wt.% wet**		**wt.% dry**	**wt.% wet**		**wt.% dry**	**wt.% wet**		**wt.% dry**
80-71-7	Cyclopenten-1-one, 2-hydroxy-3-methyl-2-	0.074	c	0.384	0.072	c	0.377	0.064	c	0.285	0.063	c	0.281
930-68-7	Cyclohexen-1-one, 2-	0.007	c	0.035	0.007	c	0.035	0.008	c	0.035	0.007	c	0.033
	3-Buten-2-one (NIST MQ 88)	0.015	#	0.079	0.015	#	0.079	0.006	c	0.026	0.006	c	0.025
	3-Buten-2-one, 3-methyl- (NIST MQ 88)	0.012	#	0.063	0.010	#	0.054	0.011	#	0.050	0.011	#	0.050
	2,3-Pentanedione	0.023	#	0.120	0.018	#	0.092	0.013	#	0.058	0.013	#	0.056
	3-Penten-2-one (NIST MQ 84)	0.020	#	0.105	0.020	#	0.103	0.024	#	0.105	0.023	#	0.104
	Isomere of 2-Cyclopenten-1-one, 3-methyl-	0.014	#	0.071	0.014	#	0.070	0.017	#	0.076	0.017	#	0.076
	2-Butanone, 1-hydroxy-3-methyl- (NIST MQ 78)	0.019	#	0.099	0.019	#	0.099	0.012	#	0.054	0.012	#	0.054
	2-Cyclopenten-1-one, x,y-dimethyl-	0.012	#	0.064	0.012	#	0.064	0.015	#	0.068	0.015	#	0.069
	1,2-Cyclopentanedione (NIST MQ 86)	0.029	#	0.150	0.029	#	0.150	0.010	#	0.045	0.010	#	0.045
	2,5-Hexanedione (NIST MQ 89)	0.009	#	0.045	0.008	#	0.043	0.042	#	0.185	0.041	#	0.183
	2-Cyclopenten-1-one, x,y-dimethyl-	0.007	#	0.034	0.006	#	0.033	0.007	#	0.032	0.008	#	0.034
	2-Cyclopenten-1-one, 2,3,4-trimethyl- (NIST MQ 88)	0.008	#	0.040	0.007	#	0.039	0.010	#	0.044	0.010	#	0.046
	Isomer of Cyclopenten-1-one, 3-ethyl-2-hydroxy-	0.005	#	0.027	0.005	#	0.027	0.011	#	0.048	0.010	#	0.045
	poss: 2-Cyclopenten-1-one, trimethyl- (NIST MQ 82)	0.004	#	0.023	0.005	#	0.024	-		-	-		-
	similar to 2-Cyclopenten-1-one, 3-ethyl-	0.006	#	0.032	0.006	#	0.030	-		-	-		-
	Aliphatic Hydrocarbons	**0.000**		**0.00**	**0.000**		**0.00**	**0.000**		**0.00**	**0.000**		**0.00**
	HETEROCYCLIC COMPOUNDS												
	Furans	**0.743**		**3.87**	**0.739**		**3.85**	**0.777**		**3.45**	**0.784**		**3.48**
98-00-0	Furfuryl alcohol, 2-	0.015	c	0.076	0.013	c	0.068	-		-	0.104	c	0.464
497-23-4	Furanone, 2(5H)-	0.084	c	0.440	0.084	c	0.437	0.104	c	0.462	0.446	c	1.984
98-01-1	Furaldehyde, 2-	0.396	c	2.062	0.394	c	2.054	0.441	c	1.960	0.033	c	0.146
498-60-2	Furaldehyde, 3-	0.032	c	0.169	0.032	c	0.167	0.031	c	0.139	0.045	c	0.198
620-02-0	Furaldehyde, 5-methyl-2-	0.047	c	0.244	0.046	c	0.242	0.045	c	0.198	0.019	c	0.085

		Run 1			Run 2			Run 3			Run 4		
CAS No.	**Compound**	**wt.% wet**		**wt.% dry**	**wt.% wet**		**wt.% dry**	**wt.% wet**		**wt.% dry**	**wt.% wet**		**wt.% dry**
1192-62-7	Ethanone, 1-(2-furanyl)-	0.020	c	0.102	0.020	c	0.102	0.019	c	0.084	0.021	#	0.096
591-11-7	Furan-2-one, 5-methyl-, (5H)-	0.023	#	0.118	0.024	#	0.126	0.022	#	0.099	0.024	c	0.107
22122-36-7	Furan-2-one, 3-methyl-, (5H)-	0.025	c	0.129	0.024	c	0.127	0.024	c	0.108	0.104	c	0.464
	Furan-2-one, 2,5-dihydro-3,5-dimethyl-	0.015	#	0.076	0.015	#	0.076	0.012	#	0.054	0.446	c	1.984
96-48-0	Butyrolactone, γ-	0.064	c	0.334	0.065	c	0.341	0.057	c	0.255	0.057	c	0.255
	2(3H)-Furanone, 5-methyl- (NIST MQ 84)	0.013	#	0.068	0.012	#	0.061	0.012	#	0.054	0.012	#	0.055
	Furan-2-one, 4-methyl-(5H)- (NIST MQ 88)	0.010	#	0.051	0.009	#	0.049	0.009	#	0.040	0.009	#	0.041
	Pyrans	**0.000**		**0.00**	**0.000**		**0.00**	**0.000**		**0.00**	**0.000**		**0.00**
	AROMATIC COMPOUNDS												
	Benzenes	**0.000**		**0.00**	**0.000**		**0.00**	**0.000**		**0.00**	**0.000**		**0.00**
	Catechols	**0.000**		**0.00**	**0.000**		**0.00**	**0.000**		**0.00**	**0.000**		**0.00**
	Aromatic Alcohols	**0.000**		**0.00**	**0.000**		**0.00**	**0.000**		**0.00**	**0.000**		**0.00**
	Aromatic Aldehydes	**0.002**		**0.01**	**0.002**		**0.01**	**0.000**		**0.00**	**0.000**		**0.00**
100-52-7	Benzaldehyde	0.002	c	0.009	0.002	c	0.010	-		-	-		-
	Aromatic Ketones	**0.000**		**0.00**	**0.000**		**0.00**	**0.000**		**0.00**	**0.000**		**0.00**
	Aromatic Esters	**0.000**		**0.00**	**0.000**		**0.00**	**0.000**		**0.00**	**0.000**		**0.00**
	Lignin-derived Phenols	**0.199**		**1.03**	**0.199**		**1.03**	**0.193**		**0.86**	**0.193**		**0.86**
108-95-2	Phenol	0.068	c	0.353	0.067	c	0.351	0.062	c	0.277	0.063	c	0.278
95-48-7	Cresol, o-	0.022	c	0.115	0.022	c	0.114	0.021	c	0.093	0.021	c	0.092
106-44-5	Cresol, p-	0.021	c	0.111	0.021	c	0.109	0.022	c	0.096	0.022	c	0.097
108-39-4	Cresol, m-	0.010	c	0.055	0.011	c	0.055	0.009	c	0.039	0.009	c	0.039
95-87-4	Phenol, 2,5-dimethyl-	0.007	c	0.037	0.007	c	0.037	0.007	c	0.030	0.007	c	0.029
105-67-9	Phenol, 2,4-dimethyl-	0.006	c	0.030	0.006	c	0.030	0.006	c	0.028	0.006	c	0.029

		Run 1			Run 2			Run 3			Run 4		
CAS No.	**Compound**	**wt.% wet**		**wt.% dry**	**wt.% wet**		**wt.% dry**	**wt.% wet**		**wt.% dry**	**wt.% wet**		**wt.% dry**
576-26-1	Phenol, 2,6-dimethyl-	0.003	c	0.014	0.003	c	0.013	0.003	c	0.012	0.003	c	0.011
90-00-6	Phenol, 2-ethyl-	0.002	c	0.010	0.002	c	0.010	0.060	c	0.268	-		-
123-07-9	Phenol, 4-ethyl-	0.057	c	0.296	0.058	c	0.300	0.062	c	0.277	0.060	c	0.269
	Phenol, ethyl-methyl-	0.003	#	0.015	0.003	#	0.015	0.003	#	0.014	0.003	#	0.014
	Guaiacols (Methoxy phenols)	**0.109**		**0.57**	**0.109**		**0.57**	**0.123**		**0.55**	**0.120**		**0.53**
90-05-1	Guaiacol	0.062	c	0.323	0.062	c	0.322	0.070	c	0.310	0.068	c	0.304
18102-31-3	Guaiacol, 3-methyl-	0.003	#	0.017	0.003	#	0.017	0.004	#	0.017	0.004	#	0.017
93-51-6	Guaiacol, 4-methyl-	0.025	c	0.132	0.025	c	0.133	0.031	c	0.137	0.030	c	0.132
2785-89-9	Guaiacol, 4-ethyl-	0.013	c	0.067	0.013	c	0.068	0.013	c	0.058	0.013	c	0.057
97-53-0	Guaiacol, 4-allyl-; (Eugenol)	0.003	c	0.018	0.004	c	0.018	0.004	c	0.017	0.004	c	0.017
2785-87-7	Guaiacol, 4-propyl-	0.002	c	0.010	0.002	c	0.010	0.002	c	0.008	0.002	c	0.007
	Syringols (Dimethoxy phenols)	**0.000**		**0.00**	**0.000**		**0.00**	**0.000**		**0.00**	**0.000**		**0.00**
	CARBOHYDRATES												
	Sugars	**0.000**		**0.00**	**0.000**		**0.00**	**0.000**		**0.00**	**0.000**		**0.00**
	OTHER ORGANIC COMPOUNDS												
	N-compounds	**0.013**		**0.07**	**0.013**		**0.07**	**0.008**		**0.04**	**0.008**		**0.04**
110-86-1	Pyridine	0.013	c	0.067	0.013	c	0.069	0.008	c	0.037	0.008	c	0.036
	Acetates	**0.000**		**0.00**	**0.000**		**0.00**	**0.000**		**0.00**	**0.000**		**0.00**
	Terpenes	**0.000**		**0.00**	**0.000**		**0.00**	**0.000**		**0.00**	**0.000**		**0.00**
	unknown compounds	**0.000**		**0.00**	**0.000**		**0.00**	**0.000**		**0.00**	**0.000**		**0.00**
	Miscellaneous	**0.015**		**0.08**	**0.015**		**0.08**	**0.015**		**0.07**	**0.015**		**0.07**
	poss: 1,4-Dioxin, 2,3-dihydro-	0.015	#	0.077	0.015	#	0.077	0.015	#	0.068	0.015	#	0.068

c = calibrated compound

n.q. = not quantified

		Run 1		Run 2		Run 3		Run 4	
CAS No.	**Compound**	**wt.% wet**	**wt.% dry**	**wt.% wet**	**wt.% dry**	**wt.% wet**	**wt.% dry**	**wt.% wet**	**wt.% dry**
	# = estimated response factor								

Table A11. GC-MS data for aqueous condensate (AC) recovered under optimum condensation temperature conditions (C1/C2 = 120 °C/50 °C) for coffee husk.

		Run 1			Run 2			Run 3			Run 4		
CAS No.	**Compound**	**wt.% wet**		**wt.% dry**	**wt.% wet**		**wt.% dry**	**wt.% wet**		**wt.% dry**	**wt.% wet**		**wt.% dry**
	NONAROMATIC COMPOUNDS												
	Acids	**8.698**		**39.54**	**8.858**		**40.26**	**9.340**		**39.41**	**9.558**		**40.33**
64-19-7	Acetic acid	7.847	c	35.667	8.010	c	36.411	8.518	c	35.943	8.733	c	36.849
79-09-4	Propionic acid	0.726	c	3.298	0.727	c	3.306	0.704	c	2.969	0.714	c	3.014
107-92-6	Butyric acid	0.125	c	0.570	0.120	c	0.547	0.118	c	0.499	0.110	c	0.466
	Nonaromatic Esters	**0.007**		**0.03**	**0.007**		**0.03**	**0.000**		**0.00**	**0.000**		**0.00**
554-12-1	Propanoic acid methyl ester	0.007	c	0.030	0.007	c	0.031	-		-			
	Nonaromatic Alcohols	**0.035**		**0.16**	**0.034**		**0.15**	**0.039**		**0.17**	**0.039**		**0.17**
	2-Propen-1-ol (NIST MQ 91)	0.026	#	0.116	0.026	#	0.117	0.027	#	0.114	0.028	#	0.116
	poss: Glycerin	0.009	#	0.043	0.008	#	0.037	0.012	#	0.052	0.012	#	0.050
	Nonaromatic Aldehydes	**0.710**		**3.23**	**0.694**		**3.15**	**0.948**		**4.00**	**0.906**		**3.82**
141-46-8	Acetaldehyde, hydroxy-	0.472	c	2.147	0.456	c	2.071	0.662	c	2.792	0.617	c	2.603
2134-29-4	Propanal, 3-hydroxy-	0.034	#	0.156	0.033	#	0.150	0.058	#	0.245	0.060	#	0.251
123-72-8	Butanal	0.008	c	0.038	0.008	c	0.039	0.008	c	0.033	0.007	c	0.030
15798-64-8	Crotonaldehyde, cis	0.044	c	0.202	0.044	c	0.202	0.049	c	0.205	0.048	c	0.203
123-73-9	Crotonaldehyde, trans	0.013	c	0.061	0.014	c	0.062	-		-	0.174	#	0.736
	Butanedial or Propanal (NIST MQ 88)	0.138	#	0.626	0.139	#	0.631	0.172	#	0.724			
	Nonaromatic Ketones	**6.726**		**30.57**	**6.669**		**30.31**	**6.520**		**27.51**	**0.000**		**0.00**
116-09-6	Acetol (Hydroxypropanone)	4.922	c	22.374	4.879	c	22.178	4.917	c	20.747	**6.570**		**27.72**
78-93-3	Butanone, 2-	0.062	c	0.281	0.062	c	0.282	0.052	c	0.220	4.964	c	20.944
5077-67-8	Butanone, 1-hydroxy-2-	0.593	c	2.697	0.588	c	2.670	0.522	c	2.204	0.050	c	0.213
431-03-8	Butandione, 2,3- (Diacetyl)	0.072	c	0.327	0.073	c	0.334	0.074	c	0.311	0.527	c	2.223
513-86-0	Acetoin (Hydroxy-2-butanone, 3-)	0.082	c	0.372	0.082	c	0.372	0.070	c	0.294	0.074	c	0.311
592-20-1	Propan-2-one, 1-acetyloxy-	0.171	c	0.778	0.156	c	0.710	0.161	c	0.679	0.071	c	0.298
120-92-3	Cyclopentanone	0.037	c	0.169	0.037	c	0.170	0.032	c	0.136	0.141	c	0.596
930-30-3	Cyclopenten-1-one, 2-	0.302	c	1.373	0.301	c	1.370	0.251	c	1.058	0.032	c	0.135
1121-05-7	Cyclopenten-1-one, 2,3-dimethyl-2-	0.015	c	0.068	0.015	c	0.068	0.010	c	0.043	0.256	c	1.078
1120-73-6	Cyclopenten-1-one, 2-methyl-2-	0.051	c	0.233	0.057	c	0.258	0.049	c	0.206	0.012	c	0.051
											0.059	c	0.247

		Run 1			Run 2			Run 3			Run 4		
CAS No.	**Compound**	**wt.% wet**		**wt.% dry**	**wt.% wet**		**wt.% dry**	**wt.% wet**		**wt.% dry**	**wt.% wet**		**wt.% dry**
2758-18-1	Cyclopenten-1-one, 3-methyl-2-	0.050	c	0.225	0.048	c	0.216	0.038	c	0.162	0.040	c	0.170
5682-69-2	Cylopenten-1-one, 3-ethyl-2-	0.007	#	0.034	0.008	#	0.036	0.006	#	0.026	0.006	#	0.026
10493-98-8	Cyclopenten-1-one, 2-hydroxy-2-	0.051	#	0.233	0.051	#	0.234	0.063	#	0.265	0.065	#	0.272
80-71-7	Cyclopenten-1-one, 2-hydroxy-3-methyl-2-	0.117	c	0.532	0.117	c	0.531	0.102	c	0.430	0.101	c	0.427
930-68-7	Cyclohexen-1-one, 2-	0.009	c	0.040	0.009	c	0.040	0.010	c	0.043	0.011	c	0.045
	3-Buten-2-one (NIST MQ 88)	0.015	#	0.066	0.015	#	0.067	0.015	#	0.063	0.015	#	0.063
	3-Buten-2-one, 3-methyl- (NIST MQ 88)	0.010	#	0.045	0.010	#	0.045	0.010	#	0.043	0.010	#	0.040
	2-Pentanone (NIST MQ 94)	0.018	#	0.081	0.020	#	0.090	-		-	0.024	#	0.101
	2,3-Pentanedione	0.024	#	0.111	0.026	#	0.116				0.020	#	0.082
	poss: 2,3-Pentanedione (or Methyl-Isobutyl Ketone) (NIST MQ 90)	-		-	-		-	0.025	#	0.105	0.016	#	0.065
	3-Penten-2-one (NIST MQ 84)	0.020	#	0.090	0.020	#	0.091	0.019	#	0.081	0.011	#	0.047
	Isomere of 2-Cyclopenten-1-one, 3-methyl-	0.017	#	0.079	0.017	#	0.076	0.015	#	0.063	0.017	#	0.070
	2-Cyclopenten-1-one, x,y-dimethyl-	0.012	#	0.056	0.012	#	0.055	0.011	#	0.048	0.009	#	0.037
	2-Cycolpenten-1-one, x,y-dimethyl-	0.015	#	0.069	0.015	#	0.068	0.016	#	0.069	0.013	#	0.054
	2,5-Hexanedione (NIST MQ 89)	0.009	#	0.042	0.009	#	0.042	0.008	#	0.036	0.013	#	0.053
	Isomere of Cyclopenten-1-one, 2,3-dimethyl-2-	0.013	#	0.057	0.012	#	0.053	0.012	#	0.050	0.009	#	0.038
	Butan-2-one, 1-(acetyloxy)- (NIST MQ 92)	0.013	#	0.057	0.013	#	0.060	0.013	#	0.057	0.015	#	0.063
	2-Cyclopenten-1-one, x,y-dimethyl-	0.008	#	0.036	0.008	#	0.036	0.009	#	0.037	0.010	#	0.040
	2-Cyclopenten-1-one, 2,3,4-trimethyl- (NIST MQ 88)	0.010	#	0.044	0.010	#	0.044	0.019	#	0.081	0.024	#	0.101
	Aliphatic Hydrocarbons	**0.000**		**0.00**	**0.000**		**0.00**	**0.000**		**0.00**	**0.000**		**0.00**
	HETEROCYCLIC COMPOUNDS												
	Furans	**0.751**		**3.41**	**0.748**		**3.40**	**0.787**		**3.32**	**0.797**		**3.36**
98-00-0	Furfuryl alcohol, 2-	0.018	c	0.081	0.019	c	0.085	0.020	c	0.085	0.018	c	0.076
497-23-4	Furanone, 2(5H)-	0.081	c	0.368	0.081	c	0.368	0.098	c	0.413	0.099	c	0.418
98-01-1	Furaldehyde, 2-	0.418	c	1.900	0.417	c	1.896	0.430	c	1.813	0.437	c	1.842
498-60-2	Furaldehyde, 3-	0.024	c	0.110	0.021	c	0.094	0.028	c	0.116	0.027	c	0.114

		Run 1			Run 2			Run 3			Run 4		
CAS No.	**Compound**	**wt.% wet**		**wt.% dry**	**wt.% wet**		**wt.% dry**	**wt.% wet**		**wt.% dry**	**wt.% wet**		**wt.% dry**
620-02-0	Furaldehyde, 5-methyl-2-	0.026	c	0.118	0.026	c	0.117	0.026	c	0.108	0.026	c	0.110
1192-62-7	Ethanone, 1-(2-furanyl)-	0.016	c	0.072	0.016	c	0.073	0.015	c	0.065	0.016	c	0.066
591-11-7	Furan-2-one, 5-methyl-, (5H)-	0.024	#	0.110	0.024	#	0.108	0.024	#	0.102	0.026	#	0.108
22122-36-7	Furan-2-one, 3-methyl-, (5H)-	0.024	c	0.109	0.024	c	0.109	0.025	c	0.106	0.026	c	0.108
	Furan-2-one, 2,5-dihydro-3,5-dimethyl-	0.015	#	0.070	0.015	#	0.069	0.014	#	0.058	0.014	#	0.059
96-48-0	Butyrolactone, γ-	0.067	c	0.305	0.067	c	0.304	0.063	c	0.264	0.064	c	0.268
696-59-3	Tetrahydrofuran (trans), 2,5-dimethoxy-	0.010	#	0.046	0.009	#	0.040	0.011	#	0.047	0.011	#	0.046
	Furan, tetrahydro-2-methoxy- (NIST MQ (80)	0.005	#	0.023	0.007	#	0.030	0.006	#	0.024	0.005	#	0.023
	2(3H)-Furanone, 5-methyl- (NIST MQ 84)	0.015	#	0.066	0.015	#	0.069	0.020	#	0.085	0.020	#	0.086
	Furan-2-one, 4-methyl-(5H)- (NIST MQ 88)	0.008	#	0.036	0.008	#	0.036	0.008	#	0.035	0.009	#	0.037
	Pyrans	**0.000**		**0.00**	**0.000**		**0.00**	**0.000**		**0.00**	**0.000**		**0.00**
	AROMATIC COMPOUNDS												
	Benzenes	**0.000**		**0.00**	**0.000**		**0.00**	**0.000**		**0.00**	**0.000**		**0.00**
	Catechols	**0.000**		**0.00**	**0.000**		**0.00**	**0.000**		**0.00**	**0.000**		**0.00**
	Aromatic Alcohols	**0.000**		**0.00**	**0.000**		**0.00**	**0.000**		**0.00**	**0.000**		**0.00**
	Aromatic Aldehydes	**0.003**		**0.01**	**0.003**		**0.01**	**0.003**		**0.01**	**0.003**		**0.01**
100-52-7	Benzaldehyde	0.003	c	0.013	0.003	c	0.013	0.003	c	0.012	0.003	c	0.012
	Aromatic Ketones	**0.000**		**0.00**	**0.000**		**0.00**	**0.000**		**0.00**	**0.000**		**0.00**
	Aromatic Esters	**0.000**		**0.00**	**0.000**		**0.00**	**0.000**		**0.00**	**0.000**		**0.00**
	Lignin-derived Phenols	**0.146**		**0.67**	**0.146**		**0.67**	**0.098**		**0.42**	**0.103**		**0.43**

		Run 1			Run 2			Run 3			Run 4		
CAS No.	**Compound**	**wt.% wet**		**wt.% dry**	**wt.% wet**		**wt.% dry**	**wt.% wet**		**wt.% dry**	**wt.% wet**		**wt.% dry**
108-95-2	Phenol	0.048	c	0.218	0.048	c	0.217	0.035	c	0.148	0.036	c	0.151
95-48-7	Cresol, o-	0.028	c	0.125	0.027	c	0.123	0.023	c	0.095	0.023	c	0.098
106-44-5	Cresol, p-	0.012	c	0.056	0.012	c	0.056	0.008	c	0.035	0.009	c	0.039
108-39-4	Cresol, m-	0.014	c	0.066	0.014	c	0.066	0.010	c	0.042	0.011	c	0.048
95-87-4	Phenol, 2,5-dimethyl-	0.009	c	0.040	0.009	c	0.039	0.008	c	0.033	0.008	c	0.034
105-67-9	Phenol, 2,4-dimethyl-	0.007	c	0.034	0.008	c	0.035	0.007	c	0.030	0.007	c	0.031
576-26-1	Phenol, 2,6-dimethyl-	0.003	c	0.013	0.003	c	0.013	0.003	c	0.011	0.003	c	0.011
123-07-9	Phenol, 4-ethyl-	0.022	c	0.101	0.023	c	0.103	0.005	c	0.022	0.005	c	0.022
	Phenol, ethyl-methyl-	0.003	#	0.013	0.003	#	0.013	-		-	-		-
	Guaiacols (Methoxy phenols)	**0.242**		**1.10**	**0.240**		**1.09**	**0.240**		**1.01**	**0.245**		**1.03**
90-05-1	Guaiacol	0.133	c	0.605	0.132	c	0.600	0.129	c	0.543	0.132	c	0.558
18102-31-3	Guaiacol, 3-methyl-	0.007	#	0.032	0.007	#	0.032	0.007	#	0.028	0.008	#	0.033
93-51-6	Guaiacol, 4-methyl-	0.064	c	0.291	0.064	c	0.289	0.066	c	0.278	0.067	c	0.284
2785-89-9	Guaiacol, 4-ethyl-	0.023	c	0.103	0.023	c	0.103	0.004	#	0.015	0.004	#	0.016
97-53-0	Guaiacol, 4-allyl-; (Eugenol)	0.010	c	0.044	0.010	c	0.044	0.021	c	0.088	0.021	c	0.090
2785-87-7	Guaiacol, 4-propyl-	0.005	c	0.023	0.005	c	0.023	0.009	c	0.039	0.009	c	0.038
	Syringols (Dimethoxy phenols)	**0.000**		**0.00**	**0.000**		**0.00**	**0.000**		**0.00**	**0.000**		**0.00**
	CARBOHYDRATES												
	Sugars	**0.000**		**0.00**	**0.000**		**0.00**	**0.000**		**0.00**	**0.000**		**0.00**
	OTHER ORGANIC COMPOUNDS												
	N-compounds	**0.029**		**0.13**	**0.029**		**0.13**	**0.026**		**0.11**	**0.026**		**0.11**
110-86-1	Pyridine	0.029	c	0.133	0.029	c	0.131	0.026	c	0.108	0.026	c	0.111
	Acetates	**0.000**		**0.00**	**0.000**		**0.00**	**0.000**		**0.00**	**0.000**		**0.00**
	Terpenes	**0.000**		**0.00**	**0.000**		**0.00**	**0.000**		**0.00**	**0.000**		**0.00**
	unknown compounds	**0.000**		**0.00**	**0.000**		**0.00**	**0.000**		**0.00**	**0.000**		**0.00**
	Miscellaneous	**0.008**		**0.04**	**0.009**		**0.04**	**0.009**		**0.04**	**0.009**		**0.04**

		Run 1			Run 2			Run 3			Run 4		
CAS No.	**Compound**	**wt.% wet**		**wt.% dry**	**wt.% wet**		**wt.% dry**	**wt.% wet**		**wt.% dry**	**wt.% wet**		**wt.% dry**
	poss: 1,4-Dioxin, 2,3-dihydro-	0.008	#	0.038	0.009	#	0.039	0.009	#	0.038	0.009	#	0.037

c = calibrated compound

n.q. = not quantified

= estimated response factor

Table A12. GC-MS data for organic-rich condensate (ORC) recovered under optimum condensation temperature conditions (C1/C2 = 120 °C/50 °C) for wheat straw.

		Run 1			Run 2			Run 3			Run 4		
CAS No.	**Compound**	**wt.% wet**		**wt.% dry**	**wt.% wet**		**wt.% dry**	**wt.% wet**		**wt.% dry**	**wt.% wet**		**wt.% dry**
	NONAROMATIC COMPOUNDS												
	Acids	**10.869**		**12.74**	**10.955**		**12.84**	**10.698**		**12.24**	**10.676**		**12.22**
64-19-7	Acetic acid	5.827	c	6.831	5.897	c	6.913	5.633	c	6.445	5.596	c	6.403
79-09-4	Propionic acid	5.042	c	5.911	5.058	c	5.930	5.065	c	5.796	5.080	c	5.812
	Nonaromatic Esters	**0.000**		**0.00**	**0.000**		**0.00**	**0.000**		**0.00**	**0.000**		**0.00**
	Nonaromatic Alcohols	**0.000**		**0.00**	**0.000**		**0.00**	**0.000**		**0.00**	**0.000**		**0.00**
	Nonaromatic Aldehydes	**0.000**		**0.00**				**0.000**		**0.00**	**0.000**		**0.00**
	Nonaromatic Ketones	**9.212**		**10.80**	**9.048**		**10.61**	**8.999**		**10.30**	**9.027**		**10.33**
116-09-6	Acetol (Hydroxypropanone)	4.165	c	4.883	4.064	c	4.764	3.780	c	4.324	3.772	c	4.315
78-93-3	Butanone, 2-	0.073	c	0.086	0.069	c	0.080	0.076	c	0.086	0.074	c	0.085
5077-67-8	Butanone, 1-hydroxy-2-	0.911	c	1.067	0.898	c	1.052	0.864	c	0.989	0.918	c	1.051
513-86-0	Acetoin (Hydroxy-2-butanone, 3-)	0.115	c	0.135	0.113	c	0.132	0.117	c	0.134	0.113	c	0.129
592-20-1	Propan-2-one, 1-acetyloxy-	0.084	c	0.098	0.085	c	0.099	0.080	c	0.092	0.080	c	0.092
120-92-3	Cyclopentanone	0.103	c	0.121	0.103	c	0.121	0.104	c	0.118	0.102	c	0.117
930-30-3	Cyclopenten-1-one, 2-	0.560	c	0.657	0.548	c	0.642	0.550	c	0.629	0.547	c	0.626
1121-05-7	Cyclopenten-1-one, 2,3-dimethyl-2-	0.195	c	0.229	0.202	c	0.237	0.212	c	0.242	0.234	c	0.268
1120-73-6	Cyclopenten-1-one, 2-methyl-2-	0.287	c	0.336	0.279	c	0.327	0.290	c	0.332	0.287	c	0.328
2758-18-1	Cyclopenten-1-one, 3-methyl-2-	0.374	c	0.438	0.374	c	0.439	0.390	c	0.446	0.394	c	0.451
5682-69-2	Cylopenten-1-one, 3-ethyl-2-										0.119	#	0.137
80-71-7	Cyclopenten-1-one, 2-hydroxy-3-methyl-2-										1.426	c	1.632
21835-01-8	Cyclopenten-1-one, 3-ethyl-2-hydroxy-2-	0.342	c	0.401	0.344	c	0.404	0.119	#	0.137	0.342	c	0.392
	Isobutyl methyl ketone (NIST MQ 91)	0.050	#	0.058	0.049	#	0.057	1.454	c	1.664	0.051	#	0.058
	2-Cyclopenten-1-one, x,y-dimethyl-	0.054	#	0.064	0.052	#	0.061	0.346	c	0.395	0.053	#	0.061
	Isomere of Cyclopenten-1-one, 2,3-dimethyl-2-	0.081	#	0.095	0.078	#	0.091	0.050	#	0.058	0.080	#	0.092
	2-Cyclopenten-1-one, x,y-dimethyl-	0.068	#	0.080	0.066	#	0.078	0.053	#	0.061	0.070	#	0.080
	1,2-Cyclopentanedione, 3-methyl- (NIST MQ 84)	1.269	#	1.488	1.246	#	1.461	0.079	#	0.091	-		-
	2-Cyclopenten-1-one, 2,3,4-trimethyl- (NIST MQ 88)	0.076	#	0.089	0.074	#	0.087	0.072	#	0.082	0.079	#	0.090
	Isomer of Cyclopenten-1-one, 3-ethyl-2-hydroxy-	0.193	#	0.227	0.193	#	0.226	0.080	#	0.092	0.190	#	0.218

		Run 1			Run 2			Run 3			Run 4		
CAS No.	**Compound**	**wt.% wet**		**wt.% dry**	**wt.% wet**		**wt.% dry**	**wt.% wet**		**wt.% dry**	**wt.% wet**		**wt.% dry**
	similar to 2-Cyclopenten-1-one, 3-ethyl-	0.132	#	0.155	0.132	#	0.155	0.191	#	0.218	-		-
	2-Heptadecanone (NIST MQ 84)	0.080	#	0.094	0.080	#	0.094	0.093	#	0.106	0.094	#	0.108
	Aliphatic Hydrocarbons	**0.000**		**0.00**	**0.000**		**0.00**	**0.000**		**0.00**	**0.000**		**0.00**
	HETEROCYCLIC COMPOUNDS												
	Furans	**1.058**		**1.24**	**1.043**		**1.22**	**0.953**		**1.09**	**0.947**		**1.08**
98-00-0	Furfuryl alcohol, 2-	0.157	c	0.184	0.157	c	0.184	0.157	c	0.180	0.158	c	0.181
98-01-1	Furaldehyde, 2-	0.204	c	0.240	0.199	c	0.233	0.184	c	0.210	0.181	c	0.207
1192-62-7	Ethanone, 1-(2-furanyl)-	0.041	c	0.048	0.040	c	0.047	0.040	c	0.046	0.039	c	0.045
22122-36-7	Furan-2-one, 3-methyl-, (5H)-	0.073	c	0.086	0.074	c	0.087	0.077	c	0.088	0.076	c	0.087
96-48-0	Butyrolactone, γ-	0.479	c	0.562	0.473	c	0.555	0.496	c	0.567	0.493	c	0.564
	Furan-2-one, 4-methyl-(5H)- (NIST MQ 88)	0.103	#	0.121	0.100	#	0.117	-		-	-		-
	Pyrans	**0.000**		**0.00**	**0.000**		**0.00**	**0.953**		**1.09**	**0.000**		**0.00**
	AROMATIC COMPOUNDS												
	Benzenes	**0.066**		**0.08**	**0.066**		**0.08**	**0.072**		**0.08**	**0.071**		**0.08**
83-33-0	Inden-1-one, 2,3-dihydro-1H-	0.066	c	0.078	0.066	c	0.077	0.072	c	0.082	0.071	c	0.081
	Catechols	**n.q.**		**n.q.**	**n.q.**		**n.q.**	**n.q.**		**n.q.**	**n.q.**		**n.q.**
123-31-9	Hydroquinone (Benzene, 1,4-dihydroxy-)	n.q.	n.q.	n.q.	n.q.	n.q.	n.q.	n.q.	n.q.	n.q.	n.q.	.	n.q.
	Benzenediol, methyl-	n.q.	n.q.	n.q.	n.q.	n.q.	n.q.	n.q.	n.q.	n.q.	-		-
6153-39-5	Resorcinol, 5-methyl-, Hydrat (Orcinol)	-		-	-		-	-		-	n.q.	.	n.q.
	Aromatic Alcohols	**0.000**		**0.00**	**0.000**		**0.00**	**0.000**		**0.00**	**0.000**		**0.00**
	Aromatic Aldehydes	**0.000**		**0.00**	**0.000**		**0.00**	**0.000**		**0.00**	**0.000**		**0.00**
	Aromatic Ketones	**0.000**		**0.00**	**0.000**		**0.00**	**0.000**		**0.00**	**0.000**		**0.00**
	Aromatic Esters	**0.000**		**0.00**	**0.000**		**0.00**	**0.000**		**0.00**	**0.000**		**0.00**

		Run 1			Run 2			Run 3			Run 4		
CAS No.	**Compound**	**wt.% wet**		**wt.% dry**	**wt.% wet**		**wt.% dry**	**wt.% wet**		**wt.% dry**	**wt.% wet**		**wt.% dry**
	Lignin-derived Phenols	**2.424**		**2.84**	**2.404**		**2.82**	**2.660**		**3.04**	**2.650**		**3.03**
108-95-2	Phenol	0.446	c	0.522	0.446	c	0.523	0.479	c	0.549	0.478	c	0.547
95-48-7	Cresol, o-	0.239	c	0.281	0.238	c	0.278	0.264	c	0.302	0.261	c	0.299
106-44-5	Cresol, p-	0.148	c	0.174	0.150	c	0.176	0.171	c	0.196	0.168	c	0.192
108-39-4	Cresol, m-	0.207	c	0.243	0.200	c	0.234	0.236	c	0.270	0.237	c	0.271
95-87-4	Phenol, 2,5-dimethyl-	0.148	c	0.173	0.139	c	0.163	0.156	c	0.179	0.158	c	0.180
105-67-9	Phenol, 2,4-dimethyl-	0.075	c	0.088	0.080	c	0.094	0.086	c	0.098	0.085	c	0.098
526-75-0	Phenol, 2,3-dimethyl-	0.037	c	0.044	0.037	c	0.043	0.042	c	0.048	0.041	c	0.047
108-68-9	Phenol, 3,5-dimethyl-	0.036	c	0.043	0.036	c	0.042	0.041	c	0.047	0.041	c	0.047
697-82-5	Phenol, 2,3,5-trimethyl-	0.023	c	0.027	0.025	c	0.029	0.038	c	0.043	0.038	c	0.044
90-00-6	Phenol, 2-ethyl-	0.034	c	0.040	0.035	c	0.041	0.180	c	0.206	0.179	c	0.204
123-07-9	Phenol, 4-ethyl-	0.452	c	0.530	0.456	c	0.535	0.476	c	0.545	0.474	c	0.542
2628-17-3	Phenol, 4-vinyl-	0.425	#	0.498	0.415	#	0.487	0.418	#	0.478	0.422	#	0.483
5932-68-3	Phenol, trans 4-propenyl-	0.048	#	0.056	0.048	#	0.056	0.071	#	0.082	-		-
	Phenol, ethyl-methyl-	0.062	#	0.073	0.058	#	0.068	**2.660**		**3.04**	0.068	#	0.078
	Phenol, x-(1-methylethyl)-	0.042	#	0.049	0.041	#	0.048	0.479	c	0.549	-		-
	Guaiacols (Methoxy phenols)	**3.984**		**4.67**	**3.988**		**4.68**	**3.955**		**4.53**	**3.935**		**4.50**
90-05-1	Guaiacol	0.603	c	0.707	0.602	c	0.706	0.578	c	0.662	0.570	c	0.652
93-51-6	Guaiacol, 4-methyl-	0.220	c	0.258	0.219	c	0.257	0.219	c	0.251	0.220	c	0.252
2785-89-9	Guaiacol, 4-ethyl-	0.490	c	0.575	0.487	c	0.571	0.495	c	0.566	0.493	c	0.564
7786-61-0	Guaiacol, 4-vinyl-	0.864	#	1.013	0.849	#	0.995	0.849	#	0.971	0.847	#	0.969
97-53-0	Guaiacol, 4-allyl-; (Eugenol)	0.119	c	0.139	0.115	c	0.135	0.115	c	0.132	0.114	c	0.130
2785-87-7	Guaiacol, 4-propyl-	0.062	c	0.072	0.059	c	0.069	0.060	c	0.069	0.058	c	0.066
97-54-1	Guaiacol, 4-propenyl- cis (Isoeugenol)	0.275	c	0.323	0.282	c	0.330	0.280	c	0.320	0.283	c	0.324
5932-68-3	Guaiacol, 4-propenyl-(trans) (Isoeugenol)	0.799	c	0.937	0.796	c	0.934	0.784	c	0.897	0.786	c	0.899
121-33-5	Vanillin	0.433	c	0.508	0.461	c	0.540	0.456	c	0.522	0.447	c	0.511
2503-46-0	Guaiacyl acetone	0.117	c	0.138	0.119	c	0.139	0.118	c	0.135	0.118	c	0.136
	Syringols (Dimethoxy phenols)	**2.316**		**2.72**	**2.328**		**2.73**	**2.216**		**2.54**	**2.248**		**2.57**
91-10-1	Syringol	0.480	c	0.563	0.474	c	0.556	0.449	c	0.513	0.457	c	0.523
6638-05-7	Syringol, 4-methyl-	0.190	c	0.222	0.191	c	0.224	0.182	c	0.208	0.184	c	0.211
14059-92-8	Syringol, 4-ethyl-	0.215	c	0.252	0.215	c	0.253	0.210	c	0.241	0.227	c	0.260

		Run 1			Run 2			Run 3			Run 4		
CAS No.	**Compound**	**wt.% wet**		**wt.% dry**	**wt.% wet**		**wt.% dry**	**wt.% wet**		**wt.% dry**	**wt.% wet**		**wt.% dry**
28343-22-8	Syringol, 4-vinyl-	0.373	#	0.437	0.371	#	0.435	0.349	#	0.400	0.355	#	0.406
6627-88-9	Syringol, 4-allyl-	0.225	c	0.263	0.222	c	0.261	0.211	c	0.242	0.212	c	0.243
26624-13-5	Syringol, 4-(1-propenyl)-, cis	0.165	#	0.193	0.171	#	0.201	0.165	#	0.189	0.168	#	0.192
20675-95-0	Syringol, 4-(1-propenyl)-, trans	0.477	#	0.559	0.486	#	0.569	0.457	#	0.523	0.449	#	0.514
2478-38-8	Acetosyringone	0.135	c	0.159	0.142	c	0.166	0.139	c	0.159	0.140	c	0.161
	Syringyl acetone	0.057	#	0.067	0.056	#	0.065	0.054	#	0.061	0.055	#	0.063
	CARBOHYDRATES												
	Sugars	**0.606**		**0.71**	**0.614**		**0.72**	**1.910**		**2.19**	**1.947**		**2.23**
4451-31-4	Dianhydro-α-D-glucopyranose, 1,4:3,6-	0.606	#	0.711	0.614	#	0.720	0.656	#	0.751	0.654	#	0.748
498-07-7	Anhydro-ß-D-glucopyranose, 1,6- (Levoglucosan)	-		-	-		-	1.254	c	1.435	1.293	c	1.480
	OTHER ORGANIC COMPOUNDS												
	N-compounds	**0.000**		**0.00**	**0.000**		**0.00**	**0.000**		**0.00**	**0.000**		**0.00**
	Acetates	**0.000**		**0.00**	**0.000**		**0.00**	**0.000**		**0.00**	**0.000**		**0.00**
	Terpenes	**0.000**		**0.00**	**0.000**		**0.00**	**0.000**		**0.00**	**0.000**		**0.00**
	unknown compounds	**0.000**		**0.00**	**0.000**		**0.00**	**0.000**		**0.00**	**0.000**		**0.00**
	Miscellaneous	**0.048**		**0.06**	**0.049**		**0.06**	**0.000**		**0.00**	**0.000**		**0.00**
	poss: 2-Pentadecanone, 6,10,14-trimethyl- (NIST MQ 88)	0.048	#	0.057	0.049	#	0.057	-		-	-		-

Table A13. GC-MS data for organic-rich condensate (ORC) recovered under optimum condensation temperature conditions (C1/C2 = 120 °C/50 °C) for *miscanthus*.

		Run 1			Run 2			Run 3			Run 4		
CAS No.	**Compound**	**wt.% wet**		**wt.% dry**	**wt.% wet**		**wt.% dry**	**wt.% wet**		**wt.% dry**	**wt.% wet**		**wt.% dry**
	NONAROMATIC COMPOUNDS												
	Acids	**11.255**		**12.97**	**11.238**		**12.95**	**11.313**		**12.86**	**11.269**		**12.81**
64-19-7	Acetic acid	6.378	c	7.348	6.341	c	7.305	6.466	c	7.348	6.418	c	7.293
79-09-4	Propionic acid	4.877	c	5.619	4.897	c	5.642	4.847	c	5.508	4.852	c	5.513
	Nonaromatic Esters	**0.000**		**0.00**	**0.000**		**0.00**	**0.000**		**0.00**	**0.000**		**0.00**
	Nonaromatic Alcohols	**0.000**		**0.00**	**0.000**		**0.00**	**0.000**		**0.00**	**0.000**		**0.00**
	Nonaromatic Aldehydes	**1.077**		**1.24**	**1.110**		**1.28**	**2.692**		**3.06**	**2.826**		**3.21**
141-46-8	Acetaldehyde, hydroxy-	0.870	c	1.003	0.903	c	1.040	2.235	c	2.539	2.345	c	2.665
2134-29-4	Propanal, 3-hydroxy-	0.123	#	0.142	0.122	#	0.141	0.239	#	0.272	0.253	#	0.288
	Butandial (or Propanal) (NIST MQ 92)	0.084	#	0.096	0.085	#	0.098	0.218	#	0.247	0.228	#	0.259
	Nonaromatic Ketones	**7.176**		**8.27**	**7.260**		**8.36**	**6.878**		**7.82**	**6.930**		**7.88**
116-09-6	Acetol (Hydroxypropanone)	4.451	c	5.128	4.515	c	5.202	4.621	c	5.251	4.705	c	5.346
5077-67-8	Butanone, 1-hydroxy-2-	0.615	c	0.708	0.622	c	0.717	0.565	c	0.642	0.558	c	0.634
592-20-1	Propan-2-one, 1-acetyloxy-	0.187	c	0.215	0.186	c	0.215	0.171	c	0.195	0.168	c	0.191
120-92-3	Cyclopentanone	0.071	c	0.082	0.069	c	0.079	0.249	c	0.283	0.248	c	0.282
930-30-3	Cyclopenten-1-one, 2-	0.308	c	0.355	0.309	c	0.356	0.110	c	0.125	0.111	c	0.126
1121-05-7	Cyclopenten-1-one, 2,3-dimethyl-2-	0.044	c	0.051	0.057	c	0.065	0.141	c	0.161	0.143	c	0.162
1120-73-6	Cyclopenten-1-one, 2-methyl-2-	0.144	c	0.166	0.146	c	0.168	0.252	#	0.287	0.230	#	0.261
2758-18-1	Cyclopenten-1-one, 3-methyl-2-	0.177	c	0.204	0.183	c	0.211	0.719	c	0.817	0.719	c	0.817
10493-98-8	Cyclopenten-1-one, 2-hydroxy-2-	0.147	#	0.169	0.157	#	0.181	0.050	#	0.057	0.049	#	0.056
80-71-7	Cyclopenten-1-one, 2-hydroxy-3-methyl-2-	0.783	c	0.902	0.770	c	0.887	**2.692**		**3.06**	**6.930**		**7.88**
21835-01-8	Cyclopenten-1-one, 3-ethyl-2-hydroxy-2-	0.144	c	0.166	0.143	c	0.164	2.235	c	2.539	4.705	c	5.346
	Isobutyl methyl ketone (NIST MQ 91)	0.050	#	0.058	0.048	#	0.055	0.239	#	0.272	0.558	c	0.634
	Isomere of Cyclopenten-1-one, 2,3-dimethyl-2-	0.054	#	0.062	0.054	#	0.063	0.218	#	0.247	-		-
	Aliphatic Hydrocarbons	**0.000**		**0.00**	**0.000**		**0.00**	**0.000**		**0.00**	**0.000**		**0.00**

		Run 1			Run 2			Run 3			Run 4		
CAS No.	Compound	wt.% wet		wt.% dry	wt.% wet		wt.% dry	wt.% wet		wt.% dry	wt.% wet		wt.% dry
	HETEROCYCLIC COMPOUNDS												
	Furans	**1.591**		**1.83**	**1.600**		**1.84**	**1.707**		**1.94**	**1.683**		**1.91**
98-00-0	Furfuryl alcohol, 2-	-		-	-		-	0.117	c	0.133	0.113	c	0.129
497-23-4	Furanone, 2(5H)-	0.406	c	0.467	0.406	c	0.468	0.499	c	0.567	0.490	c	0.556
98-01-1	Furaldehyde, 2-	0.354	c	0.408	0.357	c	0.411	0.412	c	0.468	0.409	c	0.464
620-02-0	Furaldehyde, 5-methyl-2-	0.085	c	0.098	0.087	c	0.100	0.089	c	0.101	0.087	c	0.098
591-11-7	Furan-2-one, 5-methyl-, (5H)-	0.095	#	0.109	0.097	#	0.112	-		-	0.167	#	0.189
22122-36-7	Furan-2-one, 3-methyl-, (5H)-	0.111	c	0.128	0.111	c	0.128	0.102	c	0.114	0.283	c	0.322
96-48-0	Butyrolactone, γ-	0.300	c	0.346	0.304	c	0.350	0.283	c	0.322	0.135	#	0.154
	Furan-2-one, 4-methyl-(5H)- (NIST MQ 88)	0.145	#	0.167	0.142	#	0.164	0.138	#	0.157	0.113	c	0.129
	Isomere of Furan-2-one, 2,5-dihydro-3,5-dimethyl-	0.096	#	0.111	0.097	#	0.112	-		-	-		-
	Pyrans	**0.000**		**0.00**	**0.000**		**0.00**	**0.000**		**0.00**	**0.000**		**0.00**
	AROMATIC COMPOUNDS												
	Benzenes	**0.000**		**0.00**	**0.000**		**0.00**	**0.000**		**0.00**	**0.000**		**0.00**
	Catechols	**n.q.**		**n.q.**	**n.q.**		**n.q.**	**n.q.**		**n.q.**	**n.q.**		**n.q.**
123-31-9	Hydroquinone (Benzene, 1,4-dihydroxy-)	n.q.	n.q.	n.q.	n.q.	.	n.q.	n.q.	n.q.	n.q.	n.q.	n.q.	n.q.
	Benzenediol, methyl-	n.q.	n.q.	n.q.	n.q.	.	n.q.	-		-	n.q.	n.q.	n.q.
	Aromatic Alcohols	**0.000**		**0.00**	**0.000**		**0.00**	**0.000**		**0.00**	**0.000**		**0.00**
	Aromatic Aldehydes	**0.000**		**0.00**	**0.000**		**0.00**	**0.000**		**0.00**	**0.000**		**0.00**
	Aromatic Ketones	**0.000**		**0.00**	**0.000**		**0.00**	**0.000**		**0.00**	**0.000**		**0.00**
	Aromatic Esters	**0.000**		**0.00**	**0.000**		**0.00**	**0.000**		**0.00**	**0.000**		**0.00**
	Lignin-derived Phenols	**3.794**		**4.37**	**3.816**		**4.40**	**3.456**		**3.93**	**3.528**		**4.01**
108-95-2	Phenol	0.336	c	0.387	0.333	c	0.383	0.284	c	0.323	0.284	c	0.323
95-48-7	Cresol, o-	0.132	c	0.152	0.134	c	0.154	0.109	c	0.124	0.110	c	0.125

		Run 1			Run 2			Run 3			Run 4		
CAS No.	**Compound**	**wt.% wet**		**wt.% dry**	**wt.% wet**		**wt.% dry**	**wt.% wet**		**wt.% dry**	**wt.% wet**		**wt.% dry**
106-44-5	Cresol, p-	0.198	c	0.228	0.199	c	0.229	0.171	c	0.194	0.171	c	0.195
108-39-4	Cresol, m-	0.107	c	0.123	0.111	c	0.128	0.084	c	0.095	0.082	c	0.093
95-87-4	Phenol, 2,5-dimethyl-	0.118	c	0.136	0.117	c	0.135	0.111	c	0.126	0.113	c	0.128
105-67-9	Phenol, 2,4-dimethyl-	0.061	c	0.071	0.062	c	0.071	0.056	c	0.064	0.056	c	0.064
123-07-9	Phenol, 4-ethyl-	1.024	c	1.180	1.060	c	1.221	0.842	c	0.957	0.899	c	1.021
2628-17-3	Phenol, 4-vinyl-	1.740	#	2.005	1.720	#	1.982	1.682	#	1.911	1.698	#	1.930
5932-68-3	Phenol, trans 4-propenyl-	0.079	#	0.091	0.080	#	0.092	0.071	#	0.081	0.070	#	0.079
	Phenol, ethyl-methyl-	-		-	-		-	0.046	#	0.053	0.045	#	0.052
	Guaiacols (Methoxy phenols)	**2.946**		**3.39**	**2.959**		**3.41**	**2.821**		**3.21**	**2.817**		**3.20**
90-05-1	Guaiacol	0.251	c	0.290	0.253	c	0.291	0.248	c	0.282	0.245	c	0.278
93-51-6	Guaiacol, 4-methyl-	0.214	c	0.246	0.219	c	0.253	0.216	c	0.245	0.220	c	0.250
2785-89-9	Guaiacol, 4-ethyl-	0.174	c	0.201	0.174	c	0.200	0.142	c	0.162	0.143	c	0.163
7786-61-0	Guaiacol, 4-vinyl-	0.483	#	0.556	0.485	#	0.559	0.444	#	0.505	0.450	#	0.512
97-53-0	Guaiacol, 4-allyl-; (Eugenol)	0.085	c	0.098	0.086	c	0.099	0.094	c	0.107	0.084	c	0.096
2785-87-7	Guaiacol, 4-propyl-	0.030	c	0.035	0.030	c	0.035	0.032	c	0.036	0.027	c	0.030
97-54-1	Guaiacol, 4-propenyl- cis (Isoeugenol)	0.252	c	0.290	0.251	c	0.289	0.238	c	0.271	0.252	c	0.286
5932-68-3	Guaiacol, 4-propenyl-(trans) (Isoeugenol)	0.561	c	0.647	0.557	c	0.641	0.523	c	0.595	0.529	c	0.601
121-33-5	Vanillin	0.506	c	0.583	0.491	c	0.566	0.492	c	0.559	0.478	c	0.544
498-02-2	Ethanone, 1-(4-hydroxy-3-methoxyphenyl)- (Acetoguaiacone)	0.389	c	0.448	0.414	c	0.477	0.390	c	0.443	0.388	c	0.441
	Syringols (Dimethoxy phenols)	**1.352**		**1.56**	**1.302**		**1.50**	**1.476**		**1.68**	**1.474**		**1.67**
91-10-1	Syringol	0.204	c	0.235	0.204	c	0.235	0.214	c	0.243	0.214	c	0.244
6638-05-7	Syringol, 4-methyl-	0.174	c	0.201	0.167	c	0.193	0.180	c	0.204	0.179	c	0.204
14059-92-8	Syringol, 4-ethyl-	0.061	c	0.070	0.060	c	0.069	0.054	c	0.061	0.055	c	0.062
28343-22-8	Syringol, 4-vinyl-	0.168	#	0.193	0.163	#	0.188	0.160	#	0.182	0.162	#	0.184
6627-88-9	Syringol, 4-allyl-	0.129	c	0.148	0.125	c	0.144	0.131	c	0.149	0.135	c	0.154
26624-13-5	Syringol, 4-(1-propenyl)-, cis	0.113	#	0.130	0.095	#	0.110	0.100	#	0.113	0.098	#	0.111
20675-95-0	Syringol, 4-(1-propenyl)-, trans	0.275	#	0.317	0.274	#	0.316	0.276	#	0.314	0.279	#	0.317
134-96-3	Syringaldehyde	0.164	c	0.189	0.146	c	0.169	0.173	c	0.197	0.169	c	0.192

		Run 1			Run 2			Run 3			Run 4		
CAS No.	**Compound**	**wt.% wet**		**wt.% dry**	**wt.% wet**		**wt.% dry**	**wt.% wet**		**wt.% dry**	**wt.% wet**		**wt.% dry**
2478-38-8	Acetosyringone	0.065	c	0.075	0.066	c	0.076	-		-	0.066	c	0.075
	CARBOHYDRATES												
	Sugars	**7.125**		**8.21**	**7.408**		**8.53**	**7.788**		**8.85**	**7.532**		**8.56**
51246-94-7	Anhydro-ß-D-xylofuranose, 1,5-	0.677	#	0.779	0.708	#	0.816	0.671	#	0.763	0.614	#	0.697
498-07-7	Anhydro-ß-D-glucopyranose, 1,6- (Levoglucosan)	5.847	c	6.736	6.076	c	7.000	6.119	c	6.954	5.927	c	6.735
4451-31-4	Dianhydro-α-D-glucopyranose, 1,4:3,6-	0.434	#	0.500	0.449	#	0.517	0.400	#	0.455	0.400	#	0.455
	Anhydrosugar unknown (unspecific spectrum)	-		-	-		-	0.446	#	0.507	0.441	#	0.501
	poss: 2,3-Anhydro-d-galactosan (NIST MQ 78)	0.168	#	0.193	0.174	#	0.200	0.151	#	0.172	0.150	#	0.171
	OTHER ORGANIC COMPOUNDS												
	N-compounds	**0.000**		**0.00**	**0.000**		**0.00**	**0.000**		**0.00**	**0.000**		**0.00**
	Acetates	**0.000**		**0.00**	**0.000**		**0.00**	**0.000**		**0.00**	**0.000**		**0.00**
	Terpenes	**0.000**		**0.00**	**0.000**		**0.00**	**0.000**		**0.00**	**0.000**		**0.00**
	unknown compounds	**0.000**		**0.00**	**0.000**		**0.00**	**0.000**		**0.00**	**0.000**		**0.00**
	Miscellaneous	**0.000**		**0.00**	**0.000**		**0.00**	**0.000**		**0.00**	**0.000**		**0.00**

Table A14. GC-MS data for organic-rich condensate (ORC) recovered under optimum condensation temperature conditions (C1/C2 = 120 °C/50 °C) for coffee husk.

		Run 1			Run 2			Run 3			Run 4		
CAS No.	**Compound**	**wt.% wet**		**wt.% dry**	**wt.% wet**		**wt.% dry**	**wt.% wet**		**wt.% dry**	**wt.% wet**		**wt.% dry**
	NONAROMATIC COMPOUNDS												
	Acids	**11.983**		**13.60**	**12.046**		**13.67**	**12.185**		**13.74**	**12.200**		**13.75**
64-19-7	Acetic acid	7.167	c	8.136	7.212	c	8.187	7.384	c	8.324	7.388	c	8.330
79-09-4	Propionic acid	4.815	c	5.466	4.834	c	5.487	4.801	c	5.413	4.811	c	5.424
	Nonaromatic Esters	**0.000**		**0.00**	**0.000**		**0.00**	**0.000**		**0.00**	**0.000**		**0.00**
	Nonaromatic Alcohols	**0.000**		**0.00**	**0.000**		**0.00**	**0.000**		**0.00**	**0.000**		**0.00**
	Nonaromatic Aldehydes	**0.181**		**0.21**	**0.180**		**0.20**	**0.306**		**0.34**	**0.350**		**0.39**
2134-29-4	Propanal, 3-hydroxy-	0.050	#	0.057	0.052	#	0.059	0.121	#	0.136	0.134	#	0.151
	Butanedial or Propanal (NIST MQ 88)	0.131	#	0.148	0.128	#	0.146	0.185	#	0.208	0.215	#	0.243
	Nonaromatic Ketones	**7.281**		**8.26**	**7.354**		**8.35**	**6.916**		**7.80**	**6.896**		**7.77**
116-09-6	Acetol (Hydroxypropanone)	4.037	c	4.582	4.079	c	4.630	4.263	c	4.806	4.248	c	4.789
5077-67-8	Butanone, 1-hydroxy-2-	0.714	c	0.810	0.720	c	0.817	0.664	c	0.748	0.667	c	0.751
592-20-1	Propan-2-one, 1-acetyloxy-	0.116	c	0.131	0.115	c	0.130	0.119	c	0.135	0.123	c	0.139
120-92-3	Cyclopentanone	0.075	c	0.085	0.076	c	0.086	-		-	-		-
930-30-3	Cyclopenten-1-one, 2-	0.381	c	0.432	0.385	c	0.437	0.292	c	0.329	0.296	c	0.333
1121-05-7	Cyclopenten-1-one, 2,3-dimethyl-2-	0.076	c	0.087	0.092	c	0.104	0.051	c	0.058	0.110	c	0.124
1120-73-6	Cyclopenten-1-one, 2-methyl-2-	0.164	c	0.186	0.162	c	0.184	0.128	c	0.145	0.125	c	0.141
2758-18-1	Cyclopenten-1-one, 3-methyl-2-	0.220	c	0.250	0.225	c	0.255	0.172	c	0.194	0.171	c	0.192
5682-69-2	Cylopenten-1-one, 3-ethyl-2-	0.054	#	0.061	0.054	#	0.061	-		-	-		-
10493-98-8	Cyclopenten-1-one, 2-hydroxy-2-	0.161	#	0.183	0.163	#	0.184	0.246	#	0.277	0.253	#	0.286
80-71-7	Cyclopenten-1-one, 2-hydroxy-3-methyl-2-	0.997	c	1.132	0.990	c	1.124	0.831	c	0.937	0.752	c	0.848
21835-01-8	Cyclopenten-1-one, 3-ethyl-2-hydroxy-2-	0.180	c	0.204	0.184	c	0.208	0.150	c	0.169	0.152	c	0.171
	Isobutyl methyl ketone (NIST MQ 91)	0.046	#	0.052	0.049	#	0.056	-		-	-		-
	Isomere of Cyclopenten-1-one, 2,3-dimethyl-2-	0.061	#	0.069	0.061	#	0.069	-		-	-		-
	Aliphatic Hydrocarbons	**0.000**		**0.00**	**0.000**		**0.00**	**0.000**		**0.00**	**0.000**		**0.00**
	HETEROCYCLIC COMPOUNDS												

		Run 1			Run 2			Run 3			Run 4		
CAS No.	**Compound**	**wt.% wet**		**wt.% dry**	**wt.% wet**		**wt.% dry**	**wt.% wet**		**wt.% dry**	**wt.% wet**		**wt.% dry**
	Furans	**1.408**		**1.60**	**1.441**		**1.64**	**1.394**		**1.57**	**1.399**		**1.58**
497-23-4	Furanone, 2(5H)-	0.309	c	0.351	0.318	c	0.360	0.391	c	0.441	0.399	c	0.450
98-01-1	Furaldehyde, 2-	0.369	c	0.419	0.378	c	0.429	0.400	c	0.451	0.404	c	0.456
620-02-0	Furaldehyde, 5-methyl-2-	0.048	c	0.055	0.048	c	0.055	0.047	c	0.052	0.049	c	0.055
591-11-7	Furan-2-one, 5-methyl-, (5H)-	0.090	#	0.102	0.098	#	0.111	0.088	#	0.099	0.081	#	0.091
22122-36-7	Furan-2-one, 3-methyl-, (5H)-	0.100	c	0.114	0.101	c	0.115	0.101	c	0.114	0.102	c	0.114
96-48-0	Butyrolactone, γ-	0.299	c	0.340	0.304	c	0.345	0.269	c	0.304	0.265	c	0.299
	Furan-2-one, 4-methyl-(5H)- (NIST MQ 88)	0.102	#	0.116	0.102	#	0.116	0.097	#	0.110	0.100	#	0.113
	Isomere of Furan-2-one, 2,5-dihydro-3,5-dimethyl-	0.090	#	0.102	0.093	#	0.105	-		-	-		-
	Pyrans	**0.000**		**0.00**	**0.000**		**0.00**	**0.000**		**0.00**	**0.000**		**0.00**
	AROMATIC COMPOUNDS												
	Benzenes	**0.000**		**0.00**	**0.000**		**0.00**	**0.000**		**0.00**	**0.000**		**0.00**
	Catechols	**n.q.**		**n.q.**	**n.q.**		**n.q.**	**n.q.**		**n.q.**	**n.q.**		**n.q.**
123-31-9	Hydroquinone (Benzene, 1,4-dihydroxy-)	n.q.	n.q.	n.q.	n.q.	n.q.	n.q.	n.q.	n.q.	n.q.	n.q.	n.q.	n.q.
	Benzenediol, methyl-	n.q.	n.q.	n.q.	n.q.	n.q.	n.q.	n.q.	n.q.	n.q.	n.q.	n.q.	n.q.
	Aromatic Alcohols	**0.000**		**0.00**	**0.000**		**0.00**	**0.000**		**0.00**	**0.000**		**0.00**
	Aromatic Aldehydes	**0.000**		**0.00**	**0.000**		**0.00**	**0.000**		**0.00**	**0.000**		**0.00**
	Aromatic Ketones	**0.000**		**0.00**	**0.000**		**0.00**	**0.000**		**0.00**	**0.000**		**0.00**
	Aromatic Esters	**0.000**		**0.00**	**0.000**		**0.00**	**0.000**		**0.00**	**0.000**		**0.00**
	Lignin-derived Phenols	**0.896**		**1.02**	**0.900**		**1.02**	**0.573**		**0.65**	**0.577**		**0.65**
108-95-2	Phenol	0.218	c	0.247	0.220	c	0.250	0.149	c	0.168	0.149	c	0.168
95-48-7	Cresol, o-	0.154	c	0.175	0.152	c	0.173	0.115	c	0.130	0.116	c	0.131
106-44-5	Cresol, p-	0.090	c	0.102	0.091	c	0.104	0.060	c	0.067	0.061	c	0.069
108-39-4	Cresol, m-	0.127	c	0.144	0.128	c	0.145	0.084	c	0.095	0.086	c	0.096

		Run 1			Run 2			Run 3			Run 4		
CAS No.	**Compound**	**wt.% wet**		**wt.% dry**	**wt.% wet**		**wt.% dry**	**wt.% wet**		**wt.% dry**	**wt.% wet**		**wt.% dry**
95-87-4	Phenol, 2,5-dimethyl-	0.122	c	0.139	0.121	c	0.138	0.112	c	0.126	0.109	c	0.123
105-67-9	Phenol, 2,4-dimethyl-	0.068	c	0.078	0.071	c	0.080	0.053	c	0.060	0.056	c	0.063
123-07-9	Phenol, 4-ethyl-	0.117	c	0.132	0.116	c	0.132	-		-	-		-
	Guaiacols (Methoxy phenols)	**5.265**		**5.98**	**5.298**		**6.01**	**4.694**		**5.29**	**4.757**		**5.36**
90-05-1	Guaiacol	0.499	c	0.567	0.499	c	0.567	0.463	c	0.522	0.470	c	0.530
18102-31-3	Guaiacol, 3-methyl-	0.039	#	0.045	0.039	#	0.045	-		-	-		-
93-51-6	Guaiacol, 4-methyl-	0.432	c	0.490	0.456	c	0.517	0.409	c	0.461	0.407	c	0.459
	Guaiacol, 3-ethyl-	0.038	#	0.043	0.040	#	0.045	-		-	-		-
2785-89-9	Guaiacol, 4-ethyl-	0.235	c	0.267	0.236	c	0.268	0.185	c	0.208	0.185	c	0.209
7786-61-0	Guaiacol, 4-vinyl-	0.639	#	0.726	0.645	#	0.732	0.558	#	0.629	0.565	#	0.637
97-53-0	Guaiacol, 4-allyl-; (Eugenol)	0.192	c	0.218	0.191	c	0.217	0.180	c	0.203	0.183	c	0.206
2785-87-7	Guaiacol, 4-propyl-	0.070	c	0.080	0.070	c	0.079	0.066	c	0.074	0.065	c	0.074
97-54-1	Guaiacol, 4-propenyl- cis (Isoeugenol)	0.438	c	0.497	0.440	c	0.499	0.376	c	0.424	0.385	c	0.434
5932-68-3	Guaiacol, 4-propenyl-(trans) (Isoeugenol)	1.326	c	1.505	1.311	c	1.488	1.163	c	1.311	1.173	c	1.322
121-33-5	Vanillin	0.650	c	0.737	0.671	c	0.761	0.640	c	0.722	0.656	c	0.739
498-02-2	Ethanone, 1-(4-hydroxy-3-methoxyphenyl)- (Acetoguaiacone)	0.582	c	0.661	0.578	c	0.656	0.539	c	0.607	0.548	c	0.618
2503-46-0	Guaiacyl acetone	0.122	c	0.139	0.123	c	0.139	0.116	c	0.131	0.118	c	0.133
	Syringols (Dimethoxy phenols)	**3.040**		**3.45**	**3.068**		**3.48**	**2.832**		**3.19**	**2.862**		**3.23**
91-10-1	Syringol	0.390	c	0.443	0.390	c	0.443	0.366	c	0.413	0.372	c	0.420
6638-05-7	Syringol, 4-methyl-	0.349	c	0.396	0.348	c	0.395	0.334	c	0.376	0.340	c	0.384
14059-92-8	Syringol, 4-ethyl-	0.162	c	0.184	0.168	c	0.191	0.140	c	0.158	0.141	c	0.159
28343-22-8	Syringol, 4-vinyl-	0.522	#	0.592	0.520	#	0.590	0.485	#	0.547	0.476	#	0.537
6627-88-9	Syringol, 4-allyl-	0.297	c	0.337	0.299	c	0.339	0.268	c	0.302	0.275	c	0.310
26624-13-5	Syringol, 4-(1-propenyl)-, cis	0.216	#	0.245	0.218	#	0.248	0.192	#	0.216	0.201	#	0.226
20675-95-0	Syringol, 4-(1-propenyl)-, trans	0.664	#	0.754	0.671	#	0.761	0.609	#	0.687	0.606	#	0.683
134-96-3	Syringaldehyde	0.294	c	0.334	0.303	c	0.344	0.299	c	0.337	0.306	c	0.346
2478-38-8	Acetosyringone	0.145	c	0.164	0.151	c	0.172	0.139	c	0.157	0.144	c	0.163

		Run 1			Run 2			Run 3			Run 4		
CAS No.	**Compound**	**wt.% wet**		**wt.% dry**	**wt.% wet**		**wt.% dry**	**wt.% wet**		**wt.% dry**	**wt.% wet**		**wt.% dry**
	CARBOHYDRATES												
	Sugars	**6.309**		**7.16**	**6.390**		**7.25**	**6.271**		**7.07**	**6.481**		**7.31**
51246-94-7	Anhydro-ß-D-xylofuranose, 1,5-	0.829	#	0.941	0.831	#	0.943	0.730	#	0.823	0.753	#	0.849
498-07-7	Anhydro-ß-D-glucopyranose, 1,6- (Levoglucosan)	5.022	c	5.701	5.118	c	5.809	5.169	c	5.827	5.348	c	6.029
4451-31-4	Dianhydro-α-D-glucopyranose, 1,4:3,6-	0.458	#	0.519	0.442	#	0.501	0.372	#	0.419	0.380	#	0.429
	OTHER ORGANIC COMPOUNDS												
	N-compounds	**0.107**		**0.12**	**0.104**		**0.12**	**0.097**		**0.11**	**0.097**		**0.11**
	Caffeine	0.107	#	0.121	0.104	#	0.118	0.097	#	0.109	0.097	#	0.109
	Acetates	**0.000**		**0.00**	**0.000**		**0.00**	**0.000**		**0.00**	**0.000**		**0.00**
	Terpenes	**0.000**		**0.00**	**0.000**		**0.00**	**0.000**		**0.00**	**0.000**		**0.00**
	unknown compounds	**0.000**		**0.00**	**0.000**		**0.00**	**0.000**		**0.00**	**0.000**		**0.00**
	Miscellaneous	**0.000**		**0.00**	**0.000**		**0.00**	**0.000**		**0.00**	**0.000**		**0.00**

Appendix B: *Additional Information for the Study on the Influence of Selected Quench Media on Yield and Composition of Fast Pyrolysis Bio-Oils*

Section 1: Model-Predicted Txy Plot of Water and Ethanol Showing Azeotrope Formation

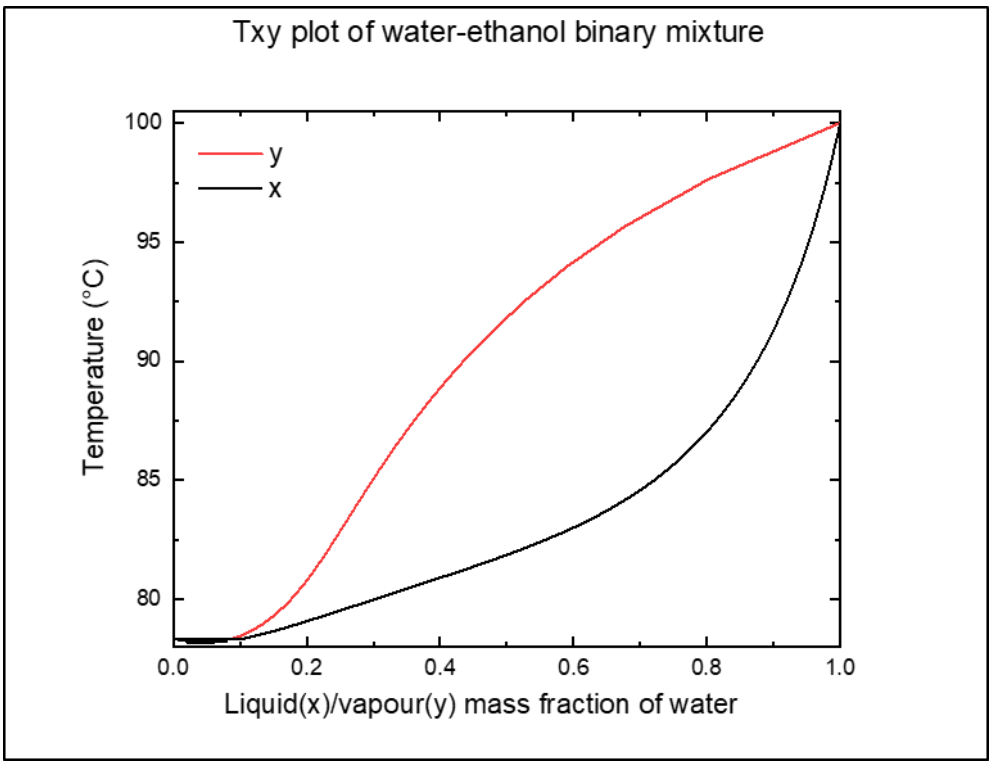

Fig. B1. Model-predicted Txy plot of water–ethanol showing azeotrope formation at 78.14 °C.

Section 2: Experimental and Model-Predicted Product Yield and Compounds Composition Ratios of ORC to AC

Table B1. Experimental and model-predicted data for the product yield ratios of ORC to AC for all investigated quench media at all m_q/m_v ratios.

Quench Medium	$m_q/m_v - 0.5$ (Exp. Data)	$m_q/m_v - 0.5$ (Model)	$m_q/m_v - 2.0$ (Exp. Data)	$m_q/m_v - 2.0$ (Model)
Isopar-V	3.56	9.03	2.59	6.90
Water	3.71	5.23	2.78	3.31
Glycol	7.88	41.97	10.20	96.27
Ethanol	3.92	63.67	5.48	115.25

Note: Exp. Data = Experimental Data

Table B2. Isopar-V: Experimental and model-predicted data for the concentration ratios of chemical compounds in ORC to AC at all m_q/m_v ratios.

Compound Class	$m_q/m_v - 0.5$ (Exp. Data)	$m_q/m_v - 0.5$ (Model)	$m_q/m_v - 2.0$ (Exp. Data)	$m_q/m_v - 2.0$ (Model)
Acids	6.70	4.80	4.23	1.98
Alcohols	10.00	11.30	4.06	6.35
Ketones	2.50	51.10	1.55	10.00
Aliphatics	7.80	54.80	0.56	50.69
Aldehydes	0.00	0.00	0.00	0.00
Furans	4.80	48.10	2.89	28.37
Phenols	38.60	165.90	24.60	67.81
Guaiacols	85.70	399.80	33.69	159.03
Syringols	1102.10	4631.40	679.21	1266.16
Sugars	∞	∞	∞	∞

Note: Exp. Data = Experimental Data; ∞ = No sugars were detected in AC.

Table B3. Water: Experimental and model-predicted data for the concentration ratios of chemical compounds in ORC to AC at all m_q/m_v ratios.

Compound Class	$m_q/m_v - 0.5$ (Exp. Data)	$m_q/m_v - 0.5$ (Model)	$m_q/m_v - 2.0$ (Exp. Data)	$m_q/m_v - 2.0$ (Model)
Acids	2.72	0.97	0.55	0.20
Alcohols	0.00	4.79	0.00	0.25
Ketones	1.80	17.90	0.65	3.66
Aldehydes	0.00	21.47	0.00	4.72
Furans	0.91	6.36	0.11	1.23
Phenols	47.24	10.55	25.12	2.10
Guaiacols	87.05	25.04	45.12	5.35
Syringols	>200	198.55	>100	17.74
Sugars	∞	∞	∞	∞

Note: Exp. Data = Experimental Data; ∞ = No sugars were detected in AC.

Table B4. Ethylene glycol: Experimental and model-predicted data for the concentration ratios of chemical compounds in ORC to AC at all m_q/m_v ratios.

Compound Class	$m_q/m_v - 0.5$ (Exp. Data)	$m_q/m_v - 0.5$ (Model)	$m_q/m_v - 2.0$ (Exp. Data)	$m_q/m_v - 2.0$ (Model)
Acids	110.71	274.71	0.00*	1704.26
Ketones	34.98	986.60	138.50	3823.58
Aldehydes	0.00	2672.43	0.00	14727.17
Furans	31.72	1341.41	71.48	8844.72
Phenols	788.10	2111.77	1837.87	14,673.47
Guaiacols	767.28	3554.41	1371.89	23,878.23
Syringols	>25,000	26,833.97	>150,000	176,498.59
Sugars	∞	∞	∞	∞

*Note: Exp. Data = Experimental Data; * = No experimental data recorded; ∞ = No sugars were detected in AC.*

Table B5. Ethanol: Experimental and model-predicted data for the concentration ratios of chemical compounds in ORC to AC at all m_q/m_v ratios.

Compound Class	$m_q/m_v - 0.5$ (Exp. Data)	$m_q/m_v - 0.5$ (Model)	$m_q/m_v - 2.0$ (Exp. Data)	$m_q/m_v - 2.0$ (Model)
Acids	39.67	686.47	212.53	2540.57
Ketones	12.26	4260.65	28.38	8526.40
Aldehydes	0.00	7186.87	0.00	22,418.12
Furans	12.15	2047.49	47.17	5666.46
Phenols	531.73	30,953.17	1755.79	175,504.26
Guaiacols	346.61	61,137.94	916.37	292,102.08
Syringols	>800,000	739,605.24	>3,000,000	3,167,142.24
Sugars	∞	∞	∞	∞

Note: Exp. Data = Experimental Data; ∞ = No sugars were detected in AC.

Section 3: GC-MS Analysis of All Condensates and Spent Quench Media for Isopar-V and Water

Table B6. GC-MS data for organic-rich condensate (ORC) recovered using ethylene glycol as the quench at quench-to-volatiles mass flow rate ratios (m_q/m_v) of 0.5 and 2.0.

	wt.% (wet)							
	m_q/m_v– 2.0				m_q/m_v– 0.5			
NONAROMATIC COMPOUNDS	**Run 1**	**Run 2**	**Run 3**	**Run 4**	**Run 1**	**Run 2**	**Run 3**	**Run 4**
Acids	**0.000**	**0.000**	**0.000**	**0.000**	**3.538**	**3.524**	**3.638**	**3.659**
Acetic acid	n/a	n/a	n/a	n/a	3.538	3.524	3.638	3.659
Nonaromatic Esters	**0.000**	**0.000**	**0.000**	**0.000**	0.000	0.000	0.000	0.000
Nonaromatic Alcohols	**138.025**	**138.025**	**135.529**	**134.137**	**100.934**	**102.902**	**94.174**	**92.003**
Ethylene glycol	138.025	138.025	135.529	134.137	100.934	102.902	94.174	92.003
Nonaromatic Aldehydes	**0.000**	**0.000**	**0.000**	**0.000**	**0.000**	**0.000**	**0.000**	**0.000**
Nonaromatic Ketones	**1.660**	**1.660**	**1.300**	**1.298**	**2.356**	**2.348**	**3.034**	**2.968**
2-Pentanone, 4-hydroxy-4-methyl- = Diacetone alcohol = impurity of Acetone	0.066	0.066	0.099	0.098	0.119	0.122	0.067	0.069
Acetol (Hydroxypropanone)	1.189	1.189	0.906	0.904	1.179	1.180	1.796	1.761
Butanone, 2-	n/a	n/a	n/a	n/a	0.029	0.030	0.027	0.026
Butanone, 1-hydroxy-2-	n.q.	n.q.	n.q.	0.081	n.q.	n.q.	n.q.	n.q.
Butandione, 2,3- (Diacetyl)							0.014	0.013
Cyclopentanone	n.q.	n.q.	n.q.	0.035	n.q.	n.q.	n.q.	n.q.
Cyclopenten-1-one, 2-	0.072	0.072	0.080	0.180	0.192	0.166	0.174	0.172
Cyclopenten-1-one, 2-methyl-2-	0.030	0.030	0.037	n/a	0.078	0.077	0.074	0.072
Cyclopenten-1-one, 3-methyl-2-	0.077	0.077	0.179	n/a	0.165	0.167	0.162	0.157
Cylopenten-1-one, 3-ethyl-2-	n/a	n/a	n/a	n/a	n/a	n/a	0.039	0.038
Cyclopenten-1-one, 2-hydroxy-3-methyl-2-	0.226	0.226	n/a	n/a	0.538	0.550	0.621	0.603
Isomer of Cyclopenten-1-one, 3-ethyl-2-hydroxy-					0.055	0.057	0.059	0.057
Aliphatic Hydrocarbons	**0.000**	**0.000**	**0.000**	**0.000**	**0.000**	**0.000**	**0.000**	**0.000**
HETEROCYCLIC COMPOUNDS								
Furans	**0.081**	**0.081**	**0.072**	**0.074**	**0.163**	**0.161**	**0.312**	**0.309**
Furanone, 2(5H)-					n/a	n/a	0.137	0.140
Butyrolactone, γ-	0.081	0.081	0.072	0.074	0.163	0.161	0.174	0.169
Pyrans	**0.000**	**0.000**	**0.000**	**0.000**	**0.000**	**0.000**	**0.000**	**0.000**
AROMATIC COMPOUNDS								
Benzenes	**0.000**	**0.000**	**0.000**	**0.000**	**0.021**	**0.021**	**0.000**	**0.000**
					0.021	0.021		
Catechols	**0.000**	**0.000**	**0.000**	**0.000**	**0.000**	**n.q.**	**n.q.**	**n.q.**
Hydroquinone (Benzene, 1,4-dihydroxy-)	n/a	n/a	n/a	n/a	n.q.	n.q.	n.q.	n.q.
Benzenediol, methyl-	n/a	n/a	n/a	n/a	n.q.	n.q.	n.q.	n.q.

Aromatic Alcohols	**0.000**	**0.000**	**0.000**	**0.000**	**0.000**	**0.000**	**0.000**	**0.000**
Aromatic Aldehydes	**0.000**	**0.000**	**0.000**	**0.000**	**0.000**	**0.000**	**0.000**	**0.000**
Aromatic Ketones	**0.000**	**0.000**	**0.000**	**0.000**	**0.000**	**0.000**	**0.000**	**0.000**
Aromatic Esters	**0.000**	**0.000**	**0.000**	**0.000**	**0.000**	**0.000**	**0.000**	**0.000**
Lignin-derived Phenols	**0.376**	**0.376**	**0.375**	**0.380**	**1.118**	**1.140**	**1.213**	**1.191**
Phenol	0.075	0.075	0.084	0.093	0.230	0.235	0.227	0.219
Cresol, o-	0.046	0.046	0.049	0.044	0.131	0.132	0.138	0.134
Cresol, p-	0.016	0.016	0.019	0.017	0.057	0.061	0.060	0.057
Cresol, m-	0.030	0.030	0.037	0.039	0.098	0.098	0.087	0.086
Phenol, 2,5-dimethyl-	0.073	0.073	0.077	0.076	0.091	0.092	0.091	0.089
Phenol, 2,4-dimethyl-	0.008	0.008	0.008	0.009	0.024	0.023	0.022	0.022
Phenol, 3-ethyl-	n/a	n/a	n/a	n/a	0.130	0.133	0.126	0.129
Phenol, 4-ethyl-	0.049	0.049	0.049	0.050	0.167	0.169	0.152	0.148
Phenol, 4-vinyl-	0.079	0.079	0.045	0.046	0.167	0.174	0.286	0.285
Phenol, ethyl-methyl-	n/a	n/a	0.007	0.008	0.022	0.022	0.023	0.023
Guaiacols (Methoxy phenols)	**0.265**	**0.265**	**0.229**	**0.215**	**0.913**	**0.930**	**1.138**	**1.102**
Guaiacol	0.076	0.076	0.055	0.055	0.166	0.151	0.202	0.190
Guaiacol, 4-methyl-	0.018	0.018	0.016	0.017	0.049	0.049	0.057	0.055
Guaiacol, 4-ethyl-	0.032	0.032	0.042	0.040	0.117	0.119	0.097	0.096
Guaiacol, 4-vinyl-	0.078	0.078	0.057	0.050	0.201	0.207	0.296	0.292
Guaiacol, 4-allyl-; (Eugenol)	n/a	n/a	n/a	n/a	0.029	0.028	0.034	0.033
Guaiacol, 4-propenyl- cis (Isoeugenol)	n/a	n/a	n/a	n/a	0.067	0.062	0.075	0.073
Guaiacol, 4-propenyl-(trans) (Isoeugenol)	0.060	0.060	0.058	0.053	0.217	0.242	0.301	0.287
Guaiacyl acetone	n/a	n/a	n/a	n/a	0.068	0.072	0.077	0.076
Syringols (Dimethoxy phenols)	**0.186**	**0.186**	**0.113**	**0.112**	**0.501**	**0.516**	**0.623**	**0.616**
Syringol	0.033	0.033	0.026	0.028	0.101	0.099	0.127	0.124
Syringol, 4-methyl-	0.016	0.016	0.024	0.024	0.042	0.044	0.050	0.050
Syringol, 4-ethyl-	0.018	0.018	0.063	0.060	0.068	0.073	0.057	0.057
Syringol, 4-vinyl-	0.073	0.073	n/a	n/a	0.118	0.114	0.166	0.165
Syringol, 4-allyl-					0.066	0.069	0.078	0.074
Syringol, 4-(1-propenyl)-, trans	0.047	0.047	n/a	n/a	0.106	0.118	0.145	0.147
CARBOHYDRATES								
Sugars	**0.000**	**0.000**	**0.000**	**0.000**	**0.000**	**0.000**	**0.000**	**0.000**
OTHER ORGANIC COMPOUNDS								
N-compounds	**0.000**	**0.000**	**0.000**	**0.000**	**0.092**	**0.094**	**0.000**	**0.000**
Oxazole, 4,5-dihydro-2,4,4-trimethyl- (NIST MQ 82)	n/a	n/a	n/a	n/a	0.069	0.071	n/a	n/a
unknown N-Compound (no NIST spectrum found)	n/a	n/a	n/a	n/a	0.023	0.023	n/a	n/a

Acetates	**0.000**	**0.000**	**0.000**	**0.000**	**0.000**	**0.000**	**0.000**	**0.000**
Terpenes	**0.000**	**0.000**	**0.000**	**0.000**				
unknown compounds	**0.000**	**0.000**	**0.000**	**0.000**				
Miscellaneous	**0.000**	**0.000**	**0.000**	**0.000**				

Table B7. GC-MS data for aqueous condensate (AC) recovered using ethylene glycol as the quench at quench-to-volatiles mass flow rate ratios (m_q/m_v) of 0.5 and 2.0.

	wt.% (wet)							
	m_q/m_v– 2.0				m_q/m_v – 0.5			
NONAROMATIC COMPOUNDS	**Run 1**	**Run 2**	**Run 3**	**Run 4**	**Run 1**	**Run 2**	**Run 3**	**Run 4**
Acids	**2.048**	**2.054**	**1.584**	**1.587**	**1.741**	**1.690**	**2.343**	**2.314**
Acetic acid	1.565	1.568	1.096	1.100	1.258	1.212	1.808	1.785
Propionic acid	0.483	0.485	0.488	0.487	0.483	0.478	0.535	0.528
Nonaromatic Esters	**0.012**	**0.013**	**0.000**	**0.000**	**0.000**	**0.000**	**0.010**	**0.010**
2-oxo-Propanoic acid methyl ester (NIST MQ 82)	0.012	0.013	n/a	n/a			0.010	0.010
Nonaromatic Alcohols	**3.772**	**3.759**	**3.328**	**3.198**	**2.785**	**2.666**	**3.709**	**3.456**
Ethylene glycol	3.737	3.725	3.301	3.170	2.758	2.639	3.682	3.430
2-Propen-1-ol (NIST MQ 91)	0.027	0.026	0.028	0.027	0.027	0.026	0.027	0.026
unknown aliphatic alcohol	0.008	0.008	n/a	n/a				
Nonaromatic Aldehydes	**0.052**	**0.051**	**0.057**	**0.057**	**0.053**	**0.052**	**0.122**	**0.122**
Acetaldehyde, hydroxy-	n/a	n/a	n/a	n/a	n/a	n/a	0.064	0.066
Butanal	0.009	0.009	0.011	0.011	0.010	0.009	0.010	0.009
Crotonaldehyde, cis	0.026	0.025	0.021	0.021	0.020	0.020	0.029	0.028
Crotonaldehyde, trans	0.017	0.017	0.019	0.020	0.018	0.018	0.020	0.019
2-Butenal, 2-methyl- (NIST MQ 92)	n/a	n/a	0.005	0.006	0.005	0.005	n/a	n/a
Nonaromatic Ketones	**4.995**	**4.868**	**4.096**	**4.164**	**4.217**	**4.069**	**5.393**	**5.407**
2-Pentanone, 4-hydroxy-4-methyl- = Diacetone alcohol = impurity of Acetone	n/a	n/a	0.005	0.005	n/a	n/a	n/a	n/a
Acetol (Hydroxypropanone)	3.093	3.025	2.040	2.046	2.129	2.051	3.453	3.383
Butanone, 2-	0.093	0.090	0.122	0.117	0.112	0.109	0.107	0.103
Butanone, 1-hydroxy-2-	0.460	0.411	0.407	0.464	0.483	0.471	0.408	0.521
Butandione, 2,3- (Diacetyl)	0.126	0.122	0.092	0.095	0.080	0.081	0.127	0.124
Acetoin (Hydroxy-2-butanone, 3-)	0.090	0.091	0.097	0.097	0.093	0.090	0.097	0.097
Propan-2-one, 1-acetyloxy-	0.062	0.061	0.040	0.041	0.042	0.040	0.061	0.060
Cyclopentanone	0.091	0.089	0.112	0.115	0.117	0.099	0.078	0.085
Cyclopenten-1-one, 2-	0.396	0.393	0.481	0.486	0.461	0.446	0.414	0.404
Cyclopenten-1-one, 2,3-dimethyl-2-	0.034	0.032	0.022	0.023	0.023	0.019	0.037	0.029
Cyclopenten-1-one, 2-methyl-2-	0.129	0.128	0.165	0.166	0.155	0.152	0.131	0.127
Cyclopenten-1-one, 3-methyl-2-	0.083	0.085	0.101	0.102	0.099	0.096	0.088	0.087
Cylopenten-1-one, 3-ethyl-2-	0.013	0.013	0.015	0.015	0.015	0.014	0.014	0.013
Cyclopenten-1-one, 2-hydroxy-3-methyl-2-	0.055	0.063	0.073	0.075	0.081	0.077	0.070	0.074
Cyclohexen-1-one, 2-	0.007	0.007	0.009	0.008	0.009	0.009	0.008	0.008
3-Buten-2-one (NIST MQ 88)	0.021	0.021	0.020	0.019	0.018	0.018	0.022	0.022
Butanone, 3-methyl-2- (NIST MQ 88)	n/a	n/a	0.004	0.004	0.003	0.003	0.006	0.006
3-Buten-2-one, 3-methyl- (NIST MQ 88)	0.005	0.005	0.005	0.005	0.005	0.005	n/a	n/a
2-Pentanone (NIST MQ 94)	0.023	0.023	0.018	0.015	0.022	0.023	0.028	0.030
3-Pentanone (NIST MQ 92)	0.009	0.008	0.008	0.005	n/a	n/a	0.011	0.011
3-Pentanone (NIST MQ 92)	n/a	n/a	0.005	0.032	0.010	0.007	n/a	n/a

2,3-Pentanedione	0.031	0.030	0.032	0.036	0.027	0.027	0.033	0.032
3-Penten-2-one (NIST MQ 84)	0.030	0.030	0.036	0.020	0.033	0.033	0.033	0.032
2,3-Hexanedione (NIST MQ 78)					0.006	0.007	n/a	n/a
Cyclopentanone, 2-methyl- (NIST MQ 87)	0.016	0.015	0.019	0.029	0.018	0.018	0.017	0.017
Cyclopentanone, 3-methyl- (NIST MQ 92)	n/a	n/a	n/a	n/a	0.019	0.019	n/a	n/a
Isomere of 2-Cyclopenten-1-one, 3-methyl-	0.024	0.024	0.029	0.020	0.027	0.026	0.025	0.024
2-Butanone, 1-hydroxy-3-methyl- (NIST MQ 78)	0.021	0.021	0.020	0.019	0.021	0.020	0.023	0.023
2-Cyclopenten-1-one, x,y-dimethyl-	0.015	0.015	0.019	0.013	0.019	0.019	0.016	0.015
2-Cycolpenten-1-one, x,y-dimethyl-	0.011	0.012	0.013	0.013	0.012	0.012	0.012	0.011
2,5-Hexanedione (NIST MQ 89)	0.014	0.013	0.012	0.024	0.013	0.012	0.013	0.012
Isomere of Cyclopenten-1-one, 2,3-dimethyl-2-	0.023	0.023	0.024	0.028	0.024	0.023	0.023	0.022
2-Cyclopenten-1-one, x,y-dimethyl-	n/a	n/a	0.027	0.010	0.019	0.022	0.013	0.010
2-Cyclopenten-1-one, 2,3,4-trimethyl- (NIST MQ 88)	0.008	0.008	0.009	0.012	0.009	0.009	0.008	0.009
Isomer of Cyclopenten-1-one, 3-ethyl-2-hydroxy-	0.012	0.012	0.012	0.005	0.012	0.012	0.014	0.013
poss: 2-Cyclopenten-1-one, trimethyl- (NIST MQ 82)	n/a	n/a	0.004	n/a	n/a	n/a	0.004	0.004
Aliphatic Hydrocarbons	**0.000**	**0.000**	**0.000**	**0.000**	**0.000**	**0.000**	**0.000**	**0.000**
HETEROCYCLIC COMPOUNDS								
Furans	**0.489**	**0.488**	**0.422**	**0.426**	**0.432**	**0.422**	**0.505**	**0.498**
Furfuryl alcohol, 2-	0.028	0.027	0.031	0.030	0.032	0.031	0.033	0.033
Furanone, 2(5H)-	0.045	0.045	n/a	n/a	n/a	n/a	0.038	0.041
Furaldehyde, 2-	0.238	0.238	0.216	0.220	0.219	0.214	0.242	0.236
Furaldehyde, 3-	0.018	0.018	0.018	0.018	0.017	0.016	0.020	0.021
Furaldehyde, 5-methyl-2-	0.019	0.019	0.020	0.021	0.021	0.020	0.020	0.019
Ethanone, 1-(2-furanyl)-	0.026	0.025	0.027	0.027	0.026	0.026	0.026	0.025
Furan-2-one, 3-methyl-, (5H)-	0.012	0.012	0.009	0.009	0.010	0.010	0.013	0.013
Furan-2-one, 2,5-dihydro-3,5-dimethyl-	0.014	0.014	0.012	0.012	0.013	0.013	0.015	0.014
Butyrolactone, γ-	0.085	0.084	0.085	0.086	0.089	0.087	0.093	0.091
Furan, tetrahydro-2-methoxy- (NIST MQ (80)	0.004	0.005	0.005	0.005	0.004	0.004	0.005	0.005
Pyrans	**0.000**	**0.000**	**0.000**	**0.000**	**0.000**	**0.000**	**0.000**	**0.000**
AROMATIC COMPOUNDS								
Benzenes	**0.002**	**0.002**	**0.000**	**0.000**	**0.002**	**0.002**	**0.002**	**0.002**
Inden-1-one, 2,3-dihydro-1H-	0.002	0.002	n/a	n/a	0.002	0.002	0.002	0.002
Catechols	**0.000**	**0.000**	**0.000**	**0.000**	**0.000**	**0.000**	**0.000**	**0.000**
Aromatic Alcohols	**0.000**	**0.000**	**0.000**	**0.000**	**0.000**	**0.000**	**0.000**	**0.000**
Aromatic Aldehydes	**0.003**	**0.003**	**0.000**	**0.000**	**0.000**	**0.000**	**0.003**	**0.003**
Benzaldehyde	0.003	0.003	n/a	n/a			0.003	0.003
Aromatic Ketones	**0.000**	**0.000**	**0.000**	**0.000**	**0.000**	**0.000**	**0.000**	**0.000**
Aromatic Esters	**0.000**	**0.000**	**0.000**	**0.000**	**0.000**	**0.000**	**0.000**	**0.000**

Lignin-derived Phenols	**0.089**	**0.090**	**0.084**	**0.084**	**0.085**	**0.081**	**0.103**	**0.100**
Phenol	0.043	0.043	0.047	0.047	0.046	0.043	0.049	0.048
Cresol, o-	0.019	0.019	0.019	0.019	0.019	0.019	0.022	0.021
Cresol, p-	0.006	0.006	0.006	0.005	0.006	0.006	0.007	0.007
Cresol, m-	0.008	0.008	0.009	0.007	0.008	0.008	0.009	0.010
Phenol, 2,5-dimethyl-	0.006	0.006	n/a	n/a	0.006	0.006	0.006	0.006
Phenol, 2,4-dimethyl-	0.002	0.002	n/a	n/a	n/a	n/a	0.002	0.002
Phenol, 4-ethyl-	0.005	0.005	0.005	0.006	n/a	n/a	0.007	0.007
Guaiacols (Methoxy phenols)	**0.081**	**0.081**	**0.069**	**0.070**	**0.079**	**0.077**	**0.087**	**0.089**
Guaiacol	0.061	0.061	0.054	0.055	0.058	0.056	0.064	0.067
Guaiacol, 4-methyl-	0.010	0.010	0.008	0.008	0.009	0.009	0.010	0.010
Guaiacol, 4-ethyl-	0.007	0.007	0.007	0.007	0.008	0.008	0.008	0.008
Guaiacol, 4-vinyl-	0.003	0.003	n/a	n/a	0.004	0.004	0.004	0.004
Syringols (Dimethoxy phenols)	**0.000**	**0.000**	**0.000**	**0.000**	**0.000**	**0.000**	**0.000**	**0.000**
CARBOHYDRATES								
Sugars	**0.000**	**0.000**	**0.000**	**0.000**	**0.000**	**0.000**	**0.000**	**0.000**
OTHER ORGANIC COMPOUNDS								
N-compounds	**0.003**	**0.003**	**0.041**	**0.042**	**0.046**	**0.042**	**0.003**	**0.003**
Oxazole, 4,5-dihydro-2,4,4-trimethyl- (NIST MQ 82)	n/a	n/a	0.027	0.027	0.031	0.028	n/a	n/a
Pyridine, 2-methyl- (NIST MQ 92)	0.003	0.003	0.004	0.004	0.003	0.004	0.003	0.003
unknown N-Compound (no NIST spectrum found)	n/a	n/a	0.010	0.010	0.011	0.010	n/a	n/a
Acetates	**0.000**	**0.000**	**0.000**	**0.000**	**0.000**	**0.000**	**0.000**	**0.000**
Terpenes	**0.000**	**0.000**	**0.000**	**0.000**	**0.000**	**0.000**	**0.000**	**0.000**
unknown compounds	**0.000**	**0.000**	**0.000**	**0.000**	**0.000**	**0.000**	**0.000**	**0.000**
Miscellaneous	**0.017**	**0.016**	**0.012**	**0.018**	**0.012**	**0.011**	**0.017**	**0.016**
1,3-Dioxolane, 2-methyl- (NIST MQ 91)	0.011	0.010	0.007	0.007	0.007	0.007	0.011	0.011
1,4-Dioxane (NIST MQ 83)	n/a	n/a	n/a	0.005	0.005	0.004	0.006	0.006
poss: 1,4-Dioxin, 2,3-dihydro-	0.006	0.006	0.005	0.005	n/a	n/a	n/a	n/a

Table B8. GC-MS data for organic-rich condensate (ORC) recovered using ethanol as the quench at quench-to-volatiles mass flow rate ratios (m_q/m_v) of 0.5 and 2.0.

	wt.% (wet)							
	$m_q/m_v - 2.0$				$m_q/m_v - 0.5$			
NONAROMATIC COMPOUNDS	**Run 1**	**Run 2**	**Run 3**	**Run 4**	**Run 1**	**Run 2**	**Run 3**	**Run 4**
Acids	**0.000**	**0.000**	**3.126**	**2.958**	**3.836**	**3.846**	**4.455**	**4.523**
Acetic acid	n/a	n/a	3.126	2.958	3.836	3.846	4.455	4.523
Nonaromatic Esters	**0.000**	**0.000**	**0.000**	**0.000**	**0.000**	**0.000**	**0.000**	**0.000**
Nonaromatic Alcohols	**64.766**	**64.766**	**62.810**	**62.810**	**24.427**	**24.427**	**20.742**	**20.675**
Ethylene glycol	n/a	n/a	n/a	n/a	n/a	n/a	0.706	0.639
Ethanol	64.766		62.810		24.427		24.036	
Nonaromatic Aldehydes	**0.000**	**0.000**	**0.000**	**0.000**	**0.000**	**0.000**	**0.000**	**0.000**
Nonaromatic Ketones	**2.434**	**2.406**	**3.034**	**3.017**	**4.359**	**4.350**	**6.087**	**6.126**
2-Pentanone, 4-hydroxy-4-methyl- = Diacetone alcohol = impurity of Acetone	0.055	0.054	0.049	0.049	0.104	0.104	0.069	0.067
Acetol (Hydroxypropanone)	0.927	0.924	1.491	1.477	1.751	1.750	3.593	3.528
Butanone, 2-	0.623	0.611	0.563	0.566	0.242	0.233	0.164	0.160
Butanone, 1-hydroxy-2-	0.269	0.264	0.359	0.354	0.504	0.500	0.731	0.725
Propan-2-one, 1-acetyloxy-					0.044	0.046	0.065	0.068
Cyclopentanone	0.073	0.071	0.067	0.067	0.124	0.126	0.135	0.135
Cyclopenten-1-one, 2-	0.132	0.131	0.140	0.139	0.397	0.398	0.372	0.390
Cyclopenten-1-one, 2-methyl-2-	0.080	0.076	0.075	0.072	0.211	0.207	0.152	0.180
Cyclopenten-1-one, 3-methyl-2-	0.089	0.089	0.087	0.086	0.243	0.242	0.201	0.214
Cylopenten-1-one, 3-ethyl-2-	n/a	n/a	n/a	n/a	0.053	0.056	0.046	0.045
Cyclopenten-1-one, 2-hydroxy-3-methyl-2-	0.152	0.151	0.182	0.183	0.502	0.509	0.525	0.576
2-Cyclopenten-1-one, x,y-dimethyl-	n/a	n/a	n/a	n/a	0.032	0.033	0.035	0.039
Isomere of Cyclopenten-1-one, 2,3-dimethyl-2-	n/a	n/a	n/a	n/a	0.044	0.045	n/a	n/a
Butanone, 3-methyl-2- (NIST MQ 88)	0.022	0.023	0.022	0.024	n/a	n/a	n/a	n/a
2-Cyclopenten-1-one, x,y-dimethyl-	0.013	0.012	n/a	n/a	0.046	0.047	n/a	n/a
Isomer of Cyclopenten-1-one, 3-ethyl-2-hydroxy-	n/a	n/a	n/a	n/a	0.061	0.055	n/a	n/a
Aliphatic Hydrocarbons	**0.000**	**0.000**	**0.000**	**0.000**	**0.000**	**0.000**	**0.000**	**0.000**
HETEROCYCLIC COMPOUNDS								
Furans	**0.078**	**0.077**	**0.228**	**0.246**	**0.376**	**0.365**	**0.655**	**0.707**
Furfuryl alcohol, 2-					0.138	0.137	0.054	0.056
Furaldehyde, 2-	n/a	n/a	0.141	0.158	0.025	0.026	0.215	0.250
Furaldehyde, 5-methyl-2-					0.213	0.203	0.020	0.023
Ethanone, 1-(2-furanyl)-	n/a	n/a	n/a	n/a	n/a	n/a	0.027	0.030
Furan-2-one, 3-methyl-, (5H)-					n/a	n/a	0.025	0.027
Butyrolactone, γ-	0.078	0.077	0.087	0.087	n/a	n/a	0.233	0.238
Furan, 2-ethoxytetrahydro- (NIST MQ 87)					n/a	n/a	0.049	0.054
Furan-2-one, 4-methyl-(5H)- (NIST MQ 88)					n/a	n/a	0.030	0.030

Pyrans	**0.000**	**0.000**	**0.000**	**0.000**	**0.000**	**0.000**	**0.000**	**0.000**
AROMATIC COMPOUNDS								
Benzenes	**0.010**	**0.009**	**0.017**	**0.018**	**0.027**	**0.028**	**0.000**	**0.000**
Toluene	0.010	0.009	0.017	0.018	0.027	0.028		
Catechols	**0.000**	**0.000**	**0.000**	**0.000**	n.q.	n.q.	n.q.	n.q.
Hydroquinone (Benzene, 1,4-dihydroxy-)	n/a	n/a	n/a	n/a	n.q.	n.q.	n.q.	n.q.
Benzenediol, methyl-	n/a	n/a	n/a	n/a	n.q.	n.q.	n.q.	n.q.
Aromatic Alcohols	**0.000**	**0.000**	**0.000**	**0.000**	**0.000**	**0.000**	**0.000**	**0.000**
Aromatic Aldehydes	**0.000**	**0.000**	**0.000**	**0.000**	**0.000**	**0.000**	**0.000**	**0.000**
Aromatic Ketones	**0.000**	**0.000**	**0.000**	**0.000**	**0.000**	**0.000**	**0.000**	**0.000**
Aromatic Esters	**0.000**	**0.000**	**0.000**	**0.000**	**0.000**	**0.000**	**0.000**	**0.000**
Lignin-derived Phenols	**0.468**	**0.443**	**0.439**	**0.441**	**1.369**	**1.387**	**0.992**	**1.216**
Phenol	0.098	0.098	0.085	0.089	0.288	0.291	0.209	0.249
Cresol, o-	0.048	0.049	0.046	0.046	0.159	0.161	0.119	0.146
Cresol, p-	0.025	0.021	0.022	0.019	0.073	0.074	0.051	0.064
Cresol, m-	0.053	0.041	0.036	0.035	0.118	0.121	0.077	0.090
Phenol, 2,5-dimethyl-	0.079	0.078	0.074	0.077	0.100	0.099	0.085	0.090
Phenol, 2,4-dimethyl-	0.012	0.010	0.010	0.010	0.032	0.034	0.018	0.026
Phenol, 3-ethyl-					0.143	0.141	0.119	0.127
Phenol, 4-ethyl-	0.084	0.081	0.066	0.065	0.242	0.250	0.124	0.171
Phenol, 4-vinyl-	0.057	0.054	0.099	0.099	0.183	0.184	0.190	0.254
Phenol, ethyl-methyl-	0.012	0.012	n/a	n/a	0.031	0.032	n/a	n/a
Guaiacols (Methoxy phenols)	**0.241**	**0.250**	**0.342**	**0.340**	**1.033**	**1.044**	**0.955**	**1.187**
Guaiacol	0.052	0.057	0.080	0.080	0.205	0.192	0.198	0.232
Guaiacol, 4-methyl-	0.018	0.017	0.021	0.021	0.062	0.064	0.050	0.062
Guaiacol, 4-ethyl-	0.046	0.046	0.040	0.041	0.155	0.156	0.082	0.107
Guaiacol, 4-vinyl-	0.056	0.057	0.106	0.107	0.224	0.229	0.219	0.286
Guaiacol, 4-allyl-; (Eugenol)	n/a	n/a	n/a	n/a	0.035	0.034	0.025	0.036
Guaiacol, 4-propenyl- cis (Isoeugenol)	n/a	n/a	n/a	n/a	0.074	0.074	0.056	0.075
Guaiacol, 4-propenyl-(trans) (Isoeugenol)	0.069	0.072	0.095	0.092	0.278	0.294	0.252	0.313
Guaiacyl acetone	n/a	n/a	n/a	n/a	n/a	n/a	0.073	0.078
Syringols (Dimethoxy phenols)	**0.046**	**0.046**	**0.128**	**0.123**	**0.469**	**0.489**	**0.498**	**0.659**
Syringol	0.025	0.024	0.043	0.040	0.113	0.115	0.125	0.140
Syringol, 4-methyl-	n/a	n/a	n/a	n/a	0.050	0.055	0.042	0.052
Syringol, 4-ethyl-	0.021	0.022	0.020	0.020	0.079	0.086	0.045	0.058
Syringol, 4-vinyl-	n/a	n/a	0.065	0.063	0.112	0.113	0.132	0.153
Syringol, 4-allyl-	n/a	n/a	n/a	n/a	n/a	n/a	n/a	0.072
Syringol, 4-(1-propenyl)-, cis	n/a	n/a	n/a	n/a	n/a	n/a	0.056	0.053
Syringol, 4-(1-propenyl)-, trans	n/a	n/a	n/a	n/a	0.114	0.121	0.099	0.132

CARBOHYDRATES								
Sugars	**0.000**	**0.000**	**0.000**	**0.000**	**0.960**	**0.993**	**1.382**	**1.408**
Anhydro-ß-D-glucopyranose, 1,6- (Levoglucosan)	n/a	n/a	n/a	n/a	0.960	0.993	1.145	1.162
Dianhydro-α-D-mannopyranose, 1,4:3,6-	n/a	n/a	n/a	n/a	n/a	n/a	0.237	0.247
OTHER ORGANIC COMPOUNDS								
N-compounds	**0.000**	**0.000**	**0.000**	**0.000**	**0.283**	**0.282**	**0.158**	**0.141**
Oxazole, 4,5-dihydro-2,4,4-trimethyl- (NIST MQ 82)	n/a	n/a	n/a	n/a	0.128	0.126	0.093	0.080
2H-Imidazole, 2,2,4,5-tetramethyl- (NIST MQ 80)	n/a	n/a	n/a	n/a	0.108	0.110	0.047	0.040
unknown N-Compound (no NIST spectrum found)	n/a	n/a	n/a	n/a	0.047	0.045	0.018	0.022
Acetates	**0.000**	**0.000**	**0.000**	**0.000**	**0.000**	**0.000**	**0.000**	**0.000**
Terpenes	**0.000**	**0.000**	**0.000**	**0.000**	**0.000**	**0.000**	**0.000**	**0.000**
unknown compounds	**0.000**	**0.000**	**0.000**	**0.000**	**0.000**	**0.000**	**0.000**	**0.000**
Miscellaneous	**0.000**	**0.000**	**0.000**	**0.000**	**0.000**	**0.000**	**0.000**	**0.000**

Table B9. GC-MS data for aqueous condensate (AC) recovered using ethanol as the quench at quench-to-volatiles mass flow rate ratios (m_q/m_v) of 0.5 and 2.0.

	wt.% (wet)							
	$m_q/m_v - 2.0$				$m_q/m_v - 0.5$			
NONAROMATIC COMPOUNDS	**Run 1**	**Run 2**	**Run 3**	**Run 4**	**Run 1**	**Run 2**	**Run 3**	**Run 4**
Acids	**0.219**	**0.218**	**0.279**	**0.279**	**0.304**	**0.310**	**0.875**	**0.872**
Acetic acid	0.219	0.218	0.279	0.279	0.304	0.310	0.525	0.523
Propionic acid	n/a	n/a	n/a	n/a	n/a	n/a	0.349	0.349
Nonaromatic Esters	**0.000**	**0.000**	**0.048**	**0.049**	**0.012**	**0.012**	**0.065**	**0.063**
Propanoic acid, 2-oxo-, ethyl ester (NIST MQ 92)			0.048	0.049	0.012	0.012	0.065	0.063
Nonaromatic Alcohols	**72.084**	**72.084**	**68.751**	**68.752**	**52.827**	**52.827**	**44.537**	**44.536**
2-Propen-1-ol (NIST MQ 91)	0.006	0.006	0.008	0.008	0.026	0.026	0.032	0.031
Ethanol	72.077		68.743		52.802		44.506	
Nonaromatic Aldehydes	**0.072**	**0.073**	**0.102**	**0.106**	**0.223**	**0.218**	**0.199**	**0.197**
Butanal	0.031	0.031	0.030	0.030	0.060	0.058	0.041	0.040
Crotonaldehyde, cis	0.016	0.016	0.035	0.036	0.071	0.070	0.079	0.078
Crotonaldehyde, trans	0.013	0.014	0.014	0.016	0.032	0.031	0.027	0.027
Butanal, 3-methyl- (NIST MQ 87)	n/a	n/a	0.006	0.006	0.011	0.011	0.010	0.010
2-Butenal, 2-methyl- (NIST MQ 92)	0.012	0.012	0.011	0.011	0.030	0.030	0.025	0.024
2-Pentenal, (E)- (NIST MQ 89)	n/a	n/a	0.006	0.006	0.019	0.019	0.019	0.018
Nonaromatic Ketones	**1.633**	**1.615**	**1.725**	**1.696**	**2.207**	**2.182**	**2.607**	**2.597**
2-Pentanone, 4-hydroxy-4-methyl- = Diacetone alcohol = impurity of Acetone	0.003	0.003	n/a	n/a	n/a	n/a	n/a	n/a
Acetol (Hydroxypropanone)	0.217	0.216	0.402	0.397	0.426	0.423	0.880	0.872
Butanone, 2-	1.019	1.023	0.908	0.888	0.716	0.702	0.548	0.548
Butanone, 1-hydroxy-2-	0.030	0.029	0.044	0.043	0.075	0.074	0.166	0.169
Butandione, 2,3- (Diacetyl)	0.059	0.040	0.046	0.044	0.122	0.128	0.133	0.141
Acetoin (Hydroxy-2-butanone, 3-)	n/a	n/a	n/a	n/a	0.037	0.036	0.111	0.039
Propan-2-one, 1-acetyloxy-	n/a	n/a	0.012	0.012	0.016	0.016	0.025	0.023
Cyclopentanone	0.030	0.030	0.028	0.027	0.088	0.087	0.078	0.077
Cyclopenten-1-one, 2-	0.044	0.043	0.047	0.047	0.136	0.134	0.164	0.163
Cyclopenten-1-one, 2,3-dimethyl-2-	0.005	0.005	0.003	0.003	0.007	0.007	0.011	0.011
Cyclopenten-1-one, 2-methyl-2-	0.020	0.020	0.020	0.020	0.067	0.067	0.074	0.074
Cyclopenten-1-one, 3-methyl-2-	0.007	0.007	0.006	0.006	0.013	0.013	0.017	0.017
Cyclohexen-1-one, 2-					n/a	n/a	0.003	0.003
3-Buten-2-one (NIST MQ 88)	0.018	0.018	0.037	0.036	0.038	0.038	0.047	0.046
Butanal, 2-methyl- (NIST MQ 94)	n/a	n/a	n/a	n/a	0.011	0.011	0.007	0.007
Butanone, 3-methyl-2- (NIST MQ 88)	0.041	0.041	0.037	0.035	0.039	0.038	0.028	0.028
3-Buten-2-one, 3-methyl- (NIST MQ 88)	0.020	0.020	0.020	0.021	0.039	0.038	0.033	0.033
1-Penten-3-one (NIST MQ 84)	0.005	0.005	0.008	0.008	0.012	0.012	n/a	n/a
2-Pentanone (NIST MQ 94)	0.022	0.022	0.019	0.018	0.052	0.051	0.036	0.036
3-Pentanone (NIST MQ 92)	0.015	0.015	0.012	0.012	0.035	0.034	0.024	0.024
2,3-Pentanedione	0.028	0.028	0.031	0.031	0.079	0.077	0.081	0.082

3-Penten-2-one (NIST MQ 84)	0.022	0.022	0.019	0.021	0.064	0.063		0.064
3-Hexanone (NIST MQ 94)	0.004	0.004	n/a	n/a	0.008	0.008		
2,3-Hexanedione (NIST MQ 78)	0.003	0.003	n/a	n/a	0.011	0.011	0.010	0.011
2-Hexanone (NIST MQ 92)	n/a	n/a	n/a	n/a	0.012	0.011	0.010	0.009
3,4-Hexanedione (NIST MQ 89)	n/a	n/a	n/a	n/a	0.006	0.006	0.005	0.006
Cyclopentanone, 2-methyl- (NIST MQ 87)	0.008	0.008	0.008	0.008	0.027	0.027	0.025	0.026
3-Hexen-2-one (NIST MQ 85)							0.007	0.007
Cyclopentanone, 3-methyl- (NIST MQ 92)	n/a	n/a	0.004	0.004	0.011	0.011	0.012	0.013
Isomere of 2-Cyclopenten-1-one, 3-methyl-	n/a	n/a	0.005	0.005	0.018	0.018	0.021	0.020
2-Butanone, 1-hydroxy-3-methyl- (NIST MQ 78)							0.005	0.005
3-Heptanone, 5-methyl- (NIST MQ 92)	0.006	0.006	n/a	n/a	n/a	n/a	n/a	n/a
2-Cyclopenten-1-one, x,y-dimethyl-	0.004	0.004	0.004	0.004	0.019	0.018	0.018	0.012
Isomere of Cyclopenten-1-one, 2,3-dimethyl-2-	0.003	0.003	0.004	0.004	0.012	0.012	0.015	0.015
Aliphatic Hydrocarbons	**0.033**	**0.033**	**0.004**	**0.004**	**0.000**	**0.000**	**0.000**	**0.000**
Tetradecane, n-	0.005	0.005	0.000	0.000	n/a	n/a	n/a	n/a
1-Decene	n/a	n/a	0.004	0.004	n/a	n/a	n/a	n/a
Pentadecane, n-	0.001	0.001	n/a	n/a	n/a	n/a	n/a	n/a
1-Undecene	0.003	0.003	n/a	n/a	n/a	n/a	n/a	n/a
Naphthalene, decahydro-2-methyl- (NIST MQ 86)	0.002	0.002	n/a	n/a	n/a	n/a	n/a	n/a
unknown aliphatic compound (C13H28) MW=184	0.007	0.007	n/a	n/a	n/a	n/a	n/a	n/a
unknown aliphatic compound MW=?	0.002	0.002	n/a	n/a	n/a	n/a	n/a	n/a
unknown aliphatic compound MW=?	0.007	0.007	n/a	n/a	n/a	n/a	n/a	n/a
unknown aliphatic compound MW=?	0.004	0.004	n/a	n/a	n/a	n/a	n/a	n/a
Heptadecane, 2,6,10,14-tetramethyl- (NIST MQ 88)	0.002	0.002	n/a	n/a	n/a	n/a	n/a	n/a
HETEROCYCLIC COMPOUNDS								
Furans	**0.040**	**0.040**	**0.076**	**0.076**	**0.194**	**0.191**	**0.295**	**0.294**
Furaldehyde, 2-	0.038	0.037	0.053	0.053	0.142	0.140	0.197	0.198
Furaldehyde, 3-	n/a	n/a	0.005	0.005	0.016	0.015	0.022	0.022
Furaldehyde, 5-methyl-2-					0.006	0.006	0.009	0.008
Ethanone, 1-(2-furanyl)-	0.003	0.003	0.006	0.006	0.011	0.011	0.017	0.017
Butyrolactone, γ-	n/a	n/a	0.009	0.009	0.013	0.013	0.019	0.019
Furaldehyde diethyl acetal, 2-,	n/a	n/a	0.003	0.004	0.005	0.005	0.004	0.004
Furan, 2-ethoxytetrahydro- (NIST MQ 87)	n/a	n/a	n/a	n/a	n/a	n/a	0.012	0.011
Furan, 2,5-diethoxytetrahydro- ; cis (NIST MQ 88)	n/a	n/a	n/a	n/a	n/a	n/a	0.005	0.005
Furan, 2,5-diethoxytetrahydro- ; trans (NIST MQ 82)	n/a	n/a	n/a	n/a	n/a	n/a	0.010	0.010
Pyrans	**0.000**	**0.000**	**0.000**	**0.000**	**0.000**	**0.000**	**0.000**	**0.000**
AROMATIC COMPOUNDS								
Benzenes	**0.073**	**0.074**	**0.071**	**0.069**	**0.104**	**0.101**	**0.064**	**0.064**
Benzene	0.004	0.005	0.009	0.009	0.006	0.005	0.004	0.004
Toluene	0.026	0.026	0.022	0.021	0.027	0.026	0.017	0.016
Toluene, 2-ethyl-	0.001	0.001	n/a	n/a	0.002	0.002	n/a	n/a

Toluene, 3-ethyl-	0.003	0.003	n/a	n/a	0.005	0.004	n/a	n/a
Toluene, 4-ethyl-	0.002	0.002	0.002	0.002	0.002	0.002	n/a	n/a
Xylene, m- (Benzene, 1,3-dimethyl-)	0.007	0.008	0.006	0.006	0.009	0.008	0.006	0.005
Xylene, p- (Benzene, 1,4-dimethyl-)	0.004	0.004	0.003	0.003	0.004	0.004	0.002	0.002
Xylene, o- (Benzene, 1,2-dimethyl-)	0.003	0.003	0.003	0.003	0.004	0.004	0.002	0.002
Benzene, ethyl-	0.010	0.011	0.009	0.009	0.012	0.012	n/a	n/a
Benzene, 1,3,5-trimethyl-					0.004	0.003	n/a	n/a
Benzene, 1,2,4-trimethyl-	0.002	0.002	0.002	0.002	0.004	0.004	0.003	0.003
Benzene, 1,2,3-trimethyl-	n/a	n/a	0.001	0.001	n/a	n/a	n/a	n/a
Benzene, propyl-	0.001	0.001	n/a	n/a	n/a	n/a	n/a	n/a
Benzofuran	n/a	n/a	0.001	0.001	0.003	0.003	n/a	n/a
Styrene	0.004	0.004	0.006	0.005	0.008	0.008	0.014	0.015
Benzene, 1-methoxy-4-methyl-					0.004	0.004	0.005	0.005
Naphthalene					0.001	0.002	0.002	0.002
Indene	0.004	0.004	0.004	0.004	0.009	0.009	0.009	0.009
Benzene, ethyl-methyl-	n/a	n/a	0.003	0.003	n/a	n/a	n/a	n/a
Catechols	**0.000**	**0.000**	**0.000**	**0.000**	**0.000**	**0.000**	**0.000**	**0.000**
Aromatic Alcohols	**0.000**	**0.000**	**0.000**	**0.000**	**0.000**	**0.000**	**0.000**	**0.000**
Aromatic Aldehydes	**0.000**	**0.000**	**0.002**	**0.002**	**0.009**	**0.008**	**0.010**	**0.010**
Benzaldehyde	n/a	n/a	0.002	0.002	0.009	0.008	0.010	0.010
Aromatic Ketones	**0.000**	**0.000**	**0.000**	**0.000**	**0.000**	**0.000**	**0.000**	**0.000**
Aromatic Esters	**0.000**	**0.000**	**0.000**	**0.000**	**0.000**	**0.000**	**0.000**	**0.000**
Lignin-derived Phenols	**0.006**	**0.005**	**0.003**	**0.003**	**0.010**	**0.010**	**0.016**	**0.016**
Phenol	0.006	0.005	0.003	0.003	0.006	0.006	0.011	0.011
Cresol, o-					0.004	0.004	0.005	0.005
Guaiacols (Methoxy phenols)	**0.005**	**0.005**	**0.006**	**0.006**	**0.009**	**0.009**	**0.025**	**0.025**
Guaiacol	0.005	0.005	0.006	0.006	0.009	0.009	0.019	0.019
Guaiacol, 4-methyl-	n/a	n/a	n/a	n/a	n/a	n/a	0.004	0.003
Guaiacol, 4-ethyl-	n/a	n/a	n/a	n/a	n/a	n/a	0.003	0.002
Syringols (Dimethoxy phenols)	**0.000**	**0.000**	**0.000**	**0.000**	**0.000**	**0.000**	**0.000**	**0.000**
CARBOHYDRATES								
Sugars	**0.000**	**0.000**	**0.000**	**0.000**	**0.000**	**0.000**	**0.000**	**0.000**
OTHER ORGANIC COMPOUNDS								
N-compounds	**0.023**	**0.022**	**0.012**	**0.012**	**0.036**	**0.036**	**0.014**	**0.015**
Propanenitrile (NIST MQ 94)	0.007	0.006	n/a	n/a	0.009	0.010	0.006	0.007
Propanenitrile, 2-methyl- (NIST MQ 88)	n/a	n/a	n/a	n/a	0.004	0.004	0.003	0.003
1H-Pyrrole, 1-methyl- (NIST MQ 82)	0.004	0.004	0.002	0.002	0.004	0.003	0.006	0.005

Butanenitrile, 3-methyl- (NIST MQ 87)	0.002	0.002	0.003	0.003	0.006	0.006	n/a	n/a
Pyrrole	0.010	0.010	0.007	0.007	0.013	0.013	n/a	n/a
Acetates	**0.000**	**0.000**	**0.000**	**0.000**	**0.000**	**0.000**	**0.000**	**0.000**
Terpenes	**0.005**	**0.005**	**0.005**	**0.004**	**0.004**	**0.003**	**0.002**	**0.002**
D-Limonene (NIST MQ 94)	0.002	0.002	0.002	0.002	0.004	0.003	0.002	0.002
2-Acetyl-5-norbornene (NIST MQ 92)	0.003	0.003	0.002	0.002	n/a	n/a		
unknown compounds	**0.000**	**0.000**	**0.000**	**0.000**	**0.000**	**0.000**	**0.000**	**0.000**
Miscellaneous	**0.005**	**0.006**	**0.025**	**0.025**	**0.138**	**0.135**	**0.321**	**0.318**
Acetaldehyde diethyl acetal	0.005	0.006	0.023	0.023	0.117	0.115	0.258	0.255
Ethane, 1-ethoxy-1-methoxy- (NIST MQ 94)	n/a	n/a	n/a	n/a	0.002	0.002	0.007	0.007
Propane, 1,1-diethoxy- (NIST MQ 92)	n/a	n/a	n/a	n/a	0.018	0.018	0.033	0.033
Propane, 2,2-diethoxy- (NIST MQ 90)	n/a	n/a	0.003	0.002	n/a	n/a	n/a	n/a
poss: 1,4-Dioxin, 2,3-dihydro-	n/a	n/a	n/a	n/a	n/a	n/a	0.003	0.003
Butane, 1,1-diethoxy- (NIST MQ 88)	n/a	n/a	n/a	n/a	n/a	n/a	0.020	0.019

Table B10. GC-MS data for organic-rich condensate (ORC) obtained using Isopar-V as the quench at quench-to-volatiles mass flow rate ratios (m_q/m_v) of 0.5 and 2.0.

	wt.% (wet)							
	$m_q/m_v - 2.0$				$m_q/m_v - 0.5$			
NONAROMATIC COMPOUNDS	**Run 1**	**Run 2**	**Run 3**	**Run 4**	**Run 1**	**Run 2**	**Run 3**	**Run 4**
Acids	**9.741**	**9.687**	**10.019**	**9.900**	**9.615**	**9.560**	**9.092**	**10.784**
Acetic acid	4.941	4.873	5.106	4.988	4.804	4.751	4.375	5.816
Propionic acid	4.800	4.814	4.913	4.912	4.811	4.809	4.717	4.968
Nonaromatic Esters	**0.000**	**0.000**	**0.000**	**0.000**	**0.000**	**0.000**	**0.000**	**0.000**
Nonaromatic Alcohols	**0.777**	**0.831**	**1.118**	**1.091**	**1.385**	**1.366**	**1.299**	**2.370**
Ethylene glycol	0.777	0.831	1.118	1.091	1.385	1.366	1.299	2.370
Nonaromatic Aldehydes	**0.000**	**0.000**	**0.000**	**0.000**	**0.000**	**0.000**	**0.000**	**0.000**
Nonaromatic Ketones	**5.530**	**5.372**	**5.406**	**5.348**	**6.462**	**6.443**	**4.767**	**7.394**
Acetol (Hydroxypropanone)	2.400	2.392	1.757	1.717	2.682	2.703	2.191	3.191
Butanone, 2-	0.043	0.043	0.057	0.053	0.050	0.052	0.043	0.062
Butanone, 1-hydroxy-2-	0.592	0.584	0.567	0.562	0.640	0.631	0.507	0.737
Propan-2-one, 1-acetyloxy-	0.092	0.087	0.069	0.068	0.100	0.096	0.063	0.116
Cyclopentanone	0.108	0.108	0.134	0.132	0.129	0.129	0.119	0.164
Cyclopenten-1-one, 2-	0.269	0.260	0.250	0.249	0.311	0.301	0.235	0.413
Cyclopenten-1-one, 2,3-dimethyl-2-	0.315	0.499	0.413	0.359	0.360	0.373	0.213	0.332
Cyclopenten-1-one, 2-methyl-2-	0.152	0.146	0.204	0.201	0.188	0.184	0.138	0.233
Cyclopenten-1-one, 3-methyl-2-	0.372	0.364	0.461	0.452	0.416	0.406	0.312	0.510
Cylopenten-1-one, 3-ethyl-2-	0.096	0.093	0.121	0.119	0.119	0.115		
Cyclopenten-1-one, 2-hydroxy-3-methyl-2-	0.910	0.614	1.031	1.103	1.192	1.181	0.783	1.360
Isomere of Cyclopenten-1-one, 2,3-dimethyl-2-	0.044	0.043	0.053	0.051	0.060	0.059	0.043	0.074
Isomer of Cyclopenten-1-one, 3-ethyl-2-hydroxy-	0.137	0.140	0.162	0.160	0.170	0.170	0.119	0.202
Aliphatic Hydrocarbons	**0.281**	**0.512**	**0.338**	**0.329**	**0.510**	**0.544**	**2.748**	**4.708**
Tetradecane, n-	0.003	0.090	0.097	0.096	0.080	0.091	0.627	1.144
Pentadecane, n-	0.051	0.080	0.042	0.031	0.078	0.081	0.280	0.483
Undecane, 2,6-dimethyl- (NIST MQ 88)	0.063	0.093	0.059	0.059	0.084	0.088	0.248	0.415
Heptane, 1-cyclohexyl- (NIST MQ 84)	0.044	0.060	0.040	0.043	0.056	0.060	0.150	0.248
Dodecane, 2,6,10-trimethyl- (NIST MQ 88)	0.068	0.103			0.099	0.105	0.323	0.540
Heptadecane, 2,6,10,14-tetramethyl- (NIST MQ 88)	0.053	0.086	0.044	0.043	0.085	0.089	0.300	0.494
HETEROCYCLIC COMPOUNDS								
Furans	**1.329**	**1.283**	**0.961**	**0.971**	**1.344**	**1.300**	**0.834**	**1.289**
Furfuryl alcohol, 2-	0.138	0.134	0.143	0.146	0.139	0.129	0.100	0.178
Furanone, 2(5H)-	0.351	0.333	n/a	n/a	0.341	0.334	0.249	0.362
Furaldehyde, 2-	0.163	0.158	n/a	n/a	0.171	0.168	0.151	0.183
Ethanone, 1-(2-furanyl)-	0.031	0.030	0.034	0.033	0.039	0.038	0.026	0.048
Furan-2-one, 3-methyl-, (5H)-	0.083	0.077	0.081	0.077	0.082	0.080	n/a	n/a
Butyrolactone, γ-	0.427	0.401	0.453	0.472	0.432	0.412	0.309	0.518

Furan-2-one, 4-methyl-(5H)- (NIST MQ 88)	0.137	0.150	0.142	0.136	0.140	0.139	n/a	n/a
Pyrans	**0.000**	**0.000**	**0.000**	**0.000**	**0.000**	**0.000**	**0.000**	**0.000**
AROMATIC COMPOUNDS								
Benzenes	**0.043**	**0.038**	**0.085**	**0.083**	**0.000**	**0.000**	**0.013**	**0.017**
Toluene							0.013	0.017
Naphthalenol, 2-	n/a	n/a	0.036	0.037				
Inden-1-one, 2,3-dihydro-1H-	0.043	0.038	0.049	0.047				
Catechols	**n.q.**	**n.q.**	**n.q.**	**n.q.**	n.q.	n.q.	n.q.	n.q.
Hydroquinone (Benzene, 1,4-dihydroxy-)	n.q.	n.q.	n.q.	n.q.	n.q.	n.q.	n.q.	n.q.
Benzenediol, methyl-	n.q.	n.q.	n.q.	n.q.	n.q.	n.q.	n.q.	n.q.
Aromatic Alcohols	**0.000**	**0.000**	**0.000**	**0.000**	**0.000**	**0.000**	**0.000**	**0.000**
Aromatic Aldehydes	**0.000**	**0.000**	**0.000**	**0.000**	**0.000**	**0.000**	**0.000**	**0.000**
Aromatic Ketones	**0.000**	**0.000**	**0.000**	**0.000**	**0.000**	**0.000**	**0.000**	**0.000**
Aromatic Esters	**0.000**	**0.000**	**0.000**	**0.000**	**0.000**	**0.000**	**0.000**	**0.000**
Lignin-derived Phenols	**3.565**	**3.428**	**3.993**	**3.891**	**3.673**	**3.627**	**2.250**	**3.816**
Phenol	0.649	0.628	0.765	0.745	0.641	0.632	0.522	0.895
Cresol, o-	0.365	0.332	0.425	0.435	0.434	0.410	n/a	n/a
Cresol, p-	0.213	0.214	0.247	0.241	0.230	0.221	0.198	0.349
Cresol, m-	0.285	0.280	0.353	0.338	0.294	0.295	0.208	0.349
Phenol, 2,5-dimethyl-	0.128	0.120	0.135	0.131	0.136	0.136	n/a	n/a
Phenol, 2,4-dimethyl-	0.067	0.070	0.083	0.078	0.091	0.098	n/a	n/a
Phenol, 3,5-dimethyl-	0.027	0.025	n/a	n/a	0.029	0.028	n/a	n/a
Phenol, 2-ethyl-	0.030	0.030	0.033	0.032	n/a	n/a	n/a	n/a
Phenol, 3-ethyl-	0.144	0.141	0.167	0.161	0.143	0.146	n/a	n/a
Phenol, 4-ethyl-	0.462	0.445	0.668	0.652	0.513	0.505	0.397	0.664
Phenol, 4-vinyl-	1.068	1.018	0.868	0.844	1.021	1.012	0.854	1.438
Phenol, trans 4-propenyl-	0.080	0.078	0.075	0.074	0.078	0.077	0.071	0.122
Phenol, ethyl-methyl-	0.049	0.048	0.066	0.061	0.064	0.065	n/a	n/a
Guaiacols (Methoxy phenols)	**2.965**	**2.859**	**3.404**	**3.280**	**4.287**	**4.262**	**3.215**	**4.874**
Guaiacol	0.336	0.325	0.331	0.324	0.466	0.459	0.271	0.474
Guaiacol, 4-methyl-	0.112	0.113	0.110	0.107	0.165	0.162	0.129	0.221
Guaiacol, 4-ethyl-	0.158	0.154	0.215	0.207	0.242	0.239	0.172	0.294
Guaiacol, 4-vinyl-	0.632	0.604	0.565	0.549	0.920	0.905	0.603	1.022
Guaiacol, 4-allyl-; (Eugenol)	0.070	0.069	0.066	0.066	0.095	0.094	0.080	0.133
Guaiacol, 4-propenyl- cis (Isoeugenol)	0.206	0.161	0.190	0.152	0.274	0.274	0.191	0.318
Guaiacol, 4-propenyl-(trans) (Isoeugenol)	0.734	0.727	0.798	0.775	0.974	0.970	0.668	0.950
Vanillin	0.510	0.520	0.451	0.445	0.519	0.524	0.538	0.765
Ethanone, 1-(4-hydroxy-3-methoxyphenyl)- (Acetoguaiacone)	n/a	n/a	0.482	0.471	0.456	0.457	0.420	0.502
Guaiacyl acetone	0.207	0.186	0.196	0.183	0.177	0.178	0.143	0.195

Syringols (Dimethoxy phenols)	**2.323**	**2.220**	**2.122**	**2.002**	**2.447**	**2.436**	**1.390**	**2.433**
Syringol	0.534	0.482	0.473	0.395	0.497	0.481	0.279	0.616
Syringol, 4-methyl-	0.147	0.143	0.148	0.145	0.167	0.168	0.107	0.179
Syringol, 4-ethyl-	0.146	0.140	0.237	0.218	0.168	0.167	0.107	0.180
Syringol, 4-vinyl-	0.438	0.414	0.351	0.343	0.489	0.484	0.286	0.476
Syringol, 4-allyl-	0.193	0.187	0.142	0.146	0.224	0.224	0.130	0.212
Syringol, 4-propyl-	n/a	n/a	0.051	0.052	n/a	n/a	n/a	n/a
Syringol, 4-(1-propenyl)-, cis	0.115	0.116	0.107	0.106	0.128	0.129	0.081	0.131
Syringol, 4-(1-propenyl)-, trans	0.421	0.414	0.419	0.414	0.465	0.479	0.282	0.430
Syringaldehyde	0.132	0.129	n/a	n/a	0.118	0.117	n/a	n/a
Acetosyringone	0.149	0.149	0.144	0.139	0.143	0.141	0.089	0.161
Syringyl acetone	0.047	0.047	0.049	0.046	0.048	0.047	0.029	0.048
CARBOHYDRATES								
Sugars	**2.003**	**2.176**	**2.308**	**2.284**	**2.650**	**2.628**	**1.572**	**2.150**
Anhydro-ß-D-glucopyranose, 1,6- (Levoglucosan)	1.218	1.283	1.399	1.402	1.642	1.611	1.572	2.150
Dianhydro-α-D-mannopyranose, 1,4:3,6-	0.785	0.893	0.909	0.882	1.007	1.017	n/a	n/a
OTHER ORGANIC COMPOUNDS								
N-compounds	**0.000**	**0.000**	**0.055**	**0.053**	**0.000**	**0.000**	**0.022**	**0.052**
Oxazole, 4,5-dihydro-2,4,4-trimethyl- (NIST MQ 82)	n/a	n/a	0.038	0.037			0.022	0.052
unknown N-Compound (no NIST spectrum found)	n/a	n/a	0.017	0.016				
Acetates	**0.000**	**0.000**	**0.000**	**0.000**	**0.000**	**0.000**	**0.000**	**0.000**
Terpenes	**0.000**	**0.000**	**0.000**	**0.000**	**0.000**	**0.000**	**0.000**	**0.000**
unknown compounds	**0.000**	**0.000**	**0.000**	**0.000**	**0.000**	**0.000**	**0.000**	**0.000**
Miscellaneous	**0.000**	**0.000**	**0.000**	**0.000**	**0.000**	**0.000**	**0.000**	**0.000**

Table B11. GC-MS data for aqueous condensate (AC) recovered using Isopar-V as the quench at quench-to-volatiles mass flow rate ratios (m_q/m_v) of 0.5 and 2.0.

	wt.% (wet)							
	m_q/m_v – 2.0				m_q/m_v – 0.5			
NONAROMATIC COMPOUNDS	**Run 1**	**Run 2**	**Run 3**	**Run 4**	**Run 1**	**Run 2**	**Run 3**	**Run 4**
Acids	**2.697**	**2.725**	**2.802**	**2.872**	**3.156**	**3.256**	**3.095**	**3.093**
Acetic acid	2.005	2.035	2.220	2.275	2.453	2.551	2.390	2.392
Propionic acid	0.627	0.629	0.582	0.597	0.638	0.643	0.644	0.643
Butyric acid	0.064	0.062			0.065	0.062	0.060	0.058
Nonaromatic Esters	**0.000**	**0.000**	**0.000**	**0.000**	**0.000**	**0.000**	**0.000**	**0.000**
Nonaromatic Alcohols	**0.306**	**0.254**	**0.269**	**0.292**	**0.351**	**0.385**	**0.323**	**0.321**
Ethylene glycol	0.279	0.226	0.243	0.265	0.322	0.356	0.295	0.293
2-Propen-1-ol (NIST MQ 91)	0.028	0.028	0.027	0.028	0.029	0.028	0.028	0.028
Nonaromatic Aldehydes	**0.021**	**0.021**	**0.040**	**0.045**	**0.067**	**0.067**	**0.038**	**0.040**
Acetaldehyde, hydroxy-	n/a	n/a	n/a	n/a	0.043	0.043	0.008	0.008
Crotonaldehyde, cis	0.008	0.008	0.011	0.011	0.043	0.043	0.012	0.012
Crotonaldehyde, trans	0.013	0.014	0.013	0.014	0.010	0.010	0.014	0.014
Butenal-2-one, 3-	n/a	n/a	0.016	0.020	0.014	0.014	0.005	0.005
Nonaromatic Ketones	**3.444**	**3.461**	**4.812**	**4.976**	**5.801**	**5.804**	**4.846**	**4.882**
Acetol (Hydroxypropanone)	1.851	1.859	3.101	3.202	3.791	3.797	3.011	3.031
Butanone, 2-	0.090	0.092	0.081	0.082	0.088	0.083	0.083	0.083
Butanone, 1-hydroxy-2-	0.343	0.342	0.477	0.497	0.560	0.562	0.491	0.495
Butandione, 2,3- (Diacetyl)	0.047	0.043	0.098	0.100	0.116	0.117	0.087	0.090
Acetoin (Hydroxy-2-butanone, 3-)	n/a	n/a	n/a	n/a	0.090	0.091	0.081	0.082
Propan-2-one, 1-acetyloxy-	0.057	0.059	0.078	0.082	0.076	0.078	0.064	0.064
Cyclopentanone	0.082	0.095	0.063	0.066	0.078	0.071	0.077	0.081
Cyclopenten-1-one, 2-	0.401	0.402	0.069	0.068	0.387	0.387	0.370	0.372
Cyclopenten-1-one, 2,3-dimethyl-2-	0.036	0.040	0.340	0.352	0.040	0.038	0.038	0.035
Cyclopenten-1-one, 2-methyl-2-	0.123	0.123	0.032	0.031	0.118	0.118	0.117	0.119
Cyclopenten-1-one, 3-methyl-2-	0.101	0.101	0.103	0.106	0.091	0.092	0.089	0.090
Cyclopenten-1-one, 2-hydroxy-3-methyl-2-	0.101	0.094	0.081	0.084	0.119	0.120	0.092	0.098
Cyclohexen-1-one, 2-	0.008	0.009	0.080	0.086	0.009	0.009	0.009	0.009
3-Buten-2-one (NIST MQ 88)	0.011	0.011	0.009	0.009	0.018	0.018	0.016	0.016
Butanone, 3-methyl-2- (NIST MQ 88)	0.003	0.003	0.016	0.016	0.003	0.003	0.003	0.003
3-Buten-2-one, 3-methyl- (NIST MQ 88)	0.005	0.005	0.005	0.005	0.005	0.005	0.005	0.005
2-Pentanone (NIST MQ 94)	0.024	0.025	0.024	0.027	0.027	0.027	0.028	0.024
3-Pentanone (NIST MQ 92)	0.009	0.009	0.008	0.008	0.008	0.009	0.009	0.008
2,3-Pentanedione	0.016	0.016	0.022	0.022	0.027	0.027	0.023	0.023
3-Penten-2-one (NIST MQ 84)	0.032	0.033	0.027	0.028	0.030	0.031	0.028	0.029
Cyclopentanone, 2-methyl- (NIST MQ 87)	0.016	0.016	0.013	0.013	0.016	0.015	0.014	0.014
Isomere of 2-Cyclopenten-1-one, 3-methyl-	0.019	0.019	0.020	0.021	0.021	0.022	0.023	0.023
2-Butanone, 1-hydroxy-3-methyl- (NIST MQ 78)	0.015	0.015	0.018	0.019	0.022	0.023	0.019	0.019
2-Cyclopenten-1-one, x,y-dimethyl-	0.014	0.014	0.011	0.012	0.013	0.013	0.013	0.013
2-Cycolpenten-1-one, x,y-dimethyl-	0.009	0.009	0.009	0.009	0.011	0.010	0.011	0.011

2,5-Hexanedione (NIST MQ 89)	0.010	0.011	0.012	0.012	0.017	0.016	0.013	0.013
Isomere of Cyclopenten-1-one, 2,3-dimethyl-2-	0.021	0.017	0.018	0.018	0.021	0.021	0.020	0.020
2-Cyclopenten-1-one, x,y-dimethyl-	n/a	n/a	n/a	n/a	n/a	n/a	0.012	0.012
Aliphatic Hydrocarbons	**0.748**	**0.753**	**0.805**	**0.791**	**0.433**	**0.428**	**0.737**	**0.745**
Undecane, n-	0.006	0.006	0.006	0.006	n/a	n/a	0.004	0.004
Tetradecane, n-	0.081	0.081	0.086	0.085	0.064	0.064	0.097	0.097
Pentadecane, n-	0.010	0.010	0.012	0.011	0.010	0.010	0.016	0.016
Hexadecane, n-	n/a	n/a	n/a	n/a	n/a	n/a	0.000	0.001
Naphthalene, decahydro-, trans- (NIST MQ 92)	0.004	0.004	0.004	0.004	n/a	n/a		
Naphthalene, decahydro-2-methyl- (NIST MQ 86)	0.039	0.042	0.042	0.040	0.019	0.019	0.028	0.028
Cyclohexane, pentyl- (NIST MQ 88)	0.011	0.011	0.011	0.010	0.005	0.005	0.008	0.008
Naphthalene, decahydro-1-methyl- (NIST MQ 86)	0.039	0.040	0.038	0.037	0.016	0.016	0.027	0.027
Undecane, methyl- (NIST MQ 84)	n/a	n/a	0.029	0.028	n/a	n/a	0.023	0.024
unknown aliphatic compound MW=?	0.023	0.023	0.023	0.026	0.012	0.012	0.019	0.020
Cyclohexane, 1-methyl-2-pentyl- (NIST MQ 82)	0.025	0.026	0.024	0.024	0.014	0.013	0.019	0.019
Naphthalene, decahydro-dimethyl-	0.032	0.032	0.032	0.031	0.017	0.017	0.025	0.025
unknown aliphatic compound (C13H28) MW=184	0.175	0.176	0.177	0.174	n/a	n/a	0.142	0.142
unknown aliphatic compound MW=?	0.061	0.062	0.060	0.058	0.036	0.036	0.055	0.054
unknown aliphatic compound MW=?	0.127	0.125	0.127	0.126	0.087	0.083	0.113	0.120
Heptane, 1-cyclohexyl- (NIST MQ 84)	0.035	0.036	0.035	0.035	n/a	n/a	0.033	0.034
Tridecane, methyl-	0.028	0.027	0.028	0.027	0.019	0.020	0.029	0.030
Tridecane, 3-methyl-	n/a	n/a	n/a	n/a	n/a	n/a	0.018	0.017
Dodecane, 2,6,10-trimethyl- (NIST MQ 88)	0.051	0.051	0.051	0.048	0.036	0.036	0.055	0.055
Heptadecane, 2,6,10,14-tetramethyl- (NIST MQ 88)	n/a	n/a	0.020	0.020	n/a	n/a	0.025	0.026
HETEROCYCLIC COMPOUNDS								
Furans	**0.437**	**0.437**	**0.489**	**0.511**	**0.557**	**0.558**	**0.505**	**0.511**
Furfuryl alcohol, 2-	0.052	0.052	0.027	0.028	0.041	0.041	0.034	0.035
Furanone, 2(5H)-	0.020	0.028	0.069	0.072	0.066	0.065	0.048	0.049
Furaldehyde, 2-	0.175	0.177	0.217	0.225	0.240	0.241	0.229	0.231
Furaldehyde, 3-	0.017	0.014	0.017	0.017	0.019	0.019	0.017	0.017
Furaldehyde, 5-methyl-2-	0.020	0.020	0.026	0.026	0.030	0.029	0.024	0.024
Ethanone, 1-(2-furanyl)-	0.026	0.026	0.026	0.027	0.028	0.028	0.027	0.027
Butyrolactone, γ-	0.119	0.113	0.101	0.108	0.125	0.126	0.118	0.120
Furan, tetrahydro-2-methoxy- (NIST MQ (80)	0.007	0.007	0.007	0.008	0.008	0.008	0.008	0.009
Pyrans	**0.000**	**0.000**	**0.000**	**0.000**	**0.000**	**0.000**	**0.000**	**0.000**
AROMATIC COMPOUNDS								
Benzenes	**0.007**	**0.007**	**0.014**	**0.017**	**0.008**	**0.014**	**0.011**	**0.011**
Toluene	0.007	0.007	0.010	0.013	0.008	0.013	0.011	0.011
Xylene, m- (Benzene, 1,3-dimethyl-)	n/a	n/a	0.004	0.004	n/a	0.002	n/a	n/a
Catechols	**0.000**	**0.000**	**0.000**	**0.000**	**0.000**	**0.000**	**0.000**	**0.000**
Aromatic Alcohols	**0.000**	**0.000**	**0.000**	**0.000**	**0.000**	**0.000**	**0.000**	**0.000**

Aromatic Aldehydes	**0.002**	**0.002**	**0.003**	**0.003**	**0.002**	**0.003**	**0.004**	**0.004**
Benzaldehyde	0.002	0.002	0.003	0.003	0.002	0.003	0.004	0.004
Aromatic Ketones	**0.000**	**0.000**	**0.000**	**0.000**	**0.000**	**0.000**	**0.000**	**0.000**
Aromatic Esters	**0.000**	**0.000**	**0.000**	**0.000**	**0.000**	**0.000**	**0.000**	**0.000**
Lignin-derived Phenols	**0.209**	**0.208**	**0.151**	**0.153**	0.176	0.178	0.194	0.197
Phenol	0.143	0.143	0.133	0.135	0.116	0.117	0.132	0.132
Cresol, p-	0.022	0.024	n/a	n/a	0.022	0.023	0.023	0.025
Cresol, m-	0.023	0.021	n/a	n/a	0.020	0.020	0.020	0.020
Phenol, 4-ethyl-	0.021	0.020	0.018	0.019	0.018	0.018	0.020	0.021
Guaiacols (Methoxy phenols)	**0.114**	**0.115**	**0.107**	**0.107**	**0.107**	**0.109**	**0.101**	**0.101**
Guaiacol	0.096	0.096	0.092	0.092	0.091	0.093	0.085	0.085
Guaiacol, 4-ethyl-	0.018	0.019	0.015	0.015	0.016	0.016	0.016	0.016
Syringols (Dimethoxy phenols)	**0.004**	**0.004**	**0.004**	**0.004**	**0.005**	**0.005**	**0.004**	**0.004**
Syringol	0.004	0.004	0.004	0.004	0.005	0.005	0.004	0.004
CARBOHYDRATES								
Sugars	**0.000**	**0.000**	**0.000**	**0.000**	**0.000**	**0.000**	**0.000**	**0.000**
OTHER ORGANIC COMPOUNDS								
N-compounds	**0.399**	**0.413**	**0.031**	**0.033**	**0.054**	**0.058**	**0.040**	**0.037**
Propanenitrile (NIST MQ 94)	0.005	0.004	n/a	n/a	0.005	0.005	0.004	0.004
Oxazole, 4,5-dihydro-2,4,4-trimethyl- (NIST MQ 82)	0.311	0.322	0.025	0.027	0.040	0.044	0.027	0.027
unknown N-Compound (no NIST spectrum found)	0.084	0.087	0.006	0.006	0.009	0.009	0.009	0.006
Acetates	**0.000**	**0.000**	**0.000**	**0.000**	**0.000**	**0.000**	**0.000**	**0.000**
Terpenes	**0.000**	**0.000**	**0.000**	**0.000**	**0.000**	**0.000**	**0.000**	**0.000**
unknown compounds	**0.000**	**0.000**	**0.000**	**0.000**	**0.000**	**0.000**	**0.000**	**0.000**
Miscellaneous	**0.000**	**0.000**	**0.005**	**0.006**	**0.000**	**0.000**	**0.006**	**0.006**
poss: 1,4-Dioxin, 2,3-dihydro-	n/a	n/a	0.005	0.006			0.006	0.006

Table B12. GC-MS data for spent Isopar-V at quench-to-volatiles mass flow rate ratios (m_q/m_v) of 0.5 and 2.0.

	wt.% (wet)							
	m_q/m_v – 2.0				m_q/m_v– 0.5			
NONAROMATIC COMPOUNDS	**Run 1**	**Run 2**	**Run 3**	**Run 4**	**Run 1**	**Run 2**	**Run 3**	**Run 4**
Acids	**0.000**	**0.000**	**0.000**	**0.000**	**0.000**	**0.000**	**0.000**	**0.000**
Nonaromatic Esters	**0.000**	**0.000**	**0.000**	**0.000**	**0.000**	**0.000**	**0.000**	**0.000**
Nonaromatic Alcohols	**0.000**	**0.000**	**0.000**	**0.000**	**0.000**	**0.000**	**0.000**	**0.000**
Nonaromatic Aldehydes	**0.000**	**0.000**	**0.000**	**0.000**	**0.000**	**0.000**	**0.000**	**0.000**
Nonaromatic Ketones	**0.000**	**0.000**	**0.000**	**0.000**	**0.000**	**0.000**	**0.000**	**0.000**
Aliphatic Hydrocarbons	**15.239**	**15.082**	**14.665**	**15.577**	**14.433**	**14.928**	**15.966**	**17.587**
Tetradecane, n-	3.697	3.654	3.687	3.907	3.689	3.822	3.783	4.176
Pentadecane, n-	1.384	1.366	1.373	1.463	1.415	1.460	1.446	1.602
Hexadecane, n-	0.346	0.346	0.353	0.377	0.366	0.378	0.376	0.421
Heptadecane, n-	0.131	0.124	0.164	0.134	0.139	0.140	0.147	0.149
Octadecane, n-	n/a	n/a	n/a	n/a			0.029	0.032
Naphthalene, decahydro-2-methyl- (NIST MQ 86)	0.177	0.176	0.176	0.184	0.131	0.136	0.129	0.143
Cyclohexane, pentyl- (NIST MQ 88)	0.045	0.044	0.044	0.046	0.034	0.036	0.034	0.037
Naphthalene, decahydro-1-methyl- (NIST MQ 86)	0.161	0.159	0.158	0.189	0.119	0.123	0.118	0.131
Undecane, methyl- (NIST MQ 84)					n/a	n/a	0.137	0.152
unknown aliphatic compound MW=?	0.145	0.143	0.144	0.152	n/a	n/a	0.119	0.131
1-Dodecene					n/a	n/a	0.164	0.180
Cyclohexane, 1-methyl-2-pentyl- (NIST MQ 82)	0.155	0.153	0.152	0.161	0.130	0.134	0.133	0.146
Naphthalene, decahydro-dimethyl-	0.188	0.187	0.186	0.199	0.160	0.169	0.166	0.183
Undecane, 2,6-dimethyl- (NIST MQ 88)	n/a	n/a	n/a	n/a	1.179	1.224	1.192	1.313
unknown aliphatic compound (C13H28) MW=184	1.349	1.331	1.333	1.408	n/a	n/a	n/a	n/a
unknown aliphatic compound MW=?	0.703	0.700	0.696	0.745	0.661	0.678	0.674	0.731
unknown aliphatic compound MW=?	1.555	1.559	1.539	1.676	1.452	1.508	1.494	1.655
Heptane, 1-cyclohexyl- (NIST MQ 84)	0.712	0.698	0.710	0.764	0.686	0.702	0.682	0.761
Tridecane, methyl-	0.775	0.760	0.772	0.816	0.763	0.783	0.777	0.857
Tridecane, 3-methyl-							0.541	0.596
Dodecane, 2,6,10-trimethyl- (NIST MQ 88)	1.577	1.556	1.578	1.661	1.563	1.617	1.595	1.744
Heptadecane, 2,6,10,14-tetramethyl- (NIST MQ 88)	1.462	1.446	1.459	1.543	1.480	1.535	1.517	1.670
Tetradecane, 3-methyl- (NIST MQ 84)	0.305	0.308	n/a	n/a	0.319	0.329	0.314	0.345
Cyclohexane, nonyl- (NIST MQ 88)	0.142	0.142	0.141	0.152	0.149	0.154	0.150	0.168
unknown aliphatic chain (MW=?)	0.228	0.228	n/a	n/a	n/a	n/a	0.248	0.264
HETEROCYCLIC COMPOUNDS								
Furans	**0.000**	**0.000**	**0.000**	**0.000**	**0.000**	**0.000**	**0.000**	**0.000**
Pyrans	**0.000**	**0.000**	**0.000**	**0.000**	**0.000**	**0.000**	**0.000**	**0.000**

AROMATIC COMPOUNDS								
Benzenes	**0.007**	**0.007**	**0.000**	**0.000**	**0.009**	**0.010**	**0.000**	**0.000**
Toluene	0.007	0.007			0.009	0.010		
Catechols	**0.000**	**0.000**	**0.000**	**0.000**	**0.000**	**0.000**	**0.000**	**0.000**
Aromatic Alcohols	**0.000**	**0.000**	**0.000**	**0.000**	**0.000**	**0.000**	**0.000**	**0.000**
Aromatic Aldehydes	**0.000**	**0.000**	**0.000**	**0.000**	**0.000**	**0.000**	**0.000**	**0.000**
Aromatic Ketones	**0.000**	**0.000**	**0.000**	**0.000**	**0.000**	**0.000**	**0.000**	**0.000**
Aromatic Esters	**0.000**	**0.000**	**0.000**	**0.000**	**0.000**	**0.000**	**0.000**	**0.000**
Lignin-derived Phenols	**0.000**	**0.000**	**0.000**	**0.000**	**0.000**	**0.000**	**0.000**	**0.000**
Guaiacols (Methoxy phenols)	**0.000**	**0.000**	**0.000**	**0.000**	**0.000**	**0.000**	**0.000**	**0.000**
Syringols (Dimethoxy phenols)	**0.000**	**0.000**	**0.000**	**0.000**	**0.000**	**0.000**	**0.000**	**0.000**
CARBOHYDRATES								
Sugars	**0.000**	**0.000**	**0.000**	**0.000**	**0.000**	**0.000**	**0.000**	**0.000**
OTHER ORGANIC COMPOUNDS								
N-compounds	**0.000**	**0.000**	**0.000**	**0.000**	**0.000**	**0.000**	**0.000**	**0.000**
Acetates	**0.000**	**0.000**	**0.000**	**0.000**	**0.000**	**0.000**	**0.000**	**0.000**
Terpenes	**0.000**	**0.000**	**0.000**	**0.000**	**0.000**	**0.000**	**0.000**	**0.000**
unknown compounds	**0.000**	**0.000**	**0.000**	**0.000**	**0.000**	**0.000**	**0.000**	**0.000**
Miscellaneous	**0.000**	**0.000**	**0.000**	**0.000**	**0.000**	**0.000**	**0.000**	**0.000**

Table B13. GC-MS data for organic-rich condensate (ORC) obtained using water as the quench at quench-to-volatiles mass flow rate ratios (m_q/m_v) of 0.5 and 2.0.

	wt.% (wet)							
	$m_q/m_v - 2.0$				$m_q/m_v - 0.5$			
NONAROMATIC COMPOUNDS	**Run 1**	**Run 2**	**Run 3**	**Run 4**	**Run 1**	**Run 2**	**Run 3**	**Run 4**
Acids	**2.998**	**3.132**	**n/a**	**n/a**	**3.368**	**3.352**	**3.490**	**3.474**
Acetic acid	2.998	3.132	n/a	n/a	3.368	3.352	3.490	3.474
Nonaromatic Esters	**0.000**	**0.000**	**0.000**	**0.000**	**0.000**	**0.000**	**0.000**	**0.000**
Nonaromatic Alcohols	**0.000**	**0.000**	**0.000**	**0.000**	**0.000**	**0.000**	**0.000**	**0.000**
Nonaromatic Aldehydes	**0.000**	**0.000**	**0.000**	**0.000**	**0.000**	**0.000**	**0.000**	**0.000**
			0.000	**0.000**				
Nonaromatic Ketones	**2.641**	**2.675**	**1.625**	**1.561**	**3.325**	**3.347**	**3.687**	**3.745**
2-Pentanone, 4-hydroxy-4-methyl- = Diacetone alcohol = impurity of Acetone	0.061	n/a	n/a	n/a	n/a	n/a	n/a	n/a
Acetol (Hydroxypropanone)	0.790	0.782	n/a	n/a	0.921	0.917	1.204	1.218
Butanone, 2-					0.051	0.050	0.036	0.040
Butanone, 1-hydroxy-2-	n/a	n/a	n/a	n/a	n/a	n/a	0.279	0.335
Cyclopentanone	0.066	0.067	n/a	n/a	0.080	0.080	0.068	0.067
Cyclopenten-1-one, 2-	0.181	0.176	0.134	0.136	0.239	0.255	0.220	0.218
Cyclopenten-1-one, 2,3-dimethyl-2-	0.107	0.097	0.039	0.050	0.158	0.170	0.117	0.116
Cyclopenten-1-one, 2-methyl-2-	0.141	0.151	0.137	0.136	0.200	0.205	0.151	0.151
Cyclopenten-1-one, 3-methyl-2-	0.231	0.239	0.236	0.208	0.328	0.356	0.279	0.280
Cylopenten-1-one, 3-ethyl-2-	0.100	0.105	0.099	0.098	0.129	0.132	0.094	0.091
Cyclopenten-1-one, 2-hydroxy-3-methyl-2-	0.498	0.558	0.516	0.492	0.694	0.657	0.827	0.823
Isomere of Cyclopenten-1-one, 2,3-dimethyl-2-	0.051	0.052	0.049	0.048	0.059	0.062	0.045	0.046
2-Cyclopenten-1-one, x,y-dimethyl-	0.052	0.054	0.051	0.049	0.066	0.069	0.021	0.023
2-Cyclopenten-1-one, 2,3,4-trimethyl- (NIST MQ 88)	0.045	0.047	0.046	0.043	0.053	0.052	n/a	n/a
Isomer of Cyclopenten-1-one, 3-ethyl-2-hydroxy-	0.091	0.095	0.086	0.085	0.127	0.129	0.116	0.117
2-Heptadecanone (NIST MQ 84)	0.201	0.223	0.232	0.215	0.220	0.213	0.165	0.155
Aliphatic Hydrocarbons	**0.000**	**0.000**	**0.000**	**0.000**	**0.000**	**0.000**	**0.000**	**0.000**
HETEROCYCLIC COMPOUNDS								
Furans	**0.000**	**0.000**	**0.079**	**0.078**	**0.173**	**0.173**	**0.206**	**0.206**
Ethanone, 1-(2-furanyl)-	n/a	n/a	n/a	n/a	n/a	n/a	0.014	0.014
Butyrolactone, γ-	n/a	n/a	0.079	0.078	0.173	0.173	0.191	0.192
Pyrans	**0.000**	**0.000**	**0.000**	**0.000**	**0.000**	**0.000**	**0.000**	**0.000**
AROMATIC COMPOUNDS								
Benzenes	**0.090**	**0.090**	**0.136**	**0.129**	**0.097**	**0.096**	**0.072**	**0.072**
Naphthalenol, 2-	n/a	n/a	0.043	0.043	0.097	0.096	0.072	0.072
Inden-1-one, 2,3-dihydro-1H-	0.090	0.090	0.093	0.086				

Catechols	**n.q.**	**n.q.**	**n.q.**	**n.q.**	n.q.	n.q.	n.q.	n.q.
Hydroquinone (Benzene, 1,4-dihydroxy-)	n/a	n/a	n/a	n/a	n.q.	n.q.	n.q.	n.q.
Benzenediol, methyl-	n.q.	n.q.	n.q.	n.q.	n.q.	n.q.	n.q.	n.q.
Aromatic Alcohols	**0.000**	**0.000**	**0.000**	**0.000**	**0.000**	**0.000**	**0.000**	**0.000**
Aromatic Aldehydes	**0.000**	**0.000**	**0.000**	**0.000**	**0.000**	**0.000**	**0.000**	**0.000**
Aromatic Ketones	**0.000**	**0.000**	**0.000**	**0.000**	**0.000**	**0.000**	**0.000**	**0.000**
Aromatic Esters	**0.000**	**0.000**	**0.000**	**0.000**	**0.000**	**0.000**	**0.000**	**0.000**
Lignin-derived Phenols	**3.599**	**3.690**	**3.491**	**3.345**	**4.197**	**4.185**	**3.128**	**3.166**
Phenol	0.356	0.366	0.365	0.352	0.543	0.549	0.406	0.405
Cresol, o-	0.304	0.314	0.291	0.281	0.370	0.372	0.310	0.312
Cresol, p-	0.167	0.171	0.170	0.166	0.209	0.214	0.151	0.153
Cresol, m-	0.239	0.243	0.251	0.243	0.334	0.332	0.212	0.216
Phenol, 2,5-dimethyl-	0.151	0.154	0.151	0.147	0.162	0.164	0.135	0.138
Phenol, 2,4-dimethyl-	0.087	0.089	0.088	0.083	0.098	0.100	0.065	0.065
Phenol, 2,6-dimethyl-	0.018	0.018	n/a		n/a	n/a	n/a	n/a
Phenol, 2,3-dimethyl-	0.041	0.042	0.041	0.039	0.045	0.048	0.033	0.040
Phenol, 3,5-dimethyl-	0.043	0.044	0.046	0.043	0.052	0.054	0.032	0.033
Phenol, 2-ethyl-	0.044	0.046	0.045	0.043	0.051	0.051	n/a	n/a
Phenol, 3-ethyl-	0.202	0.206	0.213	0.209	0.257	0.235	0.182	0.191
Phenol, 4-ethyl-	0.680	0.695	0.746	0.712	0.844	0.867	0.499	0.503
Phenol, 4-vinyl-	0.987	1.016	0.776	0.736	0.955	0.916	0.935	0.937
Phenol , cis 4-propenyl-	0.059	0.059	0.051	0.048	n/a	n/a	n/a	n/a
Phenol, trans 4-propenyl-	0.126	0.128	0.117	0.111	0.117	0.121	0.094	0.102
Phenol, ethyl-methyl-	0.098	0.099	0.098	0.093	0.113	0.112	0.075	0.073
Phenol,ethyl-methyl- (NIST MQ 87)	n/a	n/a	0.041	0.038	0.047	0.048	n/a	n/a
Guaiacols (Methoxy phenols)	**4.352**	**4.452**	**4.076**	**3.913**	**4.170**	**4.176**	**3.891**	**3.881**
Guaiacol	0.296	0.304	0.268	0.257	0.307	0.308	0.306	0.305
Guaiacol, 4-methyl-	0.158	0.162	0.146	0.142	0.151	0.153	0.135	0.135
Guaiacol, 4-ethyl-	0.417	0.424	0.471	0.449	0.504	0.505	0.313	0.307
Guaiacol, 4-vinyl-	1.138	1.161	0.995	0.951	0.955	0.952	1.011	1.004
Guaiacol, 4-allyl-; (Eugenol)	0.147	0.150	0.136	0.131	0.129	0.130	0.116	0.116
Guaiacol, 4-propyl-	0.052	0.053	0.057	0.055	0.058	0.057	0.036	0.036
Guaiacol, 4-propenyl- cis (Isoeugenol)	0.347	0.348	0.332	0.328	0.319	0.313	0.282	0.276
Guaiacol, 4-propenyl-(trans) (Isoeugenol)	1.224	1.239	1.144	1.081	1.191	1.195	1.055	1.045
Vanillin	0.428	0.463	0.394	0.387	0.400	0.406	0.481	0.495
Guaiacyl acetone	0.145	0.148	0.135	0.132	0.156	0.157	0.155	0.162
Syringols (Dimethoxy phenols)	**3.065**	**3.104**	**2.951**	**2.790**	**2.743**	**2.757**	**2.803**	**2.778**
Syringol	0.416	0.420	0.396	0.371	0.443	0.443	0.432	0.439
Syringol, 4-methyl-	0.209	0.211	0.205	0.194	0.210	0.209	0.192	0.189
Syringol, 4-ethyl-	0.293	0.295	0.358	0.337	0.357	0.368	0.233	0.231

Syringol, 4-vinyl-		0.623	0.634	0.540	0.518	0.456	0.446	0.560	0.552
Syringol, 4-allyl-		0.373	0.380	0.382	0.357	0.358	0.355	0.304	0.301
Syringol, 4-(1-propenyl)-, cis		0.219	0.220	0.201	0.191	0.179	0.181	0.173	0.163
Syringol, 4-(1-propenyl)-, trans		0.738	0.757	0.710	0.657	0.589	0.593	0.593	0.573
Syringaldehyde		n/a	n/a	n/a	n/a	n/a	n/a	0.123	0.127
Acetosyringone		0.148	0.139	0.116	0.125	0.106	0.117	0.144	0.155
Syringyl acetone		0.046	0.048	0.042	0.040	0.046	0.045	0.049	0.049
CARBOHYDRATES									
Sugars		**0.000**	**0.000**	**0.000**	**0.000**	**0.319**	**0.335**	**0.321**	**0.340**
Dianhydro-α-D-glucopyranose, 1,4:3,6-						0.319	0.335	0.321	0.340
OTHER ORGANIC COMPOUNDS									
N-compounds		**0.000**	**0.000**	**0.000**	**0.000**	**0.000**	**0.000**	**0.013**	**0.012**
unknown N-Compound (no NIST spectrum found)								**0.013**	**0.012**
Acetates		**0.000**	**0.000**	**0.000**	**0.000**	**0.000**	**0.000**	**0.000**	**0.000**
Terpenes		**0.000**	**0.000**	**0.000**	**0.000**	**0.000**	**0.000**	**0.000**	**0.000**
unknown compounds		**0.000**	**0.000**	**0.000**	**0.000**	**0.000**	**0.000**	**0.000**	**0.000**
Miscellaneous		**0.078**	**0.079**	**0.078**	**0.073**	**0.073**	**0.072**	**0.064**	**0.062**
poss: 2-Pentadecanone, 6,10,14-trimethyl-	(NIST MQ 88)	0.078	0.079	0.078	0.073	0.073	0.072	0.064	0.062

Table B14. GC-MS data for aqueous condensate (AC) obtained using water as the quench at quench-to-volatiles mass flow rate ratios (m_q/m_v) of 0.5 and 2.0.

	wt.% (wet)							
	m_q/m_v – 2.0				m_q/m_v – 0.5			
NONAROMATIC COMPOUNDS	**Run 1**	**Run 2**	**Run 3**	**Run 4**	**Run 1**	**Run 2**	**Run 3**	**Run 4**
Acids	**1.440**	**1.452**	**1.203**	**1.209**	**1.534**	**1.559**	**2.059**	**2.060**
Acetic acid	0.925	0.936	0.710	0.714	0.922	0.941	1.458	1.464
Propionic acid	0.470	0.471	0.449	0.451	0.522	0.526	0.545	0.542
Butyric acid	0.045	0.045	0.043	0.044	0.070	0.072	0.056	0.053
Propanoic acid, 2-methyl- (NIST MQ 87)	n/a	n/a	n/a	n/a	0.020	0.020		
Nonaromatic Esters	**0.000**	**0.000**	**0.000**	**0.000**	**0.000**	**0.000**	**0.000**	**0.000**
Nonaromatic Alcohols	**0.308**	**0.294**	**n/a**	**n/a**	**0.000**	**0.000**	**0.000**	**0.000**
Ethylene glycol	0.308	0.294	n/a	n/a	n/a	n/a	n/a	n/a
Nonaromatic Aldehydes	**0.023**	**0.023**	**0.000**	**0.000**	**0.022**	**0.022**	**0.022**	**0.022**
Crotonaldehyde, cis	0.012	0.011	n/a	n/a	0.009	0.009	0.011	0.011
Crotonaldehyde, trans	0.011	0.011	n/a	n/a	0.013	0.013	0.011	0.012
Nonaromatic Ketones	**2.397**	**2.421**	**1.863**	**1.886**	**2.080**	**2.122**	**3.536**	**3.510**
Acetol (Hydroxypropanone)	1.349	1.365	0.846	0.855	0.835	0.849	2.146	2.138
Butanone, 2-	0.068	0.069	0.070	0.070	0.088	0.090	0.065	0.069
Butanone, 1-hydroxy-2-	0.262	0.266	0.195	0.201	0.201	0.206	0.363	0.359
Butandione, 2,3- (Diacetyl)	0.048	0.047	0.025	0.024	0.014	0.014	0.054	0.054
Acetoin (Hydroxy-2-butanone, 3-)	0.045	0.046	0.038	0.038	0.039	0.040	0.058	0.057
Propan-2-one, 1-acetyloxy-	0.024	0.024	0.020	0.020	0.031	0.031	0.039	0.038
Cyclopentanone	n/a	n/a	0.042	0.042	0.081	0.082	0.067	0.063
Cyclopenten-1-one, 2-	0.214	0.217	0.219	0.223	0.290	0.299	0.259	0.256
Cyclopenten-1-one, 2,3-dimethyl-2-	0.024	0.019	0.016	0.016	0.030	0.025	0.030	0.028
Cyclopenten-1-one, 2-methyl-2-	0.074	0.076	0.079	0.081	0.104	0.107	0.079	0.077
Cyclopenten-1-one, 3-methyl-2-	0.057	0.058	0.059	0.061	0.076	0.078	0.071	0.071
Cylopenten-1-one, 3-ethyl-2-	0.009	0.009	0.009	0.010	0.011	0.011	0.011	0.011
Cyclopenten-1-one, 2-hydroxy-3-methyl-2-	0.066	0.069	0.079	0.078	0.076	0.086	0.108	0.104
Cyclohexen-1-one, 2-	0.004	0.004	0.004	0.004	0.005	0.005	0.007	0.006
3-Buten-2-one (NIST MQ 88)	n/a	n/a	0.009	0.010	0.007	0.007	0.012	0.012
Butanone, 3-methyl-2- (NIST MQ 88)	n/a	n/a	n/a	n/a	0.003	0.003	n/a	n/a
3-Buten-2-one, 3-methyl- (NIST MQ 88)	n/a	n/a	n/a	n/a	0.004	0.004	n/a	n/a
2-Pentanone (NIST MQ 94)	0.019	0.019	0.018	0.017	0.022	0.022	0.019	0.020
3-Pentanone (NIST MQ 92)	0.006	0.006	0.006	0.006	0.009	0.008	0.006	0.007
2,3-Pentanedione	0.014	0.014	0.010	0.010	0.007	0.006	0.014	0.015
3-Penten-2-one (NIST MQ 84)	0.015	0.015	0.016	0.016	0.023	0.023	0.015	0.015
Cyclopentanone, 2-methyl- (NIST MQ 87)	n/a	n/a	0.011	0.011	0.013	0.014	0.010	0.010
Isomere of 2-Cyclopenten-1-one, 3-methyl-	0.013	0.013	0.013	0.013	0.018	0.018	0.014	0.014
2-Butanone, 1-hydroxy-3-methyl- (NIST MQ 78)	0.012	0.012	0.009	0.009	0.010	0.009	0.016	0.015
2-Cyclopenten-1-one, x,y-dimethyl-	0.009	0.009	0.009	0.009	0.012	0.012	0.008	0.008

2-Cycolpenten-1-one, x,y-dimethyl-	0.008	0.008	0.008	0.008	0.008	0.008	0.008	0.008
2,5-Hexanedione (NIST MQ 89)	0.007	0.007	0.007	0.007	0.008	0.008	0.011	0.011
Isomere of Cyclopenten-1-one, 2,3-dimethyl-2-	0.012	0.013	0.012	0.012	0.014	0.015	0.013	0.013
2-Cyclopenten-1-one, x,y-dimethyl-	0.018	0.018	0.014	0.015	0.019	0.019	0.008	0.008
2-Cyclopenten-1-one, 2,3,4-trimethyl- (NIST MQ 88)	0.005	0.005	0.005	0.005	0.006	0.006	0.005	0.007
Isomer of Cyclopenten-1-one, 3-ethyl-2-hydroxy-	0.014	0.014	0.015	0.015	0.016	0.016	0.019	0.018
Aliphatic Hydrocarbons	**0.000**	**0.000**	**0.000**	**0.000**	**0.000**	**0.000**	**0.000**	**0.000**
HETEROCYCLIC COMPOUNDS								
Furans	**0.234**	**0.236**	**0.219**	**0.228**	**0.258**	**0.270**	**0.337**	**0.335**
Furfuryl alcohol, 2-	0.019	0.019	0.017	0.021	0.023	0.026	0.026	0.027
Furanone, 2(5H)-	n/a	n/a	n/a	n/a	n/a	n/a	0.035	0.034
Furaldehyde, 2-	0.116	0.118	0.104	0.106	0.108	0.113	0.134	0.131
Furaldehyde, 3-	n/a	n/a	0.008	0.008	0.011	0.012	0.008	0.008
Furaldehyde, 5-methyl-2-	0.012	0.012	0.010	0.010	0.012	0.012	0.013	0.013
Ethanone, 1-(2-furanyl)-	0.013	0.013	0.012	0.012	0.016	0.016	0.015	0.014
Furan-2-one, 3-methyl-, (5H)-	0.006	0.006	0.006	0.006	0.007	0.007	0.010	0.010
Furan-2-one, 2,5-dihydro-3,5-dimethyl-	0.011	0.011	0.011	0.012	0.012	0.012	0.013	0.013
Butyrolactone, γ-	0.056	0.057	0.052	0.052	0.070	0.072	0.083	0.083
Pyrans	**0.000**	**0.000**	**0.000**	**0.000**	**0.000**	**0.000**	**0.000**	**0.000**
AROMATIC COMPOUNDS								
Benzenes	**0.000**	**0.000**	**0.000**	**0.000**	**0.000**	**0.002**	**0.000**	**0.000**
Naphthalene, 1-phenyl- (impurity in IS = Fluoranthene)	n/a	n/a	n/a	n/a	n/a	0.002		
Catechols	**0.000**	**0.000**	**0.000**	**0.000**	**0.000**	**0.000**	**0.000**	**0.000**
Aromatic Alcohols	**0.000**	**0.000**	**0.000**	**0.000**	**0.000**	**0.000**	**0.000**	**0.000**
Aromatic Aldehydes	**0.000**	**0.000**	**0.000**	**0.000**	**0.000**	**0.000**	**0.000**	**0.000**
Aromatic Ketones	**0.000**	**0.000**	**0.000**	**0.000**	**0.000**	**0.000**	**0.000**	**0.000**
Aromatic Esters	**0.000**	**0.000**	**0.000**	**0.000**	**0.000**	**0.000**	**0.000**	**0.000**
Lignin-derived Phenols	**0.081**	**0.082**	**0.099**	**0.104**	**0.111**	**0.112**	**0.112**	**0.110**
Phenol	0.048	0.049	0.054	0.056	0.063	0.063	0.062	0.060
Cresol, o-	0.019	0.019	0.021	0.021	0.021	0.022	0.025	0.024
Cresol, p-	0.005	0.005	0.006	0.007	0.013	0.013	0.008	0.007
Cresol, m-	0.009	0.009	0.011	0.013	0.005	0.005	0.012	0.012
Phenol, 4-ethyl-	n/a	n/a	0.007	0.008	0.009	0.009	0.006	0.007
Guaiacols (Methoxy phenols)	**0.061**	**0.062**	**0.060**	**0.060**	**0.059**	**0.060**	**0.074**	**0.072**
Guaiacol	0.049	0.050	0.046	0.046	0.046	0.047	0.059	0.058
Guaiacol, 4-methyl-	0.007	0.007	0.007	0.007	0.007	0.007	0.009	0.008
Guaiacol, 4-ethyl-	0.005	0.005	0.006	0.006	0.006	0.006	0.006	0.006

Syringols (Dimethoxy phenols)	**0.000**	**0.000**	**0.000**	**0.000**	**0.000**	**0.000**	**0.000**	**0.000**
CARBOHYDRATES								
Sugars	**0.000**	**0.000**	**0.000**	**0.000**	**0.000**	**0.000**	**0.000**	**0.000**
OTHER ORGANIC COMPOUNDS								
N-compounds	**0.027**	**0.027**	**0.060**	**0.061**	**0.187**	**0.186**	**0.019**	**0.019**
Propanenitrile (NIST MQ 94)	0.003	0.003	n/a	n/a	0.003	0.003	0.003	0.003
unknown N-Compound (no NIST spectrum found)	0.018	0.018	0.044	0.044	0.135	0.138	0.012	0.012
unknown N-Compound (no NIST spectrum found)	0.006	0.006	0.014	0.014	0.049	0.045	0.004	0.004
unknown N-Compound (no NIST spectrum found)	n/a	n/a	0.003	0.003				
Acetates	**0.000**	**0.000**	**0.000**	**0.000**	**0.000**	**0.000**	**0.000**	**0.000**
Terpenes	**0.000**	**0.000**	**0.000**	**0.000**	**0.000**	**0.000**	**0.000**	**0.000**
unknown compounds	**0.000**	**0.000**	**0.000**	**0.000**	**0.000**	**0.000**	**0.000**	**0.000**
Miscellaneous	**0.000**	**0.000**	**0.000**	**0.000**	**0.000**	**0.000**	**0.000**	**0.000**

Table B15. GC-MS data for spent water quench at quench-to-volatiles mass flow rate ratios (m_q/m_v) of 0.5 and 2.0.

	wt.% (wet)							
	$m_q/m_v - 2.0$				$m_q/m_v - 0.5$			
NONAROMATIC COMPOUNDS	**Run 1**	**Run 2**	**Run 3**	**Run 4**	**Run 1**	**Run 2**	**Run 3**	**Run 4**
Acids	**0.924**	**0.922**	**1.005**	**1.018**	**1.922**	**1.946**	**2.485**	**2.471**
Acetic acid	0.557	0.557	0.589	0.601	1.317	1.337	1.901	1.890
Propionic acid	0.368	0.366	0.386	0.386	0.532	0.535	0.535	0.534
Butyric acid	n/a	n/a	0.030	0.030	0.073	0.075	0.049	0.047
Nonaromatic Esters	**0.000**	**0.000**	**0.000**	**0.000**	**0.000**	**0.000**	**0.009**	**0.009**
Acetic acid 2-hydroxyethyl ester							0.009	0.009
Nonaromatic Alcohols	**0.075**	**0.073**	**0.034**	**0.036**	**0.664**	**0.675**	**1.077**	**1.093**
Ethylene glycol	0.075	0.073	0.034	0.036	0.664	0.675	1.077	1.093
Nonaromatic Aldehydes	**0.000**	**0.000**	**0.000**	**0.000**	**0.000**	**0.000**	**0.000**	**0.000**
Nonaromatic Ketones	**0.537**	**0.536**	**0.489**	**0.487**	**0.763**	**0.774**	**1.852**	**1.845**
Acetol (Hydroxypropanone)	0.251	0.248	0.156	0.153	0.223	0.227	1.050	1.049
Butanone, 2-	0.006	0.006	0.006	0.006	0.016	0.016	0.011	0.012
Butanone, 1-hydroxy-2-	0.058	0.057	0.044	0.044	0.057	0.057	0.178	0.177
Butandione, 2,3- (Diacetyl)	0.001	0.001	n/a	n/a	0.002	0.002	0.004	0.004
Acetoin (Hydroxy-2-butanone, 3-)	n/a	n/a	n/a	n/a			0.018	0.017
Propan-2-one, 1-acetyloxy-	0.009	0.009	0.011	0.010	0.023	0.023	0.035	0.034
Cyclopentanone	0.015	0.016	0.016	0.015	n.q.	n.q.	n.q.	n.q.
Cyclopenten-1-one, 2-	0.042	0.047	0.052	0.052	0.088	0.089	0.096	0.095
Cyclopenten-1-one, 2-methyl-2-	0.013	0.013	0.014	0.014	0.020	0.020	0.019	0.019
Cyclopenten-1-one, 3-methyl-2-	0.024	0.023	0.029	0.029	0.048	0.049	0.050	0.050
Cylopenten-1-one, 3-ethyl-2-	0.004	0.004	0.005	0.005	0.007	0.008	0.008	0.008
Cyclopenten-1-one, 2-hydroxy-3-methyl-2-	0.103	0.103	0.119	0.120	0.203	0.208	0.297	0.294
Cyclopenten-1-one, 3-ethyl-2-hydroxy-2-	n/a	n/a	0.027	0.028	0.044	0.045	0.055	0.054
3-Penten-2-one (NIST MQ 84)	n/a	n/a	n/a	n/a	0.008	0.006	n/a	n/a
2,5-Hexanedione (NIST MQ 89)	n/a	n/a	n/a	n/a	0.005	0.006	0.009	0.008
Isomer of Cyclopenten-1-one, 3-ethyl-2-hydroxy-	0.010	0.010	0.012	0.012	0.018	0.019	0.022	0.022
Aliphatic Hydrocarbons	**0.000**	**0.000**	**0.000**	**0.000**	**0.000**	**0.000**	**0.000**	**0.000**
HETEROCYCLIC COMPOUNDS								
Furans	**0.083**	**0.091**	**0.093**	**0.093**	**0.189**	**0.193**	**0.448**	**0.470**
Furfuryl alcohol, 2-	0.010	0.010	0.012	0.011	0.022	0.023	0.028	0.028
Furanone, 2(5H)-	0.018	0.017	0.012	0.013	0.026	0.027	0.078	0.079
Furaldehyde, 2-	0.011	0.020	0.011	0.010	n/a	n/a	0.021	0.019
Ethanone, 1-(2-furanyl)-	n/a	n/a	n/a	n/a			0.004	0.004
Furan-2-one, 3-methyl-, (5H)-	0.004	0.004	0.005	0.005	0.010	0.010	0.016	0.016
Furan-2-one, 2,5-dihydro-3,5-dimethyl-	n/a	n/a	n/a	n/a			0.010	0.010
Butyrolactone, γ-	0.040	0.040	0.048	0.049	0.105	0.107	0.142	0.141

Butyrolactone, 2-hydroxy-, γ-	n/a	n/a	n/a	n/a			0.043	0.044
Furan-2-one, 4-methyl-(5H)- (NIST MQ 88)	n/a	n/a	n/a	n/a	0.017	0.017	0.025	0.034
Lactone derivative (unspecific spectrum)					n/a	n/a	0.005	0.005
Lactone derivative (unspecific spectrum)					n/a	n/a	0.076	0.091
Isomere of Furan-2-one, 2,5-dihydro-3,5-dimethyl-	n/a	n/a	0.005	0.005	0.009	0.009	n/a	n/a
Pyrans	**0.000**	**0.000**	**0.000**	**0.000**	**0.000**	**0.000**	**0.000**	**0.000**
AROMATIC COMPOUNDS								
Benzenes	**0.000**	**0.000**	**0.002**	**0.000**	**0.000**	**0.000**	**0.000**	**0.000**
Naphthalene, 1-phenyl- (impurity in IS = Fluoranthene)	n/a	n/a	0.002	n/a	n/a	n/a	n/a	n/a
Catechols	**n.q.**	**n.q.**	**n.q.**	**n.q.**	n.q.	n.q.	n.q.	n.q.
Catechol (Benzene, 1,2-dihydroxy-)	n/a	n/a	n/a	n/a	n/a	n/a	n.q.	n.q.
Hydroquinone (Benzene, 1,4-dihydroxy-)	n.q.	n.q.	n.q.	n.q.	n.q.	n.q.	n.q.	n.q.
Resorcinol (Benzene, 1,3-dihydroxy-)	n.q.	n.q.	n.q.	n.q.	n.q.	n.q.	n/a	n/a
Benzenediol, methyl-	n.q.	n.q.	n.q.	n.q.	n.q.	n.q.	n.q.	n.q.
Benzenediol, dimethyl- (NIST MQ 88)	n.q.	n.q.	n.q.	n.q.	n.q.	n.q.	n/a	n/a
Benzenediol, ethyl-	n.q.	n.q.	n.q.	n.q.	n.q.	n.q.	n/a	n/a
Aromatic Alcohols	**0.000**	**0.000**	**0.000**	**0.000**	**0.000**	**0.000**	**0.000**	**0.000**
Aromatic Aldehydes	**0.000**	**0.000**	**0.000**	**0.000**	**0.000**	**0.000**	**0.000**	**0.000**
Aromatic Ketones	**0.000**	**0.000**	**0.000**	**0.000**	**0.004**	**0.004**	**0.000**	**0.000**
Acetophenone, 3-hydroxy-	n/a	n/a	n/a	n/a	0.004	0.004	n/a	n/a
Aromatic Esters	**0.000**	**0.000**	**0.000**	**0.000**	**0.000**	**0.000**	**0.000**	**0.000**
Lignin-derived Phenols	**0.061**	**0.061**	**0.052**	**0.052**	**0.088**	**0.092**	**0.089**	**0.088**
Phenol	0.023	0.022	0.026	0.026	0.042	0.044	0.044	0.043
Cresol, o-	0.013	0.014	0.004	0.004	0.018	0.020		
Cresol, p-	0.004	0.003	0.008	0.008	n/a	n/a	0.006	0.008
Cresol, m-	0.006	0.007	0.007	0.007	n/a	n/a	0.021	0.018
Phenol, 3-ethyl-	n/a	n/a	n/a	n/a	0.010	0.010	n/a	n/a
Phenol, 4-ethyl-	0.006	0.005	0.007	0.007	0.008	0.009	0.006	0.006
Phenol, 4-vinyl-	0.009	0.009	n/a	n/a	0.009	0.009	0.012	0.012
Guaiacols (Methoxy phenols)	**0.056**	**0.052**	**0.054**	**0.055**	**0.085**	**0.085**	**0.110**	**0.109**
Guaiacol	0.016	0.015	0.017	0.017	0.022	0.022	0.028	0.028
Guaiacol, 4-methyl-	n/a	n/a	n/a	n/a	0.003	0.003	n/a	n/a
Guaiacol, 4-ethyl-	n/a	n/a	n/a	n/a	0.005	0.005	0.004	0.004
Guaiacol, 4-vinyl-	0.006	0.006	0.005	0.005	0.005	0.005	0.010	0.009
Vanillin	0.026	0.024	0.024	0.025	0.039	0.038	0.050	0.049
Guaiacyl acetone	0.008	0.007	0.008	0.008	0.011	0.011	0.018	0.018
Syringols (Dimethoxy phenols)	**0.018**	**0.018**	**0.027**	**0.027**	**0.066**	**0.071**	**0.093**	**0.103**

Syringol	0.018	0.018	0.019	0.020	0.050	0.055	0.059	0.069
Syringol, 4-methyl-	n/a	n/a	0.004	0.004	0.005	0.005	0.006	0.005
Syringol, 4-ethyl-	n/a	n/a	0.004	0.003	0.006	0.005	0.006	0.006
Syringol, 4-vinyl-	n/a	n/a	n/a	n/a	n/a	n/a	0.006	0.007
Acetosyringone	n/a	n/a	n/a	n/a	0.006	0.006	0.011	0.011
Syringyl acetone	n/a	n/a	n/a	n/a	n/a	n/a	0.005	0.005
CARBOHYDRATES								
Sugars	**0.146**	**0.144**	**0.275**	**0.280**	**0.995**	**0.974**	**1.382**	**1.410**
Anhydro-ß-D-arabinofuranose, 1,5-	0.034	0.034	0.035	0.037	0.145	0.144	0.211	0.212
Anhydro-ß-D-xylofuranose, 1,5-	0.059	0.058	0.060	0.062	0.238	0.235	0.302	0.299
Anhydro-ß-D-glucopyranose, 1,6- (Levoglucosan)	n/a	n/a	0.116	0.117	0.387	0.366	0.508	0.538
Dianhydro-α-D-glucopyranose, 1,4:3,6-	0.053	0.052	0.064	0.063	0.225	0.229	0.275	0.274
poss: 2,3-Anhydro-d-galactosan (NIST MQ 78)	n/a	n/a	n/a	n/a	n/a	n/a	0.038	0.038
poss: 2,3-Anhydro-d-mannosan (NIST MQ 84)	n/a	n/a	n/a	n/a	n/a	n/a	0.048	0.049
OTHER ORGANIC COMPOUNDS								
N-compounds	**0.093**	**0.091**	**0.135**	**0.135**	**0.378**	**0.383**	**0.285**	**0.281**
Oxazole, 4,5-dihydro-2,4,4-trimethyl- (NIST MQ 82)	0.055	0.054	0.067	0.065	0.184	0.185	n/a	n/a
unknown N-Compound (no NIST spectrum found)	0.017	0.017	0.037	0.037	0.072	0.074	0.188	0.185
unknown N- compound (no NIST spectrum found)	0.015	0.015	0.022	0.022	0.062	0.063	0.021	0.021
unknown N-Compound (no NIST spectrum found)	0.005	0.005	0.004	0.004	0.008	0.007	0.043	0.043
Acetamide (NIST MQ 94)	n/a	n/a	n/a	n/a			0.006	0.005
unknown N-compound (no NIST spectrum found)	n/a	n/a	0.006	0.006	0.006	0.007	0.007	0.007
unknown N-compound (no NIST spectrum found)	n/a	n/a	n/a	n/a	0.003	0.004	0.020	0.021
unknown N-Compound (no NIST spectrum found)	n/a	n/a	n/a	n/a	0.004	0.004	n/a	n/a
unknown N- compound (no NIST spectrum found)	n/a	n/a	n/a	n/a	0.009	0.009	n/a	n/a
unknown N-Compound (no NIST spectrum found)	n/a	n/a	n/a	n/a	0.027	0.027	n/a	n/a
unknown N-Compound (no NIST spectrum found)	n/a	n/a	n/a	n/a	0.003	0.004	n/a	n/a
Acetates	**0.000**	**0.000**	**0.000**	**0.000**	**0.000**	**0.000**	**0.000**	**0.000**
Terpenes	**0.000**	**0.000**	**0.000**	**0.000**	**0.000**	**0.000**	**0.000**	**0.000**
unknown compounds	**0.000**	**0.000**	**0.000**	**0.000**	**0.000**	**0.000**	**0.000**	**0.000**
Miscellaneous	**0.000**	**0.000**	**0.000**	**0.000**	**0.000**	**0.000**	**0.000**	**0.000**

Appendix C: *Additional Information for the Study on Water Extraction of Levoglucosan from Fast Pyrolysis Bio-Oils: Comparing Solvent Extraction and Direct-Contact Condensation*

Section 1: GC-MS Analysis of Raffinate, Extract, and Corresponding Aqueous Condensates (ACs) Following Single-Step Condensation of Pyrolysis Vapors Using Water as the Quench

Table C1. GC-MS data for the organic-rich condensate (ORC) obtained from single-step water quenching of pyrolysis vapors (wheat straw).

CAS No.	Compound	wt.% wet			
		Run 1	Run 2	Run 3	Run 4
	NONAROMATIC COMPOUNDS				
	Acids	**0.000**	**0.000**	**0.000**	**0.000**
	Nonaromatic Esters	**0.000**	**0.000**	**0.000**	**0.000**
	Nonaromatic Alcohols	**0.000**	**0.000**	**0.000**	**0.000**
	Nonaromatic Aldehydes	**0.000**	**0.000**	**0.000**	**0.000**
	Nonaromatic Ketones	**3.588**	**3.621**	**3.232**	**3.407**
116-09-6	Acetol (Hydroxypropanone)	0.867	0.886	1.116	1.077
78-93-3	Butanone, 2-	0.081	0.080	0.069	0.075
431-03-8	Butandione, 2,3- (Diacetyl)	0.024	0.024	0.025	0.025
120-92-3	Cyclopentanone	0.112	0.113	0.096	0.099

930-30-3	Cyclopenten-1-one, 2-	0.322	0.322	0.256	0.274
1120-73-6	Cyclopenten-1-one, 2-methyl-2-	0.322	0.323	0.106	0.101
2758-18-1	Cyclopenten-1-one, 3-methyl-2-	0.276	0.281	0.258	0.279
5682-69-2	Cylopenten-1-one, 3-ethyl-2-	0.129	0.133	0.231	0.245
80-71-7	Cyclopenten-1-one, 2-hydroxy-3-methyl-2-	0.705	0.722	0.095	0.103
	Cyclopentanone, 2-methyl- (NIST MQ 87)	0.035	0.036	0.509	0.609
	2-Cyclopenten-1-one, x,y-dimethyl-	0.080	0.080	0.059	0.067
	2-Cycolpenten-1-one, x,y-dimethyl-	0.060	0.061	0.045	0.050
	Isomere of Cyclopenten-1-one, 2,3-dimethyl-2-	0.121	0.124	0.089	0.097
	2-Cyclopenten-1-one, x,y-dimethyl-	0.089	0.082	n/a	n/a
	2-Cyclopenten-1-one, 2,3,4-trimethyl- (NIST MQ 88)	0.080	0.084	0.059	0.062
	Isomer of Cyclopenten-1-one, 3-ethyl-2-hydroxy-	0.099	0.100	0.085	0.094
	2-Heptadecanone (NIST MQ 84)	0.186	0.170	0.134	0.151
	Aliphatic Hydrocarbons	**0.000**	**0.000**	**0.000**	**0.000**
	HETEROCYCLIC COMPOUNDS				
	Furans	**0.213**	**0.217**	**0.198**	**0.215**
98-01-1	Furaldehyde, 2-	0.213	0.217	0.170	0.181
	Ethanone, 1-(2-furanyl)-	n/a	n/a	0.028	0.034
	Pyrans	**0.000**	**0.000**	**0.000**	**0.000**
	AROMATIC COMPOUNDS				
	Benzenes	**0.109**	**0.114**	**0.141**	**0.145**
108-88-3	Toluene	0.014	0.014	0.025	0.022
	Benzene, ethyl-	n/a	n/a	0.039	0.040
83-33-0	Inden-1-one, 2,3-dihydro-1H-	0.095	0.100	0.078	0.083
	Catechols	**n.q.**	**n.q.**	**n.q.**	**n.q.**
	Benzenediol, methyl-	n.q.	n.q.	n.q.	n.q.

	Aromatic Alcohols	**0.000**	**0.000**	**0.000**	**0.000**
	Aromatic Aldehydes	**0.000**	**0.000**	**0.000**	**0.000**
	Aromatic Ketones	**0.000**	**0.000**	**0.000**	**0.000**
	Aromatic Esters	**0.000**	**0.000**	**0.000**	**0.000**
	Lignin-derived Phenols	**4.382**	**4.427**	**3.387**	**3.707**
108-95-2	Phenol	0.538	0.546	0.407	0.444
95-48-7	Cresol, o-	0.420	0.425	0.334	0.367
106-44-5	Cresol, p-	0.245	0.251	0.183	0.206
108-39-4	Cresol, m-	0.351	0.342	0.238	0.257
95-87-4	Phenol, 2,5-dimethyl-	0.187	0.192	0.158	0.162
105-67-9	Phenol, 2,4-dimethyl-	0.122	0.122	0.084	0.100
576-26-1	Phenol, 2,6-dimethyl-	0.034	0.035		
526-75-0	Phenol, 2,3-dimethyl-	0.056	0.057	0.042	0.043
108-68-9	Phenol, 3,5-dimethyl-	0.053	0.054	0.034	0.037
90-00-6	Phenol, 2-ethyl-	0.067	0.072	0.050	0.053
620-17-7	Phenol, 3-ethyl-	0.242	0.233		
123-07-9	Phenol, 4-ethyl-	0.844	0.855	0.611	0.668
2628-17-3	Phenol, 4-vinyl-	0.889	0.902	0.999	1.097
85960-81-2	Phenol , cis 4-propenyl-	0.052	0.054	0.048	0.056
5932-68-3	Phenol, trans 4-propenyl-	0.121	0.123	0.111	0.122
	Phenol, ethyl-methyl-	0.119	0.121	0.087	0.094
	Phenol,ethyl-methyl- (NIST MQ 87)	0.042	0.043	n/a	n/a
	Guaiacols (Methoxy phenols)	**4.485**	**4.509**	**4.113**	**4.470**
90-05-1	Guaiacol	0.473	0.478	0.430	0.467
93-51-6	Guaiacol, 4-methyl-	0.221	0.223	0.195	0.214
2785-89-9	Guaiacol, 4-ethyl-	0.541	0.547	0.367	0.396
7786-61-0	Guaiacol, 4-vinyl-	1.226	1.239	1.181	1.287

97-53-0	Guaiacol, 4-allyl-; (Eugenol)	0.157	0.159	0.139	0.151
2785-87-7	Guaiacol, 4-propyl-	0.063	0.061	0.045	0.048
97-54-1	Guaiacol, 4-propenyl- cis (Isoeugenol)	0.347	0.335	0.302	0.330
5932-68-3	Guaiacol, 4-propenyl-(trans) (Isoeugenol)	1.089	1.097	0.961	1.050
121-33-5	Vanillin	0.367	0.369	0.391	0.417
	Guaiacyl acetone	n/a	n/a	0.101	0.110
	Syringols (Dimethoxy phenols)	**2.359**	**2.398**	**2.234**	**2.382**
91-10-1	Syringol	0.308	0.317	0.314	0.339
6638-05-7	Syringol, 4-methyl-	0.165	0.165	0.157	0.167
14059-92-8	Syringol, 4-ethyl-	0.253	0.256	0.163	0.178
28343-22-8	Syringol, 4-vinyl-	0.506	0.510	0.538	0.570
6627-88-9	Syringol, 4-allyl-	0.304	0.308	0.255	0.274
26624-13-5	Syringol, 4-(1-propenyl)-, cis	0.163	0.164	0.146	0.162
20675-95-0	Syringol, 4-(1-propenyl)-, trans	0.583	0.582	0.550	0.586
2478-38-8	Acetosyringone	0.077	0.098	0.111	0.105
	CARBOHYDRATES				
	Sugars	**0.000**	**0.000**	**0.000**	**0.000**
	OTHER ORGANIC COMPOUNDS				
	N-compounds	**0.000**	**0.000**	**0.000**	**0.000**
	Acetates	**0.000**	**0.000**	**0.000**	**0.000**
	Terpenes	**0.000**	**0.000**	**0.000**	**0.000**
	unknown compounds	**0.000**	**0.000**	**0.000**	**0.000**

Miscellaneous	**0.068**	**0.067**	**0.059**	**0.062**
poss: 2-Pentadecanone, 6,10,14-trimethyl- (NIST MQ 88)	0.068	0.067	0.059	0.062

Table C2. GC-MS data for the recovered quench (extract) obtained from single-step water quenching of pyrolysis vapors (wheat straw).

CAS No.	Compound	wt.% wet			
		Run 1	Run 2	Run 1	Run 2
	NONAROMATIC COMPOUNDS				
	Acids	**1.105**	**1.091**	**1.299**	**1.312**
64-19-7	Acetic acid	0.677	0.663	0.863	0.875
79-09-4	Propionic acid	0.398	0.399	0.412	0.413
107-92-6	Butyric acid	0.030	0.029	0.024	0.023
	Nonaromatic Esters	**0.000**	**0.000**	**0.000**	**0.000**
	Nonaromatic Alcohols	**0.000**	**0.000**	**0.000**	**0.000**
	Nonaromatic Aldehydes	**0.000**	**0.000**	**0.000**	**0.000**
	Nonaromatic Ketones	**0.856**	**0.856**	**1.339**	**1.355**
116-09-6	Acetol (Hydroxypropanone)	0.398	0.395	0.822	0.831
78-93-3	Butanone, 2-	0.021	0.020	0.018	0.018
5077-67-8	Butanone, 1-hydroxy-2-	0.087	0.087	0.138	0.140
431-03-8	Butandione, 2,3- (Diacetyl)	0.003	0.003	0.006	0.006
513-86-0	Acetoin (Hydroxy-2-butanone, 3-)	0.013	0.012	0.019	0.017
592-20-1	Propan-2-one, 1-acetyloxy-	0.015	0.015	0.019	0.020
120-92-3	Cyclopentanone	0.027	0.027	0.022	0.023
930-30-3	Cyclopenten-1-one, 2-	0.092	0.092	0.085	0.086
1121-05-7	Cyclopenten-1-one, 2,3-dimethyl-2-	n/a	n/a	0.026	0.015
1120-73-6	Cyclopenten-1-one, 2-methyl-2-	0.031	0.031	0.027	0.027
2758-18-1	Cyclopenten-1-one, 3-methyl-2-	0.035	0.035	0.033	0.033
5682-69-2	Cylopenten-1-one, 3-ethyl-2-	0.004	0.005	0.005	0.005
80-71-7	Cyclopenten-1-one, 2-hydroxy-3-methyl-2-	0.106	0.108	0.085	0.101
21835-01-8	Cyclopenten-1-one, 3-ethyl-2-hydroxy-2-	n/a	n/a	0.016	0.016
	3-Buten-2-one (NIST MQ 88)	n/a	n/a	0.005	0.005
	3-Penten-2-one (NIST MQ 84)	0.004	0.004	n/a	n/a

	2-Cyclopenten-1-one, x,y-dimethyl-	0.009	0.009	0.002	0.002
	Isomer of Cyclopenten-1-one, 3-ethyl-2-hydroxy-	0.012	0.012	0.011	0.011
	Aliphatic Hydrocarbons	**0.000**	**0.000**	**0.000**	**0.000**
	HETEROCYCLIC COMPOUNDS				
	Furans	**0.103**	**0.104**	**0.167**	**0.169**
98-00-0	Furfuryl alcohol, 2-	0.016	0.016	0.021	0.021
	Furanone, 2(5H)-	n/a	n/a	0.031	0.031
98-01-1	Furaldehyde, 2-	0.030	0.030	0.042	0.043
1192-62-7	Ethanone, 1-(2-furanyl)-	0.004	0.004	0.004	0.004
22122-36-7	Furan-2-one, 3-methyl-, (5H)-			0.007	0.007
	Furan-2-one, 2,5-dihydro-3,5-dimethyl-	0.007	0.008	0.008	0.008
96-48-0	Butyrolactone, γ-	0.046	0.046	0.055	0.055
	Pyrans	**0.000**	**0.000**	**0.000**	**0.000**
	AROMATIC COMPOUNDS				
	Benzenes	**0.000**	**0.000**	**0.000**	**0.000**
	Catechols	**n.q.**	n.q.	**n.q.**	**n.q.**
123-31-9	Hydroquinone (Benzene, 1,4-dihydroxy-)			n.q.	n.q.
	Benzenediol, methyl-	n.q.	n.q.	n.q.	n.q.
	Aromatic Alcohols	**0.000**	**0.000**	**0.000**	**0.000**
	Aromatic Aldehydes	**0.000**	**0.000**	**0.000**	**0.000**
	Aromatic Ketones	**0.000**	**0.000**	**0.000**	**0.000**
	Aromatic Esters	**0.000**	**0.000**	**0.000**	**0.000**

	Lignin-derived Phenols	**0.064**	**0.064**	**0.063**	**0.064**
108-95-2	Phenol	0.032	0.032	0.030	0.030
95-48-7	Cresol, o-	0.016	0.015	0.010	0.010
106-44-5	Cresol, p-	0.004	0.004	0.004	0.004
108-39-4	Cresol, m-	0.007	0.008	0.007	0.007
123-07-9	Phenol, 4-ethyl-	0.005	0.006	0.005	0.005
	Phenol, 4-vinyl-	n/a	n/a	0.007	0.007
	Guaiacols (Methoxy phenols)	**0.037**	**0.036**	**0.073**	**0.073**
90-05-1	Guaiacol	0.024	0.024	0.028	0.029
93-51-6	Guaiacol, 4-methyl-	0.004	0.003	0.005	0.005
2785-89-9	Guaiacol, 4-ethyl-	0.004	0.004	0.003	0.003
7786-61-0	Guaiacol, 4-vinyl-	0.005	0.004	0.005	0.005
121-33-5	Vanillin	n/a	n/a	0.024	0.024
	Guaiacyl acetone	n/a	n/a	0.006	0.006
	Syringols (Dimethoxy phenols)	**0.013**	**0.013**	**0.019**	**0.022**
91-10-1	Syringol	0.013	0.013	0.013	0.015
	Syringol, 4-methyl-	n/a	n/a	0.003	0.003
	Acetosyringone	n/a	n/a	0.004	0.004
	CARBOHYDRATES				
	Sugars	**0.057**	**0.059**	**0.094**	**0.094**
	Anhydro-ß-D-arabinofuranose, 1,5-	n/a	n/a	0.021	0.021
51246-94-7	Anhydro-ß-D-xylofuranose, 1,5-	0.026	0.027	0.033	0.033
4451-31-4	Dianhydro-α-D-glucopyranose, 1,4:3,6-	0.031	0.033	0.040	0.039
	OTHER ORGANIC COMPOUNDS				
	N-compounds	**0.104**	**0.104**	**0.041**	**0.041**
	unknown N-Compound (no NIST spectrum found)	0.071	0.072	0.027	0.027
	unknown N- compound (no NIST spectrum found)	0.010	0.010	0.007	0.007
	unknown N-Compound (no NIST spectrum found)	0.022	0.022	0.006	0.006

Acetates	**0.000**	**0.000**	**0.000**	**0.000**
Terpenes	**0.000**	**0.000**	**0.000**	**0.000**
unknown compounds	**0.000**	**0.000**	**0.000**	**0.000**
Miscellaneous	**0.000**	**0.000**	**0.000**	**0.000**

Table C3. GC-MS data for the aqueous condensate (AC) obtained from single-step water quenching of pyrolysis vapors (wheat straw).

CAS No.	Compound	wt.% wet			
		Run 1	**Run 2**	**Run 3**	**Run 4**
	NONAROMATIC COMPOUNDS				
	Acids	**1.197**	**1.203**	**1.646**	**1.671**
64-19-7	Acetic acid	0.764	0.771	1.116	1.137
79-09-4	Propionic acid	0.432	0.432	0.460	0.462
107-92-6	Butyric acid	n/a	n/a	0.069	0.072
	Nonaromatic Esters	**0.000**	**0.000**	**0.000**	**0.000**
	Nonaromatic Alcohols	**0.000**	**0.000**	**0.007**	**0.007**
	poss: Glycerin	n/a	n/a	0.007	0.007
	Nonaromatic Aldehydes	**0.117**	**0.112**	**0.174**	**0.176**
	Acetaldehyde, hydroxy-	n/a	n/a	0.050	0.051
123-72-8	Butanal	0.017	0.017	0.011	0.011
15798-64-8	Crotonaldehyde, cis	0.038	0.037	0.032	0.032
123-73-9	Crotonaldehyde, trans	0.027	0.024	0.020	0.021
	2-Butenal, 2-methyl- (NIST MQ 92)	0.007	0.007	n/a	n/a
	Butanedial or Propanal (NIST MQ 88)	0.028	0.027	0.061	0.061
	Nonaromatic Ketones	**2.784**	**2.716**	**2.914**	**2.967**
116-09-6	Acetol (Hydroxypropanone)	1.194	1.161	1.615	1.647
78-93-3	Butanone, 2-	0.166	0.162	0.101	0.105
5077-67-8	Butanone, 1-hydroxy-2-	0.250	0.242	0.296	0.300
431-03-8	Butandione, 2,3- (Diacetyl)	0.221	0.219	0.187	0.185
513-86-0	Acetoin (Hydroxy-2-butanone, 3-)	0.064	0.064	0.064	0.065
592-20-1	Propan-2-one, 1-acetyloxy-	0.018	0.018	0.033	0.034
120-92-3	Cyclopentanone	0.087	0.086	0.052	0.052
930-30-3	Cyclopenten-1-one, 2-	0.290	0.286	0.230	0.236

	Cyclopenten-1-one, 2,3-dimethyl-2-	n/a	n/a	0.014	0.015
1120-73-6	Cyclopenten-1-one, 2-methyl-2-	0.115	0.113	0.078	0.080
2758-18-1	Cyclopenten-1-one, 3-methyl-2-	0.045	0.041	0.029	0.029
80-71-7	Cyclopenten-1-one, 2-hydroxy-3-methyl-2-	n/a	n/a	0.014	0.013
930-68-7	Cyclohexen-1-one, 2-	n/a	n/a	0.006	0.006
5682-69-2	Cylopenten-1-one, 3-ethyl-2-	0.007	0.006	n/a	n/a
930-68-7	Cyclohexen-1-one, 2-	0.007	0.007	n/a	n/a
	3-Buten-2-one (NIST MQ 88)	0.017	0.017	0.017	0.017
	Butanone, 3-methyl-2- (NIST MQ 88)	0.005	0.005	n/a	n/a
	3-Buten-2-one, 3-methyl- (NIST MQ 88)	0.007	0.007	0.005	0.005
	2-Pentanone (NIST MQ 94)	0.025	0.024	0.020	0.020
	3-Pentanone (NIST MQ 92)	0.012	0.013	0.008	0.007
	2,3-Pentanedione	0.061	0.060	0.043	0.044
	3-Penten-2-one (NIST MQ 84)	0.041	0.040	0.026	0.025
	2,3-Hexanedione (NIST MQ 78)	0.007	0.007	n/a	n/a
	Cyclopentanone, 2-methyl- (NIST MQ 87)	0.022	0.021	0.016	0.016
	Isomere of 2-Cyclopenten-1-one, 3-methyl-	0.024	0.023	0.016	0.017
	2-Butanone, 1-hydroxy-3-methyl- (NIST MQ 78)	0.010	0.010	0.010	0.012
	2-Cyclopenten-1-one, x,y-dimethyl-	0.018	0.017	0.010	0.010
	2-Cycolpenten-1-one, x,y-dimethyl-	0.012	0.012	0.007	0.008
	2,5-Hexanedione (NIST MQ 89)	0.006	0.007	0.005	0.005
	Isomere of Cyclopenten-1-one, 2,3-dimethyl-2-	0.024	0.022	n/a	n/a
	2-Cyclopenten-1-one, x,y-dimethyl-	0.013	0.013	0.014	0.014
	2-Cyclopenten-1-one, 2,3,4-trimethyl- (NIST MQ 88)	0.005	0.005	n/a	n/a
	Isomer of Cyclopenten-1-one, 3-ethyl-2-hydroxy-	0.008	0.008	n/a	n/a
	Aliphatic Hydrocarbons	**0.000**	**0.000**	**0.000**	**0.000**
	<u>HETEROCYCLIC COMPOUNDS</u>				
	Furans	**0.281**	**0.277**	**0.256**	**0.264**
98-01-1	Furaldehyde, 2-	0.197	0.195	0.176	0.182
498-60-2	Furaldehyde, 3-	0.016	0.016	0.012	0.014
620-02-0	Furaldehyde, 5-methyl-2-	0.011	0.010	0.009	0.009

1192-62-7	Ethanone, 1-(2-furanyl)-	0.018	0.017	0.013	0.014
591-12-8	Angelicalactone, α- (Furan-2-one, 2,3-dihydro-5-methyl-)	n/a	n/a	0.015	0.015
	Furan-2-one, 2,5-dihydro-3,5-dimethyl-	0.008	0.008	n/a	n/a
96-48-0	Butyrolactone, γ-	0.031	0.031	0.030	0.030
	Pyrans	**0.000**	**0.000**	**0.000**	**0.000**
	AROMATIC COMPOUNDS				
	Benzenes	**0.000**	**0.000**	**0.000**	**0.000**
	Catechols	**0.000**	**0.000**	**0.000**	**0.000**
	Aromatic Alcohols	**0.000**	**0.000**	**0.000**	**0.000**
	Aromatic Aldehydes	**0.002**	**0.002**	**0.000**	**0.000**
100-52-7	Benzaldehyde	0.002	0.002	n/a	n/a
	Aromatic Ketones	**0.000**	**0.000**	**0.000**	**0.000**
	Aromatic Esters	**0.000**	**0.000**	**0.000**	**0.000**
	Lignin-derived Phenols	**0.066**	**0.064**	**0.058**	**0.060**
108-95-2	Phenol	0.037	0.036	0.027	0.028
95-48-7	Cresol, o-	0.013	0.013	0.011	0.011
106-44-5	Cresol, p-	0.004	0.004	0.005	0.005
108-39-4	Cresol, m-	0.008	0.007	0.008	0.007
123-07-9	Phenol, 4-ethyl-	0.004	0.004	0.008	0.009
	Guaiacols (Methoxy phenols)	**0.046**	**0.046**	**0.042**	**0.044**
90-05-1	Guaiacol	0.036	0.036	0.031	0.032
93-51-6	Guaiacol, 4-methyl-	0.005	0.005	0.006	0.006
2785-89-9	Guaiacol, 4-ethyl-	0.005	0.005	0.006	0.006

Syringols (Dimethoxy phenols)	**0.000**	**0.000**	**0.000**	**0.000**
CARBOHYDRATES				
Sugars	**0.000**	**0.000**	**0.000**	**0.000**
OTHER ORGANIC COMPOUNDS				
N-compounds	**0.005**	**0.004**	**0.000**	**0.000**
Propanenitrile (NIST MQ 94)	0.005	0.004		
Acetates	**0.000**	**0.000**	**0.000**	**0.000**
Terpenes	**0.000**	**0.000**	**0.000**	**0.000**
unknown compounds	**0.000**	**0.000**	**0.000**	**0.000**
Miscellaneous	**0.002**	**0.002**	**0.000**	**0.000**
Ethane, 1-ethoxy-1-methoxy- (NIST MQ 94)	0.002	0.002		

Table C4. GC-MS data for the organic-rich condensate (ORC) obtained from single-step water quenching of pyrolysis vapors (*miscanthus*).

CAS No.	Compound	wt.% wet			
		Run 1	Run 2	Run 3	Run 4
	NONAROMATIC COMPOUNDS				
	Acids	**3.457**	**3.430**	**3.386**	**3.386**
64-19-7	Acetic acid	3.457	3.430	3.386	3.386
	Nonaromatic Esters	**0.000**	**0.000**	**0.000**	**0.000**
	Nonaromatic Alcohols	**0.000**	**0.000**	**0.000**	**0.000**
	Nonaromatic Aldehydes	**0.000**	**0.000**	**0.000**	**0.000**
	Nonaromatic Ketones	**3.954**	**3.826**	**3.745**	**3.724**
116-09-6	Acetol (Hydroxypropanone)	1.330	1.309	1.214	1.210
78-93-3	Butanone, 2-	0.083	0.076	0.096	0.100
5077-67-8	Butanone, 1-hydroxy-2-	0.345	0.343	0.337	0.341
431-03-8	Butandione, 2,3- (Diacetyl)	0.039	0.039	0.043	0.044
592-20-1	Propan-2-one, 1-acetyloxy-	0.058	0.061	0.063	0.063
120-92-3	Cyclopentanone	0.099	0.100	0.102	0.103
930-30-3	Cyclopenten-1-one, 2-	0.324	0.327	0.326	0.327
1120-73-6	Cyclopenten-1-one, 2-methyl-2-	0.236	0.235	0.075	0.047
2758-18-1	Cyclopenten-1-one, 3-methyl-2-	0.228	0.234	0.257	0.253
5682-69-2	Cylopenten-1-one, 3-ethyl-2-	0.076	0.079	0.234	0.231
80-71-7	Cyclopenten-1-one, 2-hydroxy-3-methyl-2-	0.802	0.689	0.081	0.080
	3-Penten-2-one (NIST MQ 84)	0.092	0.083	0.635	0.645
	2-Cyclopenten-1-one, x,y-dimethyl-	0.048	0.047	0.099	0.095
	Isomere of Cyclopenten-1-one, 2,3-dimethyl-2-	0.075	0.075	0.055	0.051
	2-Cyclopenten-1-one, x,y-dimethyl-	0.073	0.083	0.081	0.081
	2-Cyclopenten-1-one, 2,3,4-trimethyl- (NIST MQ 88)	0.044	0.045	0.049	0.052
	Aliphatic Hydrocarbons	**0.000**	**0.000**	**0.000**	**0.000**

	HETEROCYCLIC COMPOUNDS				
	Furans	**0.619**	**0.614**	**0.604**	**0.608**
98-01-1	Furaldehyde, 2-	0.384	0.396	0.410	0.418
498-60-2	Furaldehyde, 3-	0.017	0.019		
620-02-0	Furaldehyde, 5-methyl-2-	0.081	0.083	0.099	0.098
1192-62-7	Ethanone, 1-(2-furanyl)-	0.024	0.023	0.027	0.026
22122-36-7	Furan-2-one, 3-methyl-, (5H)-	n/a	n/a	0.067	0.066
96-48-0	Butyrolactone, γ-	0.113	0.094	n/a	n/a
	Pyrans	**0.000**	**0.000**	**0.000**	**0.000**
	AROMATIC COMPOUNDS				
	Benzenes	**0.000**	**0.000**	**0.109**	**0.108**
135-19-3	Naphthalenol, 2-			0.045	0.043
83-33-0	Inden-1-one, 2,3-dihydro-1H-			0.064	0.065
	Catechols	**0.000**	**0.000**	**n.q.**	**n.q.**
	Benzenediol, methyl-			n.q.	n.q.
	Aromatic Alcohols	**0.000**	**0.000**	**0.000**	**0.000**
	Aromatic Aldehydes	**0.000**	**0.000**	**0.000**	**0.000**
	Aromatic Ketones	**0.000**	**0.000**	**0.000**	**0.000**
	Aromatic Esters	**0.000**	**0.000**	**0.000**	**0.000**
	Lignin-derived Phenols	**7.200**	**7.269**	**8.107**	**7.778**
108-95-2	Phenol	0.372	0.377	0.389	0.384
95-48-7	Cresol, o-	0.272	0.276	0.290	0.289
106-44-5	Cresol, p-	0.261	0.266	0.312	0.312

108-39-4	Cresol, m-	0.168	0.169	0.187	0.184
95-87-4	Phenol, 2,5-dimethyl-	0.124	0.124	0.137	0.141
105-67-9	Phenol, 2,4-dimethyl-	0.110	0.114	0.132	0.128
526-75-0	Phenol, 2,3-dimethyl-	0.042	0.042	0.044	0.043
108-68-9	Phenol, 3,5-dimethyl-	0.027	0.028	0.033	0.035
90-00-6	Phenol, 2-ethyl-	0.053	0.052	0.055	0.055
123-07-9	Phenol, 4-ethyl-	1.694	1.724	2.243	2.224
2628-17-3	Phenol, 4-vinyl-	3.574	3.585	3.723	3.431
85960-81-2	Phenol , cis 4-propenyl-	0.090	0.091	0.095	0.094
5932-68-3	Phenol, trans 4-propenyl-	0.223	0.225	0.253	0.244
	Phenol, ethyl-methyl-	0.133	0.135	0.152	0.152
	Phenol, 4-methyl-2-(2-propenyl)- (NIST MQ 88)	0.057	0.062	0.064	0.064
	Guaiacols (Methoxy phenols)	**5.816**	**5.915**	**6.266**	**6.116**
90-05-1	Guaiacol	0.379	0.385	0.383	0.378
93-51-6	Guaiacol, 4-methyl-	0.353	0.358	0.404	0.398
2785-89-9	Guaiacol, 4-ethyl-	0.358	0.363	0.426	0.423
7786-61-0	Guaiacol, 4-vinyl-	1.305	1.315	1.456	1.316
97-53-0	Guaiacol, 4-allyl-; (Eugenol)	0.222	0.222	0.248	0.245
2785-87-7	Guaiacol, 4-propyl-	0.061	0.061	0.069	0.071
97-54-1	Guaiacol, 4-propenyl- cis (Isoeugenol)	0.459	0.512	0.526	0.496
5932-68-3	Guaiacol, 4-propenyl-(trans) (Isoeugenol)	1.549	1.543	1.699	1.723
121-33-5	Vanillin	0.574	0.582	0.603	0.601
498-02-2	Ethanone, 1-(4-hydroxy-3-methoxyphenyl)- (Acetoguaiacone)	0.465	0.480	0.453	0.466
2503-46-0	Guaiacyl acetone	0.092	0.094		
	Syringols (Dimethoxy phenols)	**2.834**	**2.856**	**3.046**	**3.029**
91-10-1	Syringol	0.308	0.318	0.324	0.325
6638-05-7	Syringol, 4-methyl-	0.301	0.303	0.336	0.332
14059-92-8	Syringol, 4-ethyl-	0.131	0.133	0.151	0.146
28343-22-8	Syringol, 4-vinyl-	0.510	0.507	0.517	0.515
6627-88-9	Syringol, 4-allyl-	0.306	0.308	0.331	0.328
26624-13-5	Syringol, 4-(1-propenyl)-, cis	0.184	0.183	0.195	0.196

20675-95-0	Syringol, 4-(1-propenyl)-, trans	0.654	0.656	0.709	0.705
134-96-3	Syringaldehyde	0.205	0.204	0.225	0.228
2478-38-8	Acetosyringone	0.119	0.121	0.123	0.120
	Syringyl acetone	0.115	0.122	0.133	0.133
	CARBOHYDRATES				
	Sugars	**1.273**	**1.152**	**0.000**	**0.000**
498-07-7	Anhydro-ß-D-glucopyranose, 1,6- (Levoglucosan)	1.273	1.152		
	OTHER ORGANIC COMPOUNDS				
	N-compounds	**0.000**	**0.000**	**0.000**	**0.000**
	Acetates	**0.000**	**0.000**	**0.000**	**0.000**
	Terpenes	**0.000**	**0.000**	**0.000**	**0.000**
	unknown compounds	**0.000**	**0.000**	**0.000**	**0.000**
	Miscellaneous	**0.000**	**0.000**	**0.000**	**0.000**

Table C5. GC-MS data for the recovered quench (extract) obtained from single-step water quenching of pyrolysis vapors *(miscanthus).*

CAS No.	Compound	wt.% wet			
		Run 1	Run 2	Run 3	Run 4
	NONAROMATIC COMPOUNDS				
	Acids	**1.764**	**1.773**	**1.758**	**1.770**
64-19-7	Acetic acid	1.303	1.316	1.284	1.291
79-09-4	Propionic acid	0.405	0.405	0.414	0.417
107-92-6	Butyric acid	0.056	0.053	0.061	0.062
	Nonaromatic Esters	**0.000**	**0.000**	**0.000**	**0.000**
	Nonaromatic Alcohols	**0.067**	**0.067**	**0.054**	**0.052**
107-21-1	Ethylene glycol	0.067	0.067	0.054	0.052
	Nonaromatic Aldehydes	**0.170**	**0.174**	**0.094**	**0.096**
141-46-8	Acetaldehyde, hydroxy-	0.114	0.116	0.042	0.042
15798-64-8	Crotonaldehyde, cis	0.012	0.011	0.013	0.013
123-73-9	Crotonaldehyde, trans	0.007	0.007	0.007	0.007
	Butanedial or Propanal (NIST MQ 88)	0.038	0.040	0.033	0.034
	Nonaromatic Ketones	**1.954**	**1.955**	**1.894**	**1.917**
116-09-6	Acetol (Hydroxypropanone)	1.352	1.357	1.285	1.304
78-93-3	Butanone, 2-	0.020	0.020	0.024	0.024
5077-67-8	Butanone, 1-hydroxy-2-	0.178	0.177	0.180	0.181
431-03-8	Butandione, 2,3- (Diacetyl)	0.019	0.019	0.020	0.021
513-86-0	Acetoin (Hydroxy-2-butanone, 3-)	0.021	0.021	0.025	0.026
592-20-1	Propan-2-one, 1-acetyloxy-	0.034	0.033	0.034	0.034
120-92-3	Cyclopentanone	0.023	0.022	0.022	0.021
930-30-3	Cyclopenten-1-one, 2-	0.081	0.081	0.078	0.078
1120-73-6	Cyclopenten-1-one, 2-methyl-2-	0.019	0.019	0.020	0.020
2758-18-1	Cyclopenten-1-one, 3-methyl-2-	0.024	0.023	0.022	0.022
10493-98-8	Cyclopenten-1-one, 2-hydroxy-2-	0.026	0.024	0.026	0.025

80-71-7	Cyclopenten-1-one, 2-hydroxy-3-methyl-2-	0.130	0.129	0.118	0.119
	3-Buten-2-one (NIST MQ 88)	0.008	0.008	0.009	0.009
	3-Buten-2-one, 3-methyl- (NIST MQ 88)	n/a	n/a	0.003	0.003
	2,3-Pentanedione	n/a	n/a	0.004	0.004
	3-Penten-2-one (NIST MQ 84)	0.004	0.004	0.005	0.005
	Cyclopentanone, 2-methyl- (NIST MQ 87)	n/a	n/a	0.004	0.004
	Isomere of 2-Cyclopenten-1-one, 3-methyl-	n/a	n/a	0.003	0.003
	2-Butanone, 1-hydroxy-3-methyl- (NIST MQ 78)	0.008	0.009	0.008	0.008
	Isomer of Cyclopenten-1-one, 3-ethyl-2-hydroxy-	0.007	0.007	0.005	0.005
	Aliphatic Hydrocarbons	**0.000**	**0.000**	**0.000**	**0.000**
	HETEROCYCLIC COMPOUNDS				
	Furans	**0.279**	**0.279**	**0.269**	**0.274**
98-00-0	Furfuryl alcohol, 2-	0.029	0.028	0.029	0.029
497-23-4	Furanone, 2(5H)-	0.052	0.053	0.047	0.050
98-01-1	Furaldehyde, 2-	0.069	0.069	0.069	0.070
498-60-2	Furaldehyde, 3-	0.004	0.004	0.005	0.005
620-02-0	Furaldehyde, 5-methyl-2-	0.007	0.007	0.007	0.007
1192-62-7	Ethanone, 1-(2-furanyl)-	0.003	0.003	n/a	n/a
591-11-7	Furan-2-one, 5-methyl-, (5H)-	0.010	0.010	0.012	0.012
22122-36-7	Furan-2-one, 3-methyl-, (5H)-	0.011	0.011	0.014	0.014
	Furan-2-one, 2,5-dihydro-3,5-dimethyl-	n/a	n/a	0.011	0.011
96-48-0	Butyrolactone, γ-	0.046	0.046	0.049	0.049
19444-84-9	Butyrolactone, 2-hydroxy-, γ-	0.027	0.027	n/a	n/a
	Furan-2-one, 4-methyl-(5H)- (NIST MQ 88)	0.014	0.014	0.017	0.017
	Isomer of 2-Furanone, 2,5-dihydro-3,5-dimethyl-	0.008	0.008	0.009	0.009
	Pyrans	**0.000**	**0.000**	**0.000**	**0.000**
	AROMATIC COMPOUNDS				
	Benzenes	**0.000**	**0.000**	**0.000**	**0.000**

	Catechols	**n.q.**	n.q.	**n.q.**	**n.q.**
123-31-9	Hydroquinone (Benzene, 1,4-dihydroxy-)	n.q.	n.q.	n.q.	n.q.
	Resorcinol (Benzene, 1,3-dihydroxy-)	n/a	n/a	n.q.	n.q.
	Benzenediol, methyl-	n.q.	n.q.	n.q.	n.q.
	Aromatic Alcohols	**0.000**	**0.000**	**0.000**	**0.000**
	Aromatic Aldehydes	**0.000**	**0.000**	**0.000**	**0.000**
	Aromatic Ketones	**0.000**	**0.000**	**0.000**	**0.000**
	Aromatic Esters	**0.000**	**0.000**	**0.000**	**0.000**
	Lignin-derived Phenols	**0.113**	**0.111**	**0.122**	**0.123**
108-95-2	Phenol	0.035	0.034	0.034	0.034
95-48-7	Cresol, o-	0.015	0.014	0.014	0.014
106-44-5	Cresol, p-	0.009	0.009	0.009	0.009
108-39-4	Cresol, m-	0.006	0.006	0.006	0.006
123-07-9	Phenol, 4-ethyl-	0.023	0.023	0.026	0.027
2628-17-3	Phenol, 4-vinyl-	0.026	0.026	0.025	0.025
121-33-5	Vanillin	n/a	n/a	0.008	0.008
	Guaiacols (Methoxy phenols)	**0.074**	**0.074**	**0.106**	**0.107**
90-05-1	Guaiacol	0.024	0.024	0.022	0.022
93-51-6	Guaiacol, 4-methyl-	0.008	0.009	0.009	0.009
2785-89-9	Guaiacol, 4-ethyl-			0.003	0.003
7786-61-0	Guaiacol, 4-vinyl-	0.005	0.005	0.005	0.005
121-33-5	Vanillin	0.037	0.036	0.039	0.039
498-02-2	Ethanone, 1-(4-hydroxy-3-methoxyphenyl)- (Acetoguaiacone)	n/a	n/a	0.027	0.028
	Syringols (Dimethoxy phenols)	**0.019**	**0.019**	**0.026**	**0.026**
91-10-1	Syringol	0.012	0.013	0.013	0.013

6638-05-7	Syringol, 4-methyl-	0.006	0.006	0.006	0.006
2478-38-8	Acetosyringone	n/a	n/a	0.004	0.004
	Syringyl acetone	n/a	n/a	0.003	0.004
	CARBOHYDRATES				
	Sugars	**0.856**	**0.849**	**0.965**	**0.954**
	Anhydro-ß-D-arabinofuranose, 1,5-	0.033	0.033	0.033	0.034
51246-94-7	Anhydro-ß-D-xylofuranose, 1,5-	0.107	0.106	0.112	0.112
498-07-7	Anhydro-ß-D-glucopyranose, 1,6- (Levoglucosan)	0.583	0.579	0.681	0.675
4451-31-4	Dianhydro-α-D-glucopyranose, 1,4:3,6-	0.059	0.057	0.058	0.056
	poss: 2,3-Anhydro-d-galactosan (NIST MQ 78)	0.033	0.032	0.036	0.034
	poss: 2,3-Anhydro-d-mannosan (NIST MQ 84)	0.041	0.041	0.045	0.043
	OTHER ORGANIC COMPOUNDS				
	N-compounds	**0.000**	**0.000**	**0.000**	**0.000**
	Acetates	**0.000**	**0.000**	**0.000**	**0.000**
	Terpenes	**0.000**	**0.000**	**0.000**	**0.000**
	unknown compounds	**0.000**	**0.000**	**0.000**	**0.000**
	Miscellaneous	**0.000**	**0.000**	**0.000**	**0.000**

Table C6. GC-MS data for the aqueous condensate (AC) obtained following water quenching of pyrolysis vapors in a single-step condensation *(miscanthus)*.

CAS No.	Compound	wt.% wet			
		Run 1	**Run 2**	**Run 3**	**Run 4**
	NONAROMATIC COMPOUNDS				
	Acids	**2.057**	**2.067**	**2.013**	**1.993**
64-19-7	Acetic acid	1.552	1.558	1.501	1.484
79-09-4	Propionic acid	0.440	0.444	0.446	0.444
107-92-6	Butyric acid	0.065	0.065	0.066	0.065
	Nonaromatic Esters	**0.000**	**0.000**	**0.000**	**0.000**
	Nonaromatic Alcohols	**0.023**	**0.023**	**0.026**	**0.026**
	poss: Glycerin	0.023	0.023	0.026	0.026
	Nonaromatic Aldehydes	**0.264**	**0.262**	**0.176**	**0.177**
141-46-8	Acetaldehyde, hydroxy-	0.065	0.063	0.016	0.016
2134-29-4	Propanal, 3-hydroxy-	0.023	0.022	0.073	0.073
123-72-8	Butanal	0.012	0.013	0.022	0.023
15798-64-8	Crotonaldehyde, cis	0.060	0.060	0.006	0.006
123-73-9	Crotonaldehyde, trans	0.020	0.020	0.059	0.059
	2-Butenal, 2-methyl- (NIST MQ 92)	0.005	0.005	n/a	n/a
	2-Pentenal, (E)- (NIST MQ 89)	0.006	0.006	n/a	n/a
	Butanedial or Propanal (NIST MQ 88)	0.072	0.073	n/a	n/a
	Nonaromatic Ketones	**2.834**	**2.856**	**2.747**	**2.730**
116-09-6	Acetol (Hydroxypropanone)	1.676	1.687	1.523	1.506
78-93-3	Butanone, 2-	0.087	0.088	0.110	0.113
5077-67-8	Butanone, 1-hydroxy-2-	0.241	0.244	0.232	0.230
431-03-8	Butandione, 2,3- (Diacetyl)	0.201	0.200	0.227	0.229
513-86-0	Acetoin (Hydroxy-2-butanone, 3-)	0.042	0.045	0.039	0.040
592-20-1	Propan-2-one, 1-acetyloxy-	0.038	0.038	0.039	0.038
120-92-3	Cyclopentanone	0.038	0.038	0.039	0.039

930-30-3	Cyclopenten-1-one, 2-	0.173	0.175	0.177	0.173
1121-05-7	Cyclopenten-1-one, 2,3-dimethyl-2-	0.008	0.008	0.006	0.007
1120-73-6	Cyclopenten-1-one, 2-methyl-2-	0.054	0.055	0.058	0.058
2758-18-1	Cyclopenten-1-one, 3-methyl-2-	0.025	0.025	0.021	0.021
5682-69-2	Cylopenten-1-one, 3-ethyl-2-	0.005	0.005	n/a	n/a
80-71-7	Cyclopenten-1-one, 2-hydroxy-3-methyl-2-	0.024	0.025	0.016	0.016
930-68-7	Cyclohexen-1-one, 2-	0.004	0.004	0.005	0.005
	3-Buten-2-one (NIST MQ 88)	0.040	0.039	0.047	0.046
	Butanone, 3-methyl-2- (NIST MQ 88)	n/a	n/a	0.006	0.006
	3-Buten-2-one, 3-methyl- (NIST MQ 88)	0.014	0.014	0.018	0.017
	2-Pentanone (NIST MQ 94)	0.020	0.020	0.021	0.023
	3-Pentanone (NIST MQ 92)	0.007	0.007	0.009	0.009
	2,3-Pentanedione	0.041	0.041	0.046	0.046
	3-Penten-2-one (NIST MQ 84)	0.031	0.032	0.037	0.037
	2,3-Hexanedione (NIST MQ 78)	0.005	0.005	0.005	0.005
	Cyclopentanone, 2-methyl- (NIST MQ 87)	0.012	0.012	0.013	0.013
	Isomere of 2-Cyclopenten-1-one, 3-methyl-	0.012	0.012	0.012	0.012
	2-Butanone, 1-hydroxy-3-methyl- (NIST MQ 78)	0.010	0.011	0.008	0.008
	2-Cyclopenten-1-one, x,y-dimethyl-	0.007	0.007	0.008	0.008
	2-Cycolpenten-1-one, x,y-dimethyl-			0.006	0.006
	Isomere of Cyclopenten-1-one, 2,3-dimethyl-2-	0.009	0.010	0.010	0.010
	2-Cyclopenten-1-one, 2,3,4-trimethyl- (NIST MQ 88)	0.004	0.003	0.003	0.003
	similar to 2-Cyclopenten-1-one, 3-ethyl-	n/a	n/a	0.004	0.004
	Isomer of Cyclopenten-1-one, 3-ethyl-2-hydroxy-	0.005	0.005	n/a	n/a
	Aliphatic Hydrocarbons	**0.000**	**0.000**	**0.000**	**0.000**
	HETEROCYCLIC COMPOUNDS				
	Furans	**0.281**	**0.284**	**0.343**	**0.339**
	Furanone, 2(5H)-			0.024	0.023
98-01-1	Furaldehyde, 2-	0.203	0.206	0.236	0.233
498-60-2	Furaldehyde, 3-	0.017	0.016	0.018	0.018
620-02-0	Furaldehyde, 5-methyl-2-	0.010	0.011	0.013	0.012

1192-62-7	Ethanone, 1-(2-furanyl)-	0.008	0.008	0.009	0.009
22122-36-7	Furan-2-one, 3-methyl-, (5H)-	0.004	0.004	0.005	0.004
	Furan-2-one, 2,5-dihydro-3,5-dimethyl-	0.008	0.007	0.005	0.005
591-12-8	Angelicalactone, α- (Furan-2-one, 2,3-dihydro-5-methyl-)	0.011	0.011	0.015	0.016
96-48-0	Butyrolactone, γ-	0.021	0.021	0.018	0.018
	Pyrans	**0.000**	**0.000**	**0.000**	**0.000**
	AROMATIC COMPOUNDS				
	Benzenes	**0.000**	**0.000**	**0.000**	**0.000**
	Catechols	**0.000**	**0.000**	**0.000**	**0.000**
	Aromatic Alcohols	**0.000**	**0.000**	**0.000**	**0.000**
	Aromatic Aldehydes	**0.000**	**0.000**	**0.000**	**0.000**
	Aromatic Ketones	**0.000**	**0.000**	**0.000**	**0.000**
	Aromatic Esters	**0.000**	**0.000**	**0.000**	**0.000**
	Lignin-derived Phenols	**0.082**	**0.085**	**0.078**	**0.077**
108-95-2	Phenol	0.038	0.039	0.032	0.031
95-48-7	Cresol, o-	0.015	0.015	0.012	0.012
106-44-5	Cresol, p-	0.007	0.008	0.006	0.006
108-39-4	Cresol, m-	0.010	0.011	0.009	0.009
95-87-4	Phenol, 2,5-dimethyl-	n/a	n/a	0.006	0.006
105-67-9	Phenol, 2,4-dimethyl-	n/a	n/a	0.002	0.002
123-07-9	Phenol, 4-ethyl-	0.012	0.013	0.011	0.012
	Guaiacols (Methoxy phenols)	**0.050**	**0.052**	**0.046**	**0.045**
90-05-1	Guaiacol	0.034	0.035	0.032	0.032

93-51-6	Guaiacol, 4-methyl-	0.008	0.008	0.007	0.007
2785-89-9	Guaiacol, 4-ethyl-	0.008	0.008	0.006	0.006
	Syringols (Dimethoxy phenols)	**0.000**	**0.000**	**0.000**	**0.000**
	CARBOHYDRATES				
	Sugars	**0.000**	**0.000**	**0.000**	**0.000**
	OTHER ORGANIC COMPOUNDS				
	N-compounds	**0.000**	**0.000**	**0.000**	**0.000**
	Acetates	**0.000**	**0.000**	**0.000**	**0.000**
	Terpenes	**0.000**	**0.000**	**0.000**	**0.000**
	unknown compounds	**0.000**	**0.000**	**0.000**	**0.000**
	Miscellaneous	**0.000**	**0.000**	**0.000**	**0.000**

c = calibrated compound
n.q. = not quantified
# = estimated response factor

Section 2: GC-MS Data for All Organic-Rich Condensates (ORC) and Aqueous Condensates (AC) Obtained from the Bioliq® Facility Following Fast Pyrolysis of Wheat Straw (2018 Campaign) and *Miscanthus* (2019 Campaign)

Table C7. GC-MS data for organic-rich condensate (ORC) obtained from wheat straw fast pyrolysis using the bioliq® (2018 campaign).

		Run 1		Run 2	
CAS-No.	**Compound**	**wt.% wet**	**wt.% dry**	**wt.% wet**	**wt.% dry**
	NONAROMATIC COMPOUNDS				
	Acids	**4.952**	**5.84**	**4.990**	**5.88**
64-19-7	Acetic acid	4.952	5.840	4.990	5.884
	Nonaromatic Esters	**0.000**	**0.00**	**0.000**	**0.00**
	Nonaromatic Alcohols	**2.488**	**2.93**	**2.375**	**2.80**
107-21-1	Ethylene glycol	2.488	2.934	2.375	2.801
	Nonaromatic Aldehydes	**0.000**	**0.00**	**0.000**	**0.00**
	Nonaromatic Ketones	**6.870**	**8.10**	**6.723**	**7.93**
116-09-6	Acetol (Hydroxypropanone)	4.401	5.190	4.314	5.088
5077-67-8	Butanone, 1-hydroxy-2-	0.777	0.916	0.705	0.832
592-20-1	Propan-2-one, 1-acetyloxy-	0.068	0.081	0.070	0.083
930-30-3	Cyclopenten-1-one, 2-	0.219	0.258	0.219	0.258
1120-73-6	Cyclopenten-1-one, 2-methyl-2-	0.100	0.118	0.100	0.118
2758-18-1	Cyclopenten-1-one, 3-methyl-2-	0.179	0.212	0.181	0.213
80-71-7	Cyclopenten-3-one, 2-hydroxy-1-methyl-1-	1.016	1.198	1.021	1.204
	2-Cyclopenten-1-one, 2,3,4-trimethyl- (NIST MQ 88)	0.034	0.040	0.036	0.043
	Isomer of Cyclopenten-1-one, 3-ethyl-2-hydroxy-	0.076	0.090	0.077	0.091
	Hydrocarbons	**0.000**	**0.00**	**0.000**	**0.00**

	HETEROCYCLIC COMPOUNDS				
	Furans	**0.464**	**0.55**	**0.446**	**0.53**
497-23-4	Furanone, 2(5H)-	0.134	0.158	0.131	0.154
22122-36-7	Furan-2-one, 3-methyl-, (5H)-	0.079	0.093	0.077	0.091
96-48-0	Butyrolactone, γ-	0.251	0.296	0.238	0.281
	Pyrans	**0.000**	**0.00**	**0.000**	**0.00**
	AROMATIC COMPOUNDS				
	Benzenes	**0.021**	**0.03**	**0.024**	**0.03**
83-33-0	Inden-1-one, 2,3-dihydro-1H-	0.021	0.025	0.024	0.028
	Catechols	**n.q.**	**n.q.**	**n.q.**	**n.q.**
123-31-9	Hydroquinone (Benzene, 1,4-dihydroxy-)	n.q.	n.q.	n.q.	n.q.
608-25-3	Resorcinol, 2-methyl-	n.q.	n.q.	n.q.	n.q.
	Aromatic Alcohols	**0.000**	**0.00**	**0.000**	**0.00**
	Aromatic Aldehydes	**0.000**	**0.00**	**0.000**	**0.00**
	Aromatic Ketones	**0.000**	**0.00**	**0.000**	**0.00**
	Aromatic Esters	**0.000**	**0.00**	**0.000**	**0.00**
	Lignin-derived Phenols	**1.189**	**1.40**	**1.188**	**1.40**
108-95-2	Phenol	0.217	0.256	0.221	0.261
95-48-7	Cresol, o-	0.215	0.254	0.215	0.254
106-44-5	Cresol, p-	0.069	0.082	0.069	0.082

108-39-4	Cresol, m-	0.098	0.115	0.099	0.117
95-87-4	Phenol, 2,5-dimethyl-	0.101	0.119	0.099	0.116
105-67-9	Phenol, 2,4-dimethyl-	0.029	0.035	0.031	0.037
108-68-9	Phenol, 3,5-dimethyl-	0.012	0.014	0.012	0.014
620-17-7	Phenol, 3-ethyl-	0.122	0.144	0.121	0.142
123-07-9	Phenol, 4-ethyl-	0.102	0.120	0.109	0.128
	Phenol, 4-vinyl-	0.223	0.263	0.212	0.250
	Guaiacols (Methoxy phenols)	**2.006**	**2.37**	**2.033**	**2.40**
90-05-1	Guaiacol	0.370	0.436	0.380	0.448
93-51-6	Guaiacol, 4-methyl-	0.121	0.142	0.122	0.143
2785-89-9	Guaiacol, 4-ethyl-	0.147	0.173	0.151	0.179
7786-61-0	Guaiacol, 4-vinyl-	0.286	0.337	0.290	0.342
97-53-0	Guaiacol, 4-allyl- (Eugenol)	0.059	0.070	0.061	0.072
97-54-1	Guaiacol, 4-propenyl- cis (Isoeugenol)	0.118	0.139	0.121	0.143
5932-68-3	Guaiacol, 4-propenyl-(trans) (Isoeugenol)	0.473	0.558	0.472	0.557
121-33-5	Vanillin	0.340	0.401	0.340	0.401
2503-46-0	Guaiacyl acetone	0.092	0.108	0.095	0.112
	Syringols (Dimethoxy phenols)	**1.627**	**1.92**	**1.657**	**1.95**
91-10-1	Syringol	0.477	0.562	0.475	0.560
	Syringol, 4-methyl-	0.122	0.144	0.122	0.144
	Syringol, 4-ethyl-	0.103	0.122	0.108	0.128
	Syringol, 4-vinyl-	0.160	0.189	0.162	0.191
6627-88-9	Syringol, 4-allyl-	0.146	0.172	0.153	0.180
627-88-9	Syringol, 4-(1-propenyl)-, cis	0.050	0.058	0.054	0.064
	Syringol, 4-(1-propenyl)-, trans	0.290	0.342	0.298	0.351
134-96-3	Syringaldehyde	0.081	0.095	0.079	0.093
2478-38-8	Acetosyringone	0.141	0.166	0.150	0.177
	Syringyl acetone	0.056	0.066	0.055	0.065
	CARBOHYDRATES				

	Sugars	**1.994**	**2.35**	**1.948**	**2.30**
7732-18-5	Anhydro-ß-D-arabinofuranose, 1,5-	0.287	0.338	0.273	0.321
498-07-7	Anhydro-ß-D-glucopyranose, 1,6- (Levoglucosan)	1.367	1.612	1.339	1.579
	Dianhydro-α-D-glucopyranose, 1,4:3,6-	0.340	0.401	0.336	0.396
	OTHER ORGANIC COMPOUNDS				
	N-compounds	**0.000**	**0.00**	**0.000**	**0.00**
	Acetates	**0.000**	**0.00**	**0.000**	**0.00**
	Terpenes	**0.000**	**0.00**	**0.000**	**0.00**
	unknown compounds	**0.000**	**0.00**	**0.000**	**0.00**
	Miscellaneous	**0.000**	**0.00**	**0.000**	**0.00**

Table C8. GC-MS data for aqueous condensate (AC) obtained from wheat straw fast pyrolysis using the bioliq® (2018 campaign).

		Run 1		Run 2	
CAS-No.	**Compound**	**wt.% wet**	**wt.% dry**	**wt.% wet**	**wt.% dry**
	NONAROMATIC COMPOUNDS				
	Acids	**4.141**	**20.40**	**4.168**	**20.53**
64-19-7	Acetic acid	3.081	15.180	3.106	15.302
79-09-4	Propionic acid	1.059	5.219	1.062	5.232
	Nonaromatic Esters	**0.020**	**0.10**	**0.019**	**0.10**
	poss. Propanoic acid, ethenyl ester (NIST MQ 75)	0.020	0.101	0.019	0.096
	Nonaromatic Alcohols	**0.206**	**1.02**	**0.210**	**1.04**
107-21-1	Ethylene glycol	0.206	1.015	0.210	1.036
	Nonaromatic Aldehydes	**0.366**	**1.80**	**0.364**	**1.79**
141-46-8	Acetaldehyde, hydroxy-	0.222	1.094	0.228	1.125
	Propionaldehyde, 3-hydroxy	0.043	0.211	0.036	0.178
	2-Butenal (NIST MQ 87)	0.061	0.299	0.060	0.295
	Butandial (or Propanal) (NIST MQ 92)	0.040	0.199	0.039	0.194
	Nonaromatic Ketones	**8.253**	**40.65**	**8.271**	**40.74**
116-09-6	Acetol (Hydroxypropanone)	5.400	26.601	5.415	26.673
110-13-4	Acetonylacetone (Hexandione, 2,5-)	0.013	0.063	0.012	0.061
78-93-3	Butanone, 2-	0.206	1.015	0.206	1.016
5077-67-8	Butanone, 1-hydroxy-2-	0.697	3.432	0.695	3.425
431-03-8	Butandione, 2,3- (Diacetyl)	0.249	1.225	0.254	1.251
513-86-0	Acetoin (Hydroxy-2-butanone, 3-)	0.144	0.712	0.147	0.724
592-20-1	Propan-2-one, 1-acetyloxy-	0.117	0.577	0.118	0.580
120-92-3	Cyclopentanone	0.106	0.523	0.106	0.520
930-30-3	Cyclopenten-1-one, 2-	0.353	1.739	0.348	1.716

1121-05-7	Cyclopenten-1-one, 2,3-dimethyl-2-	0.023	0.112	0.025	0.125
1120-73-6	Cyclopenten-1-one, 2-methyl-2-	0.141	0.693	0.140	0.690
2758-18-1	Cyclopenten-1-one, 3-methyl-2-	0.074	0.363	0.074	0.365
568-26-99	Cylopenten-1-one, 3-ethyl-2-	0.009	0.046	0.009	0.045
930-68-7	Cyclohexen-1-one, 2-	0.012	0.059	0.012	0.058
	Methyl vinyl ketone = 2-Butenone (NIST MQ 84)	0.018	0.087	0.018	0.091
	poss: 2-Butanone, 3-methyl- (NIST MQ 88)	0.009	0.044	0.009	0.045
	poss: 3-Buten-2-one, 3-methyl- (NIST MQ 82)	0.017	0.085	0.017	0.084
	2-Pentanone (NIST MQ 94)	0.055	0.271	0.057	0.279
	2,3-Pentanedione	0.067	0.332	0.068	0.334
	3-Penten-2-one (NIST MQ 84)	0.049	0.242	0.049	0.244
	Cyclopentanone, 2-methyl- (NIST MQ 87)	0.037	0.182	0.034	0.169
	Cyclopentanone, 3-methyl- (NIST MQ 92)	0.027	0.132	0.028	0.140
	Isomere of 2-Cyclopenten-1-one, 3-methyl-	0.028	0.139	0.028	0.136
	2-Butanone, 1-hydroxy-3-methyl- (NIST MQ 78)	0.024	0.117	0.022	0.109
	5,9-Dodecadien-2-one, 6,10-dimethyl-, (E,E))-	0.028	0.138	0.029	0.141
	2-Cyclopenten-1-one, 3,4-dimethyl-	0.028	0.138	0.028	0.138
	Isomere of 2-Cyclopenten-1-one, 3,4-dimethyl-	0.016	0.080	0.016	0.080
	Isomere of Cyclopenten-1-one, 2,3-dimethyl-2-	0.050	0.245	0.050	0.245
	2-Cyclopenten-1-one, 3,4-dimethyl- (NIST MQ 94)	0.040	0.195	0.040	0.198
	1,2-Cyclopentanedione, 3-methyl- (NIST MQ 78)	0.170	0.840	0.165	0.815
	2-Cyclopenten-1-one, 2,3,4-trimethyl- (NIST MQ 88)	0.019	0.095	0.022	0.107
	Isomer of Cyclopenten-1-one, 3-ethyl-2-hydroxy-	0.020	0.096	0.020	0.098
	poss: 2-Cyclopenten-1-one, trimethyl- (NIST MQ 82)	0.008	0.038	0.008	0.040
	Hydrocarbons	**0.000**	**0.00**	**0.000**	**0.00**
	HETEROCYCLIC COMPOUNDS				
	Furans	**0.497**	**2.45**	**0.493**	**2.43**
98-00-0	Furfuryl alcohol, 2-	0.042	0.205	0.045	0.220
98-01-1	Furaldehyde, 2-	0.295	1.451	0.287	1.412
498-60-2	Furaldehyde, 3-	0.013	0.062	0.014	0.069

620-02-0	Furaldehyde, 5-methyl-2-	0.017	0.085	0.016	0.076
1192-62-7	Ethanone, 1-(2-furanyl)-	0.031	0.155	0.031	0.154
22122-36-7	Furan-2-one, 3-methyl-, (5H)-	0.010	0.050	0.010	0.049
96-48-0	Butyrolactone, γ-	0.080	0.395	0.082	0.403
	Furan, tetrahydro-2-methoxy- (NIST MQ (/)	0.009	0.045	0.009	0.044
	Pyrans	**0.000**	**0.00**	**0.000**	**0.00**
	AROMATIC COMPOUNDS				
	Benzenes	**0.058**	**0.29**	**0.058**	**0.28**
108-88-3	Toluene	0.012	0.059	0.012	0.058
4265-25-2	Benzofuran, 2-methyl-	0.004	0.018	0.004	0.018
104-93-8	Benzene, 1-methoxy-4-methyl-	0.008	0.040	0.007	0.037
91-20-3	Naphthalene	0.003	0.015	0.003	0.016
90-12-0	Naphthalene, 1-methyl-	0.024	0.117	0.023	0.115
95-13-6	Indene	0.008	0.038	0.008	0.040
	Catechols	**0.000**	**0.00**	**0.000**	**0.00**
	Aromatic Alcohols	**0.000**	**0.00**	**0.000**	**0.00**
	Aromatic Aldehydes	**0.008**	**0.04**	**0.007**	**0.03**
100-52-7	Benzaldehyde	0.008	0.039	0.007	0.034
	Aromatic Ketones	**0.000**	**0.00**	**0.000**	**0.00**
	Aromatic Esters	**0.000**	**0.00**	**0.000**	**0.00**
	Lignin-derived Phenols	**0.240**	**1.18**	**0.234**	**1.15**
108-95-2	Phenol	0.070	0.344	0.070	0.344
95-48-7	Cresol, o-	0.053	0.259	0.053	0.261

106-44-5	Cresol, p-	0.019	0.096	0.019	0.094
108-39-4	Cresol, m-	0.023	0.113	0.021	0.106
95-87-4	Phenol, 2,5-dimethyl-	0.020	0.098	0.020	0.098
105-67-9	Phenol, 2,4-dimethyl-	0.009	0.046	0.008	0.041
576-26-1	Phenol, 2,6-dimethyl-	0.007	0.033	0.006	0.032
90-00-6	Phenol, 2-ethyl-	0.004	0.020	0.004	0.019
123-07-9	Phenol, 4-ethyl-	0.016	0.080	0.016	0.078
	Phenol, 4-vinyl-	0.015	0.073	0.013	0.064
	Phenol, ethyl-methyl-	0.004	0.021	0.003	0.016
	Guaiacols (Methoxy phenols)	**0.356**	**1.75**	**0.351**	**1.73**
90-05-1	Guaiacol	0.195	0.959	0.196	0.964
18102-31-3	Guaiacol, 3-methyl-	0.017	0.086	0.017	0.082
93-51-6	Guaiacol, 4-methyl-	0.039	0.192	0.039	0.194
2785-89-9	Guaiacol, 4-ethyl-	0.033	0.161	0.032	0.159
7786-61-0	Guaiacol, 4-vinyl-	0.041	0.200	0.037	0.182
97-53-0	Guaiacol, 4-allyl- (Eugenol)	0.010	0.050	0.008	0.041
97-54-1	Guaiacol, 4-propenyl- cis (Isoeugenol)	0.022	0.107	0.022	0.107
	Syringols (Dimethoxy phenols)	**0.020**	**0.10**	**0.019**	**0.10**
91-10-1	Syringol	0.020	0.096	0.019	0.096
	CARBOHYDRATES				
	Sugars	**0.000**	**0.00**	**0.000**	**0.00**
	OTHER ORGANIC COMPOUNDS				
	N-compounds	**0.000**	**0.00**	**0.000**	**0.00**
	Acetates	**0.000**	**0.00**	**0.000**	**0.00**
	Terpenes	**0.022**	**0.11**	**0.022**	**0.11**

D-Limonene (NIST MQ 94)	0.015	0.076	0.015	0.075
2-Acetyl-5-norbornene (NIST MQ 92)	0.006	0.031	0.006	0.031
unknown compounds	**0.000**	**0.00**	**0.000**	**0.00**
Miscellaneous	**0.010**	**0.05**	**0.009**	**0.05**
poss: 1,4-Dioxin, 2,3-dihydro-	0.010	0.048	0.009	0.046

Table C9. GC-MS data for organic-rich condensate (ORC) obtained from *miscanthus* fast pyrolysis using the bioliq® (2019 campaign).

		Run 1		Run 2	
CAS-No.	**Compound**	**wt.% wet**	**wt.% dry**	**wt.% wet**	**wt.% dry**
	NONAROMATIC COMPOUNDS				
	Acids	**5.930**	**6.91**	**5.968**	**6.96**
64-19-7	Acetic acid	5.930	6.912	5.968	6.955
	Nonaromatic Esters	**0.323**	**0.38**	**0.329**	**0.38**
542-59-6	Acetic acid 2-hydroxyethyl ester	0.323	0.376	0.329	0.384
	Nonaromatic Alcohols	**3.876**	**4.52**	**3.898**	**4.54**
107-21-1	Ethylene glycol	3.876	4.517	3.898	4.543
	Nonaromatic Aldehydes	**2.506**	**2.92**	**2.396**	**2.79**
141-46-8	Acetaldehyde, hydroxy-	2.159	2.516	2.026	2.362
	Propionaldehyde, 3-hydroxy	0.215	0.251	0.229	0.267
	Butandial (or Propanal) (NIST MQ 92)	0.132	0.154	0.141	0.164
	Nonaromatic Ketones	**5.421**	**6.32**	**5.483**	**6.39**
116-09-6	Acetol (Hydroxypropanone)	3.961	4.617	3.993	4.654
5077-67-8	Butanone, 1-hydroxy-2-	0.573	0.667	0.597	0.695
431-03-8	Butandione, 2,3- (Diacetyl)	0.065	0.076	0.066	0.077
592-20-1	Propan-2-one, 1-acetyloxy-	0.101	0.118	0.102	0.119
930-30-3	Cyclopenten-1-one, 2-	0.140	0.164	0.146	0.170
2758-18-1	Cyclopenten-1-one, 3-methyl-2-	0.099	0.115	0.098	0.115
80-71-7	Cyclopenten-3-one, 2-hydroxy-1-methyl-1-	0.481	0.561	0.481	0.561
	Hydrocarbons	**0.000**	**0.00**	**0.000**	**0.00**
	HETEROCYCLIC COMPOUNDS				

	Furans	**1.113**	**1.30**	**1.132**	**1.32**
497-23-4	Furanone, 2(5H)-	0.405	0.472	0.414	0.483
98-01-1	Furaldehyde, 2-	0.313	0.365	0.321	0.375
591-11-17	Furan-2-one, 5-methyl-, (5H)-	0.047	0.054	0.048	0.055
22122-36-7	Furan-2-one, 3-methyl-, (5H)-	0.086	0.100	0.084	0.097
96-48-0	Butyrolactone, γ-	0.161	0.187	0.162	0.189
	Furan-2-one, 4-methyl-(5H)- (NIST MQ 88)	0.102	0.118	0.103	0.120
	Pyrans	**0.086**	**0.10**	**0.087**	**0.10**
	Pyran-4-one, 3-hydroxy-5,6-dihydro-, (4H)-	0.086	0.100	0.087	0.101
	AROMATIC COMPOUNDS				
	Benzenes	**0.019**	**0.02**	**0.020**	**0.02**
	Benzene (NIST MQ 97)	0.019	0.022	0.020	0.023
	Catechols	**n.q.**	**n.q.**	**n.q.**	**n.q.**
123-31-9	Hydroquinone (Benzene, 1,4-dihydroxy-)	n.q.	n.q.	4.278	4.986
	Benzenediol, methyl-	n.q.	n.q.	0.030	0.035
	Aromatic Alcohols	**0.000**	**0.00**	**0.000**	**0.00**
	Aromatic Aldehydes	**0.000**	**0.00**	**0.000**	**0.00**
	Aromatic Ketones	**0.000**	**0.00**	**0.000**	**0.00**
	Aromatic Esters	**0.000**	**0.00**	**0.000**	**0.00**
	Lignin-derived Phenols	**1.021**	**1.19**	**1.049**	**1.22**
108-95-2	Phenol	0.168	0.196	0.172	0.201
95-48-7	Cresol, o-	0.070	0.082	0.073	0.085
106-44-5	Cresol, p-	0.093	0.109	0.094	0.110
108-39-4	Cresol, m-	0.047	0.055	0.048	0.056

95-87-4	Phenol, 2,5-dimethyl-	0.091	0.106	0.097	0.114
105-67-9	Phenol, 2,4-dimethyl-	0.033	0.039	0.032	0.037
123-07-9	Phenol, 4-ethyl-	0.333	0.388	0.347	0.404
	Phenol, 4-vinyl-	0.155	0.181	0.153	0.179
	Phenol, ethyl-methyl-	0.031	0.036	0.032	0.037
	Guaiacols (Methoxy phenols)	**1.916**	**2.23**	**1.957**	**2.28**
90-05-1	Guaiacol	0.229	0.267	0.242	0.282
93-51-6	Guaiacol, 4-methyl-	0.167	0.195	0.179	0.208
2785-89-9	Guaiacol, 4-ethyl-	0.090	0.105	0.092	0.107
7786-61-0	Guaiacol, 4-vinyl-	0.079	0.092	0.077	0.090
97-53-0	Guaiacol, 4-allyl- (Eugenol)	0.076	0.088	0.075	0.087
2785-87-7	Guaiacol, 4-propyl-	0.029	0.034	0.027	0.032
97-54-1	Guaiacol, 4-propenyl- cis (Isoeugenol)	0.157	0.184	0.157	0.183
5932-68-3	Guaiacol, 4-propenyl-(trans) (Isoeugenol)	0.198	0.231	0.202	0.236
121-33-5	Vanillin	0.419	0.488	0.428	0.499
498-02-2	Phenylethanone, 4-hydroxy-3-methoxy- (Acetoguajacone)	0.395	0.460	0.395	0.460
2503-46-0	Guaiacyl acetone	0.076	0.089	0.081	0.095
	Syringols (Dimethoxy phenols)	**1.143**	**1.33**	**1.192**	**1.39**
91-10-1	Syringol	0.232	0.271	0.228	0.265
	Syringol, 4-methyl-	0.161	0.187	0.172	0.200
	Syringol, 4-ethyl-	0.046	0.054	0.047	0.055
	Syringol, 4-vinyl-	0.046	0.054	0.045	0.053
6627-88-9	Syringol, 4-allyl-	0.138	0.161	0.148	0.173
627-88-9	Syringol, 4-(1-propenyl)-, cis	0.085	0.099	0.089	0.103
	Syringol, 4-(1-propenyl)-, trans	0.159	0.186	0.171	0.199
134-96-3	Syringaldehyde	0.131	0.153	0.146	0.170
2478-38-8	Acetosyringone	0.057	0.066	0.064	0.075
	Syringyl acetone	0.087	0.102	0.083	0.097
	CARBOHYDRATES				
	Sugars	**5.202**	**6.06**	**5.299**	**6.18**

498-07-7	Anhydro-ß-D-glucopyranose, 1,6- (Levoglucosan)	4.889	5.698	4.971	5.793
	Dianhydro-α-D-glucopyranose, 1,4:3,6-	0.313	0.364	0.328	0.382
	OTHER ORGANIC COMPOUNDS				
	N-compounds	**0.000**	**0.00**	**0.000**	**0.00**
	Acetates	**0.016**	**0.02**	**0.018**	**0.02**
	Diethylene glycol, diacetate (NIST MQ 81)	0.016	0.019	0.018	0.021
	Terpenes	**0.000**	**0.00**	**0.000**	**0.00**
	unknown compounds	**0.000**	**0.00**	**0.000**	**0.00**
	Miscellaneous	**0.000**	**0.00**	**0.000**	**0.00**

Table C10. GC-MS data for aqueous condensate (AC) obtained from *miscanthus* fast pyrolysis using the bioliq® (2019 campaign).

		Run 1		Run 2	
CAS-No.	**Compound**	**wt.% wet**	**wt.% dry**	**wt.% wet**	**wt.% dry**
	NONAROMATIC COMPOUNDS				
	Acids	**4.130**	**21.62**	**5.343**	**27.98**
64-19-7	Acetic acid	3.515	18.401	4.706	24.641
79-09-4	Propionic acid	0.565	2.958	0.587	3.075
107-92-6	Butyric acid	0.050	0.261	0.049	0.259
	Nonaromatic Esters	**0.066**	**0.35**	**0.062**	**0.33**
554-12-1	Propanoic acid methyl ester	0.017	0.091	0.015	0.081
542-59-6	Acetic acid 2-hydroxyethyl ester	0.035	0.185	0.034	0.178
	poss. Propanoic acid, ethenyl ester (NIST MQ 75)	0.014	0.071	0.013	0.067
	Nonaromatic Alcohols	**0.863**	**4.52**	**0.827**	**4.33**
107-21-1	Ethylene glycol	0.805	4.212	0.773	4.047
	2-Propen-1-ol (NIST MQ 84)	0.058	0.306	0.054	0.282
	Nonaromatic Aldehydes	**0.950**	**4.97**	**0.811**	**4.24**
141-46-8	Acetaldehyde, hydroxy-	0.573	2.999	0.459	2.402
	Propionaldehyde, 3-hydroxy	0.092	0.482	0.072	0.377
4170-30-3	Crotonaldehyde, cis	0.161	0.843	0.019	0.098
123-73-9	Crotonaldehyde, trans	0.047	0.245	0.149	0.782
	2-Butenal, 2-methyl- (NIST MQ 92)	0.013	0.071	0.037	0.192
	poss: 2-Pentenal, (E)- (NIST MQ 89)	0.014	0.073	0.012	0.060
	Butandial (or Propanal) (NIST MQ 92)	0.050	0.261	0.013	0.066
				0.051	0.268
	Nonaromatic Ketones	**4.923**	**25.78**		
116-09-6	Acetol (Hydroxypropanone)	3.239	16.960	**4.688**	**24.54**
110-13-4	Acetonylacetone (Hexandione, 2,5-)	0.006	0.034	3.124	16.358

78-93-3	Butanone, 2-	0.133	0.699	0.006	0.029
5077-67-8	Butanone, 1-hydroxy-2-	0.324	1.696	0.125	0.656
431-03-8	Butandione, 2,3- (Diacetyl)	0.375	1.961	0.296	1.551
513-86-0	Acetoin (Hydroxy-2-butanone, 3-)	0.049	0.256	0.357	1.868
592-20-1	Propan-2-one, 1-acetyloxy-	0.081	0.425	0.046	0.241
120-92-3	Cyclopentanone	0.085	0.444	0.075	0.391
930-30-3	Cyclopenten-1-one, 2-	0.172	0.902	0.085	0.444
1121-05-7	Cyclopenten-1-one, 2,3-dimethyl-2-	0.011	0.058	0.164	0.857
1120-73-6	Cyclopenten-1-one, 2-methyl-2-	0.058	0.306	0.009	0.045
2758-18-1	Cyclopenten-1-one, 3-methyl-2-	0.026	0.136	0.057	0.301
10493-98-8	Cyclopenten-1-one, 2-hydroxy-2-	0.012	0.064	0.025	0.133
80-71-7	Cyclopenten-3-one, 2-hydroxy-1-methyl-1-	0.067	0.350	0.011	0.060
930-68-7	Cyclohexen-1-one, 2-	0.005	0.028	0.067	0.350
	Methyl vinyl ketone = 2-Butenone (NIST MQ 90)	0.018	0.092	0.005	0.024
	Methyl vinyl ketone = 2-Butenone (NIST MQ 90)	0.011	0.056	0.009	0.045
	3-Buten-2-one, 3-methyl- (NIST MQ 88)	0.035	0.184	0.029	0.154
	2,3-Pentanedione	0.067	0.351	0.060	0.312
	3-Penten-2-one (NIST MQ 84)	0.040	0.208	0.038	0.198
	2-Butanone, 4-hydroxy- (NIST MQ 84)	0.022	0.113	0.023	0.118
	poss: 2-Pentanone, 4-hydroxy- (NIST MQ 82)	0.021	0.108	0.017	0.089
	Isomere of 2-Cyclopenten-1-one, 3-methyl-	0.013	0.070	0.013	0.066
	2-Butanone, 1-hydroxy-3-methyl- (NIST MQ 78)	0.011	0.056	0.009	0.049
	2-Cyclopenten-1-one, 3,4-dimethyl-	0.014	0.075	0.014	0.074
	Isomere of Cyclopenten-1-one, 2,3-dimethyl-2-	0.020	0.107	0.019	0.099
	2-Cyclopenten-1-one, 2,3,4-trimethyl- (NIST MQ 88)	0.007	0.038	0.005	0.027
	Hydrocarbons	**0.000**	**0.00**	**0.000**	**0.00**
	HETEROCYCLIC COMPOUNDS				
	Furans	**0.739**	**3.87**	**0.700**	**3.67**
497-23-4	Furanone, 2(5H)-	0.091	0.475	0.089	0.464
98-01-1	Furaldehyde, 2-	0.457	2.392	0.434	2.273

498-60-2	Furaldehyde, 3-	0.032	0.166	0.030	0.156
620-02-0	Furaldehyde, 5-methyl-2-	0.023	0.118	0.021	0.111
1192-62-7	Ethanone, 1-(2-furanyl)-	0.024	0.124	0.023	0.121
591-11-17	Furan-2-one, 5-methyl-, (5H)-	0.019	0.099	0.018	0.093
22122-36-7	Furan-2-one, 3-methyl-, (5H)-	0.022	0.113	0.019	0.099
	Furan-2-one, 2,5-dihydro-3,5-dimethyl-	0.018	0.097	0.016	0.086
96-48-0	Butyrolactone, γ-	0.037	0.194	0.034	0.181
	Furan, tetrahydro-2-methoxy- (NIST MQ (/)	0.006	0.030	0.005	0.027
	Furan-2-one, 4-methyl-(5H)- (NIST MQ 88)	0.012	0.063	0.011	0.057
	Pyrans	**0.000**	**0.00**	**0.000**	**0.00**
	AROMATIC COMPOUNDS				
	Benzenes	**0.017**	**0.09**	**0.015**	**0.08**
104-93-8	Benzene, 1-methoxy-4-methyl-	0.006	0.030	0.005	0.025
	Benzofuran, ethyl-	0.002	0.010	0.002	0.010
	Benzofuran, dimethyl- (NIST MQ 74)	0.007	0.035	0.006	0.032
	Benzofuran, dimethyl- (NIST MQ 74)	0.002	0.011	0.002	0.011
	Catechols	**0.000**	**0.00**	**0.000**	**0.00**
	Aromatic Alcohols	**0.000**	**0.00**	**0.000**	**0.00**
	Aromatic Aldehydes	**0.015**	**0.08**	**0.014**	**0.07**
100-52-7	Benzaldehyde	0.006	0.030	0.005	0.029
90-02-8	Benzaldehyde, 2-hydroxy (Salicylaldehyd)	0.009	0.046	0.008	0.042
	Aromatic Ketones	**0.000**	**0.00**	**0.000**	**0.00**
	Aromatic Esters	**0.000**	**0.00**	**0.000**	**0.00**
	Lignin-derived Phenols	**0.166**	**0.87**	**0.160**	**0.84**

108-95-2	Phenol	0.045	0.237	0.044	0.230
95-48-7	Cresol, o-	0.022	0.117	0.021	0.111
106-44-5	Cresol, p-	0.022	0.115	0.021	0.108
95-87-4	Phenol, 2,5-dimethyl-	0.007	0.036	0.007	0.036
105-67-9	Phenol, 2,4-dimethyl-	0.007	0.037	0.007	0.035
576-26-1	Phenol, 2,6-dimethyl-	0.005	0.025	0.004	0.022
527-60-6	Phenol, 2,4,6-trimethyl-	0.002	0.008	0.001	0.008
90-00-6	Phenol, 2-ethyl-	0.003	0.017	0.003	0.016
123-07-9	Phenol, 4-ethyl-	0.048	0.251	0.047	0.245
	Phenol, ethyl-methyl-	0.005	0.027	0.005	0.026
	Guaiacols (Methoxy phenols)	**0.169**	**0.89**	**0.164**	**0.86**
90-05-1	Guaiacol	0.086	0.453	0.084	0.442
93-51-6	Guaiacol, 4-methyl-	0.041	0.217	0.040	0.211
2785-89-9	Guaiacol, 4-ethyl-	0.019	0.099	0.018	0.094
97-53-0	Guaiacol, 4-allyl- (Eugenol)	0.010	0.050	0.009	0.048
2785-87-7	Guaiacol, 4-propyl-	0.003	0.016	0.003	0.016
97-54-1	Guaiacol, 4-propenyl- cis (Isoeugenol)	0.010	0.051	0.009	0.049
	Syringols (Dimethoxy phenols)	**0.016**	**0.09**	**0.016**	**0.08**
91-10-1	Syringol	0.013	0.066	0.012	0.065
	Syringol, 4-methyl-	0.004	0.019	0.004	0.019
	CARBOHYDRATES				
	Sugars	**0.000**	**0.00**	**0.000**	**0.00**
	OTHER ORGANIC COMPOUNDS				
	N-compounds	**0.000**	**0.00**	**0.000**	**0.00**
	Acetates	**0.000**	**0.00**	**0.000**	**0.00**
	Terpenes	**0.013**	**0.07**	**0.013**	**0.07**
	5-Norbornane-2-carboxaldehyde (NIST MQ 92)	0.006	0.032	0.007	0.034

2-Acetyl-5-norbornene (NIST MQ 92)	0.006	0.034	0.006	0.033
unknown compounds	**0.000**	**0.00**	**0.000**	**0.00**
Miscellaneous	**0.041**	**0.22**	**0.041**	**0.21**
1,3-Dioxolane, 2-methyl- (NIST MQ 62)	0.013	0.066	0.012	0.065
poss: 1,4-Dioxin, 2,3-dihydro-	0.014	0.074	0.013	0.070
2,2'-Bi-1,3-dioxolane (NIST MQ 87)	0.015	0.076	0.015	0.077

Section 3: Surrogate Mixtures of ORCs and ACs Derived from Wheat Straw and Miscanthus, Used as Input for Bench-Scale Solvent Extraction Modeling in Aspen Plus

Table C11. ORC and AC surrogate mixtures from wheat straw and *miscanthus* used for solvent extraction modeling.

Surrogate compounds	Mass fraction (wt.%) of surrogate mixtures			
	Wheat Straw		*Miscanthus*	
	ORC	AC	ORC	AC
Water	0.2687	0.8325	0.1260	0.8340
Acetic acid	0.0569	0.0428	0.0917	0.0688
Propionic acid	0.0215	0.0115	0.0697	0.0089
2-Methylpropanoic acid	0.0000	0.0004	0.0000	0.0000
Ethylene glycol	0.0000	0.0000	0.0000	0.0000
Methanol	0.0000	0.0000	0.0000	0.0000
Hydroxy acetaldehyde (Glycol aldehyde)	0.0233	0.0019	0.0226	0.0104
3-hydroxypropionaldehyde	0.0000	0.0004	0.0026	0.0012
Hydroxyacetone (Acetol)	0.0530	0.0570	0.0655	0.0625
2-Butanone	0.0002	0.0024	0.0000	0.0006
1-hydroxy-2-butanone	0.0000	0.0077	0.0085	0.0054
2,3-Butanedione (Diacetyl)	0.0002	0.0028	0.0000	0.0012
2-Furaldehyde (Furfural)	0.0022	0.0035	0.0055	0.0050
5-hydroxymethyl-2-Furaldehyde	0.0000	0.0003	0.0000	0.0000
Phenol	0.0022	0.0007	0.0044	0.0008
m-Cresol	0.0011	0.0003	0.0014	0.0001

Surrogate compounds	Mass fraction (wt.%) of surrogate mixtures			
	Wheat Straw		*Miscanthus*	
	ORC	AC	ORC	AC
o-Cresol	0.0008	0.0005	0.0017	0.0003
Guaiacol	0.0042	0.0020	0.0036	0.0008
Vanillin	0.0022	0.0001	0.0070	0.0000
Syringol	0.0034	0.0003	0.0030	0.0000
Levoglucosan	0.0092	0.0000	0.0858	0.0000
Lignin (unknowns)	0.4309	0.0000	0.5010	0.0000

Academic Contributions

Publications

1. Parku, G. K., Pulicanti, S. R., Funke, A., & Dahmen, N. (2024). Phase equilibria aided optimization of levoglucosan extraction during condensation of fast pyrolysis bio-oils. *Energy & Fuels, 38*(15), 14343–14350. https://doi.org/10.1021/acs.energyfuels.4c01097.

2. Parku, G. K., Funke, A., & Dahmen, N. (2024). Influence of selected quench media used for direct contact condensation on yield and composition of fast pyrolysis bio-oils aided by thermodynamic phase equilibria modelling. *Separation and Purification Technology*, *326*, 126873. https://doi.org/10.1016/j.seppur.2024.126873.

3. Weih, N., Niebel, A., Pfitzer, C., Funke, A., Parku, G. K., & Dahmen, N. (2024). Operational experience with miscanthus feedstock at the bioliq® fast pyrolysis plant. *Journal of Analytical and Applied Pyrolysis, 177*, 106338. https://doi.org/10.1016/j.jaap.2023.106338.

4. Ajikashile, J. O., Alhnidi, M.-J., Parku, G. K., Funke, A., & Kruse, A. (2023). A study on the fast pyrolysis of millet and sorghum straws sourced from arid and semi-arid regions of Nigeria in a twin-screw mixing reactor. *Materials Science for Energy Technologies, 6*, 388–398. https://doi.org/10.1016/j.mset.2023.03.007.

5. Parku, G. K., Krutof, A., Funke, A., Richter, D., & Dahmen, N. (2023). Using fractional condensation to optimise aqueous pyrolysis condensates for downstream microbial conversion. *Industrial & Engineering Chemistry Research, 62*(6), 2792–2803. https://doi.org/10.1021/acs.iecr.2c03598.

6. Parku, G. K., Collard, F.-X., & Görgens, J. F. (2020). Pyrolysis of waste polypropylene plastics for energy recovery: Influence of heating rate and vacuum conditions on composition of fuel product. *Fuel Processing Technology, 209*, 106522. https://doi.org/10.1016/j.fuproc.2020.106522.

Conference Proceedings

1. Parku, G. K., Collard, F.-X., & Görgens, J. F. (2024, October 8–10). *Pyrolysis of waste polypropylene plastics for energy recovery: Study comparisons between bench scale and a commissioned pilot scale reactor* [Oral presentation]. ICERA 2024 – International Conference on Circular Economy, Renewable Energies and Green Hydrogen in Africa, Lomé, Togo.

2. Parku, G. K., Funke, A., & Dahmen, N. (2024, May 19–23). *Influence of quench media on yield and composition of fast pyrolysis bio-oils aided by phase equilibria modelling* [Oral presentation]. 24th International Symposium on Analytical and Applied Pyrolysis (Pyro2024), Beijing, China.

3. Parku, G. K., Collard, F.-X., & Görgens, J. F. (2024, April 28–May 2). *Pyrolysis of waste polypropylene for energy recovery: Study comparisons between bench scale and a commissioned pilot scale reactor* [Oral and Poster presentations]. CHEMREC I – 1st International Conference on Thermochemical Recycling of Plastics – Engineering Conferences International, Málaga, Spain.

4. Parku, G. K., Collard, F.-X., & Görgens, J. F. (2023, September 18–21). *Pyrolysis of waste polypropylene plastics for energy recovery: Influence of heating rate and vacuum conditions on composition of fuel product* [Oral presentation]. International Conference on Circular Economy, Renewable Energies and Green Hydrogen in Africa (ICERAfrica), Kumasi, Ghana.

5. Parku, G. K., Krutof, A., Adolf, K., Aniekwe, E. U., Funke, A., & Dahmen, N. (2023, May 7–12). *Validating the applicability of vapour–liquid phase equilibria models for fast pyrolysis bio-oils through Advanced Distillation Curves (ADC)* [Oral and Poster presentations]. PYROLIQ II – Engineering Conferences International, Schloss Hernstein, Austria.

6. Parku, G. K., Funke, A., & Dahmen, N. (2023, March 20–22). *Fine-tuning the quality of fast pyrolysis bio-oils during condensation with the aid of phase equilibria modelling* [Oral and Poster presentations]. KNT Symposium – Young Researchers Workshop on New Processes for a Circular Economy, University of Twente, Enschede, Netherlands.

7. Parku, G. K., Pulicanti, S. R., Funke, A., & Dahmen, N. (2022, September 13–14). *Water extraction of levoglucosan from fast pyrolysis bio-oils: Optimisation and scale-up* [Oral and Poster presentations]. 5th Doctoral Colloquium Bioenergy, Leipzig, Germany.

8. Parku, G. K., Krutof, A., Funke, A., Richter, D., & Dahmen, N. (2022, May 15–20). *Using fractional condensation to optimise aqueous pyrolysis condensates for downstream microbial conversion* [Poster presentation]. 23rd International Conference on Analytical and Applied Pyrolysis (PYRO 2022), Ghent, Belgium.

9. Parku, G. K., Krutof, A., Funke, A., Richter, D., & Dahmen, N. (2021, September 13–14). *Optimisation of low-temperature aqueous pyrolysis condensates for downstream microbial conversion* [Oral presentation]. 4th Doctoral Colloquium Bioenergy, Karlsruhe, Germany.

George Kofi Parku

Work : Hermann-von-Helmholtz-Platz 1, 76344, Eggenstein-Leopoldshafen, Germany

Email: george.parku@kit.edu **Phone:** (+49) 72160824338

ABOUT MYSELF

Chemical and Process Engineer with international research experience in Germany, South Africa, and the USA, skilled in process modeling, system optimization, and applied engineering solutions. Award-winning researcher with a track record of leading projects, driving sustainable energy innovation, and promoting cross-cultural collaboration.

WORK EXPERIENCE

Karlsruhe Institute of Technology

City: Karlsruhe | **Country:** Germany

[09/2019 – Current] **Research Associate**

- Researched and optimized a fractional condensation system using phase equilibrium modeling, and validated the results on a 10 kg/h fast pyrolysis pilot plant for biomass-to-fuel conversion, while supervising master's theses on thermochemical conversion processes.

Stellenbosch University

City: Stellenbosch | **Country:** South Africa

[04/2016 – 12/2018] **Research Assistant**

- Led a research project focused on the design, assembly, and commissioning of a 5 kg/h pyrolysis pilot plant for converting plastics and other carbonaceous wastes into valuable fuels and chemicals.

EDUCATION AND TRAINING

[09/2019 – Current] **PhD Chemical & Process Engineering**

Karlsruhe Institute of Technology

[04/2016 – 04/2019] **MEng Chemical Engineering**

Stellenbosch University

[08/2010 – 06/2014] **BSc Petrochemical Engineering**

Kwame Nkrumah University of Science and Technology

LANGUAGE SKILLS

Mother tongue(s): English **Other language(s):** German

STAYS ABROAD

[10/2021 – 12/2021] **Colorado State University, Fort Collins, Colorado, USA**

Advanced Distillation Curve (ADC) measurements of fast pyrolysis bio-oils (Research group of Prof. Bret Windom, Chemical Energy Conversion Laboratory).

HONOURS AND AWARDS

[06/2022] **DAAD Prize for extraordinary committed international doctoral researchers Awarding institution:** Karlsruhe Institute of Technology

[06/2022] **Business Ideas for Development Awarding institution:** German Federal Ministry for Economic Cooperation and Development (BMZ)

A grant to support start-up in sustainable solid waste management in Ghana.

[10/2018] **Green Talents International Forum for High Potentials in Sustainable Development Awarding institution:** German Federal Ministry of Education and Research (BMBF)

Link: https://www.greentalents.de/awardees_awardees2018_george-kofi-parku.php